Universitat de les Illes Balears

INIA
Instituto Nacional de Investigación
y Tecnología Agraria y Alimentaria

**Govern
de les Illes Balears**
Conselleria de Medi Ambient,
Agricultura i Pesca
Direcció General d'Agricultura
i Ramaderia

DOCTORAL THESIS
2015

EFFECTS OF GRAPEVINE LEAFROLL ASSOCIATED VIRUS 3 (GLRaV-3) CONCENTRATION, ON PLANT PHYSIOLOGY AND QUALITY PARAMETERS IN *VITIS VINIFERA* L. WHITE CULTIVARS.

Rafael Montero Silvestre

INIA

Instituto Nacional de Investigación
y Tecnología Agraria y Alimentaria

Govern
de les Illes Balears
Conselleria de Medi Ambient,
Agricultura i Pesca
Direcció General d'Agricultura
i Ramaderia

**DOCTORAL THESIS
2015**

**Doctoral Programme of Biology of the plants
under mediterranean conditions**

**EFFECTS OF GRAPEVINE LEAFROLL
ASSOCIATED VIRUS 3 (GLRaV-3)
CONCENTRATION, ON PLANT PHYSIOLOGY
AND QUALITY PARAMETERS IN VITIS VINIFERA
L. WHITE CULTIVARS.**

Rafael Montero Silvestre

**Thesis Supervisor: Josefina Bota Salort
Thesis Supervisor: Jaume Flexas Sans**

Ph. Doctor by the Universitat de les Illes Balears

Nosotros,

Dra. Josefina Bota, profesora contratada doctora interina del departamento de biología de la facultat de ciencias de la *Universitat de les Illes Balears*

Dr. Jaume Flexas, profesor titular del departamento de biología de la facultat de ciencias de la *Universitat de les Illes Balears*
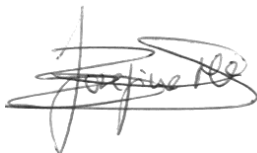
CERTIFICAMOS:

Que el presente trabajo titulado *"Effects of Grapevine leafroll associated virus 3 (GLRaV-3) concentration, on plant physiology and quality parameters in Vitis vinifera L. white cultivars"* presentado por Rafael Montero Silvestre para optar al TÍTULO universitario oficial de DOCTOR por la *Universitat de les Illes Balears* dentro del programa de doctorado de Biología de las Plantas en Condiciones Mediterráneas, se ha realizado bajo nuestra dirección.

Revisado el presente trabajo, autorizamos su presentación para que pueda ser juzgada por el tribunal correspondiente.

Palma de Mallorca, 27 de octubre del 2015

Directora	Director	Autor
Josefina Bota Salort	Jaume Flexas Sans	Rafael Montero Silvestre

A mis padres

"Ever tried. Ever failed. No matter.
Try again. Fail again. Fail better."
Samuel Beckett

AGRADECIMIENTOS-ACKNOWLEDGEMENTS

Durante el periodo de realización de la tesis, existen momentos buenos y malos. Pero todo el esfuerzo ha merecido la pena y sin duda este periodo ha sido la mejor etapa de mi vida, y todo es gracias a las personas que he encontrado en el camino. A todas ellas les quiero agradecer su ayuda, porque sin ella no hubiera sido posible la consecución de este trabajo.

Quería dar las gracias en primer lugar a todos mis compañeros del Instituto de la Vid y el Vino de Castilla-La Mancha en Tomelloso, por ayudarme a dar mis primeros pasos en la ciencia. En especial a mis "hermanicas" Adela, Laura y Noelia, por hacer que ese año fuera tan especial para mí, y a Chule y Juan Luis por todos sus consejos y por la formación que recibí de su parte.

Merci beaucoup à Dr. Thierry Simmoneau et Dr. Eric Lebon de me donner l'opportunité de poursuivre ma formation au LEPSE. Merci à tous les collègues du LEPSE de Montpellier, en particulier à Aude (merci d'être toi) et Manolo (os estaré siempre agradecido por todo lo que hicisteis por mí Rebeca y tú).

Especialmente quiero agradecer a todos los miembros del grupo de investigación de Biología de las Plantas en Condiciones Mediterráneas, y sobre todo a mis directores de tesis, Dra. Josefina Bota y Dr. Jaume Flexas, la ayuda recibida. A Josefina por confiar en mí, darme la oportunidad de realizar esta tesis y por todo lo que has hecho por mí. Eres un modelo a seguir desde el punto de vista personal y profesional. He tenido mucha suerte de conocerte y tenerte como directora de tesis. A Jaume por tus consejos y por tu capacidad para motivar. Cada reunión contigo, cada mail, ha sido un empujón más para seguir luchando.

A los doctores, Hipólito Medrano por ofrecerme su ayuda en todo momento y por sus valiosos consejos, y Pepe Escalona por su ayuda en todos los detalles más técnicos de la viticultura y enología. Al Dr. Miquel Ribas por su apoyo incondicional y sus toques de atención para no salirme del camino. A los doctores Jeroni Galmés, Alex Gallé, Xavi Gulías, Pep Cifre, Miguel Angel Conesa, por vuestro interés y consejos sobre todas las cuestiones que os he planteado.

A toda la familia "Ca'n Boom", he aprendido mucho de todos los que habéis pasado por esa oficina. Gracias a Igor, Alicia, Magdalena, Belén, Carmiña, Esther, Amani, Arantxa, Veriozka, Xurxo, Mari, Patricia, Cyril, Tià, Marcel, Nestor, Marc, Xiong, Alejandro, Antonia y Hanan por convertir estos cuatro años que he pasado en Mallorca en los mejores de mi vida. Han sido muchos momentos las que hemos vivido juntos, todos muy especiales y que siempre recordaré. Gracias a Pep Sastre, Miquel Truyols e Issac por su apoyo a en toda la parte experimental.

Gracias a Enrico y Enrique por hacerme sentir como en casa a mi llegada a Mallorca. Gracias Maruš por esa Medovina con la que empezó todo.

Gracias a Carme, Joana, Vanesa, Joan, Jaume, Bernat y Simò por vuestro apoyo en la conselleria y por introducirme en el mundo mallorquín. También quiero dar las gracias a Diego y Alicia por su ayuda en todo lo referente a sanidad vegetal.

Gracias al Dr. Leonardo Velasco por recibirme en su laboratorio del IFAPA de Málaga, por permitirme colaborar en sus experimentos y por ser mi virólogo de cabecera resolviendo todas las dudas que le planteaba.

Gracias a las doctoras Matilde Barón y Marisa Pérez Bueno por darme la oportunidad de continuar con mi formación aprendiendo nuevas técnicas en la estación experimental del Zaidín y por su colaboración en todo momento.

Grazie mille a la Dra. Cristina Marzachì e il Dr. Davide Pacifico per insegnarmi la quantificazione dei virus. Oltre a questa tecnica, grazie a loro ho imparato molto sull' efficienza e la precisione nel lavoro. Ringrazio anche tutti i colleghi dell' IVV di Torino, Flavio, Paolo, Nestor, Luciana, Dimitris, Piero, Simona, Sabrina, Domenico e soprattutto Mahnaz, per l' aiuto dentro e fuori del laboratorio.

I would like to say thanks to Dr. Mike Trought and Dion Mundy for allowing me to be part of your laboratory in New Zealand. I am also very grateful to Abby, Sharlene, Rachel, Damian, Rob, Jeff, Damian, Richard, Cherryl, Sue, Bruce, Rafidah and Lily for becoming the antipodes of my country, in my home. I am especially grateful to Claire for showing me the winery bible "making good wine", Marc and Victoria for showing me the kiwi world and of course Guillaume, for being like my brother, "Fairweathers" will miss us.

SYMBOLS AND ABBREVATIONS LIST

Symbols	Meaning
α	leaf absorptance
ABA	abscissic acid
Ac	photosynthesis limited by carboxylation
AGVd	australian grapevine viroid
Ala	alanine
A_N	net CO_2 assimilation
AOX	alternative oxidase
Aq	photosynthesis limited by RuBP regeneration
Arg	arginine
Asp	aspartic acid
ATP	adenosine triphosphate
B_L	biochemistry limitation
β	partitioning of absorbed quanta between photosystems II and I
BGF	blue and green fluorescence
C	calose
C_a	atmospheric CO_2 concentration
Caf	caffeic acid
CaMV	cauliflower mosaic virus
C_c	chloroplast CO_2 concentration
CC	companion cells
Chl	chlorophyll
Chl a	chlorophyll a
Chl b	chlorophyll b
Chl-F	chlorophyll fluorescence
Chl-FI	chlorophyll fluorescence imaging
C_i	sub-stomatal CO_2 concentration
CO_2	carbon dioxide
COX	cytochrome oxidase
CP	coat protein
CPC	crystalline protein cluster
CPm	minor coat protein
Ct	threshold cycle
CTV	citrus tristeza virus
CW	cell wall
Δ_a	oxygen isotope fractionation of the alternative oxidase pathway
Δ_c	oxygen isotope fractionation of the cytochrome oxidase pathway
DAP	diammonium phosphate
DEPC	diethylpyrocarbonate
Dhasc	dehydroascorbic acid
DIECA	na-diethyl-dithio-carbonate
DL	density of the leaves
DTT	dithiothreitol
E	leaf transpiration rate
ELISA	enzyme-linked inmunosorbent assay
ER	endoplasmic reticulum
Φ_{CO2}	apparent quantum efficiency of CO_2 fixation

Symbols	Meaning
Φ_{PSII}	photochemical efficiency of photosystem II
F_o	fluorescence signal when all reaction centers were open
f_{ias}	volume fraction of intercellular air spaces
$F440$	blue fluorescence
$F520$	green fluorescence
$F680$	red fluorescence
$F740$	far red fluorescence
FAN	total free amino acids
Flav Quer galac	flavonol quercetin-3-*O*-galactoside
Flav Quer gluc	flavonol quercetin-3-*O*-glucoside
Flav Myr rut	flavonol myricetin-3-*O*-rutinoside
F_M	fluorescence signal when all reactions centers were closed
$F_{M'}$	maximum fluorescence during a light-saturating pulse
F_s	steady-state fluorescence
FSO_2	free sulphur dioxide
F_V/F_M	maximum quantum efficiency of photosystem II
Γ^*	CO_2 compensation point in the absence of mitochondrial respiration
GC-TOF-MS	gas chromatography-time of flight-mass spectrometry
GFkV	grapevine fleck virus
GFLV	grapevine fanleaf virus
GLD	grapevine leafroll disease
GLRaVs	grapevine leafroll associated viruses
Glu	glutamic acid
Gly	glycine
g_m	mesophyll conductance
GRSPaV	Grapevine rupestris stem pitting associated virus
g_s	stomatal conductance
GTR	guanosine-5'-triphosphate
GVA	grapevine virus A
GYSVd-1	grapevine yellow speckle viroid 1
His	histidine
hsp 70	heat shock protein 70
HR	hypersensitive reaction
HRM	high-resolution melting
HSVd	hop stunt viroid
IC-PCR	immuno-capture PCR
IF	inmunofluorescence
Ile	isoleucine
JA	jasmonic acid
J_{flu}	electron transport rate determined by chlorophyll fluorescence
J_{max}	maximum capacity for electron transport rate
Kc	rubisco michaelis–menten constants for carboxylation
KCN	potassium cyanide
Ko	rubisco michaelis–menten constants for oxygenation
LAMP	loop-mediated amplification of nucleic acid
LC-MS	liquid chromatography-mass spectrometry
LEDs	light-emitting diodes
Leu	leucine
LMA	leaf mass area

Symbols	**Meaning**
L-Pro	leader protease
Lys	lysine
M	mitochondria
Mal	malate
MAP	mitogen-activated protein
MCFI	multicolour fluorescence imaging
MC_L	mesophyll limitation
MeOH	methanol
MEP	methylerythritol phosphate
Meth	methionine
mETC	mitochondrial electron transport chain
MNSV	melon necrotic spot virus
MRM	multiple reaction monitoring
MSTFA	n-methyl-n-(trimethylsilyl) trifluoroacetamide
MuLV	moloney murine leukemia virus
N	nucleus
NADH	nicotinamide adenine dinucleotide
NDVI	normalized difference vegetation index
NGS	next generation sequencing
NPQ	non-photochemical quenching
O_2	oxygen
ORFs	open reading frames
P	plastids
PAL	phenylalanine ammonia lyase
PD	plasmodesmata
PEG	polyethylene glycol
Phen	phenylalanine
PP	parietal proteins
PPFD	photosynthetically active photon flux density
PPUs	pore plasmodesmal units
PR	pathogenesis-related
PSII	photosystem II
qPCR	quantitative PCR
R_d	leaf dark respiration
RdRp	RNA dependent RNA polymerase
ROS	reactive oxygen species
RNP	ribonucleoprotein
RT-PCR	reverse transcription-PCR
RuBP	ribulose biphosphate
RW	rugose wood
SA	salicylic acid
SAR	systemic acquired resistance
SDS	sequence detection systems
SE	sieve elements
SEL	size exclusion limit
Ser	serine
sgRNAs	small guides RNAs
SHAM	salicylhydroxamic acid
S_L	stomatal limitation

Symbols	**Meaning**
SNK	student–newman–keuls
SO_2	sulphur dioxide
SPs	sieve plates
+ss	positive sense single stranded
SSCP	single-strand conformation polymorphism
τ_a	electron partitioning through the alternative pathway
TA	titratable acidity
TBE	tris-borate-EDTA
Thre	threonine
T_L	total limitation
T_{mes}	mesophyll thickness
TSO_2	total sulphur dioxide
TSS	transcriptional start sites
Tyr	tyrosine
UAV	unmanned aerial vehicle
UV	ultraviolet
V	vacuole
Val	valine
V_{alt}	activity of the alternative oxidase pathway
$V_{c,max}$	maximum carboxylation capacity
V_{cyt}	activity of the cytochrome oxidase pathway
VP	vascular parenchyma cells
V_t	total oxygen uptake rate
V_{TPU}	rate of triose-phosphate utilization
w	width of leaf anatomical section
YAN	yeast assimilable nitrogen
Ψ_{PD}	predawn leaf water potential

LIST OF PUBLICATIONS DERIVED FROM THE PRESENT THESIS

This thesis has been developed with a predoctoral fellowship (FPI-INIA) and the financial support from the National institute of Agronomic research (RTA2010-00118-00-00). Results obtained in the present thesis have resulted in the following papers:

1. Velasco L., Bota J., **Montero R.**, & Cretazzo E. (2014). Differences of three ampeloviruses multiplication in plant may explain their incidences in vineyards. *Plant Disease*, **98**, 395-400.

2. **Montero R.**, El aou ouad H., Pacifico D., Marzachì C., Castillo N., García E., Del Saz N.F., Florez-Sarasa I., Flexas J., & Bota J. (2015). Absolute quantification of *Grapevine leafroll associated virus 3* (GLRaV-3) and its effects on the physiology in asymptomatic plants of *Vitis vinifera* L. *Annals of Applied Biology*. (Submitted)

3. **Montero R.**, Pérez-Bueno M. L., Barón M., Florez-Sarasa I., Tohge T., Fernie A. R., El aou ouad H., Flexas J., & Bota J. (2015). Alterations in primary and secondary metabolism in *Vitis vinifera* L. Malvasía de Banyalbufar cv. upon infection with *Grapevine leafroll associated virus 3* (GLRaV-3). *Physiologia Plantarum* (Submitted).

4. **Montero R.**, El aou ouad H., Flexas J., & Bota J. (2015). Effects of *Grapevine Leafroll associated virus 3* (GLRaV-3) on plant carbon balance in *Vitis vinifera* L. cv. Giró Ros. *Theoretical and Experimental Plant Physiology* (Submitted).

5. **Montero R.**, Mundy D., Albright A., Grose C., Trought M.C.T., Cohen D., Chooi K.M., MacDiarmid R., Flexas J., & Bota J. (2015). Effects of *Grapevine leafroll associated virus 3* (GLRaV-3) and duration of infection on fruit composition and wine chemical profile of *Vitis vinifera* L. cv. Sauvignon Blanc. *Food Chemistry* (Accepted with minor changes).

CONTENTS

SUMMARY

Phloem systemic virus type, as *Grapevine leafroll asociated virus 3* (GLRaV-3), causes significant economic losses in many vineyards in the major wine regions around the world. The leaf symptoms of the infection are clearly visible in red cultivars, expressed as early red spotting, coalescing to a red purple colour leaving a green vein banding symptom. Leaves often curl downwards and become brittle. In white cultivars symptoms are less visually obvious and vines are asymptomatic. However, if symptoms are expressed, they are likely to include inter-veinal yellowing of leaves and leaf rolling. As a result it is more difficult to identify leafroll infected vines of white varieties in the field. These masked symptoms hinder disease diagnosis, timely insect vector control and effective removal of infected vines.

The objectives of the present Thesis were to investigate the possible reasons of the high incidence of GLRaV-3 in vineyards, to detect the most sensitive physiological parameters affected by GLRaV-3 and to estimate the influence of the virus on fruit composition.

The results showed that GLRaV-3 is able to establish and multiply more efficiently than other ampeloviruses and this could be one of the main reasons for the highest incidence in vineyards. The virus affected physiological parameters, especially net CO_2 assimilation and the electron transport rate. There was a negative correlation between these parameters and virus amount. Therefore net CO_2 assimilation and electron transport rate could be used to identify the presence of virus in asymptomatic situations. Non photochemical quenching together with blue-green fluorescence and derived ratios could also be used as disease signatures for GLRaV-3, according to the results obtained under control conditions. Flavonols such as myricetin-3-*O*-rutinoside, quercetin-3-*O*-galactoside and quercetin-3-*O*-glucoside; and hydroxycinnamic acids such as caffeic acid were identified as possibly responsible of changes observed in multicolour fluorescence imaging parameters measured in response to the infection. The detection of the virus is essential to fight against the infection spread, because it is very difficult to eliminate the virus in the field. Principal changes observed related to slower berry ripening, which in turn affects harvest date, resulting in reduced organic acid

concentrations. The length of time that vines have been infected may have a stronger effect on plant physiology than absolute virus titre measured at any given time.

Therefore this thesis has enabled a better understanding of some of the reasons for the higher GLRaV-3 incidence than other viruses in the vineyards, as well as the identification of physiological parameters sensitive to the infection that could be used for virus presence detection on large areas. Strategies to minimize virus effects on the final quality of the juice and wine have been established.

RESUMEN

Virus sistémicos de tipo floemático, como el virus del enrollado 3 (GLRaV-3), producen importantes pérdidas económicas en muchos viñedos de las mayores regiones vitícolas de todo el mundo. Los síntomas de este virus son claramente visibles en variedades tintas, con la aparición temprana de una coloración rojiza entre las nerviaciones foliares, que permanecen verdes. Las hojas se suelen enrollar hacia abajo y se vuelven frágiles. En variedades blancas, en caso de que los síntomas se expresen, estos producen el amarillamiento intervenal y enrollamiento de las hojas. Al tratarse en la mayoría de los casos de variedades asintomáticas es más difícil identificar la presencia del virus en el campo. La ausencia de síntomas, dificulta por tanto el diagnóstico de la infección y, consecuentemente, la aplicación de medidas para prevenir la dispersión del virus, como el control biológico del vector y la sustitución de las plantas infectadas por plantas sanas.

Los objetivos de la presente Tesis son indagar en las posibles causas de la alta incidencia del GLRaV-3 en los viñedos, identificar los parámetros fisiológicos más sensibles a la infección y estimar los efectos del virus en parámetros de calidad.

Los resultados obtenidos mostraron que la mayor eficiencia en la multiplicación de este virus en relación a otros virus de la vid podría ser uno de los principales motivos de su alta incidencia en los viñedos. El virus afectó a los principales parámetros fisiológicos especialmente la asimilación neta de CO_2 y la cadena de transporte de electrones, que descendieron frente a incrementos en la cantidad de virus. El coeficiente de extinción no fotoquímico junto con la fluorescencia verde, azul y los ratios derivados

se vieron también afectados considerándose buenos parámetros para ser usados como indicadores de la presencia de GLRaV-3, de acuerdo a los resultados obtenidos bajo condiciones controladas. Flavonoles como el miricetina-3-*O*-rutinósido, quercetina-3-*O*-galactosido y quercetina-3-*O*-glucósido; así como ácidos hidroxicinámicos como el ácido cafeico, fueron identificados como posibles responsables del cambio observado en los parámetros obtenidos mediante la fluorescencia multicolour en respuesta a la infección. La detección de la presencia del virus es crucial para mitigar los efectos negativos de la infección en la química básica del fruto. El retraso en la maduración del fruto fue el principal parámetro afectado, por lo que también se vio afectada la fecha de vendimia, dando lugar a la reducción de la concentración de ácidos orgánicos. El tiempo que el virus está presente en la planta podría tener un mayor efecto en la fisiología de la planta que la cantidad de virus en un momento dado.

Por tanto, la presente Tesis ha permitido entender mejor algunos de los motivos de la mayor incidencia del GLRaV-3 frente a otros virus en los viñedos, así como la identificación de parámetros fisiológicos sensibles a la infección que podrían ser utilizados para la detección precoz del virus en grandes áreas de viñedo. Además, se han establecido estrategias para minimizar el efecto en la calidad del mosto y el vino.

RESUM

Els virus sistèmics de tipus floemàtic, com el virus de l'enrotllat 3 (GLRaV-3), produeixen importants pèrdues econòmiques arreu del món. Els símptomes d'aquest virus són clarament visibles en varietats negres, amb l'aparició primerenca d'una coloració vermellosa entre els nervis de les fulles, que romanen verds. Les fulles es solen enrotllar cap avall i es tornen fràgils. En el cas de varietats blanques els símptomes són menys evidents. En cas que els símptomes s'expressin, aquests produeixen esgrogueïment entre els nervis i enrotllament de les fulles. A aquestes varietats, a ser normalment asimptomàtiques, és més difícil identificar la presència del virus al camp. L'absència de símptomes, dificulta el diagnòstic de la infecció i, conseqüentment, l'aplicació de mesures per prevenir la dispersió del virus, com el control biològic del vector i la substitució de les plantes infectades per plantes sanes.

Els objectius de la present Tesi són indagar en les possibles causes de l'alta incidència del GLRaV-3 a les vinyes, identificar els paràmetres fisiològics més sensibles a la infecció i estimar la incidència els efectes del virus sobre paràmetres de qualitat.

Els resultats obtinguts van mostrar que la major eficiència en la multiplicació d'aquest virus en relació a altres virus de la vinya podria ser un dels principals motius de la seva alta incidència a les vinyes. El virus afectà als principals paràmetres fisiològics, especialment l'assimilació neta de CO_2 i la cadena de transport d'electrons. Aquests paràmetres sofriren reduccions en funció de la quantitat de virus present a la planta. El coeficient d'extinció no fotoquímic juntament amb la fluorescència verda, blava i les ràtios derivades també es veren afectats, considerant-los bons paràmetres per ser utilitzats com a indicadors de la presència de GLRaV-3, d'acord amb els resultats obtinguts en condicions controlades. Flavonols com la miricetina-3-*O*-rutinósid, quercetina-3-*O*-galactósid i quercetina-3-*O*-glucòsid; així com àcids hidroxicinàmics com l'àcid cafeic van ser identificats com a possibles responsables del canvi observat en els paràmetres obtinguts mitjançant fluorescència multicolour en resposta a la infecció. La detecció de la presència del virus és crucial per mitigar els efectes negatius de la infecció en la química bàsica del fruit. El retard en la maduració del fruit va ser el principal paràmetre afectat, per tant, també es va veure afectada la data de verema, donant lloc a la reducció de la concentració d'àcids orgànics. El temps que el virus està present a la planta podria tenir un major efecte en la fisiologia de la planta que la quantitat de virus en un moment donat.

Per tant, aquesta Tesi ha permès entendre millor alguns dels motius de la major incidència del GLRaV-3 enfront d'altres virus a les vinyes, així com la identificació de paràmetres fisiològics sensibles a la infecció que podrien ser utilitzats per a la detecció precoç del virus en grans àrees de vinya. A més, s'han establert estratègies per minimitzar l'efecte en la qualitat del most i el vi.

Chapter 1

INTRODUCTION

1.1. GRAPEVINES AND BIOTIC STRESS.

Plant stress has been defined by Lichtenthaler (1996) as 'any unfavourable condition or substance that affects or blocks a plant's metabolism, growth or development'; by Strasser as 'a condition caused by factors that tend to alter an equilibrium'; and by Larcher as 'changes in physiology that occur when species are exposed to extraordinary unfavourable conditions that need not represent a threat to life but will induce an alarm response' (reviewed in Gaspar et al., 2002). Crop productivity worldwide is strongly constrained by stresses, with biotic stresses – i.e. diseases, pests, etc – causing some of the most important economic losses either locally or at larger scales (Boyer, 1982).

Economically, grapevine is the most important fruit species among world crops, with more than 7.4 million hectares planted (OIV, 2012). It is specially important in Spain, where grapevine is cultivated in more than 1.2 million hectares, representing about 1/7 of the world's total vineyard land, and mainly dedicated to wine production. Moreover, with more than 50.000 hectares of table grape, Spain is, after Italy, the second largest European producer with most of Spain's production being dedicated to export to foreign markets (OIV, 2012).

This crop is especially susceptible to biotic stresses. For instance, in the late 19th century, phylloxera devastated European grapevine *Vitis vinifera* L., first in France, then across the continent and eventually to the whole planet (Grannet et al., 2001). As a result of 19th century research, world viticulture was restored using resistant rootstocks to control this pest. The new worldwide pests which are not yet successfully controlled are trunk diseases. Indeed, experts are suggesting that trunk diseases could be an even larger threat than phylloxera (Smart, 2013). On the other hand, Grapevine Leafroll Disease (GLD) is also a large threat because of its worldwide spread and the current absence of cure (Charles et al., 2009; Martelli & Boudon-Padieu, 2006). Thus, GLD produces significant economic losses in many vineyards around the world (Martelli et al., 2012) with an estimated economic impact on *Vitis vinifera* cv. Cabernet franc in Finger Lakes vineyards of New York, ranging from approximately $25.000 (for a 30% yield reduction and no grape quality penalty) to $40.000 (for a 50% yield reduction and a 10% penalty for poor fruit quality) per hectare in the absence of any control measure (Atallah et al., 2012). Walker et al. (2004) examined the economical impact of this

disease on gross margins in New Zealand vineyards. These authors estimated damages of ~US\$ 21.200/ha. Cabaleiro et al. (2013) estimated more than €2000/ha per year of economic looses on Albariño cv. in Rías Baixas vineyards (north-west Spain). Despite the absence of studies quantifying the economical impact of GLD in Mediterranean regions, it is well known that GLD could produce huge damages also in these regions (Martelli et al., 2012).

1.2. GRAPEVINE LEAFROLL DISEASE.

Evidences of the presence of GLD in Mediterranean regions were observed before the introduction of phylloxera from United States (Gale, 2002). Abnormal leaf morphology was described date back to mid 1800s and explained at first as of physiological origin (Martelli & Boudon-Padieu, 2006). Also "reddening" in red cultivar leaves was observed and attributed to physiological disorders (Ravaz & Roos, 1905; Pacottet, 1906). While the most evident apparent symptoms were earlier attributed to internal physiological disorders, later it was demonstrated to be graft-transmissible between grapevines, which provided evidences for its infectious nature (Scheu, 1935).

The presence and severity of the symptoms depend on several factors such as climate conditions or cultivar. For instance, some white cultivars and rootstocks are completely symptomless while, even in susceptible cultivars, symptoms are not permanently visible, appearing only in mid-summer. However, under water stress, the symptoms of GLD appear earlier. The severity and number of symptoms increase in late summer. Initially, symptoms are only visible in basal leaves, and then they progress to the tip (Weber et al., 1993; Martelli & Boudon-Padieu, 2006; Martelli et al., 2012). The first observed leaf symptom is the reddening of interveinal areas while primary and secondary veins remain green in red cultivars. On the other hand, in those red cultivars with deeply pigmented fruit, leaves present uniform red colour without green veins. Interveinal areas of leaves in white cultivars become chlorotic, but this effect is almost unrecognizable in most cases (Figure 1). In late autumn, leaf margins roll downward, but this symptom is not equally expressed in all cultivars. Some cultivars like Chardonnay show pronounced leaf-rolling, while Sauvignon Blanc or Thomson Seedles

do not express this symptom. In fact it is difficult to observe any symptoms in these cultivars, as well as Malvasía de Banyalbufar, a Balearic Islands cultivar.

A   B
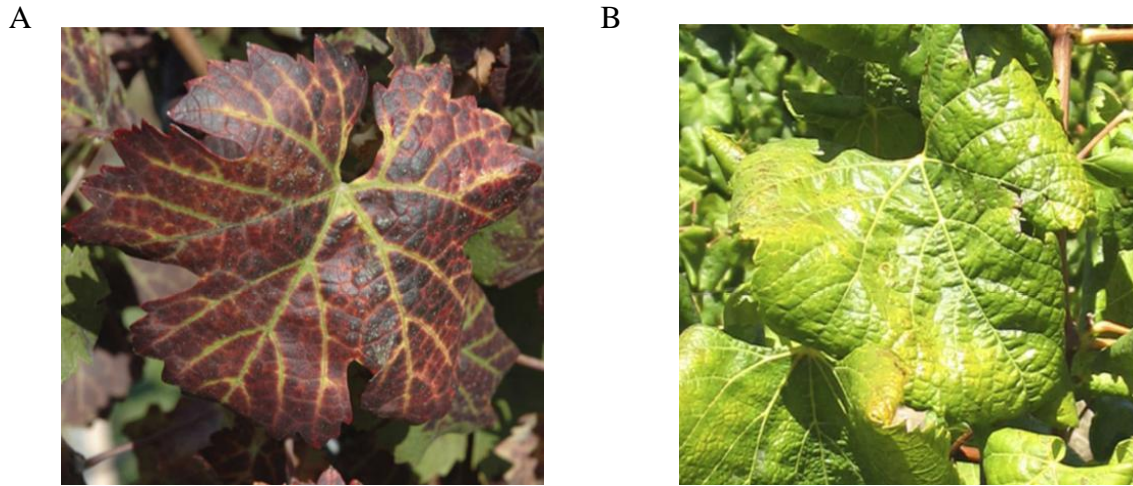
Figure 1. Leafroll disease symptoms in red cultivar *Vitis vinifera* Cabernet Franc cv. (A) and white cultivar *Vitis vinifera* Chardonay cv. (B) (From Maree et al., 2013).

Nowadays, it is well known that GLD is caused by virus infection (Almeida et al., 2013). To date, 11 Grapevine leafroll associated viruses (GLRaVs) have been described: GLRaV-1, -2, -3 -4, -5, -6, -7, -9, -Pr, -De and GLRaCV, all belonging to the *Closteroviridae* family. In particular, the *Grapevine Leafroll associated virus 3* has been identified as the most important, and characterized by higher incidence in vineyards than the other GLD (Martelli et al., 2012).

1.3. GRAPEVINE LEAFROLL ASSOCIATED VIRUS 3.

1.3.1. Morphology and genome of GLRaV-3

Grapevine leafroll associated virus 3 is member of the closteroviridae family. It is included in the genus *Ampelovirus* (Martelli et al., 2012). The particles of this virus are flexible filaments with a non-enveloped virion of approximately 1800x12 nm in size with a pitch of a primary helix of 3,5 nm (Figure 2). The structure of the filaments is helically and contains around 10 protein subunits per turn of the helix (Martelli et al., 2012). The fragility of the virions and the tendency to end-to-end aggregation contributes to the fact that a range of lengths is often given by a single virus.
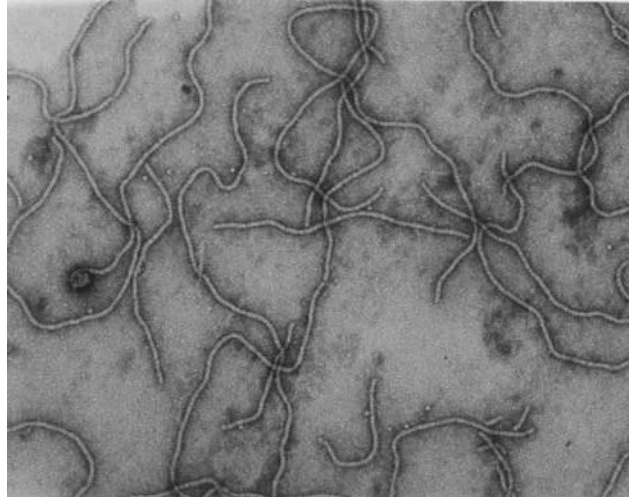
Figure 2. Negatively stained of purified GLRaV-3 particles (From Maree et al., 2013).

The virus has a positive sense single stranded (+ss) RNA genome of 18.500 nucleotides, approximately. Virions contain a single molecule, constituting 5-6% of the particle weight. The first GLRaV-3 complete sequence was established for the insolate GP18 by Maree et al. in 2008. The genome has 18.498 long-nucleotides and a 737 nucloetide-long 5' UTR with a high percentage of uracile (48.5%). This characteristic is not very common in the family *Closteroviridae.* High uracile content and large size are two factors that could explain technical problems with uncompleted sequences determined by other authors (Ling et al., 2004; Engel et al., 2008). Nowadays nine more complete genomes of different GLRaV-3 isolates are available. These isolates represent four major groups of genetic variants. Classification of the different viruses for each group is based on single-strand conformation polymorphism analysis.

The consensus genome organization of the GLRaV-3 isolates from groups I-III includes 13 open reading frames (ORFs) (Figure 3). According to the convention set out by Agranovsky et al. (1994), the ORFs are designated as 1a, 1b, and 2 to 12. *Closteroviridae* belongs to the Alphavirus-like superfamily, which has a conserved "core" that includes capping/methyltransferase, superfamily 1 RNA helicase, and RNA dependent RNA polymerase (*RdRp*) domains (Koonin & Dolja, 1993; Dolja et al., 2006) encoded by GLRaV-3 ORFs1a and1b. GLRaV-3 ORF1a hides an AlkB domain (Maree et al., 2008), which is in charge of reappearing viral RNA and systemic spread (Van den Born et al., 2008). The expression of ORF2 is uncertain. ORF3 codes for a small transmembrane protein, responsible for cell-to-cell movement protein. The major and the minor coat protein (CP and CPm, respectively) are the most abundant protein

components involved in the formation of closterovirid particles. ORF6 encodes most of the CP and is also involved in cell-to-cell movement (Alzhanova et al., 2000). The minor capsid protein (CPm) is actually a main component of the virion tail. Proteins coded by ORF4 (HSP70h), ORF5 (p55), and ORF7 (CPm) of the viral genome, might be instrumental in determining cell-to-cell and systemic transport (Dolja et al., 2006), although this has not been completely demonstrated for GLRaV-3.
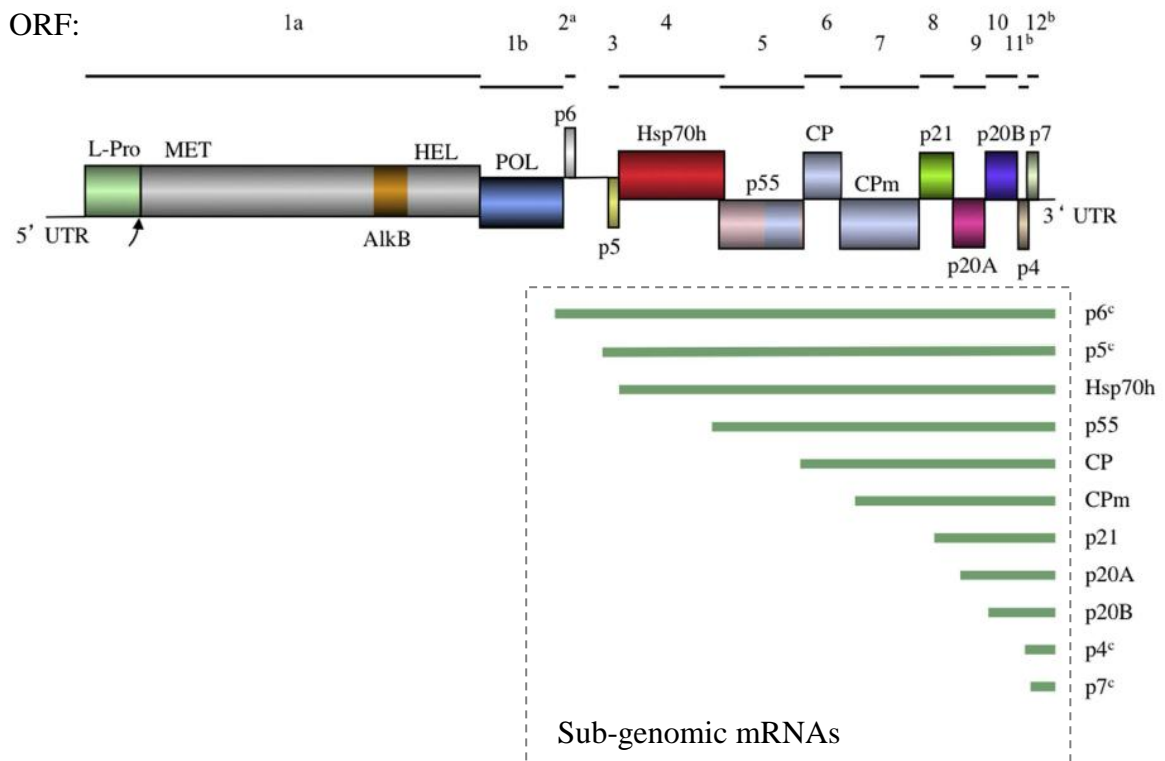
Figure 3. A schematic diagram of the GLRaV-3 genome. ORFs, numbered from 1 to 12 above the diagram, are shown as boxes with associated protein designations. L-Pro, leader proteinase; AlkB, AlkB domain; MET, HEL, and POL, methyltransferase, RNA helicase, and RNA-dependent RNA polymerase domains of the replicase, respectively; p6, a 6-kDa protein; p5, a 5-kDa protein; HSP70 h, a HSP70-homologue; p55, a 55-kDa protein; CP, major capsid protein; CPm, minor capsid protein; and p21, p20A, p20B, p4 and p7 are the 21-, 19.6-, 19.7-, 4- and 7-kDa proteins, respectively. Below the genome map, there is a representation of the 11 putative subgenomic messenger (m)RNAs for the 3' genes. (Modified from Maree et al., 2013).

ORFs 8 to 12 are not conserved outside the genus *Ampelovirus* (Ling et al., 1998), therefore it is difficult to analyse the sequences and to extract possible functions. ORFs 11 and 12 are only present in GLRaV-3. Because of the presence of many variants of GLRaV-3, ORFs change for some isolates, especially ORFs 8 to 12, hence most of their functions are not clearly characterised. Besides, difficulties in virus

isolation complicated their molecular characterisation. Therefore, it is a hard task to identify those functions and it is a big challenge of the future research (Maree et al., 2013).

1.3.2. Genome expression and replication of GLRaV-3

Once the virus enters the host cell, it releases its viral genomic RNA into the cytoplasm. ORFs1a and 1b are responsible of the virus replication encoding the replication-associated proteins with methyltransferase, RNA helicase, and *RdRp* domains. Replication occurs in viral factories. In this case viral factories are vesicles produced in the mitochondria (Kim et al., 1989). In other positive strand RNA viruses, replicase proteins produced by the virus, recruit L-Pro co-localizes with the vesicles network to form viral RNA replication complexes (Den Boon & Ahlquist, 2010). It was hypothesized that GLRaV-3 RNA replication occurs via recognition of promoter elements 3' and 5' UTRs as was demonstrated for *Citrus tristeza virus* (CTV), other member of *Closteroviridae* family (Satyanarayana et al., 2002; Gowda et al., 2003). The GLRaV-3 ORFs localized downstream of ORF1b, use nested set of sgRNAs (small guides RNAs), for the expression process of that region (Jarugula et al., 2010; Maree et al., 2010). Each sgRNA serves as monocistronic messenger for the translation of the corresponding 5'-proximal ORF. Quantitative and temporal regulation of GLRaV-3 sg RNA transcription takes place during the virus infection cycle (Jarugula et al., 2010). The 5'UTRs of the sgRNAs are irregular in size without conserved sequences around the 5'-transcriptional start sites (TSS). It does not seem to be a correlation between the length of 5'UTRs and the accumulation levels of sgRNAs, denoting different behaviour in transcriptional regulation of the genus *Ampelovirus* and the genus *Closterovirus* (Jarugula et al., 2010).

1.3.3. Virus detection

It is very common to find more than one virus infecting a host. Often, these associated diseases have similar symptoms hardening the identification viruses. In addition, other factors like virus amount, irregular distribution of the virus in the plant and the absence of clear symptoms in white cultivars, add more difficulties to the detection.

The detection of the virus is essential to fight against the infection spread, because it is very difficult to eliminate the virus in the field. Hence, detecting the virus on time and making biological control is the best way to stop the spread of the infection. Nowadays several techniques are used to detect virus associated with GLD in plant material. For this aim, biological indexing, serology, nucleic acid-based methods and next-generation sequencing have been developed. Moreover, new techniques have been proposed to identify infected plants rapidly, screening big field areas in few minutes. One of these techniques is the Unmanned Aerial Vehicle (UAV)-Based remote sensing approach with multiespectral and thermal cameras, although this method is under development and yet far for being consider a real method for accurate detection of the virus, because it is based in the detection of the principal parameters affected by the virus, like thermal canopy changes or the Normalized Difference Vegetation Index (NDVI), which can be affected by other factors (García-Ruíz et al 2013).

Biological indexing was until late 1980's the only system for testing GLD. It consists in grafting a small chip bud of the candidate vine to an indicator grapevine cultivar (Rowhani & Golino, 1995). The grafted plant is planted in the field and controlled for at least two seasons, looking after the presence of virus disease symptoms (Weber et al., 2002). There are some cultivars frequently used according to the climate conditions and/or personal preferences. Some of these cultivars are Cabernet Sauvignon, Cabernet Franc, Pinot Noir or Barbera. Another biological indexing method is the green-grafting (Pathirana & McKenzie, 2005). In this case green buds or scions are grafted to green shoots, having advantages compeering with the other system, because it is capable to defeat the graft incompatibility (Walter et al., 2008). However, biological indexing is an inefficient method regarding to the time consumed in the process and the possible incompatibilities mentioned before (Weber et al., 2002). In addition, other factors such as the lower virus amount, the irregular distribution of the virus in the different organs of the plant and the lack of symptoms depending on the different cultivars, determine the results of the indexing (Rowhani et al., 1997).

Enzyme-linked inmunosorbent assay (ELISA), inmuno-strip tests and inmunofluorescence (IF), are some of the different forms of serological diagnostic techniques that have been evolved (Schaad et al., 2003). ELISA has become the preferred method for virus detection as it is possible to analyse large number of samples in a relatively short period of time, even though it is not as sensible as nucleic acid-

based techniques. In addition, it is a simple and cost-effective detection method (Ward et al., 2004). The first antiserum against closterovirus like-particles was produce by Gugerli et al. (1984). Thereafter, many groups have made their own polyclonal antisera or monoclonal antibodies to develop ELISAs for GLRaV-3 detection (Goszczynski et al., 1995; Ling et al., 2000, 2001). However, commercial kits provided by industry are not highly efficiency detecting different GLRaV-3 strains, similarly to other viruses. For instance, in New Zealand it was found that some genetic variants were weakly detectable by commercial kits, therefore it is necessary to introduce some modifications in the protocols to provide accurate results (Cohen et al., 2012).

Recently, nucleic acid-based methods have been widely used in diagnosis assays for pathogen detection. Reverse transcription-PCR (RT-PCR) has been used for detection of pathogens with RNA genomes. Thus, GLRaV-3 can be detected by this method. However as described above, there are many different variants of this virus. Currently, are six genetic variants have been described (Jooste et al., 2010; Gouveia et al., 2011;Wang et al., 2011; Kumar et al., 2012). Therefore, multiplex PCRs were developed for the detection of most of the genetic variant group of GLRaV-3 (Bester et al., 2012; Chooi et al., 2012). Another procedure to detect GLRaV-3 is the immuno-capture PCR (IC-PCR). It is based in antibodies produced against the recombinant major CP. Antibodies immobilize on the surface of a microfuge tube and then it is amplified by RT-PCR (Ward et al., 2004; Engel et al., 2008). In woody plants, it is possible to detect pathogens in a small drop of unbuffered sap from grapevine leaf petiols. The drop is used as the template for PCR after placing it on filter paper. This system is called spot-PCR and has been successfully used for this type of detections (Osman & Rowhani, 2006). The Loop-mediated amplification of nucleic acid (LAMP) is an alternative method to PCR, based on the isothermal amplification of a target sequence. GLRaV-3 has been detected by LAMP but introducing reverse transcriptase (RT-LAMP) (Pietersen & Walsh, 2012).

However some improvements have been incorporated in order to simplify the quantification of target DNA. Using real time-PCR, unknown samples are quantified absolutely or relatively by comparison to a standard DNA or to a reference gene (Feng et al., 2008). There are two types of chemistries used to detect PCR products using Sequence Detection Systems (SDS) instruments, SYBR Green I dye chemistry and TaqMan chemistry. SYBR Green is highly specific double-stranded DNA binding dye,

used to detect PCR product and TaqMan uses a fluorogenic probe to permit the detection of specific PCR product as it accumulates during PCR cycles. The main difference between SYBR Green I and TaqMan dye chemistries is that the first one detects all double-stranded DNA, including non-specific reaction products. Therefore in that case it is necessary melting curve tests to detect the target double-stranded DNA reaction to obtain accurate results (Figure 4).
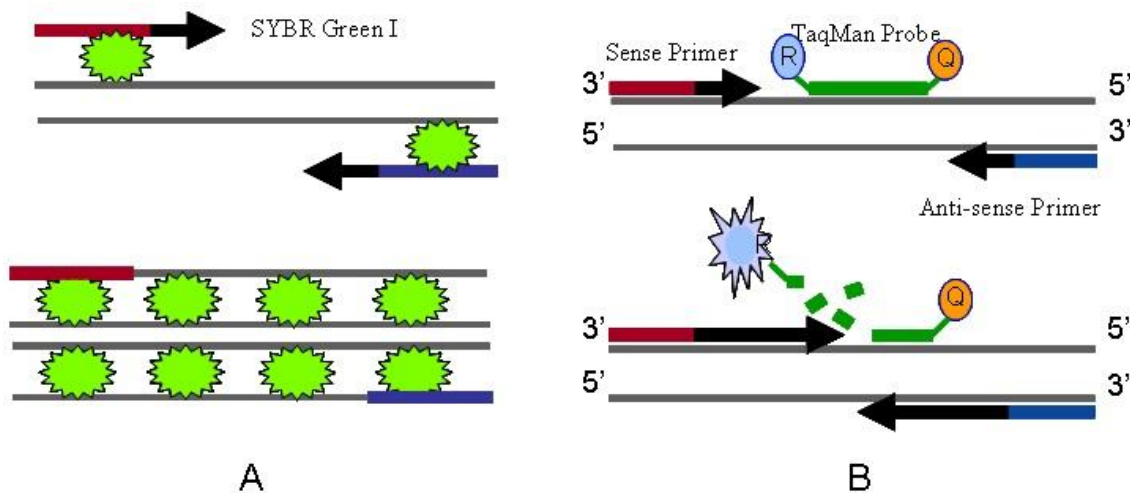
Figure 4. Two methods used to obtain fluorescent signals from the PCR products. (A) SYBR Green I; (B) TaqMan probes (From Xu et al., 2011).

Real-time TaqMan assay was developed by Osman et al. (2007) to detect simultaneously GLRaV-1, 2, 3 and 4 as well as some GLRaV-4 strains. Several modifications were introduced to real-time TaqMan assay, in a new system known as TaqMan low-density arrays. This method employs microtiter plates with dried TaqMan PCR primers/probes complexes added to the wells (Osman et al., 2008). Nowadays, a new technique has helped to identify different genetic variant groups of GLRaV-3. Real-time RT-PCR high-resolution melting (HRM) distinguishes changes in a sequence using DNA binding dye, SYTO 9 (Bester et al., 2012). There are other techniques used for differencing between genetic variants of GLRaV-3, like the single-strand conformation polymorphism (SSCP) profiles and asymmetric PCR-ELISA (APET) (Turturo et al., 2005; Jooste et al., 2010).

In the last years, methods to detect numerous genes or viruses at the same time have been developed. Oligonucleotide microarray analysis has evolved in grapevine,

with a huge amount of probes that allow the identification of 44 plant viral genome of ten grapevine viruses (Engel et al., 2010). Microarrays are a powerful tool for plant certification. Nevertheless, it is still expensive and the interpretation of the results is not straightforward. For that reason applications like macro-arrays methodology have been presented as a real alternative technology to microarrays. The equipment necessary for this methodology has been reduced to a thermocycler and a hybridization oven. In addition, macro-arrays are a good complement for other techniques described before because of its multiplexing component (Thompson et al., 2012).

The techniques described above are frequently used for virus detection, but there are some problems that those systems do not consider, for instance, the possible contribution of other viruses, known or unknown, to the disease etiology. Because of the highly specific RT-PCR protocols, different viral variants can keep being undetectable. This can be solved by metagenomic sequencing, because it sets up the total viral complement of a sample (Adams et al., 2009; Coetzee et al., 2010). Second generation or next generation sequencing (NGS), allows the determination of the sequence of all the genetic material within a sample, without previous knowledge of the organisms, using universal adaptors instead of sequence specific primers (Tucker et al., 2009). However, NGS is not used for GLRaV-3 diagnosis yet. But recently two studies successfully validated this technique to identify a new variant of GLRaV-3 never detected before in South Africa (Coetzee et al., 2010) and to assemble a complete genome sequence of GLRaV-3 (GenBank:JX559645). Nonetheless, this is a very expensive system for routine diagnosis.

1.3.4. Phloem transport of GLRaV-3

For virus survival is essential the virions to be accumulated in high levels in the whole plant. Besides, high virions amount facilitates virus transmission from plant to plant. Plant defense has evolved to fight against the infection, but viruses have strategies to protect themselves as well. This fight between plant and viruses leads to a resistance of the plant to the infection, in the case the virus is not able to defeat plant protection, or to a systemic spread, eventually ending with the host death, if the virus defense bypass the plant protection system (Hipper et al., 2013).

Virus entry into the plant, in many instances, via epidermal and mesophyll cells (Hipper et al., 2013), but filamentous viruses like particles only exist in the phloem parenchyma cells. Once the virions are in the cell the virus genome is translated and replicated in inoculated tissues. After that, viral transport complexes move from cell-to-cell and a new replication takes place in the newly infected cells (Figure 4). To allow this short-distance movement, viral movement proteins produce modifications of plasmodesmata (PD), facilitating the entry into the next cell (Schoelz et al., 2011). Viral transport in phloem tissues includes translocation from the inoculated cell to sieve elements (SE), via vascular parenchyma cells (VP) and companion cells (CC). When the virus is in the SE, it is transferred to distant location with the phloem sap exiting in another SE. To complete cell-to-cell movement and long distance movements, the virus profits plant exiting transport routes, including PD and phloem vasculature (Carrington et al., 1996).

GLRaV-3 is restricted to the phloem of infected hosts (Maree et al., 2013). Phloem transport of plant viruses is very important in the setting-up of a complete infection of a host plant (Hipper et al., 2013). Sap in the phloem is not translocated exclusively upwards or downwards. Translocation in the phloem it is not defined with respect to gravity. Indeed, sap is translocated from areas of supply, called sources, to areas of metabolism or storage, called sinks. Sources include any export organs, typically in mature leaves, while sinks include any non photosynthetic organs of the plant and organs that do not produce enough photosynthetic products to support their own growth or storage needs like roots, developing fruits and immature leaves. Not all sources supply all plant sinks, with certain sources preferentially supplying specific sinks. The importance of various sinks may shift during plant development (Taiz & Zeiger 2006). Therefore, the distribution of the virus in different tissues and organs is very irregular (Rowhani et al., 1997).

Phloem cell composition and structure have a high functional specialization in transporting molecules from source to sink tissues. SE are enucleated cells and they are maintained alive by a close association with CC. SEs are interconnected by wide sieve pores (Van Bel, 2003). A Pore Plasmodesmal Units (PPUs) is a specialized PD made of multiple channels on the CC side, and a single channel in front of the SE (Oparka & Turgeon, 1999). PPUs are more permissive than PD, because of a higher size exclusion limit (SEL). Thus some macromolecules, like proteins and RNAs, are likely to diffuse

better to the SE without specific regulation (Stadler et al., 2005). Otherwise viral particles (icosahedral or filamentous) or ribonucleoprotein (RNP) complexes are too large to freely move through PPUs by passive diffusion. If there are not compatible interaction between border connection of VP, CC and SE, the virus will not be able to traffic through these gates (Figure 5).
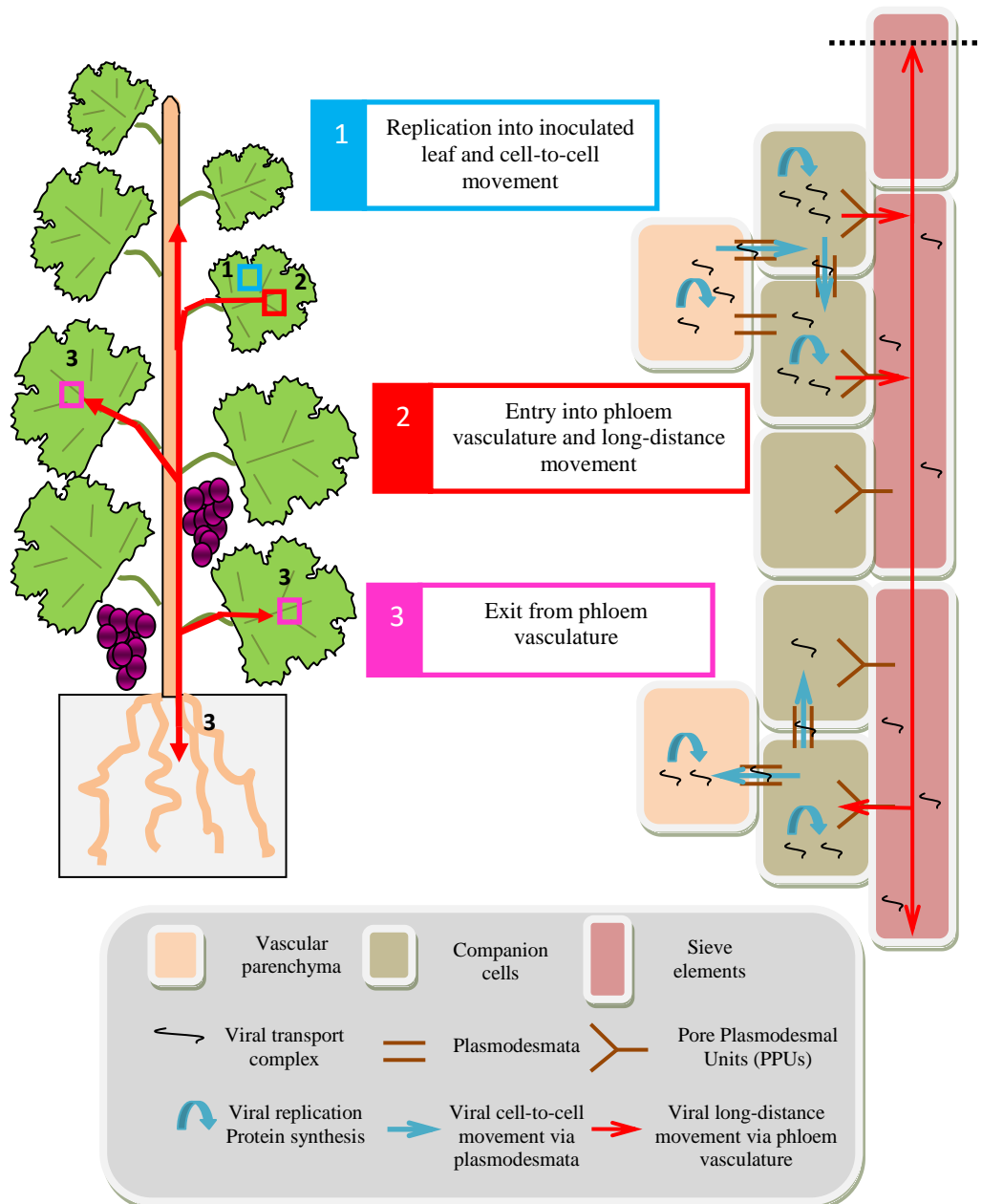
Figure 5. View of virus cell-to-cell and long-distance movement in plant tissues (Modified from Hipper et al., 2013).

Some studies suggest that PD can regulate viral transport in that borders blocking the entry by modifying its permeability (Ueki & Citovsky, 2007 and references therein). Virus entry takes place in all veins classes of source leaves, but virus exits only through major veins of sinks tissues (Oparka & Cruz, 2000; Silva et al., 2002).

Virus expands following both external and internal types of phloem, either downwards transport directed to the roots or upwards to young sink tissues, being the latter faster (Cheng et al., 2000). Roberts et al. (2007) demonstrated the similarities between the relation of symptoms appearance and virus accumulation of *Cauliflower mosaic virus* (CaMV), and the photoasssimilate distribution in sink organs. However, kinetic and spatial analyses of long-distance movement of some virus show that the direction and speed of movement can be different than those of photoassimilates. For example, *Melon necrotic spot virus* (MNSV) is first transported from cotiledons to roots in Melon plants through the external phloem. Then, the virus is transported to the shoot apex through the internal phloem (Gosalvez-Bernal et al., 2008). The reason for the slower rate of progression observed, compared to the speed of photoassimilates, could be due to the additional virus unloading and amplification step in CC before being laid on the SE (Germundsson & Valkonen, 2006). GLRaV-3 spreads quickly from trunks to new growing shoots and leaves early in the growing season. Symptoms and virus amount are higher in basal leaves, but throughout the growing season the symptoms spread to middle and apical leaves (Tsai et al., 2012).

Virus amount and time of infection besides vector activity are the principal parameters affecting the virus infection process, along with factors such as cultivar, rootstock or vine age may contribute. The natural vectors for this virus are mealybugs (Figure 6). However, GLRaV-3 can be transmited by graft and mainly spread by propagation of infected material.
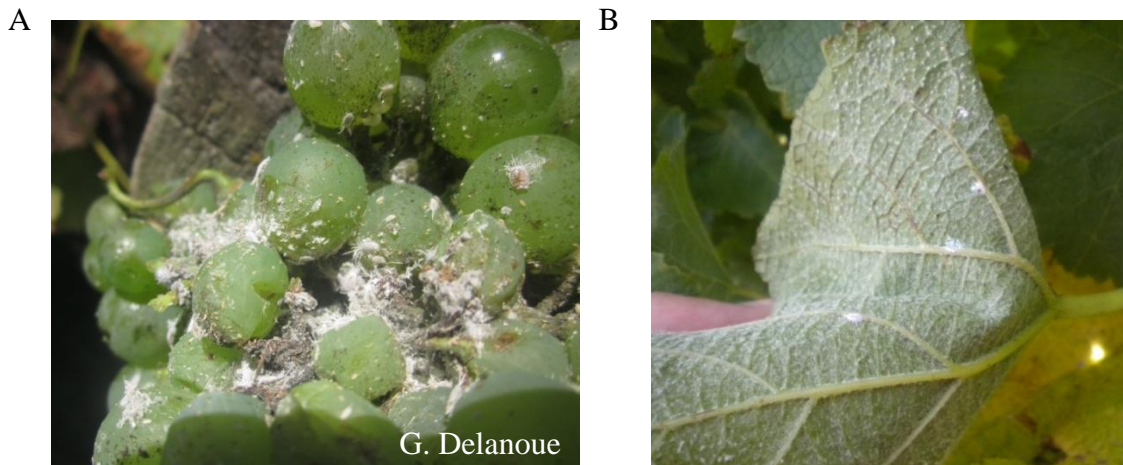
Figure 6. Mealybugs located in grapes (A) and leaves (B).

1. 4. IMPACT OF GLRaV-3 ON PLANT PHYSIOLOGY.

1.4.1. Cytopathology

Presence of GLRaV-3 produces some modifications on the structure of sieve tubes, companion cells and phloem parenchyma cells. One of those modifications are inclusion bodies made up of membranous vesicles 50-100 nm in diameter, produced by the increase of bounding of the mitochondrial membrane (Kim et al., 1989). Vesicles are released in the cytoplasm after the rupture of the mitochondria (Faoro et al., 1992). These vesicles are thought to be sites of replication as described above (Faoro & Carzaniga, 1995). Virus particles contained in the vesicles often fill the lumen of sieve tubes when vesicles lose the bundle and the virus particles group in compact aggregates. Virus clusters can be surrounded by a bounding membrane (Faoro et al., 1992). In an advanced stage of infection, when the plant has fully reddened leaves (anthocyanin deposits), in red cultivars, phloem parenchyma cell necrosis can be observed (Kim et al., 2002).

1.4.2. Limitation of phloem transport.

Primary anatomical effect of the virus is the phloem degeneration in the vascular bundles. Carbohydrate translocation from foliar parenchyma could be interrupted because sieve elements are blocked and ruptured by the effect of the virus. Therefore, starch accumulates in chloroplasts causing increased thickness and brittleness of leaf

blades, and could be the reason of the characteristic symptom of the virus, manifested by downward rolling leaves. Sugar content decreases in sinks due to transport disruption (Hoefert & Gifford, 1967; Von der Brelie & Nienhaus, 1982). Carbohydrate accumulation affects photosynthesis in source leaves by decreasing Rubisco content (Araya et al., 2006).

One of the elements responsible for blocking sieve tubes is callose. In the first stages of the morphogenesis of SE, callose platelets are accumulated around the plasmodesmata. However, these callose deposits are largely dissolved at a later stage (Evert, 1990). But callose deposited is responsible for sealing SEs (Figure 7), because it is determined to be related to sieve plates of injured sieve tubes. Besides, it was suggested that callose is involved in plasmodesmal closure sealing its sieve pores (Botha & Cross, 2000, 2001). Callose formation around PPUs in leaves may inhibit symplastic flow of solutes from companion cells into the sieve tubes, and consequently reduce phloem loading efficiency (Koh et al., 2012). Callose is responsible for long-term plugging of sieve tubes. The amount of callose accumulated determines the obstruction of sieve tubes. High levels of callose constrain transport trough PD (Maule, 2008). Diverse biotic stresses such as viral infection can increase callose synthesis in PD (Rinne & Schoot, 2003; Roberts & Oparka, 2003). The deposition of callose is a critical defense response of host plants against viral infection. This is a strategy of the plant to restrict virus movement between cells and this process takes place before its hypersensitive reaction (Li et al., 2012).
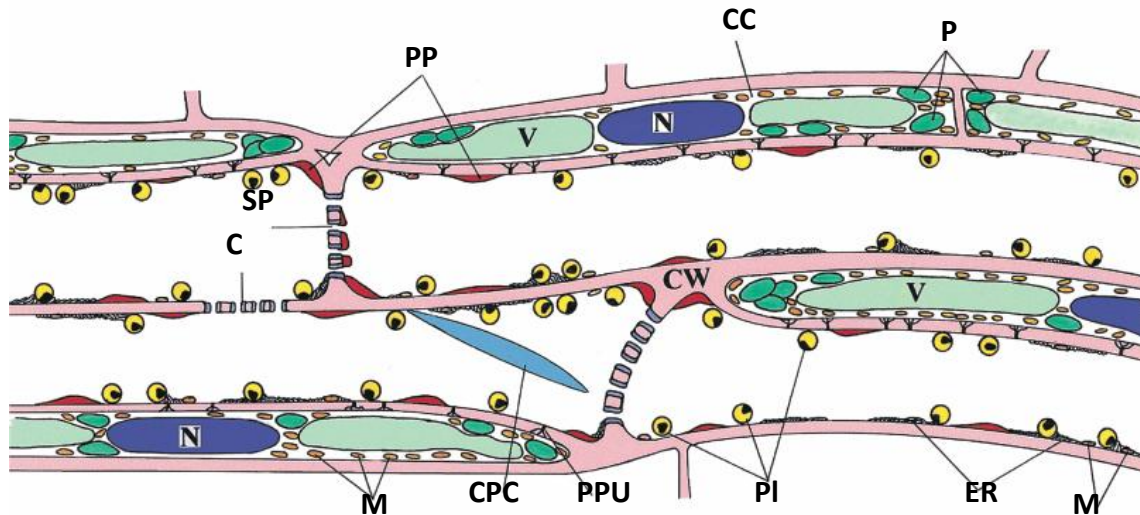
Figure 7. *In vivo* structure of sieve elements (SEs) with companion cells (CCs) in *Vicia faba*. Pore/plasmodesma units (PPUs) connect SEs and CCs. Sieve element plastids (Pl), mitochondria (M), and endoplasmic reticulum stacks (ER) are equally distributed along SE plasma membrane, whereas parietal proteins (PP) are locally accumulated. PPs and ER are sometimes located on the sieve plates (SPs) or at the margins of the sieve pores, but do not impede mass flow. A crystalline protein cluster (CPC) located close to the sieve plates (SPs) is a peculiarity of the *Fabaceae*. C, callose; CW, cell wall; N, nucleus; P, plastids; V, vacuole. (Modified from Van Bel, 2003).

1.4.3. Photosynthesis and respiration

Some of the effects of GLRaV-3 are associated with grapevine physiological disturbances, mainly associated to photosynthesis. For instance, Hristov & Abrasheva (2001) reported low levels of chlorophyll and carotenoid pigments in GLRaV-3 infected leaves of Cabernet Sauvignon vines compared to non-infected ones. In another study carried out with GFLV and GLRaV-1, -2 and -3 infected plants of Malvasía de Banyalbufar cv., Sampol et al. (2003) observed substantial declines in net assimilation rate. This decrease was attributed to a diminution in mesophyll conductance to CO_2 (g_m) and impaired Rubisco activity. More recently, Moutinho-Pereira et al. (2012) measured also photosynthetic capacity depression in GLRaV-3 infected Touriga Nacional plants cultivar associated with effects on carotenoids and chlorophyll contents, stomatal conductance and primary light reactions decrease. The virus produce loss of functionality in the chloroplast. Maximum quantum efficiency of photosystem II (F_V/F_M), photochemical efficiency of photosystem II (Φ_{PSII}) and non-photochemical quenching (NPQ) were affected by the virus, showing photoinhibition of photosystem II (PSII) and an increase in the capacity for energy dissipation.

Most of the studies, such as those cited above and others, have described the effects of virus infection on photosynthesis, however, the information about its effects on respiration have not been deeply tackled. Plant respiration consumes a great portion of the carbon assimilated by photosynthesis during the day. Therefore, this process affects carbon balance and growth, especially under stress conditions (Flexas et al., 2006). When pathogen infection takes place, the synthesis of defense compounds such as salicylic acid (SA), lignin and phytoalexin may account for a respiratory energy and carbon cost to the infected plant (Hanqing et al., 2010). Indeed, mitochondria are thought to play an important role in stress signaling under pathogen attack but less is known about mitochondrial metabolism and its control. Plant mitochondrial respiration includes different alternative pathways that allow metabolic flexibility under environmental perturbations (van Dongen et al., 2010), including pathogen infections (Hanqing et al., 2010). Notably, it is widely accepted that the two respiratory pathways, the alternative oxidase (AOX) and the cytochrome oxidase (COX) pathway, compete for the electrons of the ubiquinone pool and that the only available technique to determine their *in vivo* activities is the oxygen isotope fractionation technique (Ribas-Carbo et al., 2005). It is important to note that, the *in vivo* respiratory activities of the COX and AOX pathways are frequently not correlated with changes on the mRNA or protein levels of AOX, partly due to the tight post-translational control of the AOX protein (Florez-Sarasa et al., 2007). From this perspective, the only study dealing with the effect virus infection on leaf mitochondrial respiration essentially reported no changes of the in vivo activities of COX/AOX pathways after short-term *Tobacco mosaic virus* (TMV) infection in tobacco leaves, despite increases observed on the AOX protein level (Lennon et al., 1997). The study of virus-induced changes on plant respiration and partitioning of electrons between COX and AOX pathways can help to understand the energy efficiency on the utilization of plant carbon resources that affect grapevine growth and fruit productivity.

1.4.4. Quality parameters

Besides the reductions in net leaf photosynthesis and respiration, the virus affects content of soluble solids and vine productivity (Basso et al., 2010; Endeshaw et al., 2014; Lee et al., 2009; Mannini et al., 2012). GLRaV-3 infections alter berry sugars and organic acids that are responsible for final alcohol concentration and the taste of the wine (Bertamini et al., 2004; Cabaleiro et al., 1999; Lee & Martin, 2009). The virus also

affects the non protein nitrogen-containing compounds found in grapes, the most important nutrients needed to carry out a successful fermentation. However, the concentrations of primary and secondary metabolites in juice at harvest depends not only on vine virus status, but factors such as cultivar, vine nutrition, grape maturity and growing season (Bell et al., 2005). Certain compounds determine the fermentation rate and completion of fermentation, especially ammonia and some free amino acids. These are known as yeast assimilable nitrogen (YAN). Low YAN can produce wrong fermentation which finishes before the intended point of dryness. Such fermentation problems potentially lead to the production of undesirable off-odours in the resulting wine (Taillandier et al., 2007).

1.4.5. Secondary metabolites

There are many potential enemies (biotic) and several abiotic environmental stress in natural systems (Mazid et al., 2011). Plants have evolved specific recognition and signaling systems capable to detect pathogen invasion and initiate a potent defense response (Schaller et al., 1996). Plants produce many different natural products or secondary metabolites mainly focused in the protection against pathogens, but also against abiotic stress such as UV-B exposure, as well as for the communication between plants and other organism (Schafer et al., 2009).

Plants produce organic compounds (amino acids, nucleotides, sugars, acyl lipids), known as secondary metabolites, which, contrarily to primary metabolites, are not involved in growth and developed functions (Rosenthal et al., 1991). These substances cannot be found in the entire plant kingdom, like primary metabolites (Taiz & Zeiger, 2006). Secondary metabolites can be divided in three major chemical groups: terpenes, phenolics and nitrogen-containing compounds (Figure 8).

Terpenes establish the largest category of secondary metabolites. They have in common the biosynthetic origin from acetyl-coA or glycolytic intermediates (Gerhenzon & Croteau, 1991). There are two pathways for terpene biosynthesis; the mevalonic acid pathway and the methylerythritol phosphate (MEP) pathway (Figure 8). Most terpenes are thought to be implicated in defense as toxins and feeding dissuasion to most plant feeding insects and mammals (Gershenzon & Croteau, 1991). There are

five subclasses of terpenes: monoterpenes (C_{10}), sesquiterpenes (C_{15}), diterpenes (C_{20}), triterpenes (C_{30}) and polyterpenes ($(C_5)_n$).
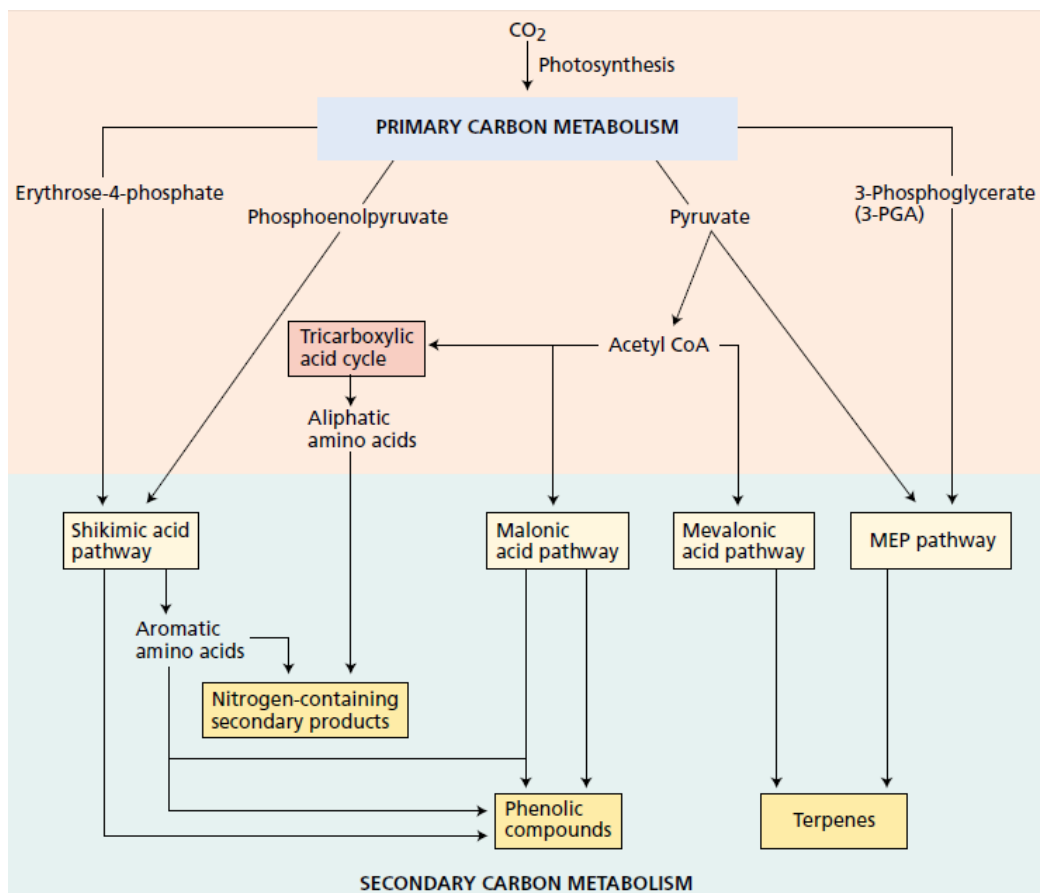
Figure 8. General view of the pathways involved in the biosynthesis of secondary metabolites and their interrelationships with primary metabolism (From Taiz & Zeiger, 2006).

There are many secondary metabolites produced by plants containing a phenol group. Phenol is a hydroxyl functional group on an aromatic ring. Plant phenolics are chemically very heterogeneous. However, shikimic acid pathway participates in the biosynthesis of most plant phenolics (Figure 8). They are very important in plant defense against diseases and pests. Thus, phenolic compounds have other functions such as reducing growth of nearby competing plants, absorbing harmful ultraviolet radiation, attracting pollinators, fruit dispersers or mechanical support (Taiz & Zeiger, 2006).

Most types of the secondary phenolic compounds in plants are derived from phenylalanine by elimination of an ammonia molecule to form cinnamic acid, which is the precursor of lignins, coumaris and flavonoids (Parker et al., 2009). The reaction is

catalyzed by phenylalanine ammonia lyase (PAL) which is located in the branch point between primary and secondary metabolism.

Some simple phenolics are activated by ultraviolet light (Lichtenthaler & Schweiger, 1998). They are widely spread in vascular plants. The structures of these compounds include the following:

- Simple phenylpropanoids, for instance trans-cinnamic acid, p-coumaric acid, and their derivates, such as caffeic acid. They have a basic phenylpropanoid carbon skeleton.
- Phenylpropanoid lactones called coumarins, with a phenylpropanoid skeleton as well.
- Benzoic acid derivates, formed from phenylpropanoids by cleavage of a two-carbon fragment from the side chain.

Phenolic compounds have an important functions in plant defense (Dixon et al., 2002). Certain coumarins have a high phototoxicity. They are known as furanocoumarins. These compounds are toxic only after being activated by light, specifically violet A (UV-A) region from sunlight (320-400 nm). Once they are active, the furanocoumarins can insert themselves into the double helix of DNA and bind to the pyramidine bases and thus blocking transcription and DNA repair, eventually leading to cell death (Rice, 1984).

Lignin is a highly complex phenolic macromolecule and a branched polymer of phenylpropanoid groups. They are formed from coniferyl, coumaryl and sinapyl, alcohols synthesized from phenylalanine via. Lignification blocks pathogens growth in response to infections or injures (Gould, 1983). Lignin is located in the cell walls of diverse kinds of supporting and conducting tissues, otherwise it is mainly found in the tracheids and vessel elements of the xylem (Lewis & Yamamoto, 1990).

There are four major groups of flavonoids, on the basis of the level of oxidation of the three-carbon bridge, which is the connection between the two aromatic rings of the carbon skeleton: the anthocyanins, the flavones, the flavonols and the isoflavones (Gutha et al., 2010).

Anthocyanins are colored flavonoids that attract animals. Animals ingest nectar or fruit pulp, but they help the plant to spread seeds and pollen (Tanaka et al., 2008). Secondary metabolites attract animals to flowers and fruits by visual and olfactory signals. Color pigments in these organs can be produced by carotenoids and flavonoids. The first one is a terpenoid that could be yellow, orange or red. Flavonoids are phenolic compounds that produce an ample range of colors (Tanaka et al., 2008). However, anthocyanins are responsible for most pink, red, purple and blue colors of plants.

Flavonoids may protect against damage by ultraviolet light (Stapleton and Walbot, 1994). Flavones and flavonols are two large groups of flavonoids. Both of them absorb light at shorter wavelengths than anthocyanins. Otherwise, some insects capable to see into the ultraviolet range, and are able to respond to flavonols and flavonoids as attracted signals.

Isoflavonoids have antimicrobial activity. In the last years, isoflavonoids have become best known for their function as phytoalexins (Durango et al., 2002).

Tannins dissuade feeding by herbivores. They are members of a second category of plant phenolic polymers with defensive functions, besides lignins. There are two categories of tannins: condensed and hydrolysable. Hydrolysable tannins are smaller than condensed tannins (Bhat et al., 1998).

Many secondary metabolites present nitrogen in their structure. The principal function of nitrogen-containing compounds is antiherbivore defense such as alkaloids and cyanogenic glycosides. Alkaloids have dramatic physiological effects on animals and cyanogenic glycosides release the poisonous hydrogen cyanide (Taiz & Zeiger, 2006).

1.5. PLANT DEFENSE AGAINST PATHOGENS

Plants have developed resistance systems to fight against pathogens. Before pathogen attacks, some antimicrobial compounds are synthesized by the plant. There are many secondary metabolites mentioned above with strong antimicrobial activity. Saponins are one of these compounds. Saponins are a group of triterpenes suggested as

responsible for the rupture of fungal membranes by binding to sterols (Papadopoulou et al., 1999).

Once a pathogen infects the host, the plant activates many defenses. Among the first ones, the hypersensitive response (HR), in which cells rapidly enclose the infection site, cutting the nutrient supply and stopping the spread. Before HR initiation, the plant often produces reactive oxygen species (ROS). Neighboring cells to the infection site, synthesize toxic compounds, produced by the reduction of molecular oxygen, like the superoxide anion, hydrogen peroxide and the hydroxyl radical. The last one is the strongest oxidant of these active oxygen species and can produce lipid peroxidation, followed by enzyme inactivation and nucleic acid degradation (Lamb & Dixon, 1997). Active oxygen species may participate to cell death as final consequence of the HR or act to kill the pathogen directly.

Some plants are able to recognize specific substances liberated by the pathogens. It is very important to know how plants feel the presence of pathogens and the way to initiate the defense. The speed and the intensity of a plant´s reaction determine the resistance or susceptibility of the plant to the pathogens. Several plant resistance genes have already been isolated (Collins et al., 1998). These genes are known as R genes, and they participate on the defense against the infection. R genes can encode protein receptors that identify and tie specific molecules released from pathogens. These molecules are known as elicitors, and they include proteins, peptides, sterols, and polysaccharides fragments of the pathogen cell wall, outer membrane or a secretion process (Boller, 1995). Elicitors warn the plant of the presence of the pathogen.

R gene products are proteins with a leucine-rich domain irregularly repeated numerous times in the amino acid sequence. These domains are likely to be implicated in pathogen recognition and elicitors binding. Moreover, R gene products initiate signaling pathways and thereby activate several antipathogen defenses. Some of these R genes codify a nucleotide binding-site that binds GTP or ATP. Other R genes encode a protein kinase domain (Young, 2000). There is not a specific location for R gene products. They are allocated in many cell sites, for instance outside the plasma membrane or in the cytoplasma to detect pathogen molecules released there or metabolic changes produced by the pathogen.

It was demonstrated that plant species are usually susceptible to the attack of specific pathogen strains and resistant to others. The interaction between the products of host R genes and pathogen avirulence genes is thought to determine the susceptibility of the plant to certain pathogens strains by encoding specific elicitors. Therefore successful resistance requires specific elicitors as a product of pathogen avirulence genes.

An important defense against infections is the RNA silencing. RNA silencing, represents a natural defense system for plant cells against viruses and is activated by the structured RNAs or the double strain RNAs produced during the replication cycles of different classes of viruses and subviral pathogens (Ding & Voinnet, 2007).

Previous pathogen infections may increase resistance to future attacks if plant survives to pathogen inclusions. This event is known as systemic acquired resistance (SAR) and it is developed after a few days since the infection (Ryals et al., 1996). Presence of SAR depends on the increase of the certain defense compounds mentioned before, like chitinases and other hydrolytic enzymes.

Salicylic acid is thought to be the principal endogenous signal for SAR induction. Besides salicylic acid, other compounds related to this benzoic acid derivative, can act as volatile SAR inducing signal transmitted to extreme parts of the plant and even to nearby plants (Shulaev et al., 1997).

1.6. GLRaV-3 MANAGEMENT

There is not cure for vines infected by this virus. Moreover, no natural immunity to GLRaV-3 has been found in *Vitis* species. The best way to maintain vineyard health is by biological control of the vector with pesticide sprays and to replace infected plants (Golino et al., 2002, 2008; Charles et al., 2006; Pietersen et al., 2009). However, GLRaV-3 can be detected in remaining roots, when vines are removed, potentially acting as long-term reservoirs of the virus (Bell et al., 2009).

Certification programs have been established to distribute plant sanitised material. The objective of these programs is to keep clean stocks, testing plant material for different virus, including some GLD. These clean stocks are obtained using

chemotherapy with *in-vitro* grown explants (Panattoni et al., 2007), somatic embryogenesis (Gambino et al., 2006), heat therapy and meristem tip culture (Savino et al., 1991).

Genetic engineering of disease resistance has become a new tool in disease management. Several transgenic grapevines resistant to grapevine viruses like *Grapevine fanleaf virus* (GFLV) (Gambino et al., 2010; Krastanova et al., 1995; Maghuly et al., 2006), GLRaV-2 or GLRaV-3 (Freeborough, 2003; Orecchia et al., 2008; Xue et al., 1999) has been successfully tested. Nevertheless, these transgenic organisms are far away from being a real solution because of ethical, commercial and environmental factors.

Therefore the difficulty of managing this virus requires new strategies to fight against the infection. Key factors to face the mitigation of virus effects is the study of plant physiology parameters affected by the infection, particularly primary metabolism (yield) and secondary metabolism (quality).

In summary, biotic stresses severely limit crop yields worldwide, resulting in important economic losses and GLRaV-3 is an important biotic stress affecting grapevines. Despite sufficient characterization of the virus inducing this disease, at presently it is poorly controlled by managing, and techniques for early detection are still in their infancy. The virus is still decreasing yields and yield qualities in grapes, particularly in the Mediterranean area, given its effect on plant primary and secondary metabolisms. These effects are exacerbated when interacting with other stresses. In consequence, it is necessary to determine GLRaV-3 effects on plant physiology in order to find new strategies to fight against the infection.

Chapter 2

OBJECTIVES

The study of plant physiological parameters affected by the infection is the key factor to face the mitigation of virus effects. The general objective of the present work was to provide new insights into the high GLRaV-3 incidence in vineyards and to determinine its influence on grapevine physiology and fruit quality parameters.

This general aim is divided in five specific objectives:

1. To investigate differences in the multiplication capacity of three ampeloviruses in order to understand the differences in their relative incidences in vineyards.

2. To explore GLRaV-3 effects on several plant physiological and morphological parameters, identifying those most affected by the infection and possible correlations with virus amount.

3. To determine whether changes in thermal and fluorescence patterns correlate with virus effects on primary and secondary metabolism.

4. To determine GLRaV-3 effects on the different components of carbon balance and biomass distribution identifying the most sensitive organs affected by the infection.

5. To study the effects of GLRaV-3 amount and the duration of the infection on fruit composition, juice and wine chemical profile.

Chapter 3

DIFFERENCES OF THREE AMPELOVIRUSES MULTIPLICATION IN PLANT MAY EXPLAIN THEIR INCIDENCES IN VINEYARDS.

DIFFERENCES OF THREE AMPELOVIRUSES MULTIPLICATION IN PLANT MAY EXPLAIN THEIR INCIDENCES IN VINEYARDS.

Leonardo Velasco[1*], Josefina Bota[2], Rafael Montero[2], Enrico Cretazzo[1]

[1]Instituto Andaluz de Investigación y Formación Agraria, Pesquera, Alimentaria y de la Producción Ecológica (IFAPA), 29140 Churriana, Málaga, Spain.

[2]Institut de Recerca i Formació Agrària i Pesquera de les Illes Balears (IRFAP), 07009 Palma de Mallorca, Spain.

*Corresponding author: leonardo.velasco@juntadeandalucia.es

ABSTRACT

Grapevine leafroll ampeloviruses have been recently grouped into two major clades, one for *Grapevine leafroll associated virus* (GLRaV) *1* and *3* and another one grouping *Grapevine leafroll associated virus 4* and its variants. In order to understand biological factors mediating differential ampelovirus incidences in vineyards, quantitative real time PCRs were performed to assess virus populations in three grapevine cultivars in which different infection status were detected: GLRaV-3 + GLRaV-4, GLRaV-3 + GLRaV-4 strain 5 and GLRaV-4 alone. Specific primers based on the RNA-dependent RNA polymerase (*RdRp*) domains of GLRaV-3, GLRaV-4 and GLRaV-4 strain 5 were used. Absolute and relative quantitations of the three viruses were achieved by normalization of data to the concentration of the endogenous gene actin. In spring, the populations of GLRaV-4 and GLRaV-4 strain 5 ranged from 1.7×10^4 to 5.0×10^5 genomic RNA copies per mg of petiole tissue, while for GLRaV-3 values were significantly higher, ranging from 5.6×10^5 and 1.0×10^7 copies·mg^{-1}. In autumn, GLRaV-4 and GLRaV-4 strain 5 populations increased significantly, displaying values between 4.1×10^5 and 6.3×10^6 mg^{-1} genome copies, while GLRaV-3 populations displayed a less pronounced boost but were still significantly higher, ranging from 4.1×10^6 to 1.6×10^7 copies·mg^{-1}. To investigate whether additional viruses may interfere in the quantifications the small RNA populations, vines were analysed by Ion Torrent high throughput sequencing. It allowed the identification of additional viruses and viroids including *Grapevine virus A* (GVA), *Hop stunt viroid* (HSVd), *Grapevine yellow speckle viroid 1* (GYSVd-1) and *Australian grapevine viroid* (AGVd). The significance of these findings is discussed.

Keywords: grapevine leafroll disease, ampelovirus, real time PCR quantitation.

INTRODUCTION

Grapevine leafroll disease (GLD) is one of the most distributed viral diseases for the grapevine (*Vitis vinifera* L.) (Almeida et al., 2013; Maree et al., 2013; Walter & Martelli, 1996). Along with Grapevine fanleaf degeneration disease, it induces the major economic losses by virus infections in viticulture (reviewed recently in ref. Maree et al., 2013). To date, 11 Grapevine leafroll associated viruses (GLRaVs) have been described: GLRaV-1, -2, -3 -4, -5, -6, -7, -9, -Pr, -De and GLRaCV, all belonging to the

Closteroviridae family. Of these viruses, GLRaV-2 is the only member of the *Closterovirus* genus; a tentative genus called *Velavirus* has been created to classify GLRaV-7, while the rest of GLRaVs belong to the *Ampelovirus* genus (Martelli & Boudon-Padieu, 2006). Among ampeloviruses, GLRaV-1 and GLRaV-3 are apparently the most common in vineyards and, together with GLRaV-2 (Bertazzon et al., 2010), the main responsible for GLD damages. These are also much more extensively studied from any point of view. The others ampeloviruses, GLRaV-4, -5, -6, -9, -Pr, -De and GLRaCV, belong to a common phylogenetic clade (Subgroup II) in the *Ampelovirus* genera and may be classified as divergent variants of one virus, GLRaV-4, instead of distinct species, according to recent taxonomical classification (Martelli et al., 2012). So far, there is not yet any specific study about the effects of GLRaV-4 like ampeloviruses on vine performance whilst only a few reports showed their transmission by some vectors in a non-specific way (reviewed in Almeida et al., 2013 and Maree et al., 2013).

The Commission Directive 2005/43/EC considers only GLRaV-1 and -3 among GLRaVs as harmful organisms in nursery stocks. However, the development of PCR diagnostics tests has allowed detecting more consistently the GLRaV-4 like ampeloviruses all around the world (Buzkan et al., 2009; Escobar et al., 2008; Esteves et al., 2012; Ito et al., 2013; Pei et al 2010). Particularly, GLRaV-4, -5, -6 and -9 have been recently identified in Spain (Padilla et al., 2010a; Padilla et al., 2010b; Padilla et al., 2013). Therefore, the genomic characterization of these viruses has accomplished an increased interest (Esteves et al., 2012; Ghanem-Sabanadzovic et al., 2012; Saldarelli et al., 2006; Thompson et al., 2012). In addition, real time quantitative PCR (qPCR) has been successfully used for detection and quantitation of GLRaVs (Osman et al., 2007; Pacifico et al., 2011; Tsai et al., 2012). In this study, absolute and relative quantitations of GLRaV-3, GLRaV-4 and GLRaV-5 (henceforth GLRaV-4 strain 5) have been achieved starting from leaf petioles extracts of vines displaying three different infection status (GLRaV-3+GLRaV-4, GLRaV-3+GLRaV-4 strain 5 and GLRaV-4 alone). Differences in concentration between GLRaVs were analysed in order to understand the differences in their relative incidences in vineyards.

MATERIAL AND METHODS

Plant material

Vines belong to three traditional Spanish cultivars: Rome and Tintilla de Rota from the Autonomous Community of Andalusia, and Gorgollassa from the Balearic Islands. For Rome and Tintilla de Rota, dormant cuttings from the grapevine germoplasm collection at the IFAPA center of Rancho de la Merced (Jerez de la Frontera, Spain) were rooted and kept in pots and transferred to an insect proof temperature-controlled greenhouse at the IFAPA center in Churriana (Malaga) in 2010. For each cultivar, 12 plants each were analysed. All of them were double infected by GLRaV-3 and GLRaV-4 strain 5. For Gorgollassa, samples came from 10 clonal replicates of 2 vines, 5 each, infected by GLRaV-4 alone and by both GLRaV-3 and GLRaV-4, respectively. They were collected directly from the Balearic Islands grapevine germoplasm collection at the IRFAP (Palma de Mallorca). Preliminary serological and/or molecular assays to check for *Grapevine fanleaf virus* (GFLV), viruses linked to *Rugose Wood* (RW) complex and GLRaVs, showed only infections by GLRaV-3, -4 and -4 strain 5. All plants exhibited only leafroll symptoms.

Ion Torrent sequencing for other viruses and viroids identification.

Small RNAs were isolated from petiole tissues collected in June, 2013 and stored in RNAlater[TM] (Ambion, Austin, TX). Samples corresponded to one individual plant from each of the cultivars studied in this work. sRNA enriched samples were obtained using the miRCURYTM RNA isolation kit (Exiqon, Woburn, MA) and quantified. The quality and profile of the sRNAs was examined with a Bioanalyzer 2100 using the RNA 6000 Nanokit (Agilent, Waldbronn, Germany). The sRNAs from the four samples were pooled in the same amount (1 ng each) for subsequent NGS sequencing. A library was constructed using the Ion AmpliSeqTM RNA Library Kit (Life Technologies, Paisley, United Kingdom) and sequenced as single reads with an Ion Torrent PGM 318 platform using the services provided by LifeSequencing (Valencia, Spain). Sequencing adapters were trimmed off and reads shorter than 20 nt, as well as low quality ones, were discarded from the sequence datasets using the CLC Genomics Workbench (CLC Bio, Aarhus, Denmark). The remaining short reads were assembled into contigs larger than 50 nt using the de novo assembly function of the CLC Genomics software. The CLC contigs were subjected to BLASTx and Blastn analysis against the non-redundant database of the NCBI using the CLC Genomics

software (http://www.ncbi.nlm.nih.gov). The E-value cut-off was set to 1.0 x 10^{-5} so that high confidence matches could be reported. Organism taxonomy was retrieved by the CLC software from NCBI. Multiple hits were counted for each organism matched per query.

Isolation of total RNA and cDNA synthesis.

Extraction of total RNA was performed in late April 2012 and October 2012 from 100 mg of medium leaf petioles using the Spectrum Plant RNA kit (Sigma, St. Louis, MO). Previous disruption and homogenization of samples were carried out by a TissueLyser (Qiagen, Valencia, CA). A NanoDrop ND-1000 spectrophotometer (NanoDrop Technologies, Wilmington, DE) was used to determine the RNA concentrations in order to prepare the opportune dilutions for subsequent reverse transcriptions (RT). The synthesis of cDNA by RT was performed in a 20 μl reaction with 200 ng of RNA, random nonamers (Takara Bio, Shiga, Japan) and *Moloney Murine Leukemia Virus* (Mu-MLV) Reverse Transcriptase, following the manufacturer's instructions (Eurogentec, Liege, Belgium).

Primer design for real-time RT-PCR.

For all three viruses (GLRaV-3, -4 and -4 strain 5), a genome sequence within the RNA dependent RNA polymerase (*RdRp*) domain was amplified by conventional PCR. For GLRaV-3 primers P3U-2 and P3D (Tsai et al., 2010) were used (Table 1). For GLRaV-4 and GLRaV-4 strain 5, primers (LR4-RP_F3, LR4-RP_R1, LR5-RP_F2 and LR5-RP_R3, Table1) were designed using FastPCR software (Kalendar et al., 2011) based on GeneBank accessions NC016416 and FR822696, respectively. All amplicons were cloned in vector pJET2.1 (Fermentas, Waltham, MA) and sequenced.

For the absolute quantitation, other sets of primers were designed for GLRaV-4 and -4 strain 5 within the *RdRp* domain (LR4-RP_F2, LR4-RP_R2, GLR5-RP_F1 and LR5-RP_R1, Table 1), based on the amplicons obtained by conventional PCR (984 and 916 bp, respectively, Table 1), using Primer3 on-line software tool (Rozen & Skaletsky, 2000). Primers LR3qrtF and LR3qrtR (Valkonen, 1992) were used for GLRaV-3 quantitation. In addition, the grapevine endogenous gene actin was amplified in parallel reactions using a specific primer pair (Gutha et al., 2010), in order to provide a control for normalization.

Table 1. Primers used in this work (see main text for description).

Primer	Sequence (5'-3')	Position in GenBak accession	Reference
ActinF	CTTGCATCCCTCAGCACCTT	GU585869 (1)	Gutha et al., 2010
ActinR	TCCTGTGGACAATGGATGGA	GU585869 (62)	Gutha et al., 2010
LR3qrtF	CTTCTACCACGGGATGGACACT	NC004667 (7585)	Tsai et al., 2012
LR3qrtR	GGTGTAGTATTGCCGGATGT	NC004667 (7680)	Tsai et al., 2012
P3U-2	GCTCATGGTGAAAGCAGAC	NC004667 (7425)	Turturo et al., 2005
P3D	TAGAACAAAAATATGGAGCAG	NC004667 (8057)	Turturo et al., 2005
LR4-RP_F2	GGCAGTGGAATTGGAAGTGT	NC016416 (8119)	This work
LR4-RP_F3	CTTTAGGGAGTGCTGGGTCA	NC016416 (7287)	This work
LR4-RP_R1	GTATTGGCTGCACCTGTCCT	NC016416 (8271)	This work
LR4-RP_R2	CTGCACCTGTCCTCCTTTGT	NC016416 (8264)	This work
LR5-RP_F1	ATCAAAATCTTGGCATCCAG	FR822696 (7139)	This work
LR5-RP_F2	CTGGTTTGATTGACGGTGTG	FR822696 (6823)	This work
LR5-RP_R1	TCTCAGCTTTAGCTGCGTCA	FR822696 (7230)	This work
LR5-RP_R3	GCTGCCCAAGTGTCCAGTAT	FR822696 (7738)	This work

Real-time RT-PCR.

Quantitations were performed in white 96-well PCR plates using a Bio-Rad iQ5 Thermal cycler. Each reaction (20 μl final volume) contained 1 μl of cDNA, 10 μl of KAPA SYBR Green qPCR mix (KAPA Biosystems, Cape Town, South Africa) and 500 nM of each primer. The cycling conditions consisted of an initial denaturation of 3 min at 95ºC and 40 cycles of 30 s at 94ºC and 15 s at 60ºC. Each qPCR, including the actin gene internal control, was repeated three times. The specificity of the amplicons obtained was checked with Bio-Rad Optical System Software v.2.1, by means of melting-curve analyses (60 s at 95°C and 60 s at 55°C), followed by fluorescence measurements (from 55 to 95°C, with increments by 0.5°C) (Bustin et al., 2009).

Standard curves generation.

For each virus, a partial *RdRp* domain was amplified. Primers used were T7-LR4-RP_F3 and LR4-RP_R1 for GLRaV-4, T7-LR5-RP_F2 and LR5-RP_R3 for GLRaV-4 strain 5, T7-P3U-2 and P3D for GLRaV-3 (Table 1), where T7 refers to the T7 promoter. Thus, for the synthesis of RNA, the amplicons from PCR were purified and used as templates in a reaction with T7 RNA polymerase (Life technologies, Grand Island, NY), according to the manufacturer instructions. Synthetic RNA was quantified and serial diluted in non infected Sugar Seedless genomic RNA for RT and qPCR standard curve generation. Taking into account the molecular weight of synthetic RNAs, the number of genomic copies of each virus was calculated in each dilution.

Thus, the absolute virus quantitation was inferred in each sample by interpolation. A standard curve for the actin gene was obtained for normalization. The efficiency (E) of amplifications was calculated from the standard curves by the equation: $E = 10^{(-1/slope)}$ (Bustin et al., 2009). In percentage, it is expressed by the formula: % = (E - 1) x 100.

Statistical analyses.

The relative and absolute amounts of viral genomic RNA detected by the RT-qPCR were compared as the means of the clonal replicates (12 Rome plants, 12 Tintilla de Rota plants, 5 Gorgollassa plants infected by GLRaV-4 alone and 4 Gorgollassa plants infected by both GLRaV-4 and -3) of their respective mother vines. The differences among virus concentrations depending on grapevine cultivars and seasons were investigated by ANOVAs and Student–Newman–Keuls (SNK) range tests. The software used was SPSS v. 13 (SPSS Inc., Chicago, IL).

RESULTS

Isolate *RdRp* domains characterization.

Partial *RdRp* domains of GLRaV-3 isolates from each of the three cultivars, GLRaV-4 strain 5 *RdRp* domains from Rome and Tintilla de Rota and GLRaV-4 *RdRp* domain from Gorgollassa were sequenced and deposited in the GeneBank under the following Acc. Nos.: KC561088, KC561089, KC561090, KC561092, KC561087, KC561091 corresponding to GLRaV-3 (Gorgollassa), GLRaV-3 (Rome), GLRaV-3 (Tintilla), GLRaV-4 strain 5 (Rome), GLRaV-4 strain 5 (Tintilla) and GLRaV-4 (Gorgollassa), respectively. Amplicons by 984 and 916 bp were obtained for GLRaV-4 and -4 strain 5, respectively. For GLRaV-3, the amplicon length was 653 bp as expected (Tsai et al., 2012). Sequencing confirmed that primers LR3qrtF and LR3qrtR were appropriate for all three GLRaV-3 isolates of this study and allowed to design the specific primers needed for GLRaV-4 and -4 strain 5 qPCR quantitation. The nucleotide identities were also investigated. Regarding the *RdRp* domains for the three GLRaV-3 isolates, the nucleotide identities were: 99.0% for the Tintilla de Rota isolate, and 99.5 % for both Rome and Gorgollassa isolates with respect to GLRaV-3 isolate 623 (Acc No. GQ352632). With respect to the *RdRp* domain of the GLRaV-4 isolates identified in both Gorgollassa cultivars resulted 99.2% when compared with the GLRaV-4 isolate LR106 (Acc. Nº. FJ467503). The nucleotide identities for the *RdRp* domains of the

GLRaV-4 strain 5 isolates of cultivars Rome and Tintilla de Rota were both 93.3% when compared with the corresponding domain of the GLRaV-4 strain 5 isolate 3138-03 (Acc. Nº. JX559639).

Standard curves generation.

Standard curves from *in vitro* synthesized RNA of GLRaV-3, -4 and -4 strain 5 *RdRp* partial gene were generated by means of serial dilutions of the amplicons. Thus, the amplification efficiency of each primer pair and target was calculated, resulting 101.2, 104.12 and 104.3% for GLRaV-3, GLRaV-4 and GLRaV-4 strain 5, respectively (Figure 1). Similarly, a standard curve was obtained for the actin gene and the efficiency of the amplification was 100.08 %.
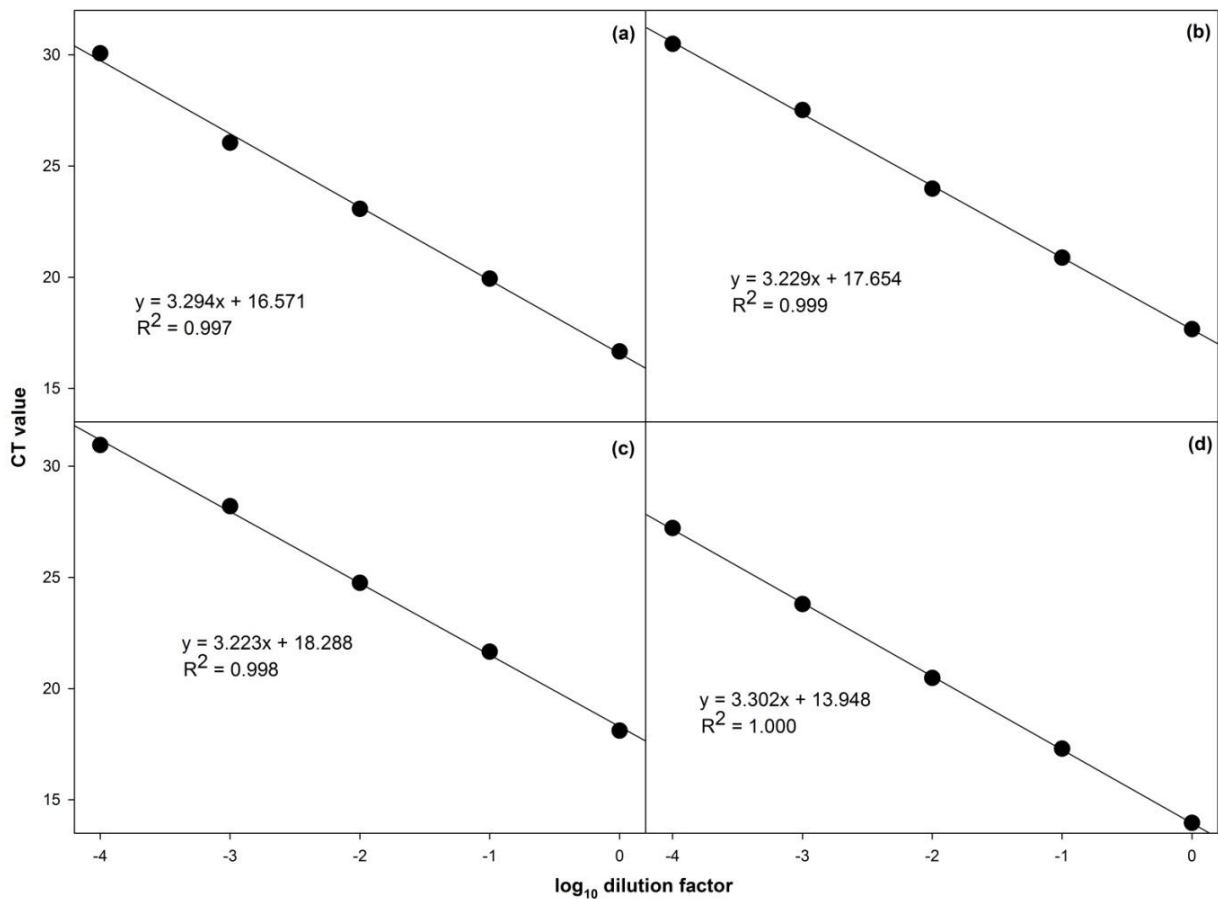
**Figure 1.** Evaluation of amplification efficiency and dynamic range of amplification of (a) *Grapevine leafroll-associated virus 3;* (b) *Grapevine leafroll-associated virus 4;* (c) *Grapevine leafroll-associated virus 4 strain 5* and (d) actin as the internal reference gene cDNA templates. Mean Cq values were obtained from serial $\log_{10}$ dilutions of reverse transcribed synthesized viral template RNAs.

Relative quantitation.

For each cultivar and season the mean $\Delta\Delta Cq = (Cq_{virusA} - Cq_{actin}) - (Cq_{virusB} - Cq_{actin})$ of GLRaV-3 versus GLRaV-4 or GLRaV-4 strain 5 was obtained, being Cq the quantification cycle at a threshold level of fluorescence (Bertolini et al., 2010). Figure 2 shows how to obtain ΔCq for relative quantification of one virus. The means $\Delta\Delta Cq$ resulted higher in April than in October in all the cases. In Gorgollassa, $\Delta\Delta Cq$ mean between GLRaV-4 and GLRaV-3 was 2.11 in April, but decreased to 0.51 in October. In Rome, $\Delta\Delta Cq$ between GLRaV-4 strain 5 and GLRaV-3 was 3.68 in April and 2.54 in October. In Tintilla de Rota, $\Delta\Delta Cq$ of GLRaV-4 strain 5 versus GLRaV-3 was 3.85 in April and 0.81 in October. In the conditions of this study, a $\Delta\Delta Cq$ by 3.3 corresponds to a difference by one magnitude order. Therefore, these $\Delta\Delta Cqs$ in April indicate differences higher than one magnitude order in Tintilla de Rota and Rome (GLRaV-3 vs. GLRaV-4 strain 5), being less consistent in Gorgollassa (GLRaV-3 vs. GLRav-4). In October, the differences between ampelovirus titers were smaller in all three cultivars.
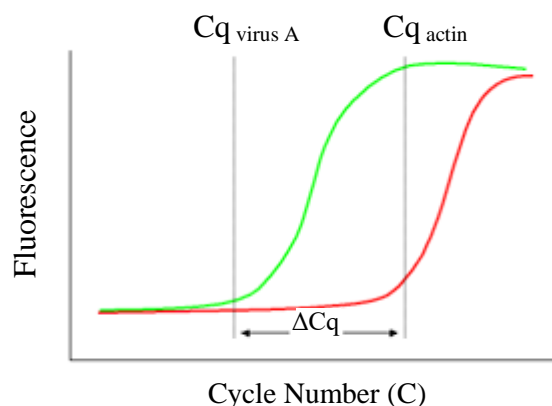
Figure 2. The relative quantity of virus A can be obtained by the difference in fractional cycle numbers between samples. Results can be normalized to a reference gen, in this case Actin.

Absolute quantitation.

Standard curves (Figure 1) allowed calculating the absolute copy number of GLRaV-3, GLRaV-4 and GLRaV-4 strain 5 for each cultivar and season. In Gorgollassa vines, the mean copy number of GLRaV-3 in the petiole was 4.9×10^6 and 4.1×10^6 mg^{-1} in April and October, respectively, being not statistically different ($P = 0.564$). With respect to the quantitation of GLRaV-4, results did not display significant differences between vines with simple (only GLRaV-4) and double (GLRaV-3 and -4)

infections ($P = 0.885$): in April, the mean number of genome copies was 5.6 x 10^5 mg^{-1} in the former and 3.2 x 10^5 mg^{-1} in the latter. Similarly, in October double-infected vines display similar values for GLRaV-4 than single infected ones (9.0 x 10^5 versus 1.1 x 10^6 mg^{-1}). In the analysis of the total virus population of GLRaV-4 in Gorgollassa vines (independently from the GLRaV-3 infection), small but significant differences are detected between seasons (4.4 x 10^5 mg^{-1} in April and 9.9 x 10^5 mg^{-1} in October, Figure 3) ($P < 0.01$).
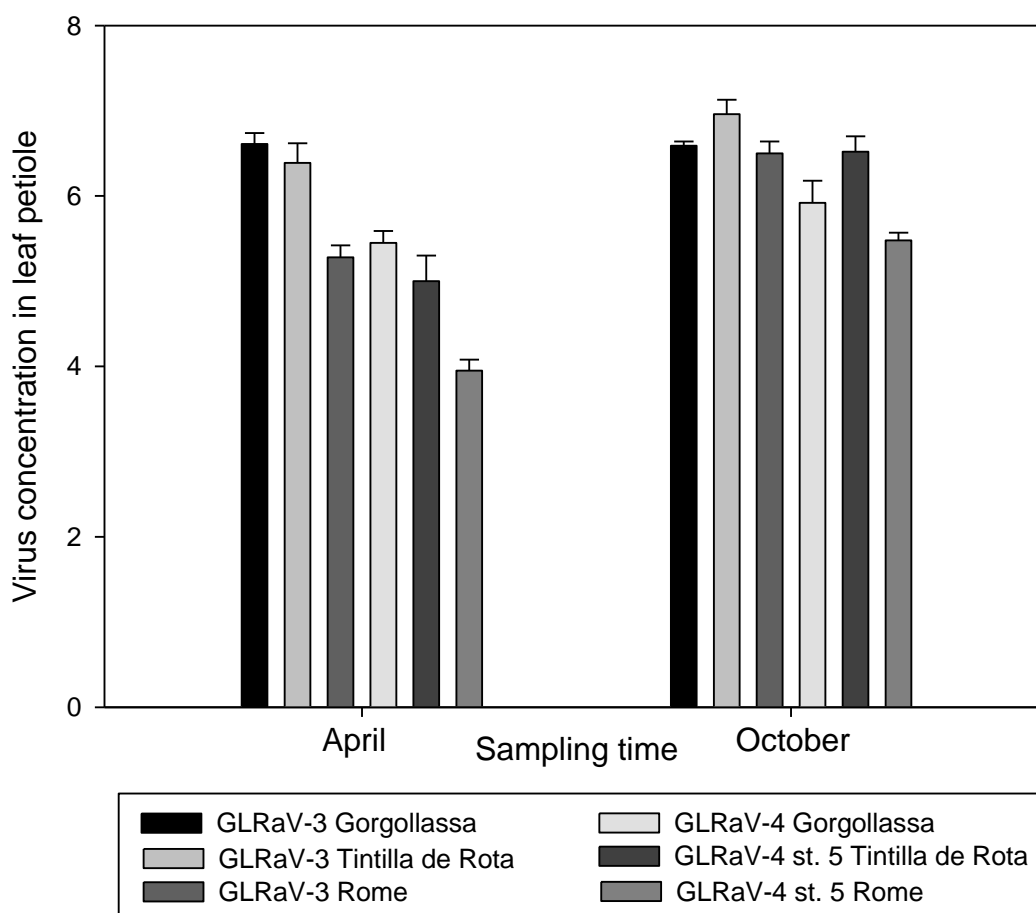
Figure 3. Mean population of *Grapevine leafroll-associated virus 3, Grapevine leafroll-associated virus 4* or *Grapevine leafroll-associated virus 4 strain 5*. Virus concentration in leaf petioles indicates the Log$_{10}$ of the number of genome copies * mg^{-1} host tissue, collected from middle sections in grapevine shoots. Vertical bars indicate standard error of the means.

In Rome, vines were double-infected by GLRaV-3 and -4 strain 5, and the mean number of genome copies was 5.6 x 10^5 for GLRaV-3 and 1.69 x 10^4 mg^{-1} for GLRaV-4 strain 5 in April, increasing to 7.5 x 10^6 mg^{-1} and 4.1 x 10^5 mg^{-1}, respectively, in

October (Figure 3). In Tintilla de Rota, vines were infected by both GLRaV-3 and -4 strain 5, resulting into mean copy number values of 1.0×10^7 mg^{-1} and 5.0×10^5 mg^{-1} in April for the former and the latter, respectively. Similarly to Rome, in Tintilla de Rota, the number of genome copies significantly increased in October for both viruses, being 1.6×10^7 mg^{-1} and 6.3×10^6 mg^{-1} for GLRaV-3 and GLRaV-4 strain 5, respectively (Figure 3).

The SNK test of $\log_{10}$[genome copy number $*$ mg^{-1}] data showed significant differences depending on grapevine cultivar, virus and their interaction (Table 2). Three groups are separated: The first includes only the mean value of GLRaV-4 strain 5 from Rome, the second is composed by GLRaV-4 strain 5 from Tintilla de Rota, GLRaV-4 from Gorgollassa and GLRaV-3 from Rome, while the third collects the GLRaV-3s from Gorgollassa and Tintilla de Rota (Table 2a).

Table 2. Student-Newman-Keuls (SNK) multiple range test for Grapevine/virus species grouping for $\log_{10}$(number of genome copies mg^{-1} host tissue). Group separation is obtained considering (a) total data ($P < 0.05$) and (b) October data only ($P < 0.05$).

(a)

Virus species	Cultivar	N	Subset for alpha = 0.05		
			1	2	3
GLRaV-4 str.	Rome	24	4.754		
GLRaV-4	Gorgollasa	20		5.691	
GLRaV-4 str.	Tintilla de Rota	24		5.918	
GLRaV-3	Rome	24		5.921	
GLRaV-3	Gorgollasa	10			6.602
GLRaV-3	Tintilla de Rota	24			6.736
	Sig.		1	0.634	0.596

(b)

Virus species	Cultivar	N	Subset for alpha = 0.05	
			1	2
GLRaV-4 str.	Rome	12	5.487	
GLRaV-4	Gorgollasa	10	5.927	
GLRaV-3	Rome	12		6.500
GLRaV-4 str.	Tintilla de	12		6.525
GLRaV-3	Gorgollasa	5		6.596
GLRaV-3	Tintilla de	12		6.962
	Sig.		0.052	0.171

Taking into account exclusively October data, only two groups can be distinguished, one composed by GLRaV-4 strain 5 from Rome and GLRaV-4 from Gorgollassa, and the second including all the rest of mean genome copies (Table 2b). This test also displays clear differences between seasons ($P < 0.001$) and viruses (GLRaV-3 versus GLRaV-4 or GLRaV-4 strain 5, $P < 0.001$).

Detection of viruses and viroids in grapevine samples using Ion Torrent sequencing.

The Ion Torrent sequencer generated 4.527.060 single reads of 16 nt-long in average from the pooled dataset composed from the four original samples. The sequence dataset was trimmed and filtered for quality and de novo assemblies were performed using CLC Genomics Workbench. A total of 478 contigs were assembled for the library. These contigs were subjected to BLASTx and BLASTn analysis in order to be characterised. Forty eigth contigs were identified corresponding to GLRaV-3, nine to GLRaV-4 and seven to GLRaV-4 strain 5 based on their homology with GenBank sequences. In addition we indentified from the pool of small RNAs enriched samples contigs corresponding to *Grapevine virus A* (GVA) and the viroids *Grapevine yellow speckle viroid-1* (GYSVd-1), *Hop stunt viroid* (HSVd-1) and *Australian grapevine viroid* (AGVd). Conventional PCR (not shown) allowed us to discriminate the presence of the organisms identified in the different cultivars. GVA, GYSVD-1 and HSVd was detected in the plants of Gorgollassa. AGVd was present in the plants of the Rome cultivar. No other GLRaV species was identified in the pool of sequences, apart from those object of this study.

DISCUSSION

GLRaV-4 type ampeloviruses have been postulated as primitive members of the genera because of their genome organization (Al Rwahnih et al., 2007; Dolja et al., 2006; Thompson et al., 2012). Althougt GLRaV-4s have been recently object of extensive genetic analysis (Esteves et al., 2012; Ghanem-Sabanadzovic et al., 2012; Ito et al., 2013; Maliogka et al., 2008; Saldarelli et al., 2006), up to the date, there are no reports of GLRaV-4s dynamics in their hosts. Therefore, their differential incidence in the vineyards and their relative epidemiological impact still needs research.

The quantitative real time PCR (qPCR) has replaced other methods such as ELISA and molecular hybridization to estimate virus populations in their hosts due to its higher sensitivity and ability to provide reliable, reproducible and consistent results (Balaji et al., 2003; Zhu et al., 2010). In addition, a RT followed by qPCR allows calculating the number of specific RNA molecules per mg of plant tissue that results into a fine estimation of the genome copy number in case of RNA viruses (Ambrós et al., 2011; Ferriol et al., 2011; Pacifico et al., 2011; Tsai et al., 2012). The *RdRp* domain is preferred for the calculation of virus genome copies to avoid the overestimation produced by genes that are shared between genomic and sub-genomic RNAs, such as the heat shock protein 70 (HSP70) or the coat protein (CP) ones (Padilla et al., 2010a; Tsai et al., 2012). To reduce possible result interference by RNA extractions and pipetting errors during PCR set up, the absolute number of viral genome copies was normalized in our analysis to the copy number of the endogenous gene actin.

The seasonal dynamics of GLRaV-3 has been already investigated in four grapevine cultivars, displaying virus populations within the same range of this study (Tsai et al., 2012). In that report, it was shown that, besides Thompson Seedless cultivar in which a slow boost was observed, the mean GLRaV-3 population in middle leaves did not increase in autumn with respect to spring, displaying even a decrease in Chardonnay. Similar value ranges for GLRaV-3 are also described in another study (Pacifico et al., 2011). In the present study, differences in virus concentration between autumn and spring are evident in Rome and Tintilla de Rota, especially with respect to GLRaV-4 strain 5. In addition, the difference in genome copies among GLRaV-3 and -4 strain 5 is significantly higher in April (more than one magnitude order) than in October, in both cultivars. Although in our conditions interactions between viruses species cannot be deduced due to the lack of vines infected by only GLRaV-3 or -4 strain 5, in a previous study GLRaV-3 populations in vines infected by only this virus (Tsai et al., 2012) displayed the same magnitude order observed in Rome and Tintilla de Rota; thus, these viruses probably do not interact between one another, at least with respect to changes in virus populations. Furthermore, data from Gorgollassa vines can support such hypothesis as no significant differences in GLRaV-4 genome copies were found between double and simple-infected vines (data not shown). In addition, GLRaV-3 population in October was in the same range from those quantified in Rome and

Tintilla de Rota. In conclusion, our results support that GLRaV-3 is able to establish more efficient multiplication rates in the host than GLRaV-4 type ampeloviruses.

In contrast to the Andalusian cultivars, in Gorgollassa both GLRaV-3 and GLRaV-4 populations did not show an appreciable variation between spring and autumn. These differential behavior observed among cultivars could be due to different experimental conditions because Rome and Tintilla de Rota vines were grown in pots in a controlled greenhouse, while Gorgollassa vines were located in a germoplasm collection in field. However, varietal differences cannot be discarded as reported previously (Tsai et al., 2012).

Apparently, GLRaV-4 like ampeloviruses are less frequent in vineyards than GLRaV-1 and -3. In Spain, this has been repeatedly observed among candidate clone vines, submitted from the different autonomous communities for the official certification (Padilla et al., 2012). The sanitary analysis showed percentages of infections in virus infected samples, by 21.6, 33.8 and 15.9 for the GLRaV-1, GLRaV-3 and GLRaV-4 clade, respectively. Most of the vines included in this study resulted to be simultaneously infected by more than one GLRaV. In another survey in the autonomous community of Valencia (Spain), GLRaV-3 was detected in 8.7% of the vines sampled, while GLRaV-4 strain 5 and GLRaV-4 were found only in the 0.8% and 3.2%, respectively (Fiore et al., 2012).

One possible explanation for the differential incidence among ampeloviruses lies in the differences in transmission by insect vectors. A very extensive literature about the capability of many mealybugs (*Hemiptera*: *Pseudococcidae*) and soft scales (*Hemiptera*: *Coccidae*) to acquire and carry GLRaV-1 and -3 is available, including several evidences of the natural virus spread in vineyards (reviewed in Almeida et al., 2013 and Marre et al., 2013). In contrast, to date, only one report in field conditions and a few ones in experimental trials have shown the transmission of the other ampeloviruses by mealybugs and soft scales. In addition, no specificity between any vector and GLRaV-4-like ampeloviruses has been proved. All the vectors reporting GLRaV-4 and its variants are also vectors for GLRaV-3 (Golino et al., 2002; Le Maguet et al., 2012; Mahfoudhi et al., 2009; Tsai et al., 2010), but more efficient in the transmission of the latter (Mahfoudhi et al., 2009).

Besides vector transmission, the spread of grapevine viruses by vegetative multiplication of infected stocks plays a very important role (Bertolini et al., 2010;

Kominek et al., 2003; López-Fabuel et al., 2013; Martelli et al., 2006), especially in local cultivars such as Rome, Tintilla de Rota and Gorgollassa where, due to the absence of certified clones, the exchange of uncontrolled or standard category material between winegrowers is very common (Cretazzo et al., 2010). Genetic analysis of GLRaV-4s supports that these viruses are well-adapted to vegetative propagation (Esteves et al., 2012; Maliogka et al., 2008). Thus, the differences in incidences of GLRaV-3 with respect to GLRaV-4 type ampeloviruses can be explained in terms of its higher efficiency in the multiplication in the host and more efficient spread by vector.

The simultaneous infection of two or more viruses and viroids in the same plant is frequent in nature. Antagonistic or synergistic interactions could result between unrelated viruses and viroids (Alabi et al., 2012; Flores et al., 2005; Syller, 2012; Valkonen, 1992). Antagonistic interactions have been previously observed for GYSVd and HSVd with GLRaV-3. However, the decrease in the GLRaV-3 small RNA concentration due to the presence of viroids reported in that study was small, fitting in the same order of magnitude (Alabi et al., 2012). Although there are differences in the concentrations of the GLRaVs for the different hosts studied in our work, these can be explained both by host genetic background, environment and the other virus and viroids found. Nevertheless, the fact that GLRaV-3 RNA concentration was around one magnitude order more abundant than GLRaV-4 and -4 strain 5 along the different virus-host combinations, suggests us to postulate biological differences among the two ampelovirus members that contribute to explain their epidemiological distribution. Finally, the two Gorgollassa vines deferred only in the presence or absence of GLRaV-3, while sharing GLRaV-4, GVA, GSYVd and HSVd. Given that the GLRaV-4 concentration in both cultivars remained similar, irrespectively of the presence or absence of GLRaV-3, it may be that the ampelovirus species do not interact each other. Finally, the real contribution to the ampeloviruses populations made by the additional virus and viroids found in the vines remains unknown until specific experiments are performed.

In this study additional insight into the biological differences between two different members of the *Ampelovirus* genera belonging to Subgroups I and II is provided, offering a complementary explanation for the differences in their relative incidences in field. Up to our knowledge, it is the first report of GLRaV-4 and -5

absolute quantitations. Also, this is the first detection of *Australian grapevine viroid* in Spain.

ACKNOWLEDGEMENTS

REFERENCES

Alabi O.J., Zheng Y., Jagadeeswaran G., Sunkar R., & Rayapati A.N. (2012). High-throughput sequence analysis of small RNAs in grapevine (*Vitis vinifera* L .) affected by grapevine leafroll disease. *Molecular Plant Pathology*, **13**, 1060–1076.

Almeida R.P.P., Daane K.M., Bell V.A., Blaisdell G.K., Cooper M.L., Herrbach E., & Pietersen G. (2013). Ecology and management of grapevine leafroll disease. *Frontiers in Microbiology*, **4**,82.

Al Rwahnih M., Uyemoto J.K., Falk B.W., & Rowhani A. (2007). Molecular characterization and detection of *Plum bark necrosis stem pitting-associated virus*. *Archives of Virology*, **152**, 2197–2206.

Ambrós S., El-Mohtar C., Ruiz-Ruiz S., Peña L., Guerri J., Dawson W.O., & Moreno, P. (2011). Agroinoculation of *Citrus tristeza virus* causes systemic infection and symptoms in the presumed nonhost *Nicotiana benthamiana*. *Molecular Plant-Microbe Interactions*, **24**, 1119–1131.

Balaji B., Bucholtz D.B., & Anderson J.M. (2003). *Barley yellow dwarf virus* and *Cereal yellow dwarf virus* quantification by real-time polymerase chain reaction in resistant and susceptible plants. *Phytopathology*, **93**, 1386–1392.

Bertazzon N., Borgo M., Vanin S., & Angelini, E. (2010). Genetic variability and pathological properties of *Grapevine leafroll-associated virus 2* isolates. *European Journal of Plant Pathology*, **127**, 185–197.

Bertolini E., García J., Yuste A., & Olmos, A. (2010). High prevalence of viruses in table grape from Spain detected by real-time RT-PCR. *European Journal of Plant Pathology*, **128**, 283–287.

Bustin S.A., Benes V., Garson J. A., Hellemans J., Huggett J., Kubista M., Mueller R., Nolan T., Pfaffl M.W., Shipley G.L., Vandesompele J., & Wittwer C.T. (2009). The MIQE guidelines: minimum information for publication of quantitative real- time PCR experiments. *Clinical Chemistry*, **55**, 611–622.

Buzkan N., Karadağ S., Kaya A., Baloğlu S., Minafra A., & Ben-Dov Y. (2009). First report of the occurrence of *Grapevine leafroll-associated virus-5* in Turkish vineyards. *Journal of Phytopatology*, **158**, 448–449.

Cretazzo E., Tomás M., Padilla C., Rosselló J., & Medrano H. (2010). Incidence of virus infection in old vineyards of local grapevine cultivars from Majorca: implications for clonal selection. *Spanish Journal of Agricultural Research*, **8**, 409–418.

Dolja V.V., Kreuze J.F., & Valkonen J.P. (2006). Comparative and functional genomics of closteroviruses. *Virus Research*, **117**, 38–51.

Escobar P.F, Fiore N., Valenzuela P.D.T., & Engel E.A. (2008). First detection of *Grapevine leafroll-associated virus 4* in Chilean grapevines. *Plant Disease*, **92**,1474.

Esteves F., Teixeira Santos M., Eiras-Dias J.E., & Fonseca F. (2012). Occurrence of *Grapevine leafroll-associated virus 5* in Portugal: genetic variability and population structure in field-grown grapevines. *Archives of Virology*, **157**, 1747–1765.

Ferriol I., Ruiz-Ruiz S., & Rubio L. (2011). Detection and absolute quantitation of *Broad bean wilt virus 1* (BBWV-1) and BBWV-2 by real time RT-PCR. *Journal of Virological Methods*, **177**, 202–205.

Fiore N., Zamorano A., Sánchez-Diana N., Pallás V., Sánchez-Navarro J. A. Survey & partial molecular characterization of grapevine virus and viroids from Valencia, Spain. Pages 196-197 in: Proc. 17th Congress of the International Council for the Study of Virus and Virus-like diseases of the Grapevine (ICVG), Davis, CA.

Flores R., Hernández C., Martínez de Alba A.E., Daròs J.A., & Di Serio F. (2005). Viroids and viroid–host interactions. *Annual Review of Phytopathology*, **43**,117–139.

Fuchs M., Martinson T.E., Loeb G.M., & Hoch, H.C. (2009). Survey for the three major leafroll disease-associated viruses in Finger Lakes vineyards in New York. *Plant Disease*, **93**, 395–401.

Ghanem-Sabanadzovic N.A., Sabanadzovic S., Gugerli P., & Rowhani A. (2012). Genome organization, serology and phylogeny of *Grapevine leafroll-associated viruses 4* and *6*: taxonomic implications. *Virus Research*, **163**, 120–128.

Golino D.A., Sim S.T., Gill R., & Rowhani A. (2002). California mealybugs can spread grapevine leafroll disease. *California Agriculture*, **56**, 196–201.

Gutha L.R., Casassa L.F., Harbertson J.F., & Naidu R.A. (2010). Modulation of flavonoid biosynthetic pathway genes and anthocyanins due to virus infection in grapevine (*Vitis vinifera* L.) leaves. *BMC Plant Biology*, **10**, e187.

Ito T., Nakaune R., Nakano M., & Koichi S. (2013). Novel variants of *Grapevine leafroll-associated virus 4* and *7* detected from a grapevine showing leafroll symptoms. *Archives of Virology*, **158**, 273–275.

Kalendar R., Lee D., & Schulman A.H. (2011). Java web tools for PCR, in silico PCR, and oligonucleotide assembly and analysis. *Genomics*, **98**, 137–144.

Kominek P., & Holleinova V. (2003). Evaluation of sanitary status of grapevines in the Czech Republic. Plant Soil Environmental, **49**, 63–66.

Le Maguet J., Beuve M., Herrbach E., & Lemaire O. (2012). Transmission of six ampeloviruses and two vitiviruses to grapevine by *Phenacoccus aceris*. *Phytopathology*, **102**, 717–723.

López-Fabuel I., Wetzel T., Bertolini E., Bassler A., Vidal E., Torres L.B., Yuste A., & Olmos A.J. (2013). Real-time multiplex RT-PCR for the simultaneous detection of the five main grapevine viruses. *Journal of Virological Methods*, **188**, 21–24.

Mahfoudhi N., Digiaro M., & Dhouibi M. H. (2009). Transmission of Grapevine leafroll viruses by *Planococcus Ficus* (*Hemiptera: Pseudococcidae*) and *Ceroplastes Rusci* (*Hemiptera: Coccidae). Plant Disease*, **93**, 999–1002.

Maliogka V.I., Dovas C.I., & Katis N.I. (2008). Evolutionary relationships of virus species belonging to a distinct lineage within the *Ampelovirus* genus. Virus Research, **135**, 125–135.

Maree H.J., Almeida R.P.P., Bester R., Chooi K.M., Cohen D., Dolja V.V, Fuchs M.F., Golino D.A, Jooste A.E.C., Martelli G.P., Naidu R.A., Rowhani A., Saldarelli P., & Burger, J. T. (2013). Grapevine leafroll-associated virus 3. Frontiers in Microbiology, **4**, 94.

Martelli G.P., Abou Ghanem-Sabanadzovic N., Agranovsky A.A., Al Rwahnih M., Dolja V.V., Dovas C.I., Fuchs M., Gugerli P., Hu J.S., Jelkmann W., Katis N.I., Maliogka V.I., Melzer M.J., Menzel W., Minafra A., Rott M.E., Rowhani A., Sabanadzovic S., & Saldarelli P. (2012). Taxonomic revision of the family *Closteroviridae* with special reference to the Grapevine leafroll-associated members of the genus *Ampelovirus* and the putative species unassigned to the family. *Journal of Plant Pathology*, **94**, 7–19.

Martelli G.P., & Boudon-Padieu E. (2006). Directory of infectious diseases of grapevines. International Centre for Advanced Mediterranean Agronomic Studies. *Options Méditerranéennes Ser. B, Studies and Research*, **55**, 59–75.

Martin R.R., Eastwell K.C., Wagner A., Lamprecht S., & Tzanetakis I.E. (2005). Survey for viruses of grapevine in Oregon and Washington. *Plant Disease*, **89**, 763–766.

Osman F., Leutenegger C., Golino D., & Rowhani, A. (2007). Real-time RT-PCR (TaqMan) assays for the detection of *Grapevine leafroll associated viruses 1-5* and *9*. *Journal of Virological Methods*, **141**, 22–29.

Pacifico D., Caciagli P., Palmano S., Mannini F., & Marzachì C. (2011). Quantitation of *Grapevine leafroll associated virus-1* and *-3*, *Grapevine virus A*, *Grapevine fanleaf virus* and *Grapevine fleck virus* in field-collected *Vitis vinifera* L. 'Nebbiolo' by real-time reverse transcription-PCR. *Journal of Virological Methods*, **172**, 1–7.

Padilla C.V., Cretazzo E., López N., García de Rosa B., Padilla V., & Velasco L. (2010a). First report of *Grapevine leafroll-associated virus 4* in Spain. *New Disease Report*, **21**, 21.

Padilla C.V., Cretazzo E., López N., Padilla V., & Velasco L. (2010b). First report of *Grapevine leafroll-associated virus 5* in Spain. *Plant Disease*, 94, 1507.

Padilla C.V., Cretazzo E., López N., Hita I., Alcalá M.J., Padilla V., & Velasco, L. (2013). First report of *Grapevine leafroll-associated virus 9* in Spain. *Journal of Plant Pathology*. In press.

Padilla C.V., García de Rosa B., López N., Velasco L., Salmerón E., Padilla V., & Hita I. (2012). Grapevine leafroll virus in candidate clones for plant certification in Spain. Pages 268-269 in: Proc. 17th Congress of the International Council for the Study of Virus and Virus-like diseases of the Grapevine (ICVG), Davis, CA.

Pei G.-Q., Dong Y.-F., Zhang Z.-P., & Fan X.-D. (2010). First Report of Grapevine leafroll- associated virus 4 and 5 in grapevines in China. *Plant Disease*, **94**, 130.

Rozen S., & Skaletsky H. J. (2000). Primer3 on the WWW for general users and for biologist programmers. Pages 365-386 in: *Bioinformatics Methods and Protocols: Methods in Molecular Biology*. S. Krawetz, and S. Misener, eds. Humana Press, Totowa, NJ.

Saldarelli P., Cornuet P., Vigne E., Talas F., Bronnenkant I., Dridi A.M., Boscia D., Gugerli P., Fuchs M., & Martelli G.P. (2006). Partial characterization of two divergent variants of grapevine leafroll-associated virus 4. *Journal of Plant Pathology*, **88**, 203–214.

Syller J. (2012). Facilitative and antagonistic interactions between plant viruses in. *Molecular Plant Pathology*, **13**, 204–216.

Thompson J.R, Fuchs M., & Perry K.L. (2012). Genomic analysis of *Grapevine leafroll associated virus-5* and related viruses. *Virus Research*, **163**, 19–27.

Tsai C.-W., Rowhani A., Golino D.A., Daane K.M., & Almeida R.P.P. (2010). Mealybug transmission of grapevine leafroll viruses: an analysis of virus-vector specificity. *Phytopathology*, **100**, 830-834.

Tsai C.-W., Daugherty M.P., & Almeida R.P.P. (2012). Seasonal dynamics and virus translocation of *Grapevine leafroll-associated virus 3* in grapevine cultivars. *Plant Pathology*, **61**, 977–985.

Valkonen J.P.T. (1992). Accumulation of *Potato virus Y* is enhanced in *Solanum brevidens* also infected with *Tobacco mosaic virus or potato spindle storage root viroid*. *Annals of Applied Biology*, **121**, 321–327.

Walter B., & Martelli G.P. (1996). Sélection clonale de la vigne: sélection sanitaire et sélection pomologique. Influence des viroses et qualité. 1ere partie: effets des viroses sur la culture de la vigne et ses produits. *Bull. O. I. V.,* **69**, 945–971.

Zhu Y.J., Lim S.T.S., Schenck S., Arcinas A., & Komor E. (2010). RT-PCR and quantitative real-time RT-PCR detection of *Sugarcane yellow leaf virus* (SCYLV) in symptomatic and asymptomatic plants of Hawaiian sugarcane cultivars and the correlation of SCYLV titre to yield. *European Journal of Plant Pathology*, **127**, 263–273.

Chapter 4

ABSOLUTE QUANTIFICATION OF GRAPEVINE
LEAFROLL ASSOCIATED VIRUS 3 (GLRaV-3) AND
ITS EFFECTS ON THE PHYSIOLOGY IN
ASYMPTOMATIC PLANTS OF *VITIS VINIFERA* L.

ABSOLUTE QUANTIFICATION OF GRAPEVINE LEAFROLL ASSOCIATED VIRUS 3 (GLRaV-3) AND ITS EFFECTS ON THE PHYSIOLOGY IN ASYMPTOMATIC PLANTS OF *VITIS VINIFERA* L.

R. Montero[1], H. El aou ouad[2], D. Pacifico[3,4], C. Marzachì[4], N. Castillo[5], E. García[5], N. F. Del Saz[2], I. Florez-Sarasa[6], J. Flexas[2], J. Bota[2*]

[1]Institut de Recerca i Formació Agrària i Pesquera (IRFAP), Conselleria d'Agricultura, Medi Ambient i Territori. Govern de les Illes Balears. C/Eusebio Estada nº 145. 07009, Palma de Mallorca, Spain.

[2]Grup de Recerca en Biologia de les Plantes en Condicions Mediterrànies, Departament de Biologia, Universitat de les Illes Balears, Carretera de Valldemossa, km 7.5, 07071, Palma de Mallorca, Balears, Spain.

[3]Istituto di Bioscienze e BioRisorse, CNR, Corso Calatafimi 414, 90129, Palermo, Italy

[4]Istituto per la Protezione Sostenibile delle Piante, CNR, Strada delle Cacce 73, 10135, Torino, Italy

[5]Instituto de la Vid y el Vino de Castilla-La Mancha (IVICAM), Ctra. Toledo-Albacete s/n, 13700, Tomelloso, Spain

[6]Max-Planck-Institute of Molecular Plant Physiology, 14476 Potsdam, Germany

*Corresponding author: j.bota@uib.es

ABSTRACT

Grapevine leafroll disease is one of the most important viral diseases of grapevine (*Vitis vinifera* L.) worldwide. *Grapevine leafroll associated virus 3* (GLRaV-3) is the most predominant strain causing this disease. Therefore, it is important to identify GLRaV-3 effects, especially in plants which do not systematically show visual symptoms. In the present study, effects of GLRaV-3 on grapevine physiology in pot-grown asymptomatic Malvasía de Banyalbufar and Cabernet Sauvignon plants were evaluated. Absolute virus quantification was performed in order to determine possible correlations between virus amount and physiology parameters. The net carbon dioxide (CO_2) assimilation rate and electron transport rate were the parameters mainly affected by the virus and they had good correlation with the virus quantity. Malvasía de Banyalbufar showed higher virus amount than Cabernet Sauvignon plants. In Malvasía de Banyalbufar plants the reduction in net CO_2 assimilation rate was attributed to CO_2 diffusion and biochemistry limitations, while in Cabernet Sauvignon plants net CO_2 assimilation rate was not affected by the virus probably due to the lower virus amount. The CO_2 diffusion was restricted principally by anatomical leaf changes and biochemistry limitation by a reduction in the activity of Rubisco. The reduction of net CO_2 assimilation rate lead to a decrease in total oxygen (O_2) uptake rate by the activity of the cytochrome oxidase pathway, producing slight differences in plant growth. However, at this virus infection level there were no evidences of the activation of the hormone response against the virus. Therefore, even though no symptoms were expressed in the plants, the effects of the virus can compromise the plant vital processes, showing the importance of early detection of the virus in order to fight against the infection spread.

Keywords: *Vitis vinifera* L., Grapevine Leafroll associated Virus 3, virus absolute quantification, chlorophyll fluorescence, leaf gas exchange, leaf anatomy, Rubisco content.

INTRODUCTION

Virus infections cause significant economic losses in many vineyards around the world. Grapevine Leafroll disease is one of the most important virus diseases in grapevine and it is widespread to all major grape-growing regions of the world. Several members from the *Closteroviridae* family are associated with Leafroll diseases (Mannini et al*.,* 2012). *Grapevine Leafroll-associated virus 3* (GLRaV-3, genus *Ampelovirus*) is regarded as the most important one because of its high incidence in the field attributed to its high replication efficiency (Velasco et al*.,* 2014 (Chapter 3)). GLRaV-3 is systemic in the vine, although it is generally localized in the vascular plant tissue (phloem) like other members of the *Closteroviridae* family. GLRaV-3 infects both white and red grape cultivars. Red cultivars symptoms are easily noticeable seen as dark-red, downward rolling leaves with green veins, but in white cultivars they are hard to visibly identify. The difficulty of detecting virus infection can lead to rapid dissemination of virus-infected material through propagation. Diagnostic methods for the detection of grapevine viruses have been developed over the last few years. These methods include: biological indexing (Habili et al., 1992), enzyme-linked immunosorbent assay (ELISA) (Frosline et al., 1996; Rowhani, 1992; Rowhani et al., 1997) and nucleic acid-based methods, mainly PCR methods (Wetzel et al., 2002; Rowhani et al., 1993; Minafra et al., 1992). However, real time qPCR has become the most used method to determine virus presence and the unique method to determine virus amount (Huggett et al., 2005). This system determines the quantification of the specific RNA molecules per milligram of plant tissue that fits, very accurately, up to genome copy number of RNA viruses (Ambrós et al., 2011; Ferriol et al., 2011). Quantification of RNA viruses was successfully achieved using the *RdRp* gene as RT-PCR target, which avoids the overestimation produced by subgenomic RNA targets while measuring viral population (Pacifico et al., 2011; Tsai et al., 2012).

Physiological consequences of biotic stress are still far from being well understood because they are highly variable (Balachandran et al., 1997; González et al., 1997; Christov et al., 2001; Sampol et al., 2003; Petit et al., 2006; Komar et al., 2007; Christov et al., 2007; Basso et al., 2010). The grapevine response to virus infection depends on several factors such as cultivar, vegetative season, environmental conditions and viral isolate (Martelli, 2009). Viruses (including GLRaV-3) are known to affect grape yield and quality (González et al., 1997; Guidoni et al., 1997; Cabaleiro et al.,

1999; Cretazzo et al., 2010; Lee and Martin, 2009; Lee et al., 2009; Basso et al., 2010). Few findings demonstrate that some of the effects of GLRaV-3 are associated with grapevine physiological disturbances, mainly associated to photosynthesis. Hristov & Abrasheva (2001) measured low levels of chlorophyll and carotenoid pigments in the leaves of GLRaV-3 infected Cabernet Sauvignon vines compared to non infected ones. In another study done in Malvasía de Banyalbufar cv., plants infected with *Grapevine Fanleaf Virus* (GFLV) and GLRaV-1, -2 and -3, Sampol et al. (2003) measured substantial declines in net assimilation rate identifying decreases in mesophyll conductance to CO_2 (g_m) and impaired Rubisco activity the principal limitations to photosynthesis. More recently, Moutinho-Pereira et al. (2012) reported photosynthetic capacity reduction in GLRaV-3 infected Touriga Nacional plants cultivar. This was associated with effects on chlorophyll and carotenoid contents, primary light reactions and a decrease in stomatal conductance. Endeshaw et al. (2014), reported similar effects in symptomatic plants of Cabernet Franc cv., and suggested that there was also impaired leaf photosynthetic performance and associated metabolic components (chlorophyll and nitrogen content) in asymptomatic plants.

While the studies cited and others have described the effects of virus infection on photosynthesis, the information about its effects on respiration remains scarce. Plant respiration can consume a great proportion of the carbon assimilated by photosynthesis during the day, thus affecting carbon balance and growth, especially under stress conditions (Flexas et al., 2006). During pathogen infection, the synthesis of defense compounds such as salicylic acid (SA), phytoalexin and lignin may account for a respiratory energy and carbon cost to the infected plant (Hanqing et al., 2010). Among different alternative pathways, the mitochondrial electron transport chain (mETC) presents an alternative oxidase (AOX) that constitutes a branching point, at the level of the ubiquinone pool, from the main electron transport pathway, the cytochrome oxidase (COX) pathway (Vanlerberghe, 2013). The electron flow to AOX greatly reduces the mitochondrial synthesis of adenosine triphosphate (ATP) because it bypasses two of the three proton pumping sites of the mETC and AOX protein by itself does not pump protons into the intermembrane space (Vanlerberghe, 2013). It is widely accepted that the two respiratory pathways compete for the electrons of the ubiquinone pool and that the only available technique to determine their *in vivo* activities is the oxygen isotope fractionation technique (Ribas-Carbo et al., 2005). While there have been numerous

reports regarding the changes of AOX protein amount in response to bacterial, viral and fungal pathogens (reviewed in Hanqing et al., 2010), studies on its *in vivo* activity are scarce (Lennon et al., 1997).

The few studies done on GLRaV-3 effects on grapevine physiology were performed in vines with visible symptoms but none of them quantified the virus infection. We hypothesize that the effects on specific physiological parameters may be related to the absolute concentrations of the virus. To test this, fluctuations in virus concentration in relation to ambient temperature at different sampling times were examined. Also, virus effects on several plant physiological and morphological parameters were determined, tryning to find those more affected by the infection.

MATERIAL AND METHODS

Plant material and growth conditions

Pot-grown virus-free and GLRaV-3 infected *Vitis vinifera* L. Malvasía de Banyalbufar cv. and Cabernet Sauvignon cv. were used for this work. Symptomless Malvasía de Banyalbufar and Cabernet Sauvignon infected mother plants were selected in experimental vineyards at IRFAP center (*Institut de Recerca i Formació Agrària i Pesquera, Conselleria d'Agricultura Medi Ambient i Territori*), on Palma de Mallorca (Balearic Island, Spain) and IMIDA center (*Instituto Murciano de Investigación y Desarrollo Agrario y Alimentario*), Murcia (Spain) respectively. Plants for the experiment were obtained by direct rooting of 0.2 m cuttings of dormant canes selected from the mother plants. Two weeks after rooting, six GLRaV-3 infected cuttings and six uninfected cuttings of each cultivar were transferred into 10 l pots filled with organic substrate and perlite mixture (5:1). All this process was done inside the greenhouse. One month later, the plants were placed outdoors. The experiment was carried out during summer 2012 and 2013 at the *Universitat de les Illes Balears* (Palma de Mallorca, Balearic Island, Spain) experimental field. In 2012, only Malvasía de Banyalbufar was tested while in 2013 the experiment was expanded introducing Cabernet Sauvignon cultivar. In both years, the Malvasía de Banyalbufar cuttings were selected from the same mother plants. Before starting the experiment, all the plants were irrigated daily, and every 15 days 2 g of organic fertilizer was added to the pots. Instead of using an

organic fertilizer the plants were irrigated with 50% Hoagland´s solution (Hoagland & Aron, 1950) every 3 days, 2 weeks before starting the measurements. The plants did not develop any fruit. In all the plants two shoots were left to carry out the experiment.

Environmental conditions and plant water status

Mean daily temperature was monitored during the experiment using a meteorological station (Meteodata 3000, Geónica SA, Madrid, Spain).

Leaf water status was determined as the predawn leaf water potential (Ψ_{PD}), using a Scholander chamber (Soil Moisture Equipment Corp., Santa Barbara, CA, USA) on five leaves per cultivar and treatment.

Virus diagnosis

The presence of GLRaV-1, 3, 4, 5, 7, 9, GFLV and *Grapevine fleck virus* (GFkV) viruses was tested in mother plants by enzyme-linked immunosorbent assay (ELISA) (Clark & Adams, 1977) using commercial coating and conjugate antibody preparations (Bioreba AG, Reinach, Switzerland). According to ELISA results non infected and single GLRaV-3 infected plants were selected for the experiment. The ELISA results were confirmed in these plants by RT-PCR using a RT- PCR system (Illumina, SD, USA) following the protocol of Pacifico et al. (2011). Total RNA was extracted from one leaf per plant (70 mg of phloem scraped from leaves) using Spectrum^{TM} Plant Total RNA Kit (Sigma-Aldrich, Inc.) according to the manufacturer's instructions. The Spectrum™ Plant total RNA Kit removes most of the DNA during RNA purification. However, for very sensitive applications, such as RT-qPCR, complete removal of traces of DNA may be necessary. On-Column DNase I Digest Set (Sigma-Aldrich Co., St Louis, MO, USA) was used to digest the DNA during RNA purification following the manufacturer´s instruction. RNA purity and concentration were measured at 260/280 nm using a spectrophotometer (NanoDrop-1000, Thermo Scientific, Villebon sur Yvette, France). First-strand cDNA synthesis was performed using 500 ng of total RNA, 200 units of recombinant *Moloney Murine Leukemia Virus* (MuLV) reverse transcriptase (Invitrogen Life Technologies, Inc.), 40 units of RNase inhibitor (RNase out, Invitrogen Life Technologies, Inc.), 0.4 mM of dNTPs, and 2 mM of random nonamers (Takara Bio, Inc.). The mixture for reverse transcription (20

µl) was incubated for 50 min at 37ºC and the reaction was inactivated by heating it at 70ºC for 15 min.

RT- PCR reactions were performed in a 10 µl mixture containing 2 µl of diluted (1:100) cDNA, 5 µl SYBR Premix Ex Taq II (Takara Bio, Inc.) and 0,2 µM of each primer in the ECO-Illumina system (ECO-Illumina) using the following PCR cycle profile: one cycle of 2 min at 95°C followed by 40 cycles of 5 s at 95°C, 20 s at 60°C. After that, melting curve was performed using the following profile: 15 s at 95ºC, 15 s at 60ºC and 15 s 95ºC. The fluorescence threshold value (Ct) was calculated using the ECO-Illumina system software (ECO-Illumina). Overall, a mean Ct value was calculated from two PCR replicates.

Sequences of primers used in this study were retrieved from literature and used for amplifying partial gene-specific sequences. A list of primer pairs and amplicon lengths used for the virus diagnosis are provided in Table 1.

Table 1. Sequences of primers used for amplification of grapevine virus, amplicon length and references.

Virus	Primers	Sequences (5′-3′)	Size (bp)	References
GLRaV-1	GLRaV 1f	CAT CGC AAG ATG AGT CTG GG	275	Sefc et al., 2000
	GLRaV 1r	TTC ACA TTG CCC ACG CTG CC		
GLRaV-2	GLRaV-2 198 F	CATTATATTCTTCATGCCTCTCAGGAT	116	Osman et al., 2007
	GLRaV-2 290 R	GATGACAACTTCTGTCCGCTATAGC		
GLRaV-3	GLRaV-3 RdRp(1) For	TACGCTCATGGTGAAAGCAG	103	This work
	GLRaV-3 RdRp(1) Rev	GGTTACGCACCTATCGTGGT		
GLRaV-4	HSP-85 F	ATATACATACCAACCGTTGTGGGTATAA	93	Osman et al., 2007
	HSP-178 R	CCCTATAAACTAGCACATCCTTCTCTAGT		
GLRaV-5	HSP-26 F	AACACTCTGCTTTTCTGCTGGC	162	Osman et al., 2007
	HSP-188 R	CTTTTTATGTCCCGATAAACGAGTACA		
GFkV	Fleck 239 f	CAACATCGAATGCCAATTTGG	89	Osman et al., 2007
	Fleck 328 r	GCCAGGCTGTAGTCGGTGTTGT		
GFLV	GFLV V1/F	ACCGGATTGACGTGGGTGAT	311	Osman et al., 2008
	GFLV C1/R	CCAAAGTTGGTTTCCCAAGA		

Modified from Pacifico et al., 2012

Standard curve construction and virus quantification

In order to obtain a GLRaV-3 standard curve, RNA-dependent RNA polymerase (*RdRp*) sequences were retrieved from GenBank (Table 2) and aligned using the software DNAman vers. 4.02 (Lynnon BioSoft, Vandreuil, Quebec, Canada). Primers designed on sequence GU812895 (Table 2), were used with the protocol described above to amplify partial *RdRp* gene from the Malvasía de Banyalbufar GLRaV3 isolate for the construction of standard RNA curve.

A template of 2 μl was used in 50 μl PCR reactions, using the following conditions: denaturation for 5 min at 94°C; followed by 35 cycles of 30 s at 94°C, 30 s at 50°C and 1 min 30 s at 72°C; and a post-well period of 10 min at 72°C.

Table 2. GenBank accession numbers of the *RdRp* genes of viruses from different geographical origins used to design primers for the amplification and cloning of *RdRp* of GLRaV-3 Malvasía de Banyalbufar isolate.

Virus	Sequence	Origin
GLRaV-3	EF508151	New Zealand
	DQ314610	Spain
	AY495340	China
	AJ748536	China
	AJ748530	Italy
	GU812895	Italy
	AJ748529	France
	AJ748526	Portugal
	AJ748525	Austria
	AJ748532	Nigeria
	AJ748531	Israel
	AJ748528	Albania
	AJ748527	Tunisia
	KP844580	Spain (This work)

Modified from Osman et al., 2008

PCR products were analysed by electrophoresis through a 1% agarose gel in 1× Tris-borate-EDTA (TBE) buffer along with a 1 kb plus DNA size marker (Gibco BRL, Paislay, UK), and observed on a UV transilluminator. Amplicons were then gel-purified using the Geneclean® Turbo kit (MP-Biomedicals, Solon, OH, USA), ligated into the

pGEM-T easy vector (Promega, Madison, WI, USA) and transformed in *E. coli* DH5α. Transformed plasmids were purified with the Fast Plasmid Mini kit (Eppendorf AG, Hamburg, Germany), and sequenced (BioFab Research, Pomezia, RM, Italy) with the universal primers M13F/R. with at least twice the sequencing coverage for each nucleotide position, raw sequence data were edited manually with the DNAman program vers. 4.02 (Lynnon BioSoft, Vandreuil, Quebec, Canada).

RdRp sequence of GLRaV-3 isolate from PCR products was compared with the sequences retrieved from GenBank (Table 2). Genetic correspondences were obtained using DNAman program vers. 4.02 (Lynnon BioSoft, Vandreuil, Quebec, Canada).

The obtained plasmid (1.3 μg), containing a fragment of the Malvasía de Banyalbufar GLRaV3 *RdRp* gene, was linearised with five units of SalI (Promega) over night at 37°C. EDTA (25 mM) was added to stop the digestion; DNA was precipitated and dissolved in 13 μl RNase-free water. The linearised plasmid was transcribed with the MAXIscript® *in vitro* Transcription Kit (Applied Biosystems), according to the manufacturer's instructions. RNA was treated with two units of RNase-free DNase I (Applied Biosystems) in the supplied buffer to eliminate plasmid DNA. Then, phenol/chloroform extraction was applied and RNA was dissolved in 30 μl of RNase-free water containing 0.1% DEPC. RNA concentration was measured in a spectrophotometer. The number of RNA copies per microliter was calculated from the concentration using the next formula: $M = C \times N/S$, where M is the number of molecules per microliter, C the RNA concentration (ng μl^{-1}), S the molecular weight of the fragment and N a factor derived from the Avogadro constant. Finally first-strand cDNA synthesis was performed from RNA extracted using the protocol mentioned above to be used as a standard for qRT-PCR.

Three tenfold serial dilution of cDNA standards in 0.1% RNAse-free water were run in duplicate for each PCR system. Standard curves were generated by linear regression analysis of the threshold cycle (Ct) value of each of the three standard dilution replicates over the Log of the copies numbers of GLRaV-3 genome present in each sample. Data acquisition and analysis were processed by the ECO-Illumina system software (ECO-Illumina), which automatically calculates the Ct values and the parameters of the standard curves. Real-time RT-PCR efficiency (E) was calculated by

the formula: $E = e^{\ln 10/-s} - 1$, where the slope (s) $=-3.322$ (E = 2) represents 100% efficiency.

Primers used for the qRT-PCR of GLRaV-3 were designed from the *RdRp* sequence of Malvasía de Banyalbufar plants sequenced in this study (Table 1).

RT-qPCR reactions were performed in a 10 µl mixture containing 2 µl of diluted (1:100) cDNA, 5 µl SYBR Premix Ex Taq II (Takara Bio, Inc.), and 0,2 µM of each primer in the ECO-Illumina system using the following PCR cycle profile: one cycle of 2 min at 95°C followed by 40 cycles of 5 s at 95°C, 20 s at 60°C. After this, a melting curve was performed using the following profile: 15 s at 95ºC, 15 s at 60ºC and 15 s 95ºC. The fluorescence threshold value (Ct) was calculated using the ECO-Illumina system software (ECO-Illumina). Overall, a mean Ct value was calculated from two PCR replicates. Three serial dilutions of virus standard RNAs were run in duplicate together with grapevine samples on the plate. RT-qPCR mix with sterile distilled water instead of RNA was used as a negative control on each plate.

Growth measurements

In both years and for each treatment the length of all leaves of all plants was measured at the begging and at the end of the experiment, and leaf area was calculated with reference to a regression equation obtained on 36 leaves per treatment. These were used to calculate leaf area. Leaf area of these leaves was measured using public domain image analysis software (ImageJ version 1.32; http.//rsb.info.nih.gov/ij/).

Total number of leaves per plant and shoot length were determined during the same week of gas exchange and chlorophyll fluorescence measurements.

Gas Exchange and Chlorophyll fluorescence measurements.

The open gas exchange system Li-6400 (Li-Cor, Lincoln, NE, USA) with an integrated fluorescence chamber head (Li-6400-40; LI-COR Inc.) was used to measure leaf gas exchange rates and chlorophyll fluorescence in mature fully expanded leaves. Five plants per treatment were used for the experiment. One leaf per plant was measured at the beginning of July and at the end of August, at mid-morning for each treatment. Photosynthesis was induced at saturating light (1500 µmol m^{-2} s^{-1}) and 400 µmol mol^{-1} CO$_2$. Leaf temperature was kept at 30ºC and leaf-to-air vapor pressure

deficit was maintained between 1 kPa and 2 kPa during all measurements. Gas exchange and chlorophyll fluorescence were first measured at a steady state of 400 µmol mol^{-1} CO_2. After a few minutes in steady state these parameters mentioned were measured at 50 µmol mol^{-1} CO_2 and after that, partial pressure in ambient air (C_a) was increased stepwise up to 1200 µmol mol^{-1} CO_2 and returned to its original value. The A_N–Cc curves were fitted based on the mechanistic model of CO_2 assimilation originally published by Farquhar et al. (1980), then later modified and developed by Sharkey (1985) and Harley et al. (1992). Net CO_2 assimilation (A_N), stomatal conductance (g_s), maximum ribulose 1,5-bisphosphatecarboxylase/oxygenase (Rubisco) carboxylation rate (V_{cmax}), regeneration of ribulose biphosphate (RuBP) controlled by electron transport rate (J_{max}) and the regeneration of RuBP controlled by the rate of triose-phosphate utilization (V_{TPU}) were determined by gas exchange. Leakage of CO_2 in and out of the leaf cuvette was measured and corrected according to Flexas et al. (2007).

Maximum quantum efficiency of photosystem II (PSII) was determined as $F_V/F_M = (F_M - F_0)/F_M$ by measuring the fluorescence signal from a dark-adapted leaf, being F_o the fluorescence signal when all reaction centers were open, using a low intensity pulsed measuring light source and during a pulse saturating light (0.7 s pulse of 8000 µmol photons m^{-2} s^{-1} of white light) and F_M the fluorescence signal when all reactions centers were closed. The actual photochemical efficiency of photosystem II (Φ_{PSII}) was calculated by measuring steady-state fluorescence (F_s) and maximum fluorescence during a light-saturating pulse of ca. 8000 µmol m^{-2} s^{-1} (F_M') following the procedures of Genty et al. (1989):

$$\Phi_{PSII} = (F_M' - F_s)/F_M'$$

Non-photochemical quenching was calculated as:

$$NPQ = (F_M - F_M')/ F_M'$$

The electron transport rate determined by chlorophyll fluorescence (J_{flu}) was then calculated as:

$$J_{flu} = \Phi_{PSII} \cdot PPFD \cdot \alpha \cdot \beta$$

where PPFD is the photosynthetically active photon flux density, α is leaf absorbance and β reflects the partitioning of absorbed quanta between photosystems II and I. The product $\alpha\beta$ was determined, following Valentini et al. (1995), from the relationship between Φ_{PSII} and Φ_{CO2} obtained by varying light intensity under non-photorespiratory conditions in an atmosphere containing less than 1% O_2.

Estimation mesophyll conductance by gas exchange and chlorophyll fluorescence.

Combining gas-exchange and Chl a fluorescence measurements, the mesophyll conductance to CO_2 (g_m) can be estimated according to Harley et al. (1992) as:

$$g_m = A_N/(C_i - (\Gamma^*(J_{flu}+8(A_N+R_d))/(J_{flu}-4(A_N+R_d))))$$

The Γ^* (chloroplast CO_2 concentration (C_c) at the CO_2 compensation point in the absence of mitochondrial respiration) was calculated from the Rubisco specificity factor (100 at 25°C for *Vitis* according to Bota et al., 2002) and corrected for leaf temperature following Epron et al. (1995) and Valentini et al. (1995). After 30 minutes of darkness R_d was measured in steady state and maintaining leaf temperature at 30°C.

Values obtained of g_m by calculations described before were used to convert A_N–C_i curves into A_N–C_c curves using the following equation:

$$C_c = C_i - (A_N/g_m)$$

Using values obtained from A_N–C_c curves, the maximum carboxylation capacity ($V_{c,max}$) and the maximum capacity for electron transport rate (J_{max}) were determinated using the temperature dependence of kinetic parameters of Rubisco described on a C_c basis by Bernacchi et al. (2002), whereby net assimilation rate is given as:

$$A_N = \min\{A_c, A_q\} - R_d$$

$$A_c = V_{cmax}(C_c - \Gamma^*)/(C_c + K_c[1 + (O/k_o)])$$

$$A_q = J(C_c - \Gamma^*)/4(C_c + 2\Gamma^*)$$

where A_c and A_q represent photosynthesis limited by carboxylation and RuBP regeneration, respectively, K_c and K_o are the Rubisco Michaelis–Menten constants for

carboxylation and oxygenation, respectively, and O is the leaf internal oxygen concentration (assumed equal to the external).

Quantitative limitation analysis

Light-saturated photosynthesis is generally limited by substrate availability at ambient CO_2 concentration. To compare the relative limitations to assimilation imposed by stomatal closure, decreased mesophyll conductance and damaged biochemistry in infected plants, the approach proposed by Grassi & Magnani (2005) with some modifications was used. This approach which needs the measurement of A_N, g_s, g_m, and $V_{c,max}$, allows the calculation of partition photosynthesis limitations into components related to stomatal conductance (S_L), mesophyll conductance (MC_L), and leaf biochemical characteristics (B_L), assuming that a reference maximum assimilation rate can be defined as a standard. In the current study, the maximum assimilation rate, associated with maximum g_s, g_m, and $V_{c,max}$, was generally reached by uninfected plants, therefore this value was used as a reference. Finally, non-stomatal limitations were defined as the sum of the mesophyll conductance and leaf biochemistry ($NS_L=MC_L+B_L$), while diffusive limitations were the sum of stomatal and mesophyll conductance components ($D_L=S_L+MC_L$).

Stomatal density

To determine stomatal density, areas of the abaxial side of six mature fully expanded leaves per treatment and cultivar were coated with clear nail enamel (Fisher, 1985), in between the principal nerves. Once the enamel was dry, the cast was stripped using clear tape and placed on microscope slides.

Stomata were counted from each cast at magnification of 200×. The microscope (model BX51, Olympus America Inc., Melville, N.Y.) was attached to a digital camera (U-TVO.5XC, Olympus) interfaced with a personal computer.

Photosynthetic pigments, Total soluble protein and Rubisco analysis

One leaf disc of 5.3 cm^2 from different plants of the experiment were collected and immediately frozen in liquid nitrogen. Five replicates per treatment were reduced to powder in a mortar with liquid nitrogen; 1 ml extraction buffer was added and mixed until the mixture was dissolved. The extraction buffer was composed of 100 mM N,N-

bis (2-hydroxyethyl) glycine (Bicine)-NaOH (pH 8), 11 mM Na-diethyl-dithio-carbonate (DIECA), 1 M dithiothreitol (DTT), 6% polyethylene glycol (PEG), 1% (v:v) protease inhibitor cocktail (sigma-Aldrich Co., St.Louis, Mo,USA). Extracts were centrifuged at 14.500 g, at 4ºC for 2 minutes.

In order to determine pigments, 50 μl of crude extract were diluted in 950 μl of ethanol and after 10 minutes in the dark, extracts were clarified by centrifugation (12000 g at 4ºC for 2 min.) and Chl a, Chl b and carotenoids were quantified by spectrophotometry and values obtained were used to determine the final pigment concentration according to Lichtenthaler & Wellburn (1983).

Leaf soluble protein concentration was obtained spectrophotometrically according to Bradford (1976). Aliquots of extracts obtained for pigment quantification were used for total protein content and Rubisco quantification. These aliquots contained 3.5 μg of leaf soluble proteins. They were loaded in 12.5% SDS-polyacrylamide gel to quantify the amount of Rubisco by quantitative electrophoresis by densitometry. Total proteins were divided by 0.75 mm thick of SDS-PAGE gel (12.5% resolving and 5% stacking). After that the gels were fixed in a mixture with water, methanol and acetic acid for 1 hour, spotted in EZ Blue Gel Staining (Sigma) solution for 1 hour, and finally washed in water to eliminate excess stain. Gels were taken with a Chemidoc XRS densitometer (Bio-Rad) and images were processed by software Quantity one 1-D (Bio-Rad).

Respiration and oxygen-isotope fractionation measurements

One leaf disc of 10 cm^2 per plant was harvested, weighed and placed in a 3 ml stainless-steel closed cuvette that was maintained at 25°C using a copper plate and a copper coil connected to a temperature-controlled water bath.

Respiration and oxygen-isotope fractionation measurements were done as described in Florez-Sarasa et al. (2007) with some modifications. Each measurement was performed in approximately 75 min; values of the isotope ratios between m/z 34/32 ($^{18}O_2/^{16}O_2$) and m/z 32/28 ($^{16}O_2/^{28}N_2$) were determined from a standard and the sample air via dual-inlet analysis with six replicate cycles. Calculations of the oxygen-isotope fractionation were made according to Ribas-Carbo et al. (2005), and the electron partitioning between the two pathways in the absence of inhibitors was obtained as

described by Guy et al. (1989). The r^2 values of all unconstrained linear regressions between –ln f and ln ($R/R0$), with at least five data points, were close to 0.995 (Ribas-Carbo et al., 1997). In order to obtain the oxygen isotope fractionation of the alternative oxidase pathway (Δ_a), leaf discs were incubated for 30 min between medical wipes soaked with a water solution of 10 mM potassium cyanide (KCN), and the mean ± SE value obtained was of 30.9 ± 0.07‰. For the oxygen isotope fractionation of the cytochrome oxidase pathway (Δ_c), leaf discs were cut into 2- to 4-mm slices to facilitate the inclusion of the reagent into the tissues, and incubated for 30 min in 25 mM salicylhydroxamic acid (SHAM) solution; the mean ± SE value obtained was of 20.0 ± 0.2‰. All stock solutions were freshly prepared before use. Finally, the total mitochondrial ATP synthesis rate was calculated according to Noguchi et al. (2001).

Microscopy

In 2013, two small leaf pieces 1x1 mm were collected from three plants per treatment cutting between the main veins of the leaves. The leaf material was immediately fixed under vacuum with 4% glutaraldehyde and 2% paraformaldehyde in 0.1 M phosphate buffer (pH 7.2). Once the primary fixation was done, the tissue was washed three times in the same buffer used in the prior step. After that, samples were fixed in 1% osmium tetroxide between 1 to 2 hours (h) and dehydrated in a graded ethanol series (from 30% to absolute ethanol). Afterwards ethanol was replaced by propylene oxide and washed three times. The solvent propylene oxide was mixed with Spurr's resin (Monocomp Instrumentación, Madrid, Spain) and placed into vials with the dehydrated segments. Slowly, the resin-solvent ratio was increased until sheer Spurr's resin was employed. The pure resin specimens were put into moulds and preserved in an oven at 60ºC for 48 h. The semi-thin (0.8 μm) cross sections were cut with an ultramicrotome (Reichert & Jung model Ultracut E).

Semi-thin cross sections (0.8 μm) were stained with 1% toluidine blue and observed under Olympus light microscope BX60. Pictures were captured at 200x magnifications with a digital camera (U-TVO.5XC, Olympus) to measure the thickness of epidermal layers, spongy mesophyll and palisade, and whole leaf thickness.

$$f_{ias}=1-(\ \Sigma S_s/T_{mes}\ w)$$

The total cross sectional area of mesophyll cells (ΣSs), the width of the section (w) and the mesophyll thickness between the two epidermises (T_{mes}), are required to determine the volume fraction of intercellular air spaces.

All images were processed with Image analysis software (Image J; Wayne Rasband/NIH, Bethesda, MD, USA) in 4-6 different fields of view, making ten measurements for spongy tissue and ten for palisade parenchyma cells for each anatomical trait.

Abscisic acid, jasmonic acid and salicylic acid quantification.

The sap of each plant was extracted at mid-morning using a Scholander chamber (Soil Moisture Equipment Corp., Santa Barbara, CA, USA). Between 15 and 25 µl of leaf sap were collected from leaf petioles with a pipette, after applying 0.2 MPa more than the pressure needed for extracting the first drop sap. Sap was put into a 1.5 ml tube and immediately frozen in liquid nitrogen. The eppendorfs with leaf sap were sent to IVICAM (*Instituto de la Vid y el Vino de Castilla-La Mancha*), where the analysis was carried out. The samples were diluted three folds with Milli-Q water. The analysis of abscissic acid (ABA), jasmonic acid (JA), and salicylic acid (SA) phytohormones were performed by HPLC-ESI-MS/MS using a Agilent 1200 Series HPLC system (Agilent, Santa Clara, California, USA), coupled to an 3200 QTRAP (Applied Biosystems, California, USA). Chromatographic separation was carried out on a reversed-phase column Ascentis Express C18 (4.6 mm x 150 mm; 2.7 µm particle size; Agilent), thermostatized at 16 ºC. The solvent A was water/methanol/formic acid (97:2:1, v/v/v) and the solvent B was methanol 100%. The linear gradient for solvent B was as follows: 0 min, 50%¸1 min 50%; 14 min, 80%; 24 min, 90%; 26 min, 50%; 30 min, 50%. The flow rate was 0.3 ml min^{-1}, and the injection volume was 30 µl.

The quantification of the phytohormones was made using Multiple Reaction Monitoring (MRM) of ion pairs appropriated for each compound. The transitions used was: SA 137 > 93 and 137>65; ABA 263 > 153 and 263 > 219; JA 209 > 59 and 209 > 165.

The electrospray ionization was operated in negative mode in the following conditions: Temperature 400°C, Ion source gas 1, 50 psi, Ion source gas 2, 30 psi, Ion spray voltage -4500 V, curtain gas 15 psi, collision gas setting high; DP (-30 V), CXP (-

1). The following parameters were specific for each compound: SA EP -5, CE -40; ABA EP -12, CE -20; JA EP -5, CE -20.

Statistical analysis

The data was analysed using R (http://.rproject.org/). T-Student, one-way ANOVA and LSD tests were used for determining differences in between the treatments for the parameters measured.

RESULTS

Climatic conditions

According to mean daily temperatures recorded in 2012 and 2013 from May to September, those years were very different.
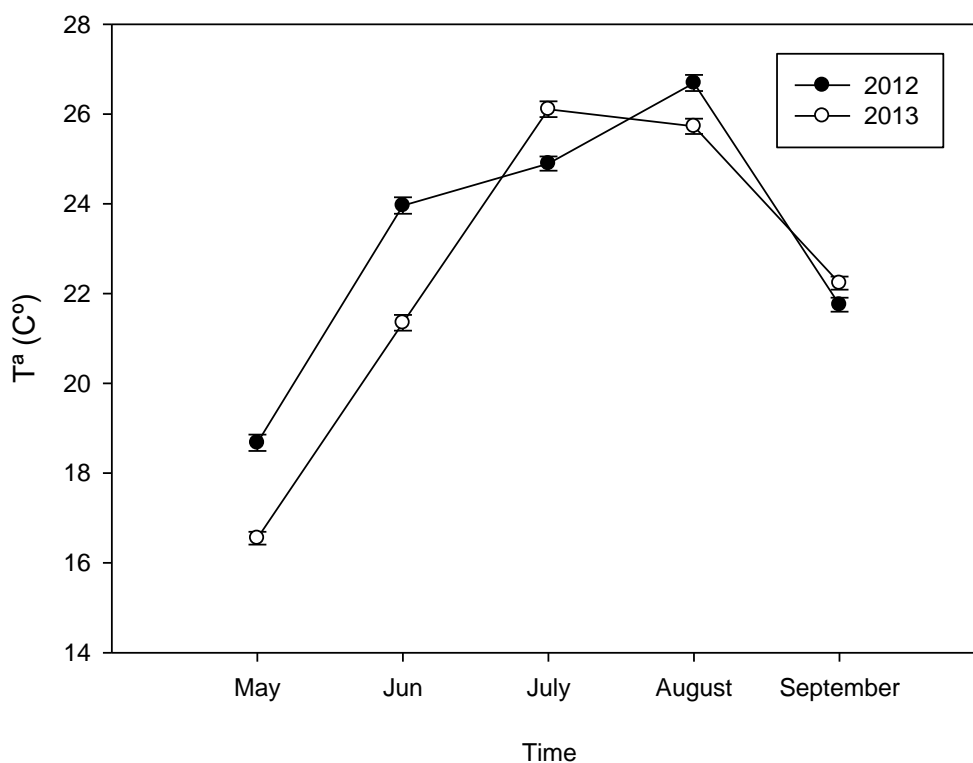
Figure 1. Mean daily temperature (ºC) recorded from May to September in 2012 and 2013. Vertical bars indicate standard error of the means.

The temperatures were significantly lower by 2ºC in 2013 in May and June compared with 2012. However, in July of 2013 the temperature was 2ºC higher than July 2012. Therefore, in 2013 the mean temperature increased was 4.8ºC from June to July, while in 2012 that increase was 0.8ºC. From July to August, the temperature decreased by 0.5ºC in 2013, while it increased by 1.8ºC in 2012. Despite the seasonal differences in 2012 and 2013 the mean temperature in September was close to 22ºC (Figure 1).

Virus diagnosis and absolute quantification by SYBR green one-step RT-PCR assay.

None of potted-grown virus-free and GLRaV-3 infected plants showed symptoms of leafroll disease. GLRaV-3 was detected by ELISA and RT-qPCR and was found to be present in all infected plants, while none of the tested viruses was detected in non-infected ones. For the absolute quantification of viral genome units, specific standard curves were obtained by running three 10-fold serial dilutions of *in vitro* transcribed RNA. For the absolute quantification of GLRaV-3 the correlation coefficient (R^2) of the standard curve was 1 and 83.1% was the reaction efficiency (Figure 2). Samples were amplified in RT-qPCR reactions together with at least three dilutions of the specific *in vitro* transcribed target RNA. No amplification was obtained in the absence of template RNA (water control), in the RT-PCR mix devoid SYBR Green (not shown) nor when total RNA from plants singly infected with any of the viruses not under test was used as a template.

Specific GLRaV-3 *RdRp* amplicons were obtained, with Ct values within the dynamic range of the standard curve, ranging between 19.5 and 32.2, corresponding to 10^6 and 10^2 GLRaV-3 genome units, respectively (Figure 2).
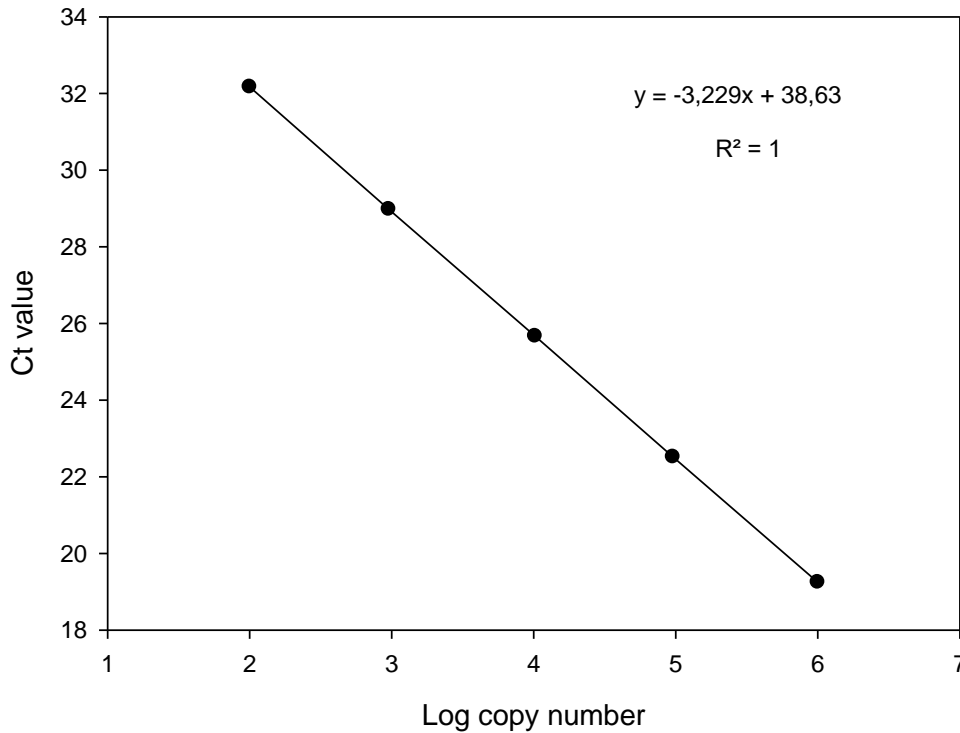
Figure 2. Amplification efficiency and dynamic range of amplification of GLRaV-3 *RdRp*. Mean quantification cycle values were obtained from serial Log_{10} dilutions of reverse transcribed synthesized viral template RNAs with known log copy number. Ct = cycle threshold.

Significant differences were found in viral concentration values obtained for GLRaV-3 between the different samplings in 2012 and 2013 (Figure 3). Viral concentration in Malvasía de Banyalbufar plants was 10% higher in August cultivar than in July in 2012, however in 2013 the virus concentration decreased by 12% in August compared with July. The lower virus concentration in 2013 matched with the highest observed in 2012. The maximum virus concentration, 6.0 Log virus copy numbers, was observed in July 2013. In Cabernet Sauvignon plants, the virus concentration was very low, below the values obtained in Malvasía de Banyalbufar cv. In this case the virus concentration also diminished from July to August around 16%, with minimum values around 3.5 Log virus copy numbers (Figure 3).
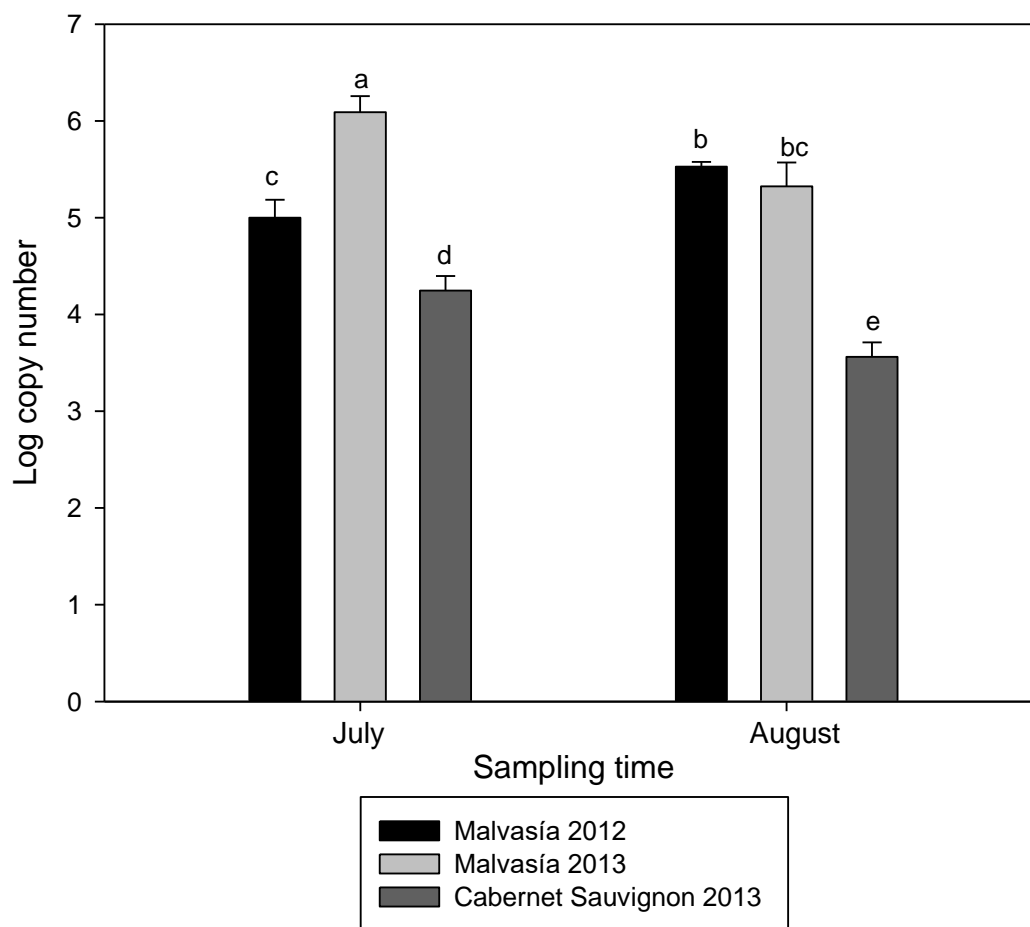
Figure 3. Virus concentration (Log copy number) of *Grapevine leafroll-associated virus 3* (GLRaV-3) in leaves of Malvasía de Banyalbufar and Cabernet Sauvignon cultivars in two sampling times, July and August, in 2012 and 2013. Mean population of the virus was expressed as $\log_{10}$ of the viral copy numbers per 70 mg of leaves, collected from middle sections of grapevine shoots, used in the RNA extractions. Vertical bars indicate standard error of the means. Figures were obtained from five replicates for each treatment (different letters indicate significant differences at $P = 0.05$, LSD test).

Water status and growth parameters

Both treatments presented similar water status during both experimental years. Pre-dawn leaf water potential was always kept above –0.2 MPa.

There were not significant differences in shoot length and number of leaves per plant between infected and non-infected plants (Table 3). Total leaf area values were very similar throughout the growing season in both years and in both cultivars, with the

exception of July 2013 when leaf expansion of non-infected plants of Malvasía de Banyalbufar cv. was significantly higher (P<0.05) than infected ones (71.34±9.39 cm^2 and 44.37±10.27 cm^2 respectively). However, this difference was not significant at the end of the growing period (Table 3).

Table 3. Total increment of leaves per shoot, shoot length and total leaf area, in each cultivar studied, Malvasía de Banyalbufar and Cabernet Sauvignon, for non-infected (GLRaV-3 (-)) and virus infected (GLRaV-3 (+)) plants, during the summer of 2012 and 2013. ns denote no significant difference at P=0.05. Figures were obtained from five replicates for each treatment.

Cultivar	Year	Treatment	Δ Leaves per shoot	Δ Shoot lenght (cm)	Δ total leaf area (cm^2)
Malvasía	2012	GLRaV-3 (-)	10.7±1.3	89.8±11.2	1265.4±142.5
		GLRaV-3 (+)	10.1±1.4	105.9±14.8	1265.8±98.5
Significance			ns	ns	ns
	2013	GLRaV-3 (-)	12.2±1.3	93.4±12.9	1634.0±222.3
		GLRaV-3 (+)	12.0±1.1	112.5±16.1	1164.8±160.1
Significance			ns	ns	ns
Cabernet	2013	GLRaV-3 (-)	18.0±1.0	75.1±4.5	2212.3±83.2
Sauvignon		GLRaV-3 (+)	17.3±2.3	64.7±11.5	2286.0±42.2
Significance			ns	ns	ns

Photosynthetic parameters and limitation analysis.

In Cabernet Sauvignon cv. no significant differences were observed between non-infected and infected plants in any of the photosynthetic parameters determined. In Malvasía de Banyalbufar cv., net photosynthesis in non infected plants was higher than in GLRaV-3 infected ones. The infection caused a reduction of 32% in the assimilation rates in July of both years. The difference was even higher in August, with a A_N reduction of 34% in 2012 and 50% of reduction in 2013 (Figure 4). In relation to CO_2 diffusion, g_s was reduced between 30-43% in GLRaV-3 infected plants in both periods and years; in August of 2012 this reduction was not statistically significant (Figure 4). Stomatal density did not differ between treatmentes in July (195±8 stomata per mm^2 and 202±12 stomata per mm^2, for GLRaV-3 infected and non infected plants respectively) either in August (196±6 stomata per mm^2 and 200±4 stomata per mm^2, for GLRaV-3 infected and non infected plants respectively). Reductions between 30-50%

on g_m were also measured in GLRaV-3 infected plants. This difference was significant only in August of 2012 (Figure 4).
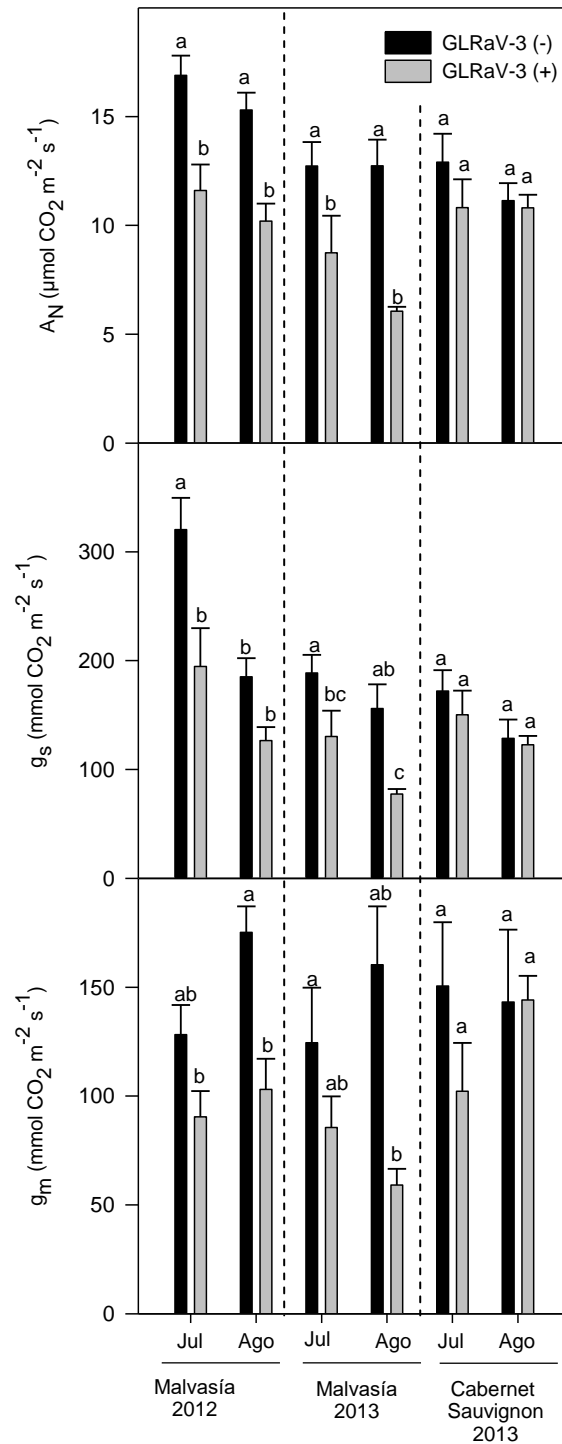
Figure 4. Net CO2 assimilation (A_N), stomatal conductance (g_s) and mesophyll conductance (g_m), in Malvasía de Banyalbufar and Cabernet Sauvignon, for non-infected (GLRaV-3 (-)) and virus infected (GLRaV-3 (+)) plants, during the summer of 2012 and 2013. Figures were obtained from five replicates for each treatment (different letters indicate significant differences at $P = 0.05$, LSD test).

In both periods and years, infected vs. non-infected Malvasía de Banyalbufar plants presented differences in A_N-C_i curves. A_N-C_i curves from Cabernet Sauvignon plants did not differ (Figure 5).
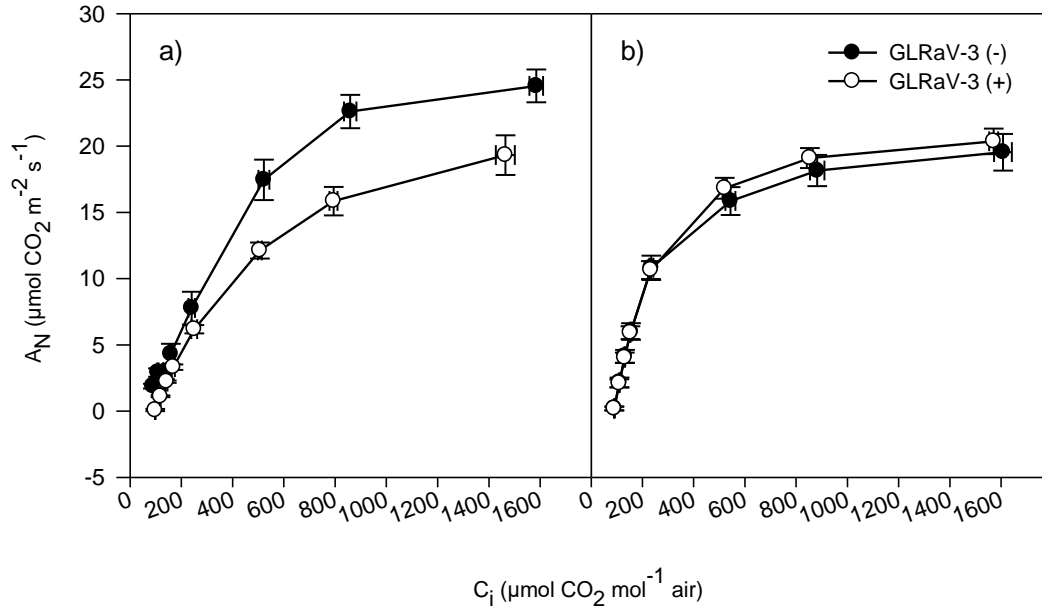
Figure 5. Example of results obtained in the relationship between net CO_2 assimilation (A_N) and substomatal CO_2 concentration (C_i) in potted-grown non-infected (GLRaV-3 (-)) and virus infected (GLRaV-3 (+)) *Vitis vinifera* L. plants, at the beginning of July 2013 in Malvasía de Banyalbufar plants (a) and at the same period in Cabernet Sauvignon plants (b).

In the estimation of mesophyll conductance, A_N-C_i curves were transformed to A_N-C_c curves. Parameters derived from A_N-C_c curves, V_{cmax} and J_{max} were significantly higher in non-infected Malvasía de Banyalbufar plants in both growth periods than infected ones in 2012, while V_{TPU} did not change (Table 4). The following year the results were very similar, otherwise the variability of values obtained in the different plants of the same treatment was higher, thus there was only significant differences J_{max} measured in August.

Table 4. Maximum ribulose 1, 5-bisphosphatecarboxylase/oxygenase (Rubisco) carboxylation rate (V_{cmax}), regeneration of ribulose biphosphate (RuBP) controlled by electron transport rate (J_{max}) and the regeneration of RuBP controlled by the rate of triose-phosphate utilization (V_{TPU}) in noninfected (GLRaV-3 (-)) and virus infected (GLRaV-3 (+)) plants of Malvasía de Banyalbufar and Cabernet Sauvignon cultivar, in July and August 2012 and 2013, estimated for A_N-C_c curves. There are five replicates per treatment in each period (letters; P = 0.05, LSD test).

Year			2012		
Cultivar	Month	Treatment	V_{cmax}	J_{max}	V_{TPU}
			(μmol CO_2 m^{-2} s^{-1})	(μmol CO_2 m^{-2} s^{-1})	(μmol CO_2 m^{-2} s^{-1})
Malvasía	July	GLRaV-3 (-)	196.4±10.7a	125.4±9.1ab	5.9±0.4a
		GLRaV-3 (+)	143.5±6.0b	85.8±8.9c	5.1±0.5a
	August	GLRaV-3 (-)	162.3±8.6a	146.2±9a	6.9±0.4a
		GLRaV-3 (+)	130.8±7.3b	108.7±9.9bc	5.2±0.5a
Year			2013		
Cultivar	Month	Treatment	V_{cmax}	J_{max}	V_{TPU}
			(μmol CO_2 m^{-2} s^{-1})	(μmol CO_2 m^{-2} s^{-1})	(μmol CO_2 m^{-2} s^{-1})
Malvasía	July	GLRaV-3 (-)	210.7±21.2a	151.0±12.0a	7.6±1.1a
		GLRaV-3 (+)	169.28±25.4ab	120.4±15.3ab	6.2±0.7a
	August	GLRaV-3 (-)	196.7±24.8ab	146.1±15.9a	6.7±0.7a
		GLRaV-3 (+)	129.59±9.9b	99.8±12.6b	5.4±0.3a
Cabernet Sauvignon	July	GLRaV-3 (-)	231.79±12.9a	145.49±4.3a	7.43±0.9a
		GLRaV-3 (+)	225.95±29.5a	138.89±12.35a	7.32±0.7a
	August	GLRaV-3 (-)	225.04±19.6a	129.4±9.4a	5.6±0.5a
		GLRaV-3 (+)	208.22±15.4a	125.1±7.4a	6.4±0.4a

The fluorescence measurements of leaves previously exposed to sunlight corroborate that J_{flu} significantly decreased due to the effect of the presence of virus (Table 5). The reduction percentage was 27% in all the cases. On the other hand, F_V/F_M and NPQ did not change significantly at any time.

Table 5. The maximum quantum efficiency of photosystem II (PSII) (F_V/F_M), the electron transport rate (J_{flu}) and non-photochemical quenching (NPQ) in non-infected (GLRaV-3 (-)) and virus infected (GLRaV-3 (+)) plants of Malvasía de Banyalbufar and Cabernet Sauvignon cultivar, in July and August 2012 and 2013. There are five replicates per treatment in each period (letters; P = 0.05, LSD test).

Year				2012	
Cultivar	Month	Treatment	F_V/F_M	J_{flu}	NPQ
				(µmol e$^-$ m^{-2} s^{-1})	
Malvasía	July	GLRaV-3 (-)	-	167.1±10.9a	-
		GLRaV-3 (+)	-	121.2±7.0b	-
	August	GLRaV-3 (-)	-	122.4±7.7b	-
		GLRaV-3 (+)	-	88.8±4.4c	-
Year				2013	
Cultivar	Month	Treatment	F_V/F_M	J_{flu}	NPQ
				(µmol e$^-$ m^{-2} s^{-1})	
Malvasía	July	GLRaV-3 (-)	0.794±0.005a	151.1±12.8a	2.37±0.22a
		GLRaV-3 (+)	0.797±0.002a	115.1±15.9ab	2.74±0.20a
	August	GLRaV-3 (-)	0.806±0.026a	148.4±18.1a	2.45±0.20a
		GLRaV-3 (+)	0.791±0.017a	88.4±9.9b	2.41±0.10a
Cabernet Sauvignon	July	GLRaV-3 (-)	0.804±0.003a	148.1±5.1a	2.77±0.15a
		GLRaV-3 (+)	0.800±0.002ab	138.7±13.7a	2.53±0.13a
	August	GLRaV-3 (-)	0.789±0.005b	131.9±8.7a	2.60±0.08a
		GLRaV-3 (+)	0.792±0.003b	133.9±9.7a	2.41±0.27a

The limitation analysis to photosynthesis was done for Malvasía de Banyalbufar cv.. In July 2012, the analysis revealed that virus induced a total limitation (T_L) of 30%. The components of the total limitation, stomatal (S_L), mesophyll (MC_L) and biochemistry limitation (B_L) were very similar, with a 9, 11 and 10% respectively (Figure 6). In August 2012 S_L increased 2%, M_L and B_L decreased 1% and 2% respectively, throughout the summer. In 2013, the total limitation in plants infected by the virus was 32% in July and 46% in August. In July S_L was 12%, MC_L 11% and B_L 9%. In August S_L and M_L increased 5%, and B_L increased 4%.
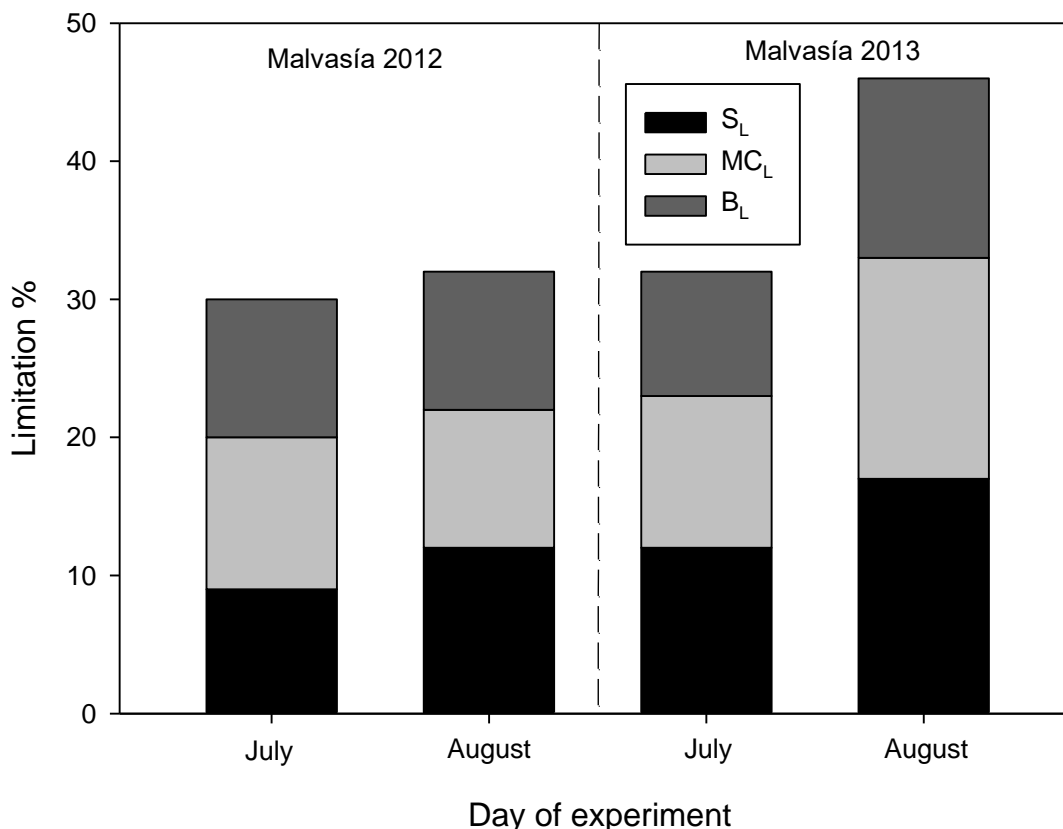
Figure 6. Total limitation to the photosynthesis (Limitation %), presented as the sum of the percentage of stomatal conductance limitation (S_L), mesophyll conductance limitation (MC_L) and biochemistry limitation (B_L), in non-infected (GLRaV-3 (-)) and virus infected (GLRaV-3 (+)) plants of Malvasía de Banyalbufar cultivar, in July and August 2012 and 2013.

Photosynthetic pigments, total soluble protein and Rubisco content.

There were no changes in pigments, soluble proteins and Rubisco content due to GLRaV-3 infection between treatments in 2012 (Table 6). Both treatments improved soluble protein values and Rubisco content in August (Table 6). In 2013, no differences were observed in most of the parameters described above in both cultivars. The only difference was found in August, where infected plants of Malvasía de Banyalbufar cv. showed less Rubisco content.

Table 6. Chlorophyll content (Chl a+b), carotenoids content, total soluble protein, Rubisco concentration in non-infected (GLRaV-3 (-)) and virus infected (GLRaV-3 (+)) plants of Malvasía de Banyalbufar and Cabernet Sauvignon cultivar, in July and August 2012 and 2013. There are five replicates per treatment in each period (letters; P = 0.05, LSD test).

Year				2012		
Cultivar	Month	Treatment	Chl a+b (mg g^{-1})	Carotenoids (mg g^{-1})	Soluble protein (mg g^{-1})	Rubisco (mg g^{-1} SP)
Malvasía	July	GLRaV-3 (-)	1.5±0.2b	0.35±0.04b	35.8±1.9b	175.1±30.1b
		GLRaV-3 (+)	1.9±0.2ab	0.43±0.03ab	37.1±1.4b	180.1±30.1b
	August	GLRaV-3 (-)	2.7±0.1a	0.58±0.03a	51.3±3.9a	240.1±41.2ab
		GLRaV-3 (+)	2.1±0.3ab	0.44±0.09ab	54.3±2,8a	290.1±22.2a
Year				2013		
Cultivar	Month	Treatment	Chl a+b (mg g^{-1})	Carotenoids (mg g^{-1})	Soluble protein (mg g^{-1})	Rubisco (mg g^{-1} SP)
Malvasía	July	GLRaV-3 (-)	2.0±0.5a	0.32±0.10a	51.4±3.5a	137.4±11.6b
		GLRaV-3 (+)	1.8±0.2a	0.31±0.06a	41.0±2.8a	160.4±18.7b
	August	GLRaV-3 (-)	1.5±0.4a	0.20±0.03a	57.0±8.8a	305.7±14.4a
		GLRaV-3 (+)	1.3±0.2a	0.25±0.03a	53.0±7.1a	158.3±12.2b
Cabernet Sauvignon	July	GLRaV-3 (-)	2.3±0.4a	0.41±0.07a	48.8±2.8b	106.7±14.0ab
		GLRaV-3 (+)	2.2±0.7a	0.40±0.11a	43.7±5.2b	94.2±6.5b
	August	GLRaV-3 (-)	1.6±0.2a	0.32±0.05a	69.0±4.7a	86.7±2.0b
		GLRaV-3 (+)	1.4±0.4a	0.27±0.07a	66.3±9.2a	174.4±38.8a

In Cabernet Sauvignon plants, measured only in 2013, Rubisco content was 48% higher in GLRaV-3 infected plants than in non infected ones, in August.

Respiration

No significant differences on total respiration and the activities of COX and AOX pathways were observed between infected and non-infected leaves of Cabernet Sauvignon plants. On the other hand, total respiration was 30% lower in leaves of infected Malvasía de Banyalbufar plants measured in July (Figure 7). Such reduction in respiration was mainly due to a significant 23% reduction of the *in vivo* COX pathway activity while AOX pathway remained unaltered (Figure 7). Due to the predominant contribution of COX on the ATP synthesis, the calculated ATP synthesis rate was then also 27% lower in GLRaV-3 infected plants (69.71±2.88 nmol ATP g^{-1} s^{-1}) than in non infected ones (95.40±10.88 nmol ATP g^{-1} s^{-1}).
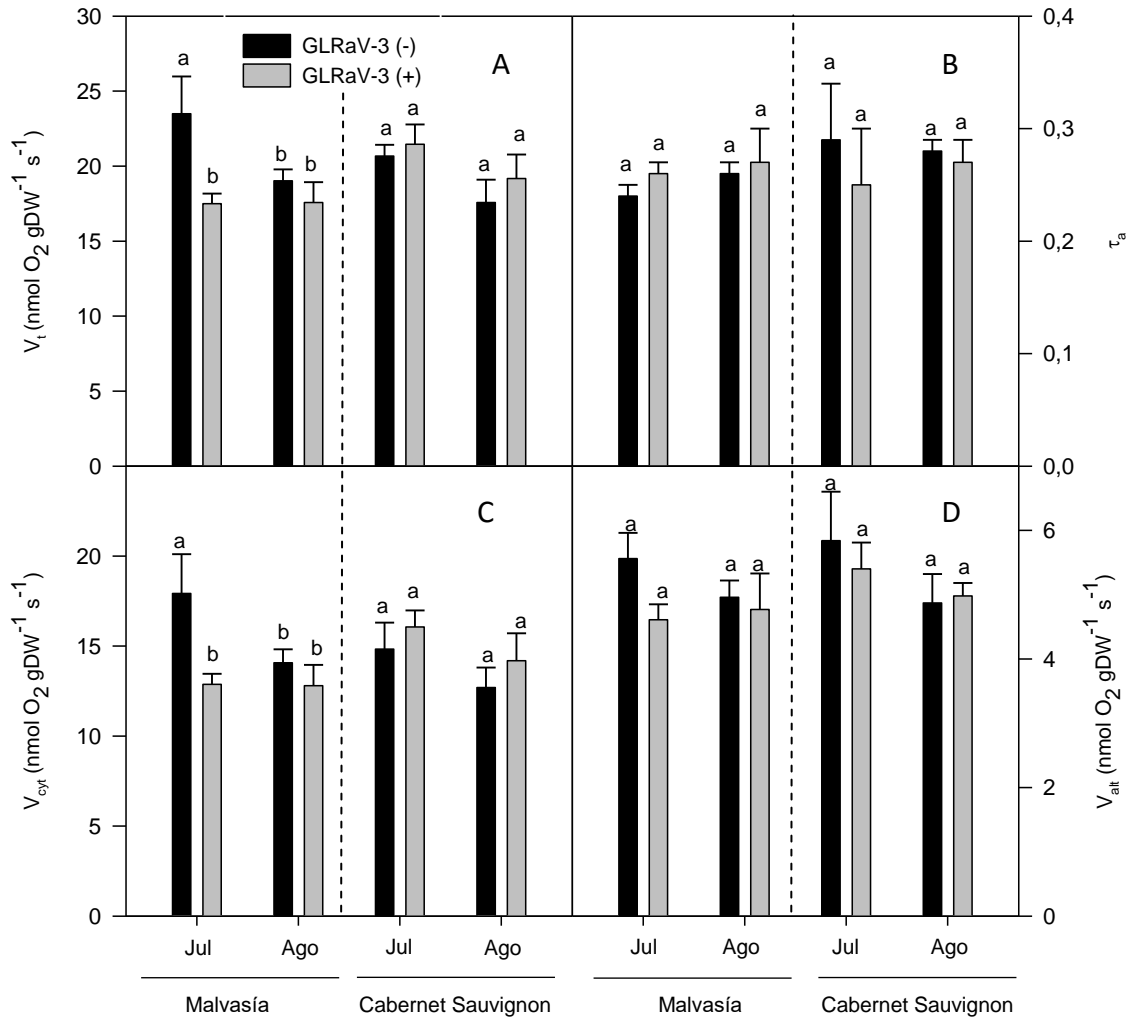
Figure 7. A. Total oxygen uptake rate (V_t), B. the electron partitioning through the alternative pathway (τ_a), C. activity of the cytochrome oxidase pathway (V_{cyt}) and D. activity of the alternative oxidase pathway (V_{alt}) in non-infected (GLRaV-3 (-)) and virus infected (GLRaV-3 (+)) plants of Malvasía de Banyalbufar and Cabernet Sauvignon cultivar, in July and August 2013. There are five replicates per treatment in each period (letters; $P = 0.05$, LSD test).

Anatomy and hormone response

There were differences in the anatomic parameters measured between treatments, mainly in Malvasía de Banyalbufar plants. Leaves of GLRaV-3 infected plants were 20% thicker than the non infected ones (Table 7). Besides this, significant differences in the two leaf layers were observed. Upper and lower epidermis, pallisade and spongy mesophyll of the leaves in the infected plants were significantly thicker. However, no significant differences were observed in the percentage of porosity in the pallisade and spongy mesophyll, as well as in leaf mass area (LMA). In Cabernet Sauvignon plants the upper epidermis, the pallisade mesophyll and the mesophyll

thickness were also modified by the virus, being thicker in the infected plants. Otherwise, the percentage of increased in thickness was 5% (Table 7).

Table 7. Leaf mass area (LMA), leaf thickness, upper epidermis thickness, lower epidermis thickness, pallisade mesophyll thickness, spongy mesophyll thicknes, mesophyll thickness, % porosity pallisade and % porosity spongy in non-infected (GLRaV-3 (-)) and virus infected (GLRaV-3 (+)) plants of Malvasía de Banyalbufar and Cabernet Sauvignon cultivar, in July 2013. There are five replicates per treatment in each period (letters; P = 0.05, LSD test).

	Malvasía			Cabernet Sauvignon		
	GLRaV-3 (-)	GLRaV-3 (+)	Sig.	GLRaV-3 (-)	GLRaV-3 (+)	Sig.
LMA (g m^{-2})	53.5±5.0	69.8±7.5	ns	61.2±2.4	61.1±4.6	ns
Leaf thickness (μm)	150.3±1.6	187.2±1.2	***	163.9±1.9	172.8±4.4	*
Upper epidermis thickness (μm)	11.3±0.2	15.7±0.6	***	11.6±0.4	12.7±0.5	ns
Lower epidermis thickness (μm)	10.3±0.3	13.9±0.5	***	12.4±0.5	12.0±0.4	ns
Pallisade mesophyll thickness (μm)	65.9±1.2	69.6±1.7	**	61.4±1.6	70.8±1.8	***
Spongy mesophyll thicknes (μm)	64.2±1.0	89.9±1.6	***	77.4±1.6	78.2±2.6	ns
Mesophyll thickness (μm)	127.1±1.6	159.5±1.2	***	138.8±2.2	148.8±4.2	*
%Porosity pallisade	8.8±2.1	7.1±1.1	ns	3.5±0.6	3.8±0.8	ns
%Porosity Spongy	17.3±2.2	22.5±3.4	ns	21.2±2.4	20.3±2.1	ns

In 2013 ABA, SA and JA, hormones involved in plant defense response, were determined in both cultivars. Even though seasonal differences were observed in ABA and SA, no significant differences were observed between GLRaV-3 infected and non infected plants in hormone content in any cultivar and period (Figure 8).

Figure 8. ABA, SA and JA concentration in non-infected (GLRaV-3 (-)) and virus infected (GLRaV-3 (+)) plants of Malvasía de Banyalbufar and Cabernet Sauvignon cultivar, in July and August 2013. There are five replicates per treatment in each period (letters; P = 0.05, LSD test).

DISCUSSION

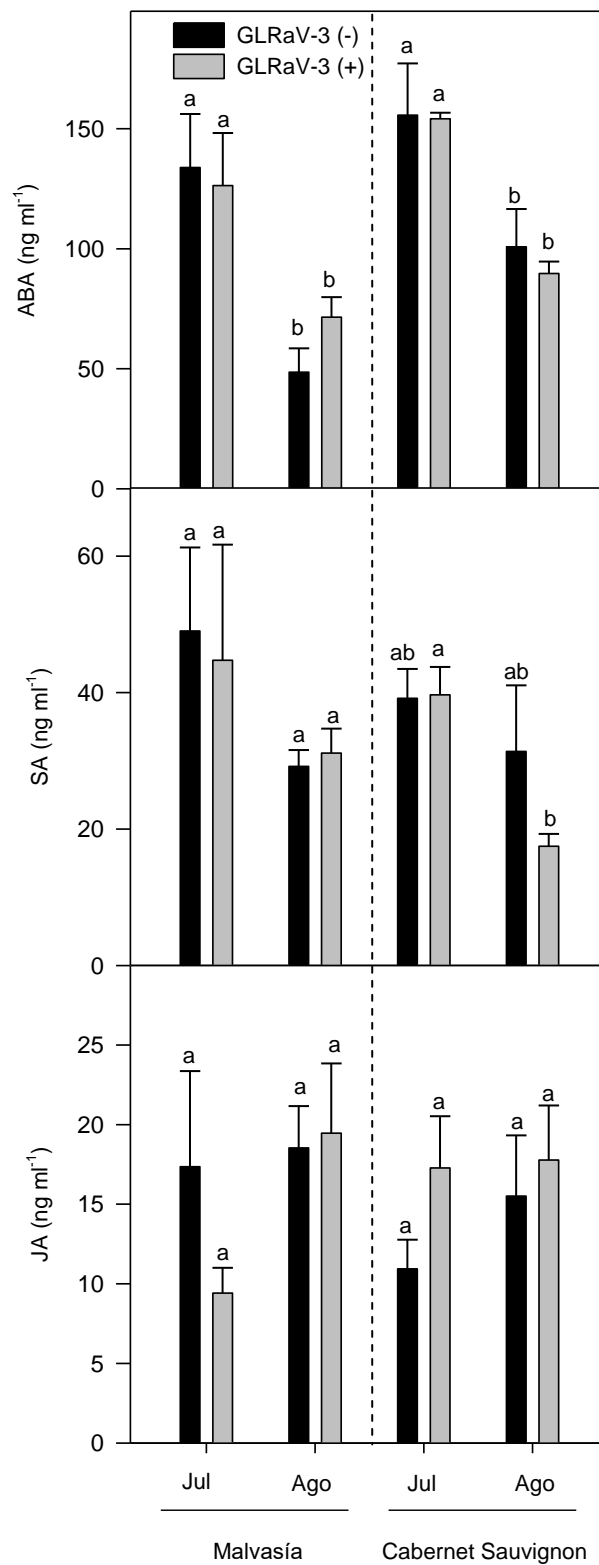Prevention and control of viruses are critical, as there is no cure for virus infected grapevines. The possibility of absolute quantification of GLRaV-3 genomes enables there to be a greater understanding of plant physiological consequences due to viral infections. To our knowledge, none of the previous studies on GLRaV-3 effects on grapevine performance determined the virus amount. Some of them have compared symptomatic with asymptomatic infected leaves (Moutinho-Pereira et al., 2012; Endeshaw et al., 2014), but in some cases, as in white cultivars, the symptoms may be subtle or non-existent, requiring proper experiments to demonstrate the effects of the virus. Sampol et al. (2003) compared young low-level infected with old highly infected plants determined by ELISA. The present work is the first time that an absolute quantitative determination of the GLRaV-3 has been carried out in order to determine its effects on grapevine physiology. Moreover, the absolute quantification is the only way to compare between seasons or tissues. By doing this it has enabled the authors to relate results from different studies (Tsai et al, 2012; Velasco et al., 2014 (Chapter 3), Gambino et al., 2012).

The results confirmed that GLRaV-3 viral population may vary during the growing season (Tsai et al., 2012; Velasco et al., 2014 (Chapter 3)), indicating that climate conditions and phenology status of the plant determine virus movement and concentration. Even though Cabernet Sauvignon cv. presented the lowest virus concentration; the trend of viral population in both cultivars during summer 2013 was similar, with higher concentration in July than in August. Surprisingly the previous results in 2012 showed a completely opposite trend with an increase in virus population during the season. This different trend between both years can be attributed to differences in mean daily temperatures during the growing seasons. During summer of 2012, the highest value mean daily temperature was registered in August, while in 2013 was slightly lower and registered in July (Figure 1). These periods of high temperatures correspond to highest virus concentrations measured in each cultivar (Figure 3). These results do not concern with those obtained by Gambino et al. (2012) on work on *Grapevine Rupestris Stem Pitting associated Virus* (GRSPaV), where warm temperatures were associated with low virus concentration. In addition, it has been pointed out that high temperatures in the field can act as natural thermotherapy, stopping virus replication (Valero et al., 2003; Bota et al., 2014). However, in the

present study it seems that changes observed in virus concentration were affected mainly by the temperature of the previous month to the sampling day. As it was mentioned before, Cabernet Sauvignon had lower virus concentration than Malvasía de Banyalbufar cv., probably being the reason of the absence of virus effects on the parameters measured in the first one.

The results showed that A_N is one of the main parameters affected by the virus and figure 9A shows how A_N reduction is correlated to virus amount. This A_N reduction was accompanied by a reduction in g_s in Malvasía de Banyalbufar infected plants (Figure 4), as it was reported in other studies (Cabaleiro et al., 1999; Bertamini et al., 2004).
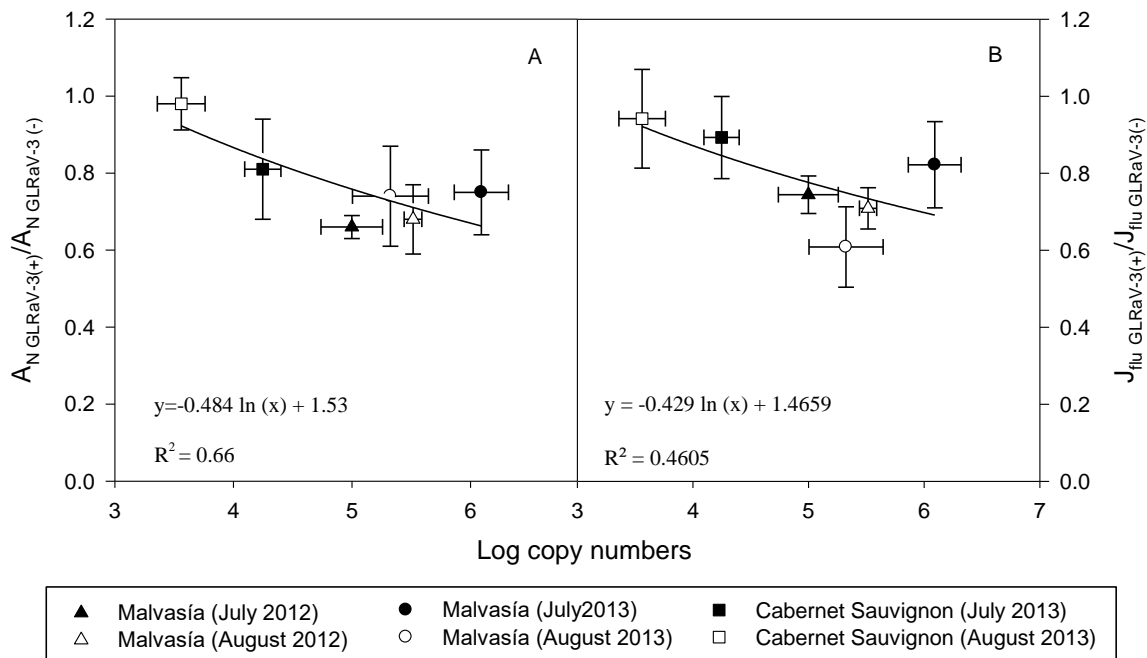
Figure 9. A. Correlation between the ratio net CO_2 assimilation rate (A_N) from infected plants (GLRaV-3 (+)) and non-infected plants (GLRaV-3 (-)), and the log copy numbers of the virus. B. Correlation between the ratio electron transport rate (J_{flu}) from infected plants (GLRaV-3 (+)) and non-infected plants (GLRaV-3 (-)), and the log copy numbers of the virus. A_N and J_{flu} were expressed as the ratio of the value of each replicate of infected plants divided for the corresponding mean of the non-infected plants for each cultivar, treatment and period of measurements.

The results showed that g_s reductions cannot be attributed to plant water status or increases in ABA content (Figure 8) as there were no statistically significant differences. Previous studies showed that the infection by GLRaV-3 was related to increases in ABA-responsive genes expression (Espinoza et al., 2007). ABA is

implicated in the disease-resistance response more directly than expected, and ABA action in the defense system is under spatial and temporal regulation (Asselbergh et al., 2008; Ton et al., 2009). Otherwise, no significant changes were observed in other hormones involved in the plant defense response, such as Salycilic Acid (SA) and Jasmonic Acid (JA) (Figure 8) (Whitham et al., 2006). Also, there were no differences in the number of stomata in either of the cultivars or between the time periods of measurements, thus the reduction in g_s is due to stomatal closure. There may be other factor affecting g_s such as hydraulic conductance. Even if the plant is in good water status, carbon metabolism and hydraulics are coupled via multiple interactions, therefore virus effects on A_N could lead to effects on hydraulic conductance and stomatal closure (McDowel, 2011).

Decreased CO_2 diffusion through the mesophyll (g_m) was found as an important factor limiting photosynthesis in plants of Malvasía de Banyalbufar cv. infected by GLRaV and GFLV (Sampol et al., 2003). In the present study, the reduction of g_m in GRLaV-3 infected Malvasía de Banyalbufar seems not to be the main factor limiting A_N. Nevertheless, anatomic changes were observed between treatments (Table 7). Among liquid and lipid conductance, where it is commonly located the diffusion limitation, cell walls and chloroplast membranes have been proposed as the most important factors affecting CO_2 diffusion inside leaves (Terashima et al., 2011; Tomás et al., 2013). Leaves of infected plants were thicker (Table 7). Thicker leaves, such as leaves of the infected plants, have a lower proportion of mesophyll cell surface area exposed to intercellular air spaces per unit leaf surface area (Moutinho-Pereira et al., 2012), making CO_2 diffusion more difficult and limiting photosynthesis.

Despite the diffusion limitations to net CO_2 assimilation, the photosynthetic mechanism may not only be constrained by lower CO_2 diffusion but also by changes on photochemical and carbon metabolism processes. Chlorophyll content in non-infected plants significantly increased in August with respect to July, while in infected ones it did not change significantly. This result indicates that virus presence can affect this parameter. Other studies reported changes in chlorophyll content due to virus infection (Bertamini et al., 2004; Sampol et al., 2003; Moutinho-Pereira et al., 2012). In regards to the biochemistry of photosynthesis, the present results demonstrate that GLRaV-3 infection can lead to metabolism impairment related with Rubisco activity reduction. Despite virus concentration, V_{cmax}, and J_{max} were lower in infected Malvasía de

Banyalbufar plants, and these reductions were more evident in 2012 than in 2013. Reduction in V_{cmax} cannot be attributed to Rubisco content since this was unaffected, therefore it should be attributed to lower activity of the enzyme. In other studies virus infection induced a reduction of the carboxylation capacity through impairment of Rubisco activity due to a decrease in the activation state of the enzyme (Sampol et al., 2003). In addition, in this present work reductions in electron transport rate (J_{flu}) due to GLRaV-3 infection were observed. This parameter also showed a good correlation with virus concentration including data from cultivars, seasons and years (Figure 9B), suggesting a relationship between virus quantity and the negative effects on grapevine performance. The reductions in J_{flu} were observed mainly in Malvasía de Banyalbufar plants the first year of the experiment. The fluorescence measurements in other studies demonstrated that electron transport rate significantly decreased due to virus infection (Sampol et al., 2003, Moutinho-Pereira et al., 2012). However, this reduction in electron transport rate was not related to photo injury as F_V/F_M and NPQ were not strongly affected by virus presence (Table 5). Balachandran et al. (1994) also suggested that virus infection did not induce photo-inibitory damage. However, Moutinho-Pereira et al. (2012) described NPQ as sensible parameter to virus infection in Touriga Nacional cv.

Plant respiration is an important factor in carbon metabolism process determining plant growth, and therefore it is necessary to take it into account. Only growth increment in infected plants of Malvasía de Banyalbufar cv. in July 2013 was lower than non-infected plants in the same time period. Together with this observed reduction on growth, the rate of ATP-coupled respiration (i.e. Δ_c) was lower in infected plants (Figure 7C). A_N increase on maintenance respiration could be expected in infected plants because of higher metabolic requirements for the biosynthesis of defense compounds against the virus infection. Furthermore, it has been suggested that AOX pathway activity may allow the supply of carbon intermediates (i.e. from the TCA cycle) to be used for the biosynthesis of defense related compounds. This is done by maintaining the activity of mitochondrial electron transport chain under conditions when COX pathway may be inhibited by effect of the pathogen infection (Hanqing et al., 2010). However, v_{alt} was not changed in Malvasía de Banyalbufar plants (Figure 7D), thus suggesting that the GLRaV-3 virus affects mainly leaf growth respiration; this is in line with previous observations on the higher contribution of COX than AOX pathways to leaf growth rates (Florez-Sarasa et al., 2007). Despite the slight growth

decrease of infected Malvasía de Banyalbufar plants observed in July 2013, total growth at the end of the period was not significantly different between infected and non-infected plants (Table 3).

Although most of the parameters studied showed a trend with virus concentration, A_N and J_{flu} were the ones with better correlation as it was mentioned above (Figure 9A and 9B). These parameters decreased with the increase in virus amount. Thus, differences in virus concentration could explain the great variability of physiological consequences of this biotic stress observed among the studies. The low virus concentration found in Cabernet Sauvignon plants could explain the absence of effects in most of the evaluated parameters, suggesting a compatible level of infection. Nevertheless, some results such as high leaf thickness and Rubisco content in infected plants may reflect some leaf adaptations to minimize the virus effect on the plant.

The results of this study performed with asymptomatic grapevine plants showed the existence of virus effects on physiology parameters, especially A_N and J_{flu} in Malvasía de Banyalbufar plants, where virus concentration was higher than in Cabernet Sauvignon cv.. Moreover, these parameters could be used for virus presence indicators in asymptomatic situations. The decrease in A_N in the first stage of GLRaV-3 infection was mainly due to CO_2 diffusion limitations. Biochemistry limitation to photosynthesis resulted from a reduction in Rubisco activity, while anatomical changes were the main reason of CO_2 diffusion limitation. This study highlights the importance of virus concentration on virus effects. Therefore it must be taken into account in future studies of virus impact in physiological parameters, especially in white cultivars. Further investigations are recommended to confirm this, by introducing different levels of infection.

ACKNOWLEDGEMENTS

and Flavio Veratti for their help in the laboratory and Victoria Raw for English-language editing.

REFERENCES

Ambrós S., El-Mohtar C., Ruiz-Ruiz S., Peña L., Guerri J., Dawson W.O., & Moreno P. (2011). Agroinoculation of *Citrus tristeza virus* causes systemic infection and symptoms in the presumed nonhost *Nicotiana benthamiana*. *Molecular Plant-Microbe Interaction,* **24**, 1119-1131.

Asselbergh B., De Vleesschauwer D., & Hofte M. (2008). Global switches and fine-tuning-ABA modulates plant pathogen defense. *Molecular Plant Microbe Interaction*, **21**, 709–719.

Balachandran S., Osmond C.B., & Makino A. (1994). Effects of two strains of tobacco mosaic virus on photosynthetic characteristics and nitrogen partitioning in leaves of *Nicotiana tabacum* cv xanthi during photoaclimation under two nitrogen nutrition regimes. *Plant Physiology*, **104**, 1043–1050.

Balachandran S., Hurry V.M., Kelley S.E., Osmond C.B., Robinson S.A., Rohozinski J., Seaton G.G.R., & Sims D.A. (1997). Concepts of plant biotic stress. Some insights into stress physiology of virus-infected plants, from the perspective of photosynthesis. Physiologia *Plantarum*, **100**, 203–213.

Basso M.F., Fajardo T.V.M., Eiras M., Ayub R.A., & Nickel O. (2010). Detecção e identificação molecular de vírus associados a videiras sintomáticas e assintomáticas. *Ciência Rural*, **40**, 2249-2255.

Bernacchi C.J., Portis A.R., Nakano H., Von Caemmerer S., & Long S.P. (2002). Temperature response of mesophyll conductance. Implications for the determination of Rubisco enzyme kinetics and for limitations to photosynthesis *in vivo*. *Plant Physiology*, **130**, 1992–1998.

Bertamini M., Muthuchelian K., & Nedunchezhian N. (2004). Effect of grapevine leafroll on the photosynthesis of field grown grapevine plants (*Vitis vinifera* L. cv. Lagrein). *Journal of Phytopathology*, **152**, 145–152.

Bota J., Flexas J., Keys A.J., Loveland J., Parry M.A.J., & Medrano H. (2002). CO_2/O_2 specificity factor of ribulose- 1,5-bisphosphate carboxylase/oxygenase in grapevines (*Vitis vinifera* L.): first *in vitro* determination and comparison to *in vivo* estimations. Vitis, **41**, 163–168.

Bota J., Cretazzo E., Montero R., Rossello J., & Cifre J. (2014). *Grapevine fleck virus* (GFkV) elimination in a selected clone of Manto negro Cv. and its effects on the photosynthesis. *Journal International des Science de la Vigne et du Vine*, **48**, 11-19.

Bradford M.M. (1976). A rapid and sensitive method for the quantitation of microgram quantities of protein utilizing the principle of protein dye binding. *Analytical Biochemistry*, **72**, 248–254.

Cabaleiro C., Segura A., & Garcia-Berrios J.J. (1999). Effects of *Grapevine leafroll-associated virus 3* on the physiology and must of *Vitis vinifera* L. cv. Albarino following contamination in the field. *American Journal of Enology and Viticulture*, **50**, 40–44.

Christov I., Stefanov D., Goltsev V., & Abracheva P. (2001). Effects of *Grapevine fanleaf* and *Stem pitting viruses* on the photosynthetic activity of grapevine plants grown *in vitro*. *Russian Journal of Plant Physiology*, **48**, 473–7.

Christov I., Stefanov D., Velinov T., Goltsev V., Georgieva K., & Abracheva P. (2007). The symptomless leaf infection with *Grapevine leafroll associated virus 3* in grown *in vitro* plants as a simple model system for investigation of viral effects on photosynthesis. *Journal of Plant Physiology*, **164**, 1124–1133.

Clark M.F., & Adams A.N. (1977). Characteristics of the microplate method of enzyme-linked immunosorbent assay for the detection of plant viruses. *Journal of General Virology*, **34**, 475-483.

Cretazzo E., Tomás M., Padilla C., Rosselló J., Medrano H., Padilla V., & Cifre J. (2010). Incidence of virus infection in old vineyards of local grapevine cultivars from

Majorca: implications for clonal selection strategies. *Spanish Journal of Agricultural Research*, **8**, 409–418.

Endeshaw S.T., Sabbatini P., Romanazzi G., Schilder A.C., & Neri D. (2014). Effects of *Grapevine leafroll associated virus 3* infection on growth,leaf gas exchange, yield and basic fruit chemistry of *Vitis vinifera* L. cv. Cabernet Franc. *Scientia Horticulturae*, **170**, 228–236.

Epron D., Godard G., Cornic G., & Genty B. (1995). Limitation of net CO_2 assimilation rate by internal resistances to CO_2 transfer in the leaves of two tree species (Fagus sylvatica and Castanea sativa Mill.). *Plant, Cell and Environment*, **18**, 43–51.

Espinoza C., Cramer G., Arce-Johnson P., Schlauch K., Vega A, & Medina C. (2007). Gene expression associated with compatible viral diseases in grapevine cultivars. *Functional and Integrative Genomics*, **7**, 95-110.

Farquhar G.D., von Caemmerer S., & Berry J.A. (1980). A biochemical model of photosynthetic CO_2 assimilation in leaves of C3 species. *Planta*, **149**, 78–90.

Ferriol I., Ruíz-Ruíz, S., & Rubio L. (2011). Detection and absolute quantitation of *Broad bean wilt virus 1* (BBWV-1) and BBWV-2 by real time RT-PCR. *Journal of Virolological Methods*, **177**, 202-205.

Fisher D.G. (1985). Morphology and anatomy of the leaf of *Coleus blurnei* (Lamiaceae). *American Journal of Botany*, **72**, 392-406.

Flexas J., Bota J., Galmes J., Medrano H., & Ribas-Carbo M. (2006). Keeping a positive carbon balance under adverse conditions: responses of photosynthesis and respiration to water stress. *Physiologia Plantarum*, **127**, 343-352.

Flexas J., Díaz-Espejo A., Berry J.A., Galmés J., Cifre J., Kaldenhoff R., Medrano H., & Ribas-Carbo M. (2007). Leakage in leaf chambers in open gas exchange systems: quantification and its effects in photosynthesis parameterization. *Journal of Experimental Botany*, **58**, 1533–1543.

Florez-Sarasa I.D., Bouma T.J., Medrano H., Azcon-Bieto J., & Ribas-Carbo M. (2007). Contribution of the cytochrome and alternative pathways to growth respiration

and maintenance respiration in Arabidopsis thaliana. *Physiologia Plantarum*, **129**, 143–151.

Frosline P.L., Hoch J., Limboy W.F., Mc Ferson J.R., Golino D., & Gonsalves D. (1996). Comparative effectiveness of symptomatology and ELISA for detecting two isolates of grapevine leafroll in Cabernet Franc. *American Journal of Enology and Viticulture*, **47**, 239–243.

Gambino G., Cuozzo D., Fasoli M., Pagliarani C., Vitali M., Boccacci P., Pezzotti M., & Mannini F. (2012). Co-evolution between Grapevine rupestris stem pittingassociated virus and *Vitis vinifera* L. leads to decreased defense responses and increased transcription of genes related to photosynthesis. *Journal of Experimental Botany*, **63(16)**, 5919-5933.

Genty B., Briantais J.M., & Baker N.R. (1989). The relationship between the quantum yield of photosynthetic electron transport and quenching of chlorophyll fluorescence. *Biochimica et Biophysica Acta*, **990**, 87–92.

González E., Mosquera M.V., San José M.C., & Díaz T. (1997). Influence of virus on the chlorophyll, carotenoid and polyamide contents in grapevine microcuttings. *Journal of Phytopathology*, **145**, 185–187.

Guidoni S., Mannini F., Ferrandino A., Argamante N., & Di Stefano R. (1997). The effect of grapevine leafroll and rugose wood sanitation on agronomic performance and berry phenolic content of Nebbiolo clone (*Vitis vinifera* L.). *American Journal of Enological Viticulture*, **48**, 438–442.

Grassi G., & Magnani F. (2005). Stomatal, mesophyll conductance and biochemical limitations to photosynthesis as affected by drought and leaf ontogeny in ash and oak trees. *Plant, Cell and Environment*, **28**, 834–849.

Guy R.D., Berry J.A., Fogel M.L., & Hoering T.C. (1989). Differential fractionation of oxygen isotopes by cyanide-resistant and cyanide-sensitive respiration in plants. *Planta*, **177**, 483–491.

Habili N., Krake L.R., Barlass M., & Rezaian M.A. (1992). Evaluation of biological indexing and dsRNA analysis in grapevine virus elimination. *Annals Applied Biology*, **121**, 277–283.

Hanqing F., Kun S., Mingquan L., Hongyu L., Xin L., Yan L., & Yifeng W. (2010). The expression, function and regulation of mitochondrial alternative oxidase under biotic stresses. *Molecular Plant Pathology*, **11**, 429–40.

Harley P.C., Loreto F., Di Marco G., & Sharkey T.D. (1992). Theoretical considerations when estimating mesophyll conductance to CO_2 flux by analysis of the response of photosynthesis to CO_2. *Plant Physiology*, **98**, 1429-1436.

Hoagland D.R., & Arnon D.I. (1950). The water-culture method for growing plants without soil. *California Agricultural Experiment Station*, **347**.

Hristov I., & Abrasheva P. (2001). Effect of *Grapevine fanleaf virus* and *Grapevine leafroll associated virus 3* on vine plants under conditions of *in vitro* cultivation. *Rastenievudni Nauki*, **38**, 269–274.

Huggett J., Dheda K., Bustin S., & Zumla A. (2005). Real-time RT–PCR normalisation: strategies and considerations. *Genes Immunology*, **6**, 279–284.

Komar V., Vigne E., Demangeat G., & Fuchs M. (2007). Beneficial effect of selective virus elimination on the performance of *Vitis vinifera* cv. Chardonnay. *American Journal of Enology and Viticulture*, **58**, 202–210.

Lee J., & Martin R.R. (2009). Influence of grapevine leafroll associated viruses (GLRaV-2 and -3) on the fruit composition of Oregon *Vitis vinifera* L. cv. Pinot noir: Phenolics. *Food Chemistry*, **112**, 889–896.

Lee J., Keller K.E., Rennaker C., & Martin R.R. (2009). Influence of *Grapevine leafroll associated viruses* (GLRaV-2 and -3) on the fruit composition of Oregon *Vitis vinifera* L. cv. Pinot noir: Free amino acids, sugars, and organic acids. *Food Chemistry*, **117**, 99-105.

Lennon A.M., Neuenschwander U.H., Ribas-Carbo M., Giles L., Ryals J.A., & Siedow J.N. (1997). The effects of salicylic acid and *Tobacco mosaic virus* infection on the alternative oxidase of tobacco. *Plant Physiology*, **115**, 783-791.

Lichtenthaler H.K., & Wellburn A.R. (1983). Determinations of total carotenoids and chlorophylls a and b of leaf extracts in different solvents. *Biochemical Society Transactions*, **11**, 591 - 592.

McDowel N.G. (2011). Mechanisms linking drought, hydraulics, carbon metabolism, and vegetation mortality. *Plant Physiology*, **155 (3)**, 1051-1059.

Mannini F., Mollo A., & Credi R. (2012). Field performance and wine quality modification in a clone of *Vitis vinifera* cv. Dolcetto after GLRaV-3 elimination. *American Journal of Enology and Viticulture*, **63**, 144–147.

Martelli G. (2009). Grapevine virology highlights 2006–2009. *In: le Progrès Agricole et Viticole (Ed.), Proceedings of the 16th Meeting of the International Council for the Study of Virus and Virus-like Diseases of the Grapevine.* ICVG, Dijon, France, pp. 15–23.

Minafra A., Hadidi A., & Martelli GP. (1992). Detection of *Grapevine closterovirus A* in infected tissue by reverse transcription-polymerase chain reaction. *Vitis*, **31**, 221–227.

Moutinho-Pereira J., Correia C.M., Gonçalves B., Bacelar E.A., Coutinho J.F., Ferreira H.F., Lousada J.L., & Cortez M.I. (2012). Impacts of leafroll-associated viruses (GLRaV-1 and -3) on the physiology of the Portuquese grapevine cultivar "Touriga Nacional" growing under field conditions. *Annals of Applied Biology*, **160(3)**, 237-249.

Noguchi K., Go C.S., Terashima I., Ueda S., & Yoshinari T. (2001). Activities of the cyanide-resistant respiratory pathway in leaves of sun and shade species. *Australian Journal of Plant Physiology*, **28**, 27–35.

Osman F., Leutenegger C., Golino D., & Rowhani A. (2007). Real-time RT-PCR (TaqMan®) assays for the detection of Grapevine Leafroll associated viruses 1–5 and 9. *Journal of Virological Methods*, **141**, 22-29.

Osman F., & Rowhani A. (2008). Real-time RT-PCR (TaqMan®) assays for the detection of viruses associated with Rugose wood complex of grapevine. *Journal of Virological Methods*, **154**, 69–75.

Pacifico D., Caciagli P., Palmano S., Mannini F., & Marzachì C. (2011). Quantitation of *Grapevine leafroll associated virus-1 and -3, Grapevine virus A, Grapevine fanleaf virus and Grapevine fleck virus* in field-collected *Vitis vinifera* L. 'Nebbiolo' by real-time reverse transcription-PCR. *Journal of Virological Methods*, **172**, 1-7.

Petit A.N., Vaillant N., Boulay M., Clement C., & Fontaine F. (2006). Alteration of photosynthesis in grapevines affected by esca. *Phytopathology*, **96**, 1060-1066.

Ribas-Carbo M., Lennon A.M., Robinson S.A., Giles L., Berry J.A., & Siedow J.N. (1997). The regulation of electron partitioning between the cytochrome and alternative pathways in soybean cotyledon and root mitochondria. *Plant Physiology*, **113**, 903- 911.

Ribas-Carbo M., Robinson S.A., & Giles L. (2005). The application of the oxygen-isotope technique to assess respiratory pathway partitioning. In Plant Respiration: From Cell to Ecosystem, *Advances in Photosynthesis and Respiration Series* (eds H. Lambers & M. Ribas-Carbo), **18**, 31–42. Springer, Dordrecht, The Netherlands.

Rowhani A. (1992). Use of F (ab')$_2$ antibody fragment in ELISA for detection of grapevine viruses. *American Journal of Enolology and Viticulture*, **43**, 38–40.

Rowhani A., Chay C., Golino D.A., & Falk B.W. (1993). Development of a polymerase chain reaction technique for the detection of *Grapevine fanleaf virus* in grapevine tissue. *Phytopathology*, **83**, 749–753.

Rowhani A., Uyemoto J.K., & Golino D.A. (1997). A comparison between serological and biological assays in detecting grapevine leafroll associated viruses. *Plant Disease*, **81**, 799–801.

Sampol B., Bota J., Riera D., Medrano H., & Flexas J. (2003). Analysis of the virus-induced inhibition of photosynthesis in malmsey grapevines. *New Phytologist*, **160**, 403–412.

Sefc K.M., Leonhardt W., & Steinkellner H. (2000). Partial sequence identification of *Grapevine-leafroll-associated virus-1* and development of a highly sensitive IC-RT-PCR detection method. *Journal of Virological Methods*, **86**, 101-106.

Sharkey T.D., Berry J.A., & Raschke K. (1985). Starch and sucrose synthesis in Phaseolus vulgaris as affected by light, CO_2, and abscisic acid. *Plant Physiology*, **77**, 617–620.

Terashima I., Hanba Y.T., Tholen D., & Niinemets Ü. (2011). Leaf functional anatomy in relation to photosynthesis. *Plant Physiology*, **155**, 108-116.

Tomás M., Flexas J., Copolovici L., Galmés J., Hallik L., Medrano H., Ribas-Carbó M., Tosens T., Vislap V., & Niinements Ü. (2013). Importance of leaf anatomy in determining mesophyll diffusion conductance to CO_2 across species: quantitative limitations and scaling up by models. *Journal Experimental Botany*, **64(8)**, 2269-2281.

Ton J., Flors V., & Mauch-Mani B. (2009). The multifaceted role of ABA in disease resistance. *Trends Plant Science*, **14**, 310–317.

Tsai C.W., Daugherty M.P., & Almeida R.P.P. (2012). Seasonal dynamics and virus translocation of *Grapevine leafroll-associated virus 3* in grapevine cultivars. *Plant Pathology*, **61**, 977–985.

Valentini R., Epron D., De Angelis P., Matteucci G., & Dreyer E. (1995). *In situ* estimation of net CO_2 assimilation, photosynthetic electron flow and photorespiration in Turkey oak (*Quercus cerris* L.) leaves: diurnal cycles under different levels of water supply. *Plant Cell Environment*, **18**, 631–640.

Valero M., Ibanez A., & Morte A. (2003). Effects of high vineyard temperatures on the *Grapevine leafroll associated virus* elimination from *Vitis vinifera* L. cv. Napoleon tissue culture. *Scientia Horticulturae*, **97**, 289–296.

Vanlerberghe G.C. (2013). Alternative oxidase: a mitochondrial respiratory pathway to maintain metabolic and signaling homeostasis during abiotic and biotic stress in plants. *International Journal of Molecular Sciences*, **14**, 6805–6847.

Velasco L., Bota J., Montero R., & Cretazzo E. (2014). Differences of three ampeloviruses multiplication in plant contribute to explain their incidences in vineyards. *Plant disease*, **98**, 395-400.

Wetzel T., Jardakb R., Meuniera L., Ghorbelb A., Reustlea G.M., & Krczala G. (2002). Simultaneous RT/PCR detection and differentiation of arabis mosaic and grapevine fanleaf nepoviruses in grapevines with a single pair of primers. *Journal of Virological Methods*, **101**, 63–69.

Whitham S.A., Yang C., & Goodin M.M. (2006). Global Impact: Elucidating Plant Responses to Viral Infection. *Molecular Plant-Microbe Interactions*, **19**, 1207-1215.

Chapter 5

ALTERATIONS IN PRIMARY AND SECONDARY
METABOLISM IN *VITIS VINIFERA* L. MALVASÍA DE
BANYALBUFAR CV. UPON INFECTION WITH
GRAPEVINE LEAFROLL ASSOCIATED VIRUS 3
(GLRaV-3).

ALTERATIONS IN PRIMARY AND SECONDARY METABOLISM IN *VITIS VINIFERA* L. MALVASÍA DE BANYALBUFAR CV. UPON INFECTION WITH GRAPEVINE LEAFROLL ASSOCIATED VIRUS 3 (GLRaV-3).

R. Montero[1], M.L. Pérez-Bueno[2], M. Barón[2], I. Florez-Sarasa[3], T. Tohge[3], A.R. Fernie[3], H. El aou ouad[4], J. Flexas[4], J. Bota[4*].

[1]Institut de Recerca i Formació Agrària i Pesquera (IRFAP), Conselleria d'Agricultura, Medi Ambient i Territori. Govern de les Illes Balears. C/Eusebio Estada nº 145. 07009, Palma de Mallorca, Spain.

[2]Department of Biochemistry and Molecular and Cell Biology of Plants, Estación Experimental del Zaidín, Spanish Council of Scientific Research (CSIC), Profesor Albareda 1, 18008 Granada, Spain

[3]Max-Planck-Institute for Molecular Plant Physiology, 14476 Potsdam, Germany.

[4]Grup de Recerca en Biologia de les Plantes en Condicions Mediterrànies, Departament de Biologia, Universitat de les Illes Balears, Carretera de Valldemossa, km 7.5, 07071, Palma de Mallorca, Balears, Spain.

*Corresponding author: j.bota@uib.es

ABSTRACT

Plant defence mechanisms against pathogens result in differential regulation of various processes of primary and secondary metabolism. Imaging techniques, such as fluorescence imaging and thermography, are a very valuable tool providing spatial and temporal information about these processes. In this study, effects of GLRaV-3 on grapevine physiology were analysed in pot-grown asymptomatic plants of the Malvasía de Banyalbufar cultivar. The virus triggered changes in the activity of photosynthesis and secondary metabolism. There was a decrease in the photorespiratory intermediates glycine and serine in infected plants, possibly as a defense response against the infection. The content on malate, which plays an important role in plant metabolism, also decreased. These results correlate with the increased non-photochemical quenching found in infected plants. On the other hand, the concentration of flavonols (represented by myricetin, kaempferol and quercetin derivatives) and hydroxycinnamic acids (which include derivatives of caffeic acid) increased following infection by the virus. These compounds could be responsible for the increase in multicolour fluorescence F440, F520 on the abaxial side of the leaves, and changes in the fluorescence parameters F440/680, F440/740, F520/680, F520/740 and F680/740. The combined analysis of chlorophyll fluorescence kinetics and blue-green fluorescence emitted by phenolics could constitute disease signatures allowing the discrimination between GLRaV-3 infected and non-infected plants at very early infection stage, prior to the development of symptoms.

Keywords: Virus absolute quantification; chlorophyll fluorescence; leaf gas exchange; multicolour fluorescence; metabolites; *Vitis vinifera*.

INTRODUCTION

Virus infections are very important for the wine industry since they can detrimentally affect both yield and grape quality. *Grapevine leafroll associated virus 3* (GLRaV-3) is one of the most important virus affecting grapevines provoking considerable economic losses in many vineyards around the world (Martelli, 2012). GLRaV-3 is a phloem-limited virus, member of the genus *Ampelovirus*, family *Closteroviridae* and it infects both white and red grape varieties. Symptoms in red

varieties are characterized by dark-red, downward rolled leaves with green veins. In the white varieties, symptoms are not so clear or even absent. Depending on the white variety, interveinal yellowing and rolling of the leaf margin can be observed in infected plants (Maree et al., 2013). These masked symptoms hinder disease diagnosis, timely insect vector control and effective removal of infected vines (Charles et al., 2009).

Diagnostic methods for the detection of grapevine viruses have evolved in recent years. However, real time qPCR has been established as the routine technique for virus detection and quantification (Pacifico et al., 2011) and there is a lack of methods for rapid on-site diagnosis. In this sense, the wine industry is in need for new methods for rapid on-site diagnosis of infected plants. One strategy could be the determination of appropriate physiological parameters that could work as indicators of the virus presence in the plant. The impact of viral infection on plant metabolism is still far from being fully understood, since viruses produce a very wide range of effects depending on the host-pathogen system (Balachandran et al., 1997; Sampol et al., 2003; Petit et al., 2006; Komar et al., 2007; Christov et al., 2007; Basso et al., 2010; Barón et al., 2012). However, several findings demonstrate that some of the effects of GLRaV-3 are associated with physiological disturbances on the photosynthesis of grapevine (Charles et al., 2009; Maree et al., 2013).

In some plant-virus interactions photosynthesis and processes related to primary metabolism, such as degradation or synthesis of carbohydrates, lipids and amino acids, are strongly affected (Gambino et al., 2012). GLRaV-3 has a direct effect on the metabolism of the host plant, thus manipulating its metabolism in order to promote infection by a diverse array of effectors, as well as to help replication and spreading within the plant (Gutha et al., 2010).

The analysis of chlorophyll fluorescence (Chl-F) kinetics allows the study of photosynthetic performance in terms of PSII activity, and it is a common technique in plant physiology based on the high sensitivity of PSII to stress (Murchie & Lawson, 2013). Several plant-virus interactions have been analysed by Chl-F imaging (Balachandran & Osmond, 1994; Balachandran et al., 1997; Osmond et al., 1998; Lohaus et al., 2000; Chaerle et al., 2004; Pérez-Bueno et al., 2006). Similar experiments were carried out with phytopathogenic fungi (Scholes & Rolfe, 2009; Chou et al., 2000; Swarbrick et al., 2006; Granum et al., 2015) and bacteria (Berger et al., 2004, 2007;

Bonfig et al., 2006; Rodríguez-Moreno et al., 2008; Pérez-Bueno et al., 2014). Touriga Nacional cv. grapevine infected with GLRaV-3 shows a decrease the PSII quantum yield (Φ_{PSII}), electron transport rate (J_{flu}), photochemical quenching (qP), and an increase in non-photochemical quenching (NPQ) (Moutinho-Pereira et al., 2012). However, the maximum quantum efficiency of PSII (F_V/F_M), another Chl-FI parameter quantifying the photosynthetic efficiency, was not affected under field conditions (Moutinho-Pereira et al., 2012). Endeshaw et al. (2014) determined that the appearance of the symptoms, in August and until harvest, produced a significant reduction of F_V/F_M. Alongside Chl-F measurements, UV-excited autofluorescence have developed into a sensitive and specific tool for determining the physiological status of plants before the symptoms produced by abiotic or biotic stresses are evident (Buschmann et al., 1998; Cerovic et al., 2002; Lichtenthaler et al., 1997).

On the other hand, host plants also reorganize their primary and secondary metabolism to deal with the infection. Pathogen infection often activates the phenylpropanoid pathway, leading to the production of both phytoalexins and lignin/suberin precursors for cell wall strengthening (Parker et al., 2009). These phenolic compounds are able to establish physical and chemical barriers against infection (Dixon et al., 2002). In addition some of them are the major emitters of blue (440 nm) and green (520 nm) fluorescence (F440 and F520, respectively), in green leaves excited with ultraviolet (UV) light (Buschmann et al., 1998). Ratios such as F440 ∕ F690 (red fluorescence: at 690 nm) and F440 ∕ F740 (far-red fluorescence: at 740 nm) can be very early stress indicators (Buschmann et al., 1998; Buschmann et al., 2000; Lichtenthaler et al., 1997). Within the hydroxycinnamic acids, chlorogenic acid has been determined as the main BGF fluorophore in artichoke and tobacco leaves (Morales et al., 2005). Therefore an increase in those compounds could be detected by multicolour fluorescence imaging (MCFI).

The aim of this work is to analyse the alterations in primary and secondary metabolism of grapevine induced by GLRaV-3, to evaluate the use of thermal and fluorescence imaging to detect the infection. We propose the use of Chl-F parameters and BGF as disease signatures that could be applied in diagnosis prior to the development of visible symptoms.

MATERIAL AND METHODS

Plant material and growth conditions

Pot-grown virus-free and GLRaV-3 infected plants of *Vitis vinifera* L. Malvasía de Banyalbufar cv., were evaluated for the virus infection as described in the next section. Malvasía de Banyalbufar plants were obtained by direct rooting of 0.2 m cuttings of dormant canes selected from mother plants growing under field conditions in a twelve year old experimental vineyard sited at IRFAP center (*Institut de Recerca i Formació Agrària i Pesquera, Conselleria d'Agricultura Medi Ambient i Territori*), Palma de Mallorca (Balearic Island, Spain). Infected mother plants did not show symptoms under field conditions. Two weeks after rooting, the roots were strong enough to transfer them to pots. Four infected cuttings with GLRaV-3 and four non-infected of each cultivar were planted in pots of 4 l volume filled with organic substrate and perlite mixture (5:1). Plants were grown at the greenhouse where the temperature was kept at $27.0\pm0.5^{\circ}$C and the photosynthetic photon flux density (PPFD) was 400 µmol (photon) m^{-2} s^{-1}. The experiment was carried out during June 2013, when the plants were still young (3 months age). Before starting the experiment all the plants were irrigated daily, and each 15 days organic fertilizer was added to the pots. Instead organic fertilized, the plants were irrigated with 50% Hoagland´s solution (Hoagland & Aron, 1950) every 3 days, 2 weeks before starting the measurements. The experiments were carried out prior to the flowering time. In all the plants one shoot around 0.7 m high was left to carry on the experiment.

Virus diagnosis and quantification.

The presence of GLRaV-1, 3, 4, 5, 7, 9, GFLV and GFkV viruses was tested by enzyme-linked immunosorbent assay (ELISA) (Clark & Adams, 1977) using commercial coating and conjugate antibodies preparations (Bioreba AG, Reinach, Switzerland). Field grown mother plants were tested, and then Malvasía de Banyalbufar non-infected and single GLRaV-3 infected plants were selected for the experiment. The ELISA results were confirmed by RT-PCR using a Real time PCR system (Illumina, SD, USA). GLRaV-1, 2, 3, 4, 5, GFLV and GFkV were tested with this technique. Total RNA was extracted from one leaf per plant (70 mg of phloem scraped from leaves) using SpectrumTM Plant Total RNA Kit (Sigma-Aldrich, Inc.) according to

manufacturer's instructions. The Spectrum™ Plant total RNA Kit removes most of the DNA during RNA purification. However, for very sensitive applications, such as quantitative RT-PCR, complete removal of traces of DNA may be necessary. On-Column DNase I Digest Set (Sigma-Aldrich Co., St Louis, MO, USA) was used to digest the DNA during RNA purification following the manufacturer´s instruction. RNA purity and concentration were measured at 260/280 nm using a spectrophotometer (NanoDrop-1000, Thermo Scientific, Villebon sur Yvette, France). First-strand cDNA synthesis was performed using 500 ng of total RNA, 200 units of recombinant *Moloney Murine Leukemia Virus* (MuLV) reverse transcriptase (Invitrogen Life Technologies, Inc.), 40 units of RNase inhibitor (RNase out, Invitrogen Life Technologies, Inc.), 0.4 mM of dNTPs, and 2 mM of random nonamers (Takara Bio, Inc.). The mixture for reverse transcriptase (20 μl) was incubated for 50 min at 37 ºC and the reaction was inactivated by heating it at 70ºC for 15 min.

Quantification of the viral content were performed by real-time PCR reactions in a 10 μl mixture containing 2 μl of diluted (1:100) cDNA, 5 μl iQ SYBR Green Reaction-Mix (Bio-Rad), and 0,2 μM of each primer in the ECO-Illumina system (ECO-Illumina) using the following PCR cycle profile: one cycle of 2 min at 95 °C followed by 40 cycles of 5 s at 95 °C and 20 s at 60 °C. The fluorescence threshold value (Ct) was calculated using the ECO-Illumina system software (ECO-Illumina). Overall, a mean Ct value was calculated from two PCR replicates.

Sequences of primers used in this study were retrieved from literature and used for amplifying partial gene-specific sequences. A list of primer pairs and amplicon lengths used for the virus diagnosis are provided in Montero et al. (2015) (Chapter 4). GLRaV-3 standard curve for virus quantification was performed according to Montero et al. (2015) (Chapter 4).

Gas exchange and chlorophyll content.

One leaf per plant was used for the gas exchange measurement at mid-morning in infected and non-infected plants. Photosynthesis was induced at saturating light (1500 μmol m^{-2} s^{-1}) and 400 μmol mol^{-1} CO_2. Leaf-to-air vapour pressure deficit was kept between 1 kPa and 2 kPa during all measurements. Net CO_2 assimilation (A_N) and

stomatal conductance (g_s) were determined simultaneously on leaves using an open gas exchange system Li-6400 (Li-Cor, Lincoln, NE, USA).

Relative chlorophyll concentrations were estimated in the same leaves used for gas exchange using a SPAD-502 chlorophyll meter (Minolta, Tokyo, Japan). Chlorophyll readings (expressed as SPAD units) were taken repeatedly at the three apices of a triangle drawn on the leaf lamina.

Chlorophyll fluorescence kinetics

Chl-F kinetics measurements were carried out by an Open FluorCam 700MF (PSI, Brno, Czech Republic) kinetic imaging fluorometer controlled by FluorCam5 (PSI) software (Pineda et al., 2008a). Chl-F emission from a leaf was excited by two panels of light-emitting diodes (LEDs) (λmax $\approx$ 635 nm) that generate measuring flashes (10 µs) and actinic light. Brief and intense saturating radiation pulses [1500 µmol(photon) m^{-2} s^{-1}, 1 s] were generated by a 250-W "white" (λ = 400$-$700 nm) halogen lamp. The Chl-F emission transients are captured by a CCD (charged coupled device) camera in series of images at 12-bit resolution in 512×512 pixels, taking fifty images per second. The reflected radiation is blocked by a far-red filter (RG697, Schott, Mainz, Germany).

This quenching analysis was previously described by Pérez-Bueno et al. (2006). Here, F_0 (The fluorescence signal when all reaction centers were open) and F_M (the fluorescence signal under saturating light pulse in the dark adapted state) measurements on dark-adapted leaves were followed by 16 s of dark. Then, the leaves were irradiated with continuous actinic light corresponding to the cultivation irradiance (400 µmol (photon) m^{-2} s^{-1}) for 302 s, supplemented with 11 saturating pulses to measure F_M' (the maximum fluorescence during a saturating light pulse) (at 2, 5, 10, 20, 30, 60, 90, 120, 180, 240, and 300 s after turning on the actinic light). All measurements were carried out on attached leaves. Four repetitions of the infection process were carried out, with four plants for every treatment.

Thermal imaging

Infrared images of plant leaves of the different treatments were taken in the growth chamber using a Photon 640 camera (FLIR Systems, Wilsonville, OR) vertically

positioned (Pérez-Bueno et al., 2014). Thermal images were recorded at midmorning. All measurements were performed in attached leaves. Numerical data from at least four regions of interest pear plant were analysed. The experiment was repeated twice with similar results.

Multicolour fluorescence imaging

MCFI was performed using an Open FluorCam FC 800-O (Photon Systems Instruments, Brno, Czech Republic) according to Pérez-Bueno et al. (2014). Multicolour fluorescence emission of the adaxial and abaxial side of the leaf was excited with UV light at 360 nm. Images in blue (F440), green (F520) and red (F680) regions of the spectrum were acquired sequentially for each sample. Black and white images corresponding to measured fluorescence and calculated fluorescence ratios (F440/F680 and F520/F680) are displayed using a false colour scale applied by FLUORCAM software version 7.1.0.3 (Photon Systems Instruments Brno, Czech Republic). Measurements were carried out on GLRaV-3 infected and non-infected plants. Four different plants per treatment were analysed and the experiments were repeated four times with similar results. All measurements were performed on attached leaves.

Metabolic profiling

Leaf samples were collected at midday (12.00 a.m.), immediately frozen in liquid nitrogen and stored at -80ºC. Grinding was also performed under frozen conditions using liquid nitrogen. Grapevine leaf powder (50 mg) was extracted in 100% methanol following the methodology previously described in Roessner et al. (2001). Metabolite extractions, derivatization and gas chromatography-time of flight-mass spectrometry (GC-TOF-MS) analyses were carried out as described previously (Lisec et al., 2006). The GC-TOF-MS system was composed of a CTC CombiPAL autosampler, an Agilent 6890N gas chromatograph and a LECO Pegasus III time-of-flight mass spectrometer running in EI+ mode. Metabolites were identified by comparison with database entries of authentic standards (Kopka et al., 2005; Schauer et al., 2005).

Before sample derivatization, and aliquot from the metabolite extraction described above was dried in the speed-vac (Savant SVC 200H) and then resuspended in 150 µl of 80% Methanol absolute ULC/MS (MeOH ULC) for liquid chromatography-mass

spectrometry (LC-MS). LC-MS was performed on HPLC system Surveyor (Thermo Finnigan, USA) coupled to Finnigan LTQ-XP system (Thermo Finnigan, USA) as described by Tohge and Fernie (2010).

Metabolite data were normalized with respect to the mean response calculated for non-infected plants (to allow statistical assessment, individual plants from this set were also normalized in the same way).

Statistical analysis

The data was analysed using R (http://.rproject.org/). One-way ANOVA were used to determine differences between the treatments in the measured parameters.

RESULTS

Effects of GLRaV-3 on plant primary metabolism.

Despite the low virus concentration (virus amount was 5.09 ± 0.05 log copy number/70 mg and plants did not developed symptoms of GLRaV-3 infection), the impact of GLRaV-3 on photosynthesis affected both the CO_2 fixation rate and PSII efficiency in an early stage of growth period. A_N decreased in infected plants but gs and leaf temperature measured by thermal imaging (images not shown) were not significantly different between treatments (Table 1).

Table 1. Relative chlorophyll content (SPAD), net CO_2 assimilation (A_N), stomatal conductance (g_s) and leaf temperature extracted from thermal images, for non-infected (GLRaV-3 (-)) and virus infected plants (GLRaV-3 (+)). Means and standard error of at least four plants are shown. Symbols * and ** denotes significant differences at $P < 0.05$ and <0.01, respectively; ns, not significant ($P > 0.05$).

Treatment	Relative chlorophyll content (SPAD)	A_N (μmol CO_2 m^{-2} s^{-1})	g_s (mmol CO_2 m^{-2} s^{-1})	Leaf temperature (ºC)
GLRaV-3 (-)	31.75±0.78	9.07±0.63	92.19±11.39	21.38±0.15
GLRaV-3 (+)	27.05±0.73	7.06±0.70	74.18±6.12	21.16±0.24
Significance	**	*	ns	ns

Relative chlorophyll content was also lower in infected plants. Those differences were close to 22% and 15%, in A_N and relative chlorophyll content, respectively.

Figure 1 shows the effect of GLRaV-3 infection on the photosynthesis of grapevine leaves, analysed in terms of PSII efficiency.
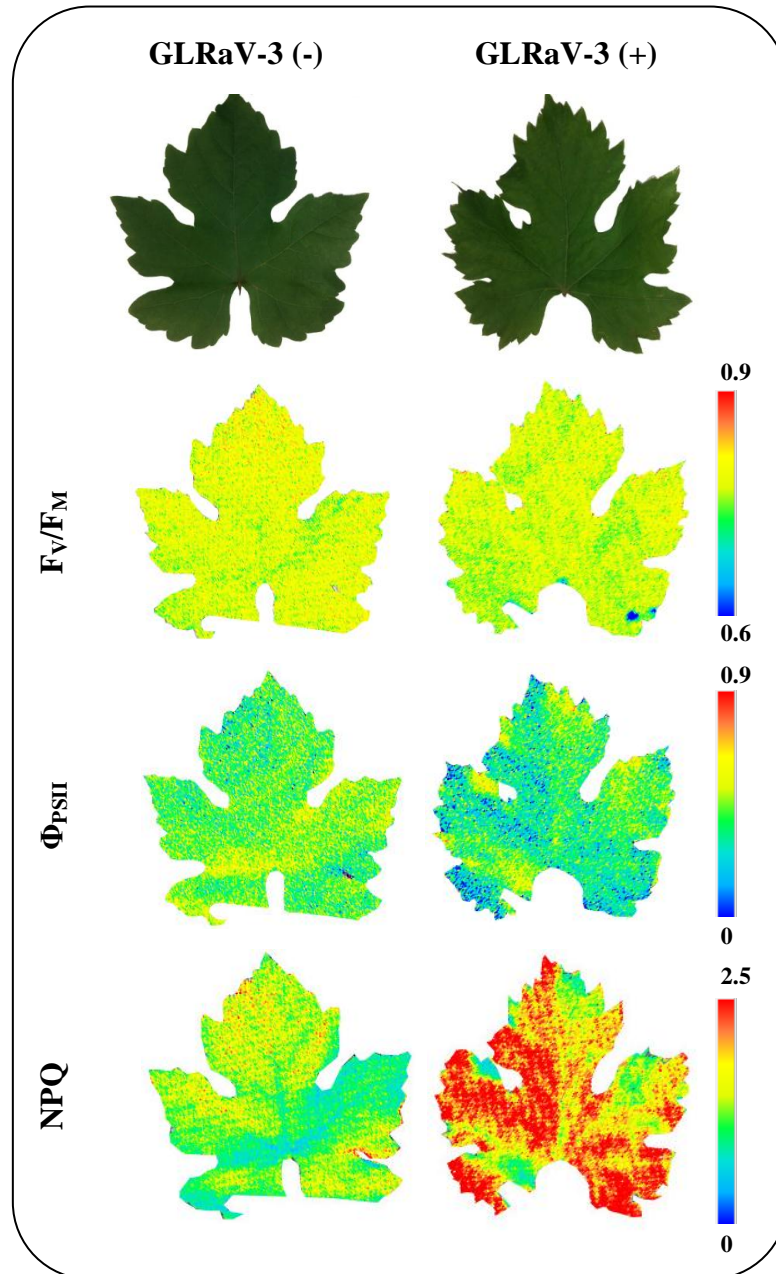
Figure 1. Impact of GLRaV-3 infection on the photosynthesis of grapevine leaves analysed in terms of PSII efficiency (F_V/F_M, Φ_{PSII}) and NPQ measured for the adaxial side of the leaves. Representative images are shown.

F_V/F_M, Φ_{PSII} and NPQ in the adaxial side of one leaf per plant were measured by Chl-FI (Figure 1). Imaging of these parameters showed no specific spatial pattern for photosynthetic activity that could be related to viral infection.

However, leaves of infected plants showed a small but statistically significant decrease in F_V/F_M together with a decrease in Φ_{PSII} and an increase in NPQ (Table 2), relative to the values found for non-infected plants. No differences were found in the values of irreversible NPQ (data not shown), meaning that the increase in NPQ was due to the activation of reversible NPQ.

Table 2. The maximum quantum efficiency of photosystem II (PSII) (F_V/F_M), the actual photochemical efficiency of photosystem II (Φ_{PSII}) and non-photochemical quenching (NPQ) in non-infected (GLRaV-3 (-)) and virus infected (GLRaV-3 (+)) plants of Malvasía de Banyalbufar. Values presented are point measurements of the interest area extracted from the images Chl-FI. Means and standard error of at least four plants are shown. Symbols ** and *** denotes significant differences at P <0.01 and <0.001, respectively; ns, not significant (P > 0.05).

Treatment	F_V/F_M	Φ_{PSII}	NPQ
GLRaV-3 (-)	0.784±0.003	0.40±0.01	1.28±0.08
GLRaV-3 (+)	0.770±0.002	0.33±0.01	1.84±0.16
Significance	***	**	**

Leaf extracts were analysed by gas chromatography mass spectrometry (GC-MS) (after derivatization with MSTFA), and 42 compounds detected in polar leaf extracts, including several amino acids, organic acids, sugars and sugar alcohols related to primary metabolism (Table 3). Only six among all metabolites quantified presented significant differences in their abundance between treatments. Glycine, serine and malate were 40-60% lower in infected plants than in non-infected ones. Dehydroascorbic acid and both cis- and trans- isomers of caffeic acid were 22%, 45% and 39% respectively higher in infected plants than in non-infected ones (Figure 2A). On the other hand, some metabolites such as shikimic and proline also decreased by the effect of the virus almost 75%, but these differences were not significant due to the high variability among replicates in the amount of those compounds.

Table 3. Compounds detected by GC-MS and LC-MS in non-infected (GLRaV-3 (-)) and infected plants (GLRaV-3 (+)) of Malvasía de Banyalbufar. Metabolites were grouped in amino acids, organic acids, sugars, sugar alcohols and flavonols. Means and standard error of at least four plants are shown. Symbols * and ** denotes significant differences at $P < 0.05$ and <0.01, respectively; ns, not significant ($P > 0.05$).

	Treatment	GLRaV-3 (-)	GLRaV-3 (+)	Sig.
Amino acids	Threonine	1.00±0,14	0,59±0,16	ns
	Valine	1.00±0,20	0,58±0,29	ns
	Isoleucine	1.00±0,18	0,58±0,34	ns
	Glycine	1.00±0,19	0,50±0,05	*
	Proline	1.00±0,56	0,25±0,08	ns
	Serine	1.00±0,22	0,36±0,11	*
	Lysine	1.00±0,22	0,72±0,39	ns
	Phenylalanine DL	1.00±0,25	0.40±0.09	ns
Organic acids	Pyruvic Acid	1.00±0,14	1,00±0,17	ns
	Guanidine	1.00±0,37	0,64±0,12	ns
	Shikimic Acid	1.00±0,10	0.26±0.10	ns
	Phosphoric Acid	1.00±0,06	0,98±0,07	ns
	Glyceric Acid	1.00±0,05	0,89±0,18	ns
	Fumaric Acid	1.00±0,05	0,87±0,10	ns
	Malic Acid	1.00±0,17	0,45±0,04	*
	Butyric Acid, 4-amino-	1.00±0,24	1,06±0,14	ns
	Aspartic Acid	1.00±0,15	0,98±0,38	ns
	Erythronic Acid-1,4-lactone	1.00±0,36	0,63±0,10	ns
	Glutamic Acid	1.00±0,10	0,63±0,14	ns
	Tartaric Acid	1.00±0,06	0,98±0,07	ns
	Glutaric Acid	1.00±0,11	0,85±0,06	ns
	Glucose, 1,6-anhydro, beta-D-	1.00±0,16	1,11±0,19	ns
	Quinic Acid	1.00±0,42	0,51±0,14	ns
	Citric Acid	1.00±0,17	1,02±0,12	ns
	Galactonic Acid-1,4-lactone	1.00±0,08	1,12±0,20	ns
	Dehydroascorbic Acid dimer	1.00±0,06	1,22±0,04	*
	Gluconic Acid	1.00±0,36	0,93±0,13	ns
	Ascorbic Acid	1.00±0,04	1,06±0,12	ns
	Glucuronic Acid-e-lactone	1.00±0,06	0,99±0,07	ns
	Cinnamic Acid, 4-hydroxy-, trans-	1.00±0,47	0,89±0,16	ns
	Caffeic Acid, cis-	1.00±0,05	1,45±0,08	**
	Caffeic Acid, trans-	1.00±0,04	1,39±0,15	*
Sugars	Fructose-6-phosphate	1.00±0,15	0,64±0,20	ns
	Sucrose, D-	1.00±0,06	0,99±0,07	ns
	Maltose, D-	1.00±0,08	1,38±0,20	ns
	Trehalose, alpha,alpha'-, D-	1.00±0,10	0,87±0,08	ns
	Fructose	1.00±0,10	0,77±0,19	ns
	Glucose	1.00±0,23	0,68±0,39	ns
	Rhamnose	1.00±0,07	0,58±0,21	ns
	Xylose	1.00±0,21	0,76±0,27	ns
Sugars-alcohols	Glycerol	1.00±0,04	0,95±0,05	ns
	Inositol	1.00±0,10	0.81±0.11	ns
Flavonols	Myricetin-3-*O*-rutinoside	1.00±0.02	1.41±0.09	**
	Myricetin-3-*O*-galactoside	1.00±0.34	1.98±0.26	ns
	Myricetin-3-*O*-glucoside	1.00±0.27	1.19±0.21	ns
	Myricetin-3-*O*-glucuronoside	1.00±0.18	1.73±0.30	ns
	Quercetin-3-*O*-rutinoside	1.00±0.18	0.90±0.23	ns
	Quercetin-3-*O*-galactoside	1.00±0.17	2.70±0.57	*
	Quercetin-3-*O*-glucoside	1.00±0.12	2.63±0.51	*
	Quercetin-3-*O*-glucuronoside	1.00±0.07	1.17±0.09	ns
	kaempferol-3-*O*-rutinoside	1.00±0.17	0.82±0.23	ns
	kaempferol-3-*O*-galactoside	1.00±0.15	5.48±2.28	ns
	kaempferol-3-*O*-glucoside	1.00±0.15	6.72±2.66	ns
	kaempferol-3-*O*-glucuronoside	1.00±0.14	1.22±0.26	ns
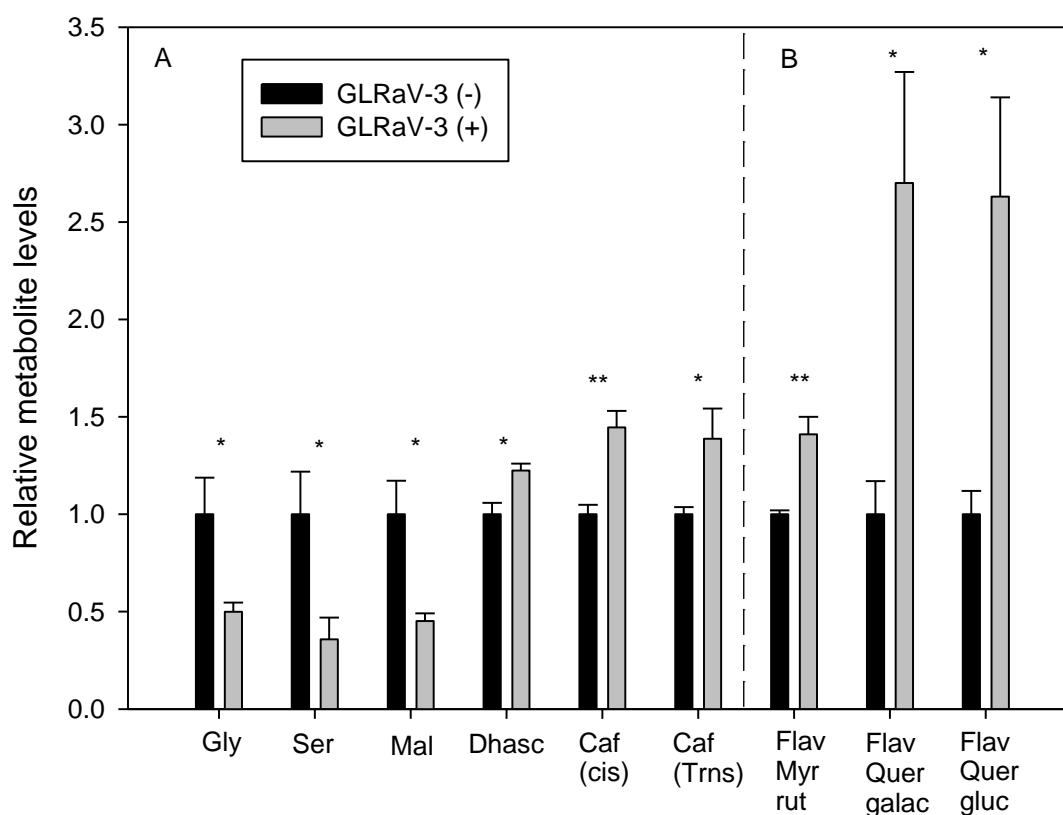
Figure 2. A. Primary metabolites: Glycine (Gly), serine (Ser), malic acid (Mal), dehydroascorbic acid (Dhasc), caffeic acid cis (Caf (cis)) and caffeic acid trans (Caf (trans)) expressed as relative metabolite levels comparing non-infected (GLRaV-3 (-)) and infected plants (GLRaV-3 (+)). **B.** Secondary metabolites: Myricetin-3-*O*-rutinoside (Flav Myr rut), quercetin-3-*O*-galactoside (Flav Quer galac) and quercetin-3-*O*-glucoside (Flav Quer gluc) expressed as relative metabolite levels comparing non-infected (GLRaV-3 (-)) and infected plants (GLRaV-3 (+)). Means and standard error of at least four plants are shown.

Effects of GLRaV-3 in plant secondary metabolism.

The up-regulation of the secondary metabolism induced in virus infected plants was analysed in leaves by MCFI. Fluorescence images were obtained for non-infected and infected plants in both sides of the leaf, corresponding to the blue (F440), green (F520), red (F680) and far-red (F740) fluorescence emission (Table 4). In the adaxial side of the leaves only differences in F520 were observed, being 9% higher in infected plants than in non-infected ones.

116

Table 4. Mean values of blue (F440), green (F520), red (F680), far-red (F740) fluorescence and ratios (F440/F520, F440/680, F440/740, F520/680, F520/740, F680/740) in non-infected (GLRaV-3 (-)) and infected plants (GLRaV-3 (+)) of Malvasía de Banyalbufar in adaxial and abaxial side of the leaf. Means and standard error of at least four plants are shown. Symbols *, ** and *** denotes significant differences at $P < 0.05$, <0.01 and <0.001, respectively; ns, not significant ($P > 0.05$).

	Adaxial side			Abaxial side		
	GLRaV-3 (-)	GLRaV-3 (+)	Sig.	GLRaV-3 (-)	GLRaV-3 (+)	Sig.
F440	174.25±1.46	181.87±3.57	ns	188.53±1.89	199.45±1.65	***
F520	211.47±2.31	234.49±10.78	*	288.88±5.11	314.08±5.17	**
F680	473.95±32.38	500.99±70.31	ns	1430.07±43.38	1363.88±50.24	ns
F740	872.87±57.93	906.18±160.50	ns	2394.37±73.36	2240.01±83.37	ns
F440/520	0.825±0.002	0.781±0.019	ns	0.651±0.005	0.636±0.005	ns
F440/680	0.377±0.024	0.398±0.037	ns	0.132±0.004	0.147±0.004	*
F440/740	0.205±0.012	0.233±0.027	ns	0.078±0.002	0.088±0.003	*
F520/680	0.458±0.028	0.503±0.037	ns	0.203±0.006	0.232±0.006	**
F520/740	0.250±0.014	0.293±0.029	ns	0.120±0.003	0.141±0.003	**
F680/740	0.543±0.011	0.575±0.018	ns	0.596±0.002	0.608±0.002	**

On the contrary, on the abaxial side of the leaf F440, F520, F440/680, F440/740, F520/680, F520/740 and F680/740, were significantly higher for infected plants. F440 and F520 increased 5% and 9%, respectively. F440/680, F440/740, F520/680, F520/740 increased 12% and F680/740 increased 2%. MCFI show that the marginal part of the leaf was most strongly affected by the virus (Figure 3).
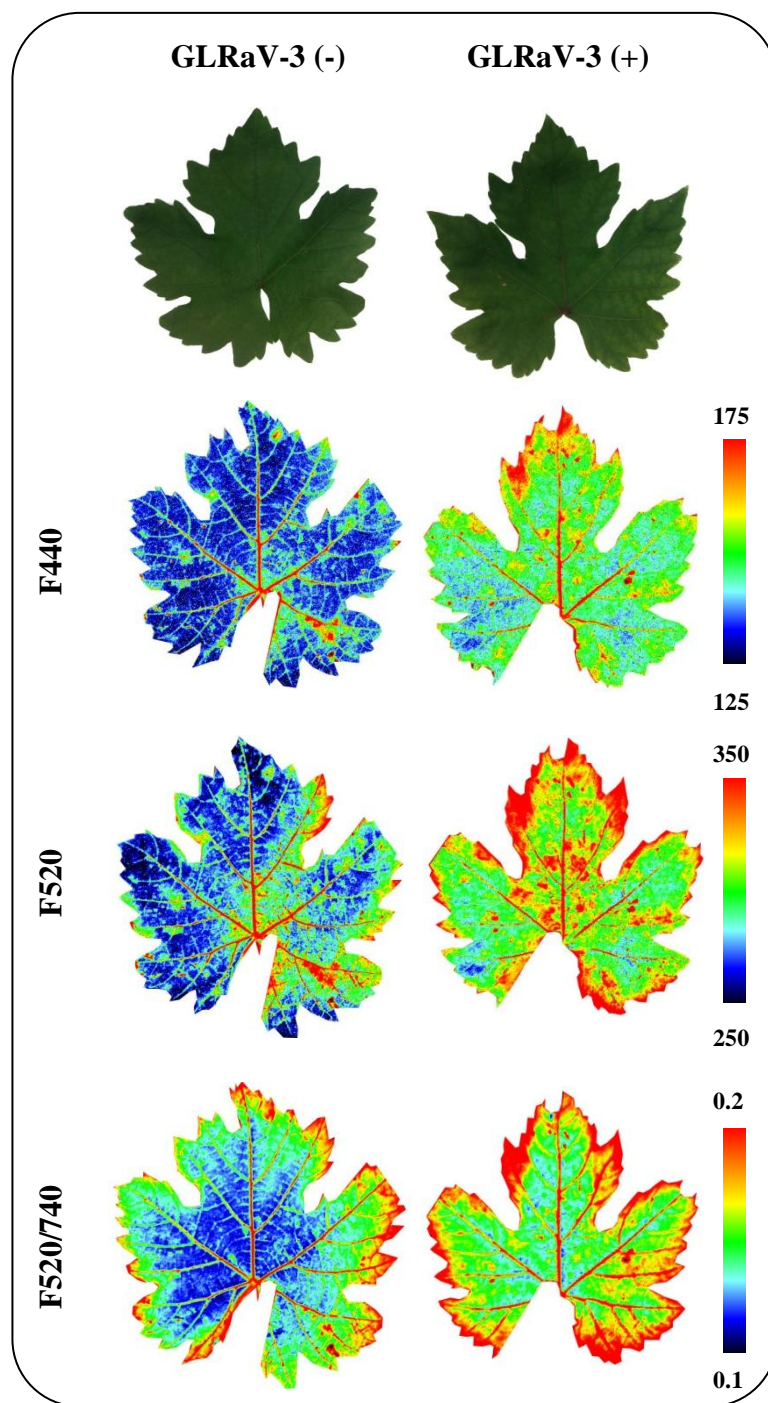
Figure 3. Impact of GLRaV-3 infection on secondary metabolism of grapevine leaves. Representative multicolour fluorescence images corresponding to F440, F520 and F520/F740 registered on the abaxial side of leaves are shown.

Leaf extracts were additionally analysed by liquid chromatography mass spectrometry (LC-MS), and 12 compounds were detected and identified (Table 3). Flavonols, such as myricetin, kaempferol and quercetin derivatives; and hydroxycinnamic acids, including derivatives of caffeic acid, increased upon infection.

Myricetin-3-*O*-rutinoside was significantly increased by 1.41-fold in infected plants, while quercetin-3-*O*-galactoside and quercetin-3-O-glucoside were 2.70-fold and 2.63-fold increased, respectively (Figure 2B). Otherwise, some metabolites such as kaempferol-3-*O*-galactoside or kaempferol-3-*O*-glucoside showed a 6-fold increase in infected plants, but this difference was not statistically significant due to the high variability in the concentration of those compounds between replicates (Table 3).

DISCUSION

Prevention and control of viruses are the main strategy to fight against the infection spread since there is no cure for virus infected grapevines. To date, most studies on GLRaV-3 have been focused on symptomatic plants of red cultivars (Moutinho-Pereira et al., 2012; Endeshaw et al., 2014). In contrast, little attention has been paid to the impact of viral infection on white varieties that develop no symptoms. In this work, asymptomatic plants of the white cultivar Malvasía de Banyalbufar were studied at the beginning of the growing season in order to evaluate the validity of Chl-F and MCFI parameters for identifying virus-infected plants.

At the beginning of the growing season virus concentration is low (Tsai et al., 2012). This would explain why in the present study the virus amount was lower than the values obtained in other studies (Velasco et al., 2014 (Chapter 3)). Although the virus concentration was low and no symptoms of the infection were observed, infected plants showed physiological disturbances.

Photosynthesis was slightly affected and therefore it was confirmed as a sensitive parameter affected by the virus (Table 1). Moutinho-Pereira et al. (2012) suggested stomatal conductance as the main factor responsible of photosynthesis depression in GLRaV-1 and GLRaV-3 infected plants under field conditions. However, in the present study, stomatal limitation could not be responsible for the decrease in net photosynthesis, as there were neither changes in g_s nor leaf temperature (Table 1). Therefore, mesophyll or biochemical limitations (Sampol et al., 2003) could affect photosynthesis in infected plants. Indeed, the results obtained by Chl-FI indicate a loss of functionality in the chloroplast. F_V/F_M, Φ_{PSII} and NPQ showed photoinhibition of PSII and an increase in the capacity for energy dissipation.

In previous studies under field conditions, F_V/F_M was not affected by the infection of grapevines by GLRaV-3 (Sampol et al., 2013; Moutinho-Pereira et al., 2012). However, in this study, F_V/F_M was decreased in infected plants relative to the value for the non-infected ones, pointing to a small permanent damage of PSII. The decrease in this parameter might be related to changes in the antenna complexes in the PSII, as suggested by the smaller Chl content (Table 1) and the increased F680/F740 value (Table 4) found in infected plants.

NPQ is considered to be a good indicator of infection in many plant pathogen systems, including viral, bacterial and fungal infections (Dodds & Rathjen, 2010; Rodríguez-Moreno et al. 2008; Pérez-Bueno et al., 2014; Granum et al., 2015). NPQ is composed of rapidly-reversible ΔpH-dependent quenching (qE or feedback de-excitation), and slowly reversible and irreversible processes such as state transition quenching (qT) and irreversible quenching (qI). In the present study, the viral infection affected mainly the reversible component of NPQ, since no significant difference was found in the irreversible quenching. This result implies an activation of photoprotective processes.

Virus-infected plants present not only alterations in photosynthesis but also in other metabolic pathways, in order to modulate respiration and other processes required for the defence against pathogen attack (Berger et al., 2007). Photorespiration seems to play an important role in active plant defence, partly because of being the major source of intracellular H_2O_2 (Kangasjärvi et al., 2012; Sørhagen et al., 2013). The decrease in the concentration of glycine and serine suggests the presence of virus might lead to inhibition of photorespiration (Figure 2A). Usually, when A_N decreases slightly, there is an increase on photorespiration. Only when A_N is strongly affected, photorespiration is also decreased.

Dehydroascorbic acid increased in infected plants comparing to non-infected ones. Post-transcriptional gene silencing is a plant defence mechanism against viruses in which dehydroascorbic acid plays an important role (Fujiwara et al., 2013). Ascorbic acid and derivates have the ability to interfere with the binding between viral small interfering RNAs and viral RNA silencing suppressor proteins *in vitro*. Therefore an increase in those compounds in plants would increase the tolerance to virus infection (Fujiwara et al., 2013) (Figure 2A).

GLRaV-3 infection also caused a reduction on the concentration of malate (Figure 2A). This metabolite has been described as an important factor driving the response of the stomatal guard cells (Araújo et al., 2011). Considering that no changes were observed in g_s, such effect is unlikely to occur in our host-pathogen system. However, malate could play different roles besides stomatal regulation, such as maintaining osmotic pressure, in amino acid biosynthesis, phosphorous and iron uptake. Malate is also involved in symbiotic nitrogen fixation and aluminium tolerance (Schulze et al., 2002) and serves as a respiratory substrate for adenosine triphosphate (ATP) and nicotinamide adenine dinucleotide (NADH) synthesis (Kovermann et al., 2007).

Although a strict line between primary and secondary metabolism cannot be drawn, activation of phenylpropanoid metabolism is considered to play a pivotal role in channelling carbon flux from primary metabolism to synthesis of phenolic compounds (Bauer et al., 2011). In the present study, phenylpropanoid compounds, including flavonols and caffeic acid, were accumulated in infected plants of Malvasía de Banyalbufar cultivar (Figure 2A and 2B). According to Gutha et al. (2010), transcripts encoding components of the phenylpropanoid biosynthesis pathway would be induced in the host plant by GLRaV-3 infection. Vega et al. (2011) already reported that grapevines infected with GLRaV-3 accumulate phenylpropanoids. However none of the studies explored correlated the accumulation of these compounds with the emission of autofluorescence. For most species, the intensity of the BGF signals is higher in abaxial than in adaxial side of the leaves, which have a thicker epidermis and its palisade parenchyma is more tightly packed. Most of the BGF comes from the cuticle, cell walls from epidermis and vascular tissues, while Chl-F comes mostly from mesophyll and occlusive cells of the stomata (Buschman et al., 1998; Cerovic et al., 1999). The increase in the amplitude of F440 and F520 correlates with the higher concentration of phenylpropanoids in infected plants: flavonols such as myricetin-3-*O*-rutinoside, quercetin-3-*O*-galactoside and quercetin-3-*O*-glucoside; and hydroxycinnamic acids such as caffeic acid. Similar increases were reported after point measurements in Chinese cabbage infected with *pepper mild mottle virus* and *turnip yellow mosaic virus* (Pineda et al., 2008b; Szigeti et al., 2002).

Based on these results, we conclude that the combination of NPQ with the MCFI parameters F440, F520, F440/680, F440/740, F520/680, F520/740 and F680/740 (measured on the abaxial side of the leaves), could be an useful tool for the

identification of asymptomatic Malvasía de Banyalbufar plants as potentially infected by GLRaV-3.

ACKNOWLEDGEMENTS

REFERENCES.

Araújo W.L., Nunes-Nesi A., Osorio S., Usadel B., Fuentes D., Nagy R., Balbo I., Lehmann M., Studart-Witkowski C., Tohge T., Martinoia E., Jordana X., DaMatta F., & Fernie A.R. (2011). Antisense inhibition of the iron-sulphur subunit of succinate dehydrogenase enhances photosynthesis and growth in tomato via an organic acid–mediated effect on stomatal aperture. *Plant Cell*, **23**, 600–627.

Balachandran S., Hurry V.M., Kelley S.E., Osmond C.B., Robinson S.A., Rohozinski J., Seaton G.G.R., & Sims D.A. (1997). Concepts of plant biotic stress. Some insights into the stress physiology of virus-infected plants, from the perspective of photosynthesis. *Physiologia Plantarum*, **100**, 203–213.

Balachandran S., & Osmond B.C. (1994). Susceptibility of tobacco leaves to photoinhibition following infection with two strains of *Tobacco mosaic virus* under different light and nitrogen nutrition regimes. *Plant Physiology*, 104, 1051–1057.

Barón M., Flexas J, & Delucia E.H. (2012). Photosynthetic responses to biotic stress. Terrestrial Photosynthesis in a Changing Environment: A Molecular, Physiological, and

Ecological Approach. J. Flexas, F. Loreto and H. Medrano. Cambridge, Cambridge University Press: 331-350.

Basso M.F., Fajardo T.V.M., Eiras M., Ayub R.A., & Nickel O. (2010). Detecção e identificação molecular de vírus associados a videiras sintomáticas e assintomáticas. *Ciência Rural*, **40**, 2249-2255.

Bauer N., Fulgosi H., & Jelaska S. (2011). Overexpression of Phenylalanine Ammonia-Lyase in Transgenic Roots of Coleus blumei Alters Growth and Rosmarinic Acid Synthesis. *Food Technology and Biotechnology*, **49 (1)**, 24–31.

Berger S., Benediktyová Z., Matouš K., Bonfig K., Mueller M.J., Nedbal L., & Roitsch T. (2007). Visualization of dynamics of plant-pathogen interaction by novel combination of chlorophyll fluorescence imaging and statistical analysis: Differential effects of virulent and avirulent strains of *Pseudomonas syringae* and of oxylipins on *Arabidopsis thaliana*. *Journal Experimental Botany*, **58**, 797–806.

Berger S., Papadopoulos M., Schreiber U., Kaiser W., & Roitsch T. (2004). Complex regulation of gene expression, photosynthesis and sugar levels by pathogen infection in tomato. *Physiologia Plantarum*, **122**, 419-428.

Bonfig K.B., Schreiber U., Gabler A., Roitsch T., & Berger S. (2006). Infection with virulent and avirulent P. syringae strains differentially effects photosynthesis and sink metabolism in Arabidopsis leaves. *Planta*, **225**, 1-12.

Buschmann C., Langsdorf G., & Lichtenthaler H.K. (2000). Imaging of the blue, green, and red fluorescence emission of plants: An overview. *Photosynthethica*, **38**, 483–491.

Buschmann C., & Lichtenthaler H.K. (1998). Principles and characteristics of multi-colour fluorescence imaging of plants. *Journal of Plant Physiology*, **152**, 297–314.

Cerovic Z.G., Ounis A., Cartelat A., Latouche G., Goulas Y., Meyer S., & Moya I. (2002). The use of chlorophyll fluorescence excitation spectra for the non-destructive *in situ* assessment of UV-absorbing compounds in leaves. *Plant Cell Environment*, **25**, 1663–1676.

Cerovic Z.G., Samson G., Morales F., Tremblay N., & Moya I. (1999). Ultraviolet-induced fluorescence for plant monitoring: Present state and prospects. *Agronomie*, **19**, 543–578.

Chaerle L., Hagenbeek D., De Bruyne E., Valcke R., & Van Der Straeten D. (2004). Thermal and chlorophyll-fluorescence imaging distinguish plant pathogen interaction at an early stage. *Plant Cell Physiology*, **45**, 887-896.

Charles J.G., Froud K.J., van der Brink R., & Allan D.J. (2009). Mealybugs and the spread of *Grapevine leafroll-associated virus 3* (GLRaV-3) in a New Zealand vineyard. *Australasian Plant Pathology*, **38**, 576-583.

Chou H.M., Bundock N., Rolfe A.S., & Scholes D.J. (2000). Infection of Arabidopsis thaliana leaves with Albugo candida (white blister rust) causes a reprogramming of host metabolism. *Molecular Plant Pathology*, **2**, 99-113.

Clark M.F., & Adams A.N. (1977). Characteristics of the microplate method of enzyme-linked immunosorbent assay for the detection of plant viruses. *Journal of General Virology*, **34**, 475-483.

Christov I., Stefanov D., Velinov T., Goltsev V., Georgieva K., & Abracheva P. (2007). The symptomless leaf infection with *Grapevine leafroll associated virus 3* in grown *in vitro* plants as a simple model system for investigation of viral effects on photosynthesis. *Journal of Plant Physiology*, **164**, 1124–1133.

Dixon R.A., Achnine L., Kota P., Liu C.J., Reddy MS, & Wang L. (2002). The phenylpropanoid pathway and plant defense – a genomics perspective. *Molecular Plant Pathology*, **3**, 371–390.

Dodds P.N., & J.P. (2010). Plant immunity: towards an integrated view of plant–pathogen interactions. *Nature Reviews Genetics*, **11**, 539–548.

Endeshaw S.T., Sabbatini P., Romanazzi G., Annemiek C., Schilder A.C., & Neri D. (2014). Effects of *Grapevine leafroll associated virus 3* infection on growth,leaf gas exchange, yield and basic fruit chemistry of *Vitis vinifera* L. cv. Cabernet Franc. *Scientia Horticulturae*, 170, 228–236.

Fujiwara A., Shimura H., Masuta C., Sano S., & Inukai T. (2011). Exogenous ascorbic acid derivatives and dehydroascorbic acid are effective antiviral agents against *Turnip mosaic virus* in Brassica rapa. *Journal of General Plant Pathology*, **79**, 198–204.

Gambino G., Cuozzo D., Fasoli M., Pagliarani C., Vitali M., Boccacci P., Pezzotti M., & Mannini F. (2012). Co-evolution between *Grapevine rupestris stem pitting associated virus* and *Vitis vinifera* L. leads to decreased defense responses and increased transcription of genes related to photosynthesis. *Journal of Experimental Botany*, **63(16)**, 5919–5933.

Granum E., Pérez-Bueno M.L., Calderón C.E., Ramos C., de Vicente A, Cazorla F.M., & Barón M. (2015). Metabolic responses of avocado plants to stress induced by Rosellinia necatrix analysed by fluorescence and thermal imaging. *European Journal of Plant Pathology*, **142(3)**, 625–632.

Gutha R.L., Casassa L.F., Harbertson J.F., Rayapati A., & Naidu R.A. (2010). Modulation of flavonoid biosynthetic pathway genes and anthocyanins due to virus infection in grapevine (*Vitis vinifera* L.) leaves. *BMC Plant Biology*, **10**, 187.

Hoagland D.R., & Arnon D.I. (1950). The water-culture method for growing plants without soil. *California Agricultural Experiment Station*, **347**, 1–32.

Kangasjärvi S., Neukermans J., Li S., Aro E.M., & Noctor G. (2012). Photosynthesis, photorespiration, and light signalling in defense responses. *Journal Experimental Botany*, **63**, 1619–1636.

Kovermann P., Meyer S., Hortensteiner S., Picco C., Scholz-Starke J., Ravera S., Lee Y., & Martinoia E. (2007). The Arabidopsis vacuolar malate channel is a member of the ALMT family. *Plant Journal*, **52**, 1169–1180.

Komar V., Vigne E., Demangeat G., & Fuchs M. (2007). Beneficial effect of selective virus elimination on the performance of Vitis vinifera cv. Chardonnay. *American Journal of Enology and Viticulture*, **58**, 202–210.

Kopka J., Schauer N., Krueger S., Birkemeyer C., Usadel B., Bergmüller E., Dörmann P., Weckwerth W., Gibon Y., Stitt M., Willmitzer L., Fernie A.R., & Steinhauser D.

(2005). GMD@CSB.DB: the Golm Metabolome Database. *Bioinformatics*, **21**, 1635–1638.

Lichtenthaler H.K., & Miehé JA. (1997). Fluorescence imaging as a diagnostic tool for plant stress. *Trends in Plant Science*, **2**, 316–320.

Lisec J., Schauer N., Kopka J., Willmitzer L., & Fernie A.R. (2006). Gas chromatography mass spectrometry-based metabolite profiling in plants. *Nature Protocols*, **1**, 387–396.

Lohaus G., Heldt H.W., & Osmond C.B. (2000). Infection with phloem limited *Abutilon mosaic virus* causes localized carbohydrate accumulation in leaves of Abutilon striatum: relationships to symptom development and effects on chlorophyll fluorescence quenching during photosynthetic induction. *Plant Biology*, **2**, 161-167.

Maree H.J., Almeida R.P.P., Bester R., Chooi K.M., Cohen D., Dolja V.V., Fuchs M.F., Golino D.A., Jooste A.E.C., Martelli G.P., Naidu R.A., Rowhani A., Saldarelli P., & Burger J.T. (2013). *Grapevine leafroll-associated virus 3*. *Frontiers in Microbiology*, **4**, 82.

Martelli G.P. (2012). Grapevine virology highlights 2010–2012. Proceedings of the 17th Meeting of the International Council for the Study of Virus and Virus-like Diseases of the Grapevine. ICVG, Davids, California, USA, October 7-14, 2012, pp. 13–32.

Montero R., El aou ouad H., Pacifico D., Marzachì C., Castillo N., García E., Del Saz N.F., Florez-Sarasa I., Flexas J., & Bota J. (2015). Absolute quantification of *Grapevine Leafroll associated Virus 3* (GLRaV-3) and its effects on the physiology in asymptomatic plants of *Vitis vinifera* L. (Submitted)

Morales F., Cartelat A., Alvarez-Fernández A., Moya I., & Cerovic Z.G. (2005). Time-resolved spectral studies of blue-green fluorescence of artichoke (*Cynara cardunculus* L. Var. Scolymus) leaves: identification of chlorogenic acid as one of the major fluorophores and age-mediated changes. *Journal of Agricultural Food Chemistry*, **53(25)**, 9668-9678.

Moutinho-Pereira J., Correia C.M., Gonçalves B., Bacelar E.A., Coutinho J.F., Ferreira H.F., Lousada J.L., & Cortez M.I. (2012). Impacts of leafroll-associated viruses (GLRaV-1 and -3) on the physiology of the Portuquese grapevine cultivar "Touriga Nacional" growing under field conditions. *Annals of Applied Biology*, **3**, 47–46.

Murchie E.H., & Lawson T. (2013). Chlorophyll fluorescence analysis: a guide to good practice and understanding some new applications. *Journal Experimental Botany*, **64**, 3983–3998.

Osmond C.B., Daley P.F., Badger M.R., & Lüttge U. (1998). Chlorophyll fluorescence quenching during photosynthetic induction in leaves of Abutilon striatum Dicks infected with *Abutilon mosaic virus* observed with a field-portable imaging system. *Botanica Acta*, **111**, 390-397.

Pacifico D., Caciagli P., Palmano S., Mannini F., & Marzachì C. (2011). Quantitation of *Grapevine leafroll associated virus-1 and -3, Grapevine virus A, Grapevine fanleaf virus and Grapevine fleck virus* in field-collected Vitis vinifera L. 'Nebbiolo' by real-time reverse transcription-PCR. *Journal of Virological Methods*, **172**, 1-7.

Parker D., Beckmann M., Zubair H., Enot D.P., Caracuel-Rios Z., Overy D.P., Snowdon S., Talbot N.J., & Draper J. (2009). Metabolomic analysis reveals a common pattern of metabolic re-programming during invasion of three host plant species by Magnaporthe grisea. *Plant Journal*, **59**, 723–737.

Pérez-Bueno M.L., Ciscato M., vandeVen M., García-Luque I., Valcke R., & Barón M. (2006). Imaging viral infection: studies on *Nicotiana benthamiana* plants infected with the *pepper mild mottle tobamovirus*. *Photosynthesis Research*, **90**, 111–123.

Pérez-Bueno M.L., Pineda M., Díaz-Casado E., & Barón M. (2014). Spatial and temporal dynamics of primary and secondary metabolism in *Phaseolus vulgaris* challenged by *Pseudomonas syringae*. *Physiologia Plantarum*, DOI: 10.1111/ppl.12237.

Petit A.N., Vaillant N., Boulay M., Clement C., & Fontaine F. (2006). Alteration of photosynthesis in grapevines affected by esca. *Phytopathology*, **96**, 1060–1066.

Pineda M., Soukupova J., Matouš K., Nedbal L., & Barón M. (2008a). Conventional and combinatorial chlorophyll fluorescence imaging of tobamovirus-infected plants. *Photosynthetica*, **46(3)**, 441-451.

Pineda M., Gáspár L., Morales F., Szigeti Z., & Barón M. (2008b). Multicolour Fluorescence Imaging of Leaves—A Useful Tool for Visualizing Systemic Viral Infections in Plants. *Photochemistry and Photobiology*, **84**, 1048–1060.

Rodríguez-Moreno L., Pineda M., Soukupová J., Macho A.P., Beuzón C.R., M. Barón M., & Ramos C. (2008). Early detection of bean infection by *Pseudomonas syringae* in asymptomatic leaf areas using chlorophyll fluorescence imaging. *Photosynthesis Research*, **96(1)**, 27–35.

Roessner U., Luedemann A., Brust D., Fiehn O., Linke T., Willmitzer L., & Fernie A.R. (2001). Metabolic profiling allows comprehensive phenotyping of genetically or environmentally modified plant systems. *The Plant Cell*, **13**, 11–29.

Sampol B., Bota J., Riera D., Medrano H., & Flexas J. (2003). Analysis of the virus-induced inhibition of photosynthesis in malmsey grapevines. *New Phytologist*, **160**, 403–412.

Schauer N., Steinhauser D., Strelkov S., Schomburg D., Allison G., Moritz T., Lundgren K., Roessner-Tunali U., Forbes M.G., Willmitzer L., Fernie A.R., & Kopka J. (2005). GC-MS libraries for the rapid identification of metabolites in complex biological samples. *Febs letters*, **579 (6)**, 1332-1337.

Scholes J.D., & Rolfe S.A. (2009). Chlorophyll fluorescence imaging as tool for understanding the impact of fungal diseases on plant performance: a phenomics perspective. *Functional Plant Biology*, **36 (10-11)**, 880-892.

Schulze J., Tesfaye M., Litjens R.H.M.G., Bucciarelli B., Trepp G., Miller S., Samac D., Allan D., & Vance C.P. (2002). Malate plays a central role in plant nutrition. *Plant and soil*, **247**, 133-139.

Sørhagen K., Laxa M., Peterhansel C., & Reumann S. (2013). The emerging role of photorespiration and non-photorespiratory peroxisomal metabolism in pathogen defense. *Plant Biology*, **15**, 723–736.

Swarbrick P.J., Schulze-Lefert P., & Scholes J.D. (2006). Metabolic consequences of susceptibility and resistance (race-specific and broad-spectrum) in barley leaves challenged with powdery mildew. *Plant Cell Environment*, **29**, 1061-1076.

Szigeti Z., Almási A., & Sárvári E. (2002). Changes in the photosynthetic functions in leaves of Chinese cabbage infected with *Turnip yellow mosaic virus*. *Acta Biologica Szegediensis*, **46**, 137–138.

Tohge T., & Fernie A.R. (2010). Combining genetic diversity, informatics and metabolomics to facilitate annotation of plant gene function. *Nature Protocols*, **5**, 1210–1227.

Tsai C.W., Daugherty M.P., & Almeida R.P.P. (2012). Seasonal dynamics and virus translocation of *Grapevine leafroll-associated virus 3* in grapevine cultivars. *Plant Pathology*, **61**, 977–985.

Vega A., Gutierrez R., Penña-Neira A., Cramer G., & Arce-Johnson P. (2011). Compatible GLRaV-3 viral infections affect berry ripening decreasing sugar accumulation and anthocyanin biosynthesis in *Vitis vinifera* L.. *Plant Molecular Biology*, **77**, 261–274.

Velasco L., Bota J., Montero R., & Cretazzo E. (2014). Differences of three ampeloviruses multiplication in plant contribute to explain their incidences in vineyards. *Plant disease*, **98**, 395–400.

Chapter 6

EFFECTS OF GRAPEVINE LEAFROLL ASSOCIATED
VIRUS 3 (GLRaV-3) EFFECTS ON PLANT CARBON
BALANCE IN VITIS VINIFERA L. CV. GIRÓ ROS

EFFECTS OF GRAPEVINE LEAFROLL ASSOCIATED VIRUS 3 (GLRaV-3) ON PLANT CARBON BALANCE IN VITIS VINIFERA L. CV. GIRÓ ROS.

R. Montero[1], H. El aou ouad[2], J Flexas[2], J. Bota[2]

[1]Institut de Recerca i Formació Agrària i Pesquera de les Illes Balears (IRFAP), 07009 Palma de Mallorca, Spain.

[2]Grup de Recerca en Biologia de les Plantes en Condicions Mediterrànies, Departament de Biologia, Universitat de les Illes Balears, Carretera de Valldemossa, km 7.5, 07122, Palma de Mallorca, Balears, Spain.

*Corresponding author: j.bota@uib.es

ABSTRACT

Phloem systemic viruses like GLRaV-3 cause significant economic losses in many vineyards around the world. Previous studies have shown that this virus could limit carbon assimilation, without affecting aerial plant growth. However, most of the studies were focused only in the effects of the virus on photosynthesis, i.e. a reduction in the availability of fixed carbon, neglecting the importance carbon losses by respiration, not only in leaves, but in all plant tissues. In this study, we analysed the effects of GLRaV-3 on the plant carbon balance. The results showed an absence of virus effects on the total biomass increment despite the fact that there was a reduction in carbon assimilation. The discrepancy was found due to an adjustment of carbon losses by respiration caused by the presence of the virus, which compensated the lower carbon assimilation with the result that the total plant carbon balance was unaffected. The carbon balance estimated by measuring photosynthesis and respiration in different plant organs matched well with that measured as total biomass increments. In addition, upper leaves and roots were identified as the most sensitive parts of the plant to GLRaV-3 infection.

Keywords: Leaf gas exchange, plant carbon balance, assimilate transport, *Vitis vinifera*.

INTRODUCTION

Within several Grapevine leafroll viruses, the so-called *Grapevine leafroll associated virus-3* (GLRaV-3) is one of the most important because it is widespread worldwide and produces significant economic losses around the world (Mannini et al., 2012). The incidence of multiple and single viral infections is very high in Majorcan viticulture and GLRaV-3 is the predominant virus in local varieties (Cretazzo et al., 2010).

The spread of a systemic virus in a plant is influenced by the direction of carbohydrate movement in the phloem (Hull, 2002). Phloem-limited viruses, such as GLRaV-3, are mainly spread with the remobilisation of sugars in the roots and trunk during the spring (Charles et al., 2006). Moreover, viruses exploit plants inter- and intracellular connection systems to facilitate their systemic spread. On the other hand,

carbohydrate translocation from foliar parenchyma could be interrupted because sieve elements are blocked and ruptured by the effect of this virus. Consequently starch cannot be transported from the leaf to other leaves and other parts of the plant, producing the characteristic symptom of the virus manifested by downward rolling leaves (Martelli, 2009).

Even when visual symptoms are not apparent, as occurs in white varieties, GLRaV-3 produces important effects in plant physiology of grapevines (Endeshaw et al., 2014). The virus has been shown to affect photosynthesis, primary metabolism and respiration (Mannini et al., 1996; Sampol et al., 2003; Mannini et al., 2012), suggesting that plant carbon balance (PCB) could be altered by the infection. In addition the virus effects on mesophyll cells and/or sieve elements will affect the source-sink ratio and consequently the assimilate distribution and final PCB. Within season, grapevine carbohydrate dynamics rely on the balance between carbon supply from canopy assimilation and carbon demand, which depends on growth and maintenance of the different sinks (berries, leaves, stems, trunk and root). Sugar translocation in grapevines predominantly occurs towards young expanding shoots and, once shoots are matured, then sugars move predominantly from the leaves to developing fruit and into the canes, trunk and roots (Williams, 1996). Sugar transport and allocation of assimilates between sources and sinks are major parameters controlling crop productivity (Gifford et al., 1984). Carbon balance disorders can result in lower sink sugar content (Hoefert & Gifford, 1967; Von der Brelie & Nienhaus, 1982).

GLRaV-3 effects on carbon balance in the whole plant and assimilate distribution have not been studied in depth. Thus, the aim of this work is to determine how GLRaV-3 affects the different components of carbon balance and biomass distribution, identifying the relative sensitivity of different organs to infection.

MATERIAL AND METHODS

Plant material and growth conditions

Pot-grown virus-free and GLRaV-3 infected plants of *Vitis vinifera* L. cv. Girò Ros, a white cultivar, were compared. Plants were obtained by direct rooting of 0.2 m

cuttings of dormant canes selected from mother plants growing under field conditions in a thirteen year old experimental vineyard sited at IRFAP center (*Institut de Recerca i Formació Agrària i Pesquera, Conselleria d'Agricultura Medi Ambient i Territori*), Palma de Mallorca (Balearic Islands, Spain). Cuttings were collected from infected vines, not showing virus symptoms in the field. Two weeks after rooting, five cuttings infected with GLRaV-3 and five non-infected cuttings were planted in pots of 10 l volume and trained to a single shoot with no fruit. The pots were filled with organic substrate and perlite mixture (5:1). This process was done inside the greenhouse, where the temperature was kept at 27±0.5ºC. The experiment was carried out during July and August 2014 under outdoor conditions. Before starting the experiment all the plants were irrigated daily, and every 15 days organic fertilizer was added to the pots. Starting two weeks before the onset of the experiment, the organic fertilizer was replaced every three days with 50% Hoagland´s solution (Hoagland & Aron, 1950).

Environmental conditions and plant water status

Environmental conditions were recorded during the experiment using a meteorological station (Meteodata 3000, Geónica SA, Madrid, Spain). Maximum and minimum daily air temperature and integrated daily photosynthetic active radiation were monitored during the days of the experiment. Leaf water status was determined in leaves as the predawn leaf water potential, using a Scholander chamber (Soil Moisture Equipment Corp., Santa Barbara, CA, USA) in the same day of gas exchange measurements.

Virus diagnosis

The presence or absence of GLRaV-1, 3, 4, 5, 7, 9, GFLV (Grapevine Fanleaf Virus) and GFkV (Grapevine Fleck virus) viruses was tested by enzyme-linked immunosorbent assay (ELISA) (Clark & Adams, 1977) using commercial coating and conjugate antibodies preparations (Bioreba AG, Reinach, Switzerland). Field grown mother plants were tested, and then non-infected and single GLRaV-3 infected plants were selected for the experiment. The ELISA results were confirmed in selected plants by RT-PCR using a Real time PCR system (Illumina, SD, USA). GLRaV-1, 2, 3, 4, 5, GFLV and GFkV were tested with this technique. Total RNA was extracted from one leaf per plant (70 mg of phloem scraped from leaves) using Spectrum[TM] Plant Total

RNA Kit (Sigma-Aldrich, Inc.) according to manufacturer's instructions. The Spectrum™ Plant total RNA Kit removes most of the DNA during RNA purification. However, for very sensitive applications, such as quantitative RT-PCR, complete removal of traces of DNA may be necessary. On-Column DNase I Digest Set (Sigma-Aldrich Co., St Louis, MO, USA) was used to digest the DNA during RNA purification following the manufacturer´s instruction. RNA purity and concentration were measured at 260/280 nm using a spectrophotometer (NanoDrop-1000, Thermo Scientific, Villebon sur Yvette, France). First-strand cDNA synthesis was performed using 500 ng of total RNA, 200 units of recombinant *Moloney Murine Leukemia Virus* (MuLV) reverse transcriptase (Invitrogen Life Technologies, Inc.), 40 units of RNase inhibitor (RNase out, Invitrogen Life Technologies, Inc.), 0.4 mM of dNTPs, and 2 mM of random nonamers (Takara Bio, Inc.). The mixture for reverse transcriptase (20 μl) was incubated for 50 min at 37ºC and the reaction was inactivated by heating it at 70ºC for 15 min.

Quantification of the viral content were performed by real-time PCR reactions in a 10 μl mixture containing 2 μl of diluted (1:100) cDNA, 5 μl iQ SYBR Green Reaction-Mix (Bio-Rad), and 0,2 μM of each primer in the ECO-Illumina system (ECO-Illumina) using the following PCR cycle profile: one cycle of 2 min at 95°C followed by 40 cycles of 5 s at 95°C and 20 s at 60°C. The fluorescence threshold value (Ct) was calculated using the ECO-Illumina system software (ECO-Illumina). Overall, a mean Ct value was calculated from two PCR replicates.

A list of primer pairs and amplicon lengths used for the virus diagnosis are reported in Pacifico et al. (2011). Sequences of primers used in this study were identified and partial gene-specific sequences amplified. GLRaV-3 standard curve for virus quantification was performed according to Montero et al. (2015a)(Chapter 4) using RNA dependent RNA polymerase sequence (KP844580).

Growth measurements

Total leaf area was measured at the beginning of July and middle August, when the two diurnal time cycles of net photosynthesis were carried out. Total number of leaves per plant, shoot length and total leaf area were determined during the same week of gas exchange. Leaf area was measured. Thirty six leaves of different sizes were used

to develop a linear regression describing the relationship between leaf area (using public domain image analysis software (ImageJ version 1.32; http.//rsb.info.nih.gov/ij/) and leaf length. The length of each leaf on the vine was then used to estimate the total vine leaf area.

Photosynthesis and respiration

Gas exchange parameters were measured in non-infected and infected plants using a Li-6400 (Li-Cor Inc., Lincoln, Nebraska, USA) under ambient temperature and relative humidity and at 1500 µmol m^{-2} s^{-1} of photosynthetic photon flux density (PPFD) and 400 µmol CO_2 mol^{-1} air. Flow was set at 350 µmol s^{-1}. Fully expanded leaves from either apical or basal parts of the stem of five plants per treatment were measured. Two diurnal time courses of leaf gas exchange were completed during the experiment at the beginning of July and mid-August, respectively, by measuring at six time intervals between 7:00 and 19:00 h (solar time). Dark respiration (R_d) was measured in dark adapted leaves with a 6 cm^2 leaf chamber and air flow was set at flow 150 µmol s^{-1}. Additionally, R_d was measured at 20, 25, 30 and 35°C in non-infected and infected plants when R_d values reached steady state for each temperature. Measurements were done after 8–10 h of dark period in a controlled room temperature in five leaves per treatment. Carbon losses during diurnal leaf respiration are implicitly included in the measurements of A_N, because this equals gross photosynthesis minus the sum of photorespiration and mitochondrial respiration. Leaf respiration values at different temperatures were used to develop calibration curves for the temperature response of leaf respiration in non-infected and infected plants. Root respiration (R_{root}) was estimated by measuring soil CO_2 efflux at 400 µmol CO_2 mol^{-1} air with an open gas exchange system (Li-6400, Li-Cor Inc.), attached to a soil chamber (Li-Cor 6400-09, Li-Cor Inc.). Five plants per treatment were measured once during the experiment at substrate temperatures of approximately 20, 25 and 35°C. All measurements were performed outdoors, considering the natural variations of substrate temperature during the day, except for 20°C, for which pots were left overnight in a controlled temperature room. At each temperature, pots containing the same substrate but no plant were also measured to account for the respiration of soil microorganisms. R_{root} was estimated as the difference between CO_2 efflux in pots containing and no containing plants (Koerber et al., 2010). CO_2 efflux values at different substrate temperatures were used to develop

calibration curves for the response of R_{root} to temperature in non-infected and infected plants, which were later used to estimate R_{root} rates during the whole experiment using the substrate temperature. Stem respiration (R_{stem}) was also measured using a Li-6400 gas-exchange system (Li-cor Inc. Lincoln, NE, USA) with a 6 cm^2 leaf chamber. CO_2 concentration in the leaf chamber was set at 400 µmol CO_2 mol^{-1} air and air flow at 150 µmol s^{-1}. Gaskets were perforated to introduce the stem without cutting it. Leaks were avoided putting Blu-Tack (Bostik) between gasket surface and the stem. Both apical and intermediate stem sections were measured. In this case, temperature response curve were not determined because of absence of variation in R_{stem} to temperature changes (Escalona et al., 2012).

Whole plant carbon gain and estimated plant carbon balance

In order to estimate plant carbon balance (PCB), two diurnal time cycles of net photosynthesis were carried out at the beginning of July and middle August as mentioned above. These cycles corresponded to the beginning and the end of the experiment respectively (44 days between the two cycles). Estimation of carbon gain by photosynthesis ($A_{N\ leaf}$) in upper and lower leaves was obtained from the sum of the daily multiplier of A_N by total leaf area. The daily carbon gain per leaf area was estimated as the integral of the A_N vs time curve. Two values were obtained, one for upper and one for lower leaf types. Multiplying each value by the total leaf area of each canopy fraction, the total daily carbon gain by the total leaves of each type was obtained. The sum of the two values equals the total plant carbon gain during one day.

To obtain CO_2 inputs during the whole experiment, data from the two cycles were used. During the first 22 days of the experiment A_N was assumed to be equal to the diurnal time cycle performed in July, and during the last 22 days experiment A_N was assumed to be equal to the diurnal time cycle performed in August. Every day, the total leaf area was estimated assuming a linear increment of leaf area from the beginning to the end of the experiment. Total CO_2 assimilation during each period was obtained multiplying daily A_N by the corresponding days. The CO_2 input of whole experiment was estimated as the sum of the two periods.

Respiration of the different organs of the plant produces carbon losses. Using respiration values measured for each organ (leaves, stem and roots) and determining

changes in these values by temperature variations, it is possible to estimate total carbon losses by respiration in the whole plant throughout the experiment. Estimation of R_{root} was derived from a single exponential function derived from dataset of R_{root} and soil temperature (T_{soil}) previously obtained for non-infected and infected plants of Girò Ros under controlled conditions. This exponential function was used for the calculation of daily R_{root} considering hourly changes of T_{soil} and daily linear increases during the experiment. Estimation of total leaf dark respiration (R_{Dleaf}) for upper and lower leaves was obtained from a single exponential function derived from dataset of leaf respiration at 20, 25, 30 and 35ºC for non-infected and infected plants. This function was used for the calculation considering hourly changes of T_{air} and increment of leaf area as described earlier. Total R_{stem} for apical and intermediate stems was considered constant due to absence of variation in R_{stem} to temperature changes (Escalona et al., 2012).

Finally, the difference between carbon gains by net CO_2 assimilation and carbon looses by respiration is the PCB during the whole experiment as shows the following equation:

$$PCB = A_{N\text{ upper leaf}} + A_{N\text{ lower leaf}} - R_{D\text{ upper leaf}} - R_{D\text{ lower leaf}} - R_{\text{upper stem}} - R_{\text{lower stem}} - R_{\text{root}}$$

PCB obtained by this method should match with the total biomass (dry mass) increment along the study period. Whole biomass and plant growth were measured throughout the summer, in five plants per treatment. Biomass was obtained from dry weights of roots, stems and leaves. These tissues were separated in upper leaves, lower leaves, upper stem, lower stem and roots. Then they were dried in an oven at 60°C until constant weight and their respective dry biomass were recorded. Total plant biomass increment was obtained from the different in weight in four plants per treatment before carrying out the first diurnal time cycles of net photosynthesis (initial biomass) and five plants per treatment at end of the experiment (final biomass). Then carbon content in this biomass was calculating according to Grechi et al. (2007), to determine the coincidence with carbon content as measured by the method mentioned above.

Statistical analysis

The data was analyzed using R (http://.rproject.org/). Student-T was used for determining differences in between the treatments for the parameters measured.

RESULTS

Environmental conditions and plant water status

Environmental conditions were measured during the experiment (Figure 1). Changes in T_{air} and PPFD were typical for a summer period in Mallorca. However at the end of the experiment there were some days of somewhat reduced temperatures and PPFD.
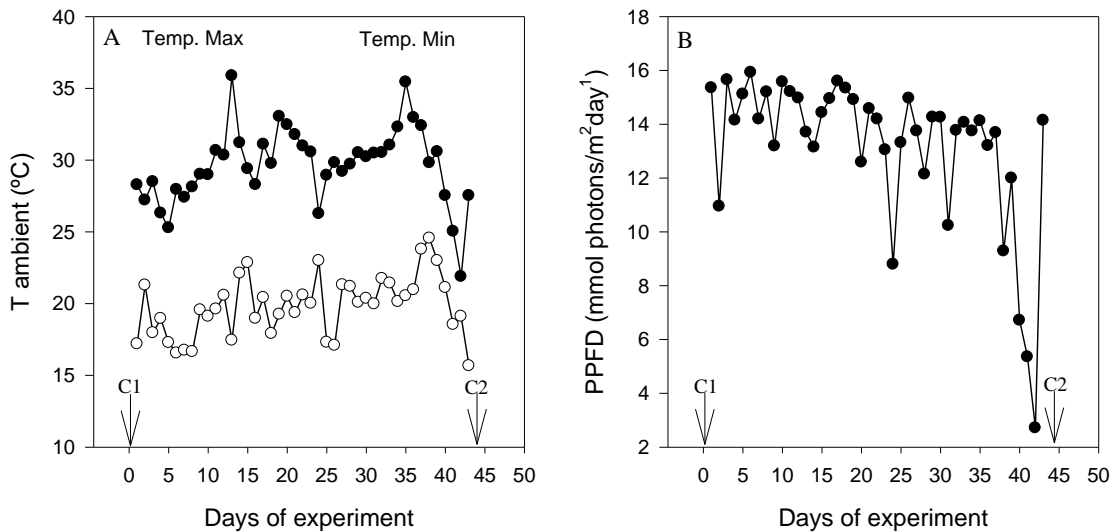
Figure 1. Maximun (Black cycles) and minimum (White cycles) daily air temperature (A), and integrated daily photosynthetic photon flux density (B). C1 represents the diurnal time cycles of net photosynthesis at the beginning of July and C2 the diurnal time cycles of net photosynthesis at middle August. Data are mean of five replicates ± standard error.

Pre-dawn leaf water potential was always maintained above –0.2 MPa throughout the experiment, indicating vines were not water stressed.

Carbon gain by leaf photosynthesis

Virus status (virus amount was 4.16±0.07 log copy number/70 mg (Fresh weight) and infected plants did not develop visual symptoms of GLRaV-3 infection) had no effect on the total biomass increment, or in the fractional biomass of the different parts of the plant during the 44 days of the experiment (Table 1). Likewise, there were no differences in plant growth as measured by total leaf area (Table 1).

140

Table 1. Increment leaf area and biomass of leaves, stem and roots, total biomass increment (TBI) and carbon content measured in non-infected (GLRaV-3 (-)) and infected (GLRaV-3 (+)) plants. Data are mean of five replicates ± standard error.

	GLRaV-3 (-)	GLRaV-3 (+)	Significance
Upper leaf area (m^2)	0.03±0.01	0.03±0.01	ns
Lower leaf area (m^2)	0.14±0.01	0.12±0.01	ns
Upper leaf biomass (g)	3.75±1.16	4.33±0.91	ns
Lower leaf biomass (g)	29.83±2.60	31.73±1.29	ns
Upper stem biomass (g)	2.77±1.33	2.02±1.06	ns
Lower stem biomass (g)	70.68±9.20	75.66±3.40	ns
Root biomass (g)	23.85±1.20	23.56±1.22	ns
TBI (g)	130.88±9.93	137.28±5.05	ns
Carbon content (g)	57.58±4.36	60.40±2.22	ns

Within these 44 days, two diurnal time cycles of net photosynthesis were carried out at the beginning of July (A) and middle August (B) (Figure 2). Virus infection had no significant effect on A_N, there were not significant changes between treatments in A_N in any point of the day, neither between upper and lower leaves of different treatments in July (Figure 2A). Diurnal time cycle performed in August followed different trend as compared to July. At the end of the experiment, A_N decreased in both treatments at midday. Globally, values were lower in this period than in July. A_N in the upper leaves ($A_{N\ upper\ leaf}$) was significantly lower in infected plants than non-infected ones at early morning and afternoon-evening (Figure 2B).
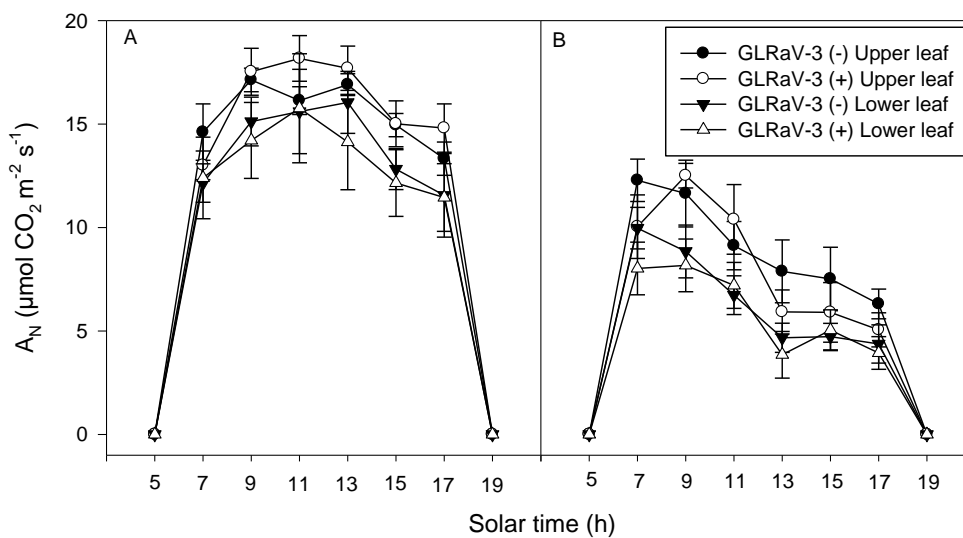


Figure 2. Diurnal time cycles of net photosynthesis (A_N) in upper and lower leaves of non-infected (GLRaV-3 (-)) and infected (GLRaV-3 (+)) Girò Ros plants. The two diurnal cycles were performed at the beginning of July (A) and middle August (B). Data are means ± standard error of five replicates.

Multiplying the A_N during the whole day by the leaf area, the carbon assimilated at the end of the day by upper and lower leaves was calculated. Virus infection resulted in a significant, 38% reduction in A_N of the upper leaf in August (Table 2). In respiration, only root respiration (R_{root}) was significantly affected by the infection. Despite R_{root} decreased 36% in infected plants in July, this difference did not produce a significant change in PCB in this period. Similarly the $R_{D\ upper\ leaf}$ was 31% lower in infected plants than in non-infected ones. This compensated the decrease of $A_{N\ upper\ leaf}$ and as a result the August PCB was not significantly affected by the infection, although in infected plants this parameter was 14% lower than in non-infected ones (Table 1).

Table 2. Plant carbon balance (PCB) (g CH_2O/plant) in the diurnal time cycles of July and August calculated as the difference between carbon gain by leaf net photosynthesis ($A_N=A_{N\ upper\ leaves}+ A_{N\ lower\ leaves}$), and daily losses by aerial part of the plant ($R_{D\ aerial}=R_{D\ upper\ leaves}+ R_{D\ lower\ leaves}+ R_{upper\ stem}+ R_{lower\ stem}$) and root ($R_{root}$). Data are mean of five replicates ± standard error.

July	$A_{N\ upper}$ leaves (g/day)	$A_{N\ lower}$ leaves (g/day)	$R_{D\ upper}$ leaves (mg/day)	$R_{D\ lower}$ leaves (mg/day)	R_{upper} stem (mg/day)	R_{lower} stem (mg/day)	R_{root} (mg/day)	PCB (g/day)
GLRaV-3 (-)	0.28±0.03	1.68±0.15	22.3±3.1	96.1±15.7	6.3±0.7	18.6±4.7	480.05±39.19	1.34±0.17
GLRaV-3 (+)	0.35±0.04	1.55±0.10	31.4±4.8	101.4±14.8	6.8±0.6	27.8±3.2	304.03±31.99	1.43±0.11
Significance	ns	ns	ns	ns	ns	ns	*	ns
August	$A_{N\ upper}$ leaves (g/day)	$A_{N\ lower}$ leaves (g/day)	$R_{D\ upper}$ leaves (mg/day)	$R_{D\ lower}$ leaves (mg/day)	R_{upper} stem (mg/day)	R_{lower} stem (mg/day)	R_{root} (mg/day)	PCB (g/day)
GLRaV-3 (-)	0.44±0.06	1.03±0.14	41.4±5.5	111.4±13.4	0.8±0.3	14.1±5.1	431.86±56.48	0.88±0.22
GLRaV-3 (+)	0.27±0.02	1.01±0.15	28.2±4.8	105.1±6.3	4.1±1.8	23.3±9.7	370.92±37.45	0.76±0.18
Significance	*	ns	*	ns	ns	ns	ns	ns

For calculations of some components of the total PCB, respiration of the different parts of the plant was determined at different temperatures in order to obtained accuracy results in PCB estimation. Only R_{root} was affected and the difference between treatments increased once the temperature reached 30ºC (Figure 3A). Q_{10} was 57% lower for infected plants. However, no significant differences were observed for instance in $R_{D\ lower\ leaf}$ or in the Q_{10} (Figure 3B).
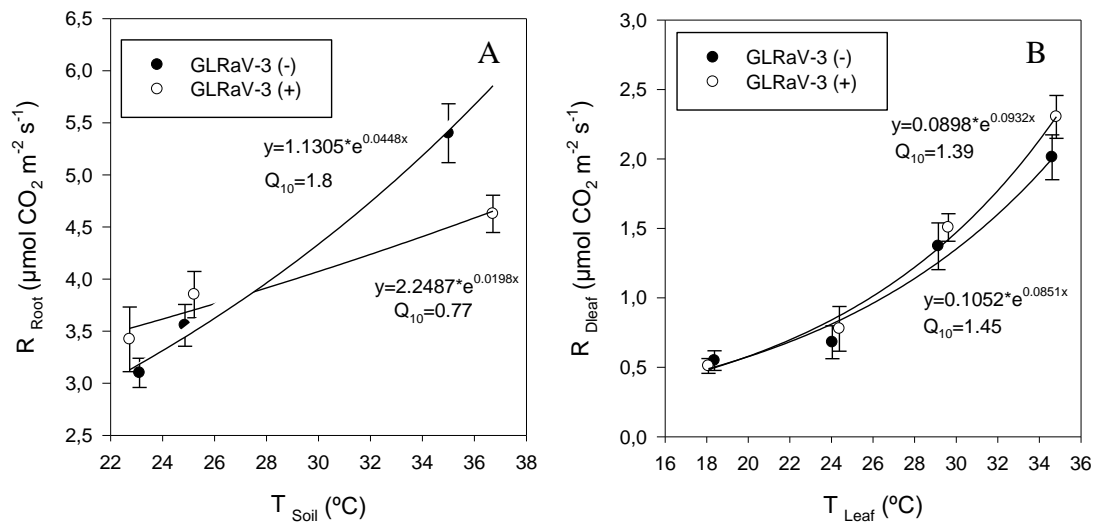
Figura 3. Changes of root respiration (A) and leaf dark respiration (B), in non-infected (GLRaV-3 (-)) and infected (GLRaV-3 (+)) plants of Girò Ros cv. in July. Data are mean of five replicates ± standard error.

PCB was calculated based on two diurnal time cycles of net photosynthesis and the respiration of the different organs, taking into account the variations of this parameter by changes in temperature, and the increment of leaf area for the 44 days between July and August. There were not significant differences in PCB after 44 days of experiment (Table 3). During the whole experiment daily losses by roots were significantly lower for infected plants, but those differences were compensated by carbon gain of leaves, although they are not significant differences, and therefore no changes were observed in total PCB. Total PCB estimation was very similar to the carbon content obtained from the final biomass (Table 1), validating this method for the estimation of total PCB in the whole plant.

Table 3. Plant carbon balance (PCB) (g CH_2O/plant) during the 44 days of experiment calculated as the difference between carbon gain by leaf net photosynthesis (A_N=$A_{N\ upper\ leaves}$ + $A_{N\ lower\ leaves}$), and daily losses by aerial part of the plant ($R_{D\ aerial}$=$R_{D\ upper\ leaves}$+ $R_{D\ lower\ leaves}$+ $R_{upper\ stem}$+ $R_{lower\ stem}$) and root (R_{root}). Data are mean of five replicates ± standard error.

Total	A_N (g)	$R_{D\ aerial}$ (g)	R_{root} (g)	PCB (g)
GLRaV-3 (-)	79.36±4.22	7.04±0.37	19.60±1.85	52.71±5.60
GLRaV-3 (+)	73.46±2.98	7.41±0.60	14.51±0.67	51.54±3.53
Significance	ns	ns	*	ns

DISCUSION

We have evidence that the virus affects photosynthesis, primary and secondary metabolism at leaf level and some findings demonstrate that these effects depend on the amount of virus (Gambino et al., 2012; Montero et al., 2015a (Chapter 4)). However, the results in the present study show that there are not differences in total biomass increment between treatments (Table 1). The low virus titer measured comparing to other studies (Tsai et al., 2012; Velasco et al., 2014 (Chapter 3)), may explain this absence of differences in total biomass increment between virus infected and non-infected plants.

There is a successfully tested method to estimate plant carbon balance (PCB) based on gas exchange measurements (Escalona et al., 2012). This method enables the carbon balance to be determined at both the whole plant and the individual plant organ level and during different periods. The present study assessed virus-induced differences in the PCB and its components. The absence of differences between the virus infect and non-infected plant in July could be due to low virus concentration, but there are evidences of the compensation of carbon assimilate limitations by respiration. In July, when roots are still growing, there were significantly lower carbon daily losses by root in infected plants, while in August there was no difference (Table 2). The decrease in R_{root} was compensated by higher carbon daily losses by the stem and lower carbon gain by leaves, however, those differences were not significant (Table 2), and therefore PCB in this period did not change between treatments. Reducing carbon losses compensates the lower rate of carbon fixation caused by the virus. GLRaV-3 virus effects on roots were not extensively studied by Charles et al. (2006). However, it is known that the virus remains in the trunk and roots of grapevines in the field throughout the year, remaining after pruning for the next season (Charles et al., 2006). Thus, each year, the effects of the virus could increase in these parts of the plant, with enhanced blockage of the sieve tubes. As a consequence the importance of the duration of the infection is important in determining the degree of damage caused by the virus.

Once the plant mobilise assimilates, the virus is transmitted to the whole plant through sap flow and starts to accumulate in different parts of the plant. In early August the roots are mature and cease their growth (Christensen, 2000) while the aerial part of the plant keeps growing. In this period only the upper leaves were affected by the

infection (Figure 2). The A_N and R_D of upper leaves decreased , with the result the leaf and total carbon balance did not change significantly between treatments. Differences obtained in leaf carbon balance in August followed the same trend as in previous studies (Montero et al., 2015a (Chapter 4)). At a leaf level, where virus concentrations were high there was a large decrease in A_N. However, virus infection also reduced respiration, with the result there was little effect on vine growth (Montero et al., 2015a (Chapter 4)). In the present study, although non-significant, there was 14% of reduction of PCB in infected plants (Table 2). While the absence of significance can be due to the low precision of the method used to capture small differences a 14% decrease during the later stages of vine development, if confirmed, could explain significant virus-induced changes in grape berry composition (Montero et al., 2015b (Chapter 7)).

The efficiency in the invasion in different tissues could be the reason of virus distribution and consequently, virus effects. In other systemic viruses it has been demonstrated a higher capacity of replication in active sink tissues such as the young leaves and root system (Gosalvez-Bernal et al., 2008). Viral unloading at distal young organs could take place in the major veins probably due to the immature status of the minor veins (Silva et al., 2002). The exact destination of the virus will depend on specific cell boundaries. Low virus titre (amount) measured in plants selected for the experiment suggest that this could be the reason of the absence of differences on growth but it evidences the strategies used by plants to fight against the infection and the most sensitive organs affected by the virus. Growth parameters have been described in other studies as one of the factors affected by the virus (Endeshaw et al., 2014; Credi et al., 1997; Mannini et al., 1996; Sampol et al., 2003). However, in these studies symptoms were visible at the end of the growing season evidencing higher virus concentration.

The results of this study using asymptomatic infected grapevine plants showed that virus infection resulted in small decreases in total PCB. This was possibly partly due to low virus concentration, but mostly explained by the lower photosynthetic carbon assimilation being compensated by reduced respiration losses. Upper leaves and root were identified as the most sensitive parts of the plant to GLRaV-3. Also plant behaviour in first stage of infection was characterised, being the capacity of the plant to compensate carbon gains and losses in different parts of the plant, the main strategy to fight against the infection. However, in the experiment described here, non-fruiting vines were used. In fruiting vines berries are the most active sink of photosynthates

post-veraison and they can import up to 70-80% of the total assimilates obtained by photosynthesis at this time (Bota et al., 2004). Additional experiments should be performed using fruiting plants to confirm the present results.

REFERENCES

Bota J., Stasyk O., Flexas J., & Medrano H. (2004). Effects of water stress on partitioning of 14C labelled photosynthates in *Vitis vinifera*. *Functional Plant Biology*, **31**, 697–708.

Clark M.F., & Adams A.N. (1977). Characteristics of the microplate method of enzyme-linked immunosorbent assay for the detection of plant viruses. *Journal of General Virology*, **34**, 475–483.

Charles J.G., Cohen D., Walker J.T.S., Forgie S.A., Bell V.A., & Breen K.C. (2006). A review of the ecology of Grapevine leafroll associated virus type 3 (GLRaV-3). *New Zealand Plant Protect*, **59**, 330–337.

Credi R., & Babini A.R. (1997). Effects of virus and virus-like infections on growth, yield and fruit quality of Albana and Trebbiano Romagnolo grapevines. *American Journal of Enology and Viticulture*, **48**, 7–12.

Cretazzo E., Tomás M., Padilla C., Rosselló J., Medrano H., Padilla V., & Cifre J. (2010). Incidence of virus infection in old vineyards of local grapevine varieties from Majorca: implications for clonal selection strategies. *Spanish Journal of Agricultural Research*, **8(2)**, 409–418.

Christensen P.L. (2000). Raisin Production Manual. UCANR Publications.

Escalona J.M., Tomàs M., Martorell S., Medrano H., Ribas-Carbó M., & Flexas J. (2012). Carbon balance in grapevines under different soil water supply: importance of whole plant respiration. *Australian Journal of Grape and Wine Research*, **18**, 308–318.

Endeshaw S.T., Sabbatini P., Romanazzi G., Schilder A.C., & Neri D. (2014). Effects of grapevine leafroll associated virus 3 infection on growth,leaf gas exchange, yield and basic fruit chemistry of *Vitis vinifera* L. cv. Cabernet Franc. *Scientia Horticulturae*, **170**, 228–236.

Gambino G., Cuozzo D., Fasoli M., Pagliarani C., Vitali M., Boccacci P., Pezzotti M., & Mannini F. (2012). Co-evolution between Grapevine rupestris stem pitting associated virus and *Vitis vinifera* L. leads to decreased defence responses and increased transcription of genes related to photosynthesis. *Journal of Experimental Botany*, **63(16)**, 5919–5933.

Gifford R.M., Thorne J.H., Hitz W.D., & Giaquinta R.T. (1984). Crop productivity and assimilate partitioning. *Science*, **1225**, 801–808.

Gosalvez-bernal B., Genoves A., Navarro J.A., Pallas V., & Sánchez-Pina M.A. (2008). Distribution and pathway for phloem-dependent movement of Melon necrotic spot virus in melon plants. *Molecular Plant Pathology*, **9 (4)**, 447–461.

Grechi I., Vivin Ph., Hilbert G., Milin S., Robert T., & Gaudillère J.P. (2007). Effect of light and nitrogen supply on internal C:N balance and control of root-to-shoot biomass allocation in grapevine. *Environmental and Experimental Botany*, **59**, 139–149

Hoagland D.R., & Arnon D.I. (1950). The water-culture method for growing plants without soil. *California Agricultural Experiment Station*, **347**, 1–32.

Hoefert L.L., & Gifford E.M. (1967). Grapevine leafroll virus. History and anatomical effects. *Hilgardia*, **38**, 403-426.

Hull R. (2002). Matthews' Plant Virology. 4th Edition. Academic Press, San Diego, CA.

Koerber G.R., Hill P.W., Jones G.E., & Jones D.L. (2010). Estimating the component of soil respiration not dependent on living plant roots: comparison of the indirect y-

intercept regression approach and direct bare plot approach. *Soil Biology & Biochemistry*, **42**, 1835–1841.

Mannini F., Argamante N., & Credi R. (1996). Improvements in the quality of grapevine Nebbiolo clones obtained by sanitation. *Acta Horticulturae*, **427**, 319–324.

Mannini F., Mollo A., & Credi R. (2012). Field performance and wine quality modification in a clone of *Vitis vinifera* cv. Dolcetto after GLRaV-3 elimination. *American Journal of Enology and Viticulture*, **63**, 144–147.

Martelli G. (2009). Grapevine virology highlights 2006–2009. In: le Progrès Agricole et Viticole (Ed.), Proceedings of the 16th Meeting of the International Council for the Study of Virus and Virus-like Diseases of the Grapevine. ICVG, Dijon, France, pp. 15–23.

Montero R., El aou ouad H., Pacifico D., Marzachì C., Castillo N., García E., Fernández N., Florez-Sarasa I., Flexas J., & Bota J. (2015a). Absolute quantification of Grapevine Leafroll associated Virus 3 (GLRaV-3) and its effects on the physiology in asymptomatic plants of *Vitis vinifera* L. *Annals of Applied Biology* (Submitted).

Montero R., Mundy D., Albright A., Grose C., Trought M.C.T., Cohen D., Chooi K.M., MacDiarmid R., Flexas J., & Bota J. (2015b). Effects of Grapevine leafroll associated virus 3 (GLRaV-3) and duration of infection on fruit composition and wine chemical profile of *Vitis vinifera* L. cv. Sauvignon Blanc. *Food Chemistry* (Submitted).

Pacifico D., Caciagli P., Palmano S., Mannini F., & Marzachì C. (2011). Quantitation of Grapevine leafroll associated virus-1 and -3, Grapevine virus A, Grapevine fanleaf virus and Grapevine fleck virus in field-collected *Vitis vinifera* L. 'Nebbiolo' by real-time reverse transcription-PCR. *Journal of Virological Methods*, **172**, 1–7.

Sampol B., Bota J., Riera D., Medrano H., & Flexas J. (2003). Analysis of the virus-induced inhibition of photosynthesis in malmsey grapevines. *New Phytologist*, **160**, 403–412.

Silva M.S., Wellink J., Goldbach R.W., & van Lent J.W. (2002). Phloem loading and unloading of Cowpea mosaic virus in Vigna unguiculata. *Journal of General Virology*, **83(6)**, 1493–1504.

Tsai C.W., Daugherty M.P., & Almeida R.P.P. (2012). Seasonal dynamics and virus translocation of Grapevine leafroll-associated virus 3 in grapevine cultivars. *Plant Pathology*, **61**, 977–985.

Velasco L., Bota J., Montero R., & Cretazzo E. (2014). Differences of three ampeloviruses multiplication in plant contribute to explain their incidences in vineyards. *Plant disease*, **98**, 395–400.

Von der Brelie D., & Nienhaus F. (1982). Histological and cytological studies on the infectious leafroll disease of the grapevine. *Zeitschrift für Pflanzenkrankheiten und Pflanzenschutz*, **89**, 508–517.

Williams, L.E. (1996). Grapes. In E Zamski and AA Schaffer (eds.), photoassimilate distribution in plants and crops: source-sink relationships. Marcel Dekker, New York.

Chapter 7

EFFECTS OF GRAPEVINE LEAFROLL ASSOCIATED VIRUS 3 (GLRaV-3) AND DURATION OF INFECTION ON FRUIT COMPOSITION AND WINE CHEMICAL PROFILE OF *VITIS VINIFERA* L. CV. SAUVIGNON BLANC.

EFFECTS OF GRAPEVINE LEAFROLL ASSOCIATED VIRUS 3 (GLRaV-3) AND DURATION OF INFECTION ON FRUIT COMPOSITION AND WINE CHEMICAL PROFILE OF *VITIS VINIFERA* L. CV. SAUVIGNON BLANC.

R. Montero[1], D. Mundy[2], A. Albright[2], C. Grose[2], M.C.T. Trought[2], D. Cohen[3], K. M. Chooi[3], R. MacDiarmid[3], J Flexas[4], J. Bota[4,*]

[1] Institut de Recerca i Formació Agrària i Pesquera (IRFAP), Conselleria d'Agricultura, Medi Ambient i Territori. Govern de les Illes Balears. C/Eusebio Estada nº 145. 07009, Palma de Mallorca, Spain.

[2] The New Zealand Institute for Plant & Food Research Limited, Marlborough Wine Research Centre, PO Box 845, Blenheim, New Zealand.

[3] The New Zealand Institute for Plant & Food Research Limited, Private Bag 92169, Auckland, New Zealand.

[4] Grup de Recerca en Biologia de les Plantes en Condicions Mediterrànies, Departament de Biologia, Universitat de les Illes Balears, Carretera de Valldemossa, km 7.5, 07071, Palma de Mallorca, Balears, Spain.

*Corresponding author: j.bota@uib.es

ABSTRACT

In order to determine the effects of Grapevine Leafroll associated virus 3 (GLRaV-3) on fruit composition and chemical profile of juice and wine from *Vitis vinifera* L. cv. Sauvignon blanc grown in New Zealand, composition variables were measured on fruit from vines either infected with GLRaV-3 (established or recent infections) or uninfected vines. Physiological ripeness (20.4 ºBrix) was the criterion established to determine the harvest date for each of the three treatments. Date of grape ripeness was strongly affected by virus infection. In juice and wine, GLRaV-3 infection prior to 2008 reduced titratable acidity compared with the uninfected control. Differences observed in amino acids from the three infection status groups did not modify basic wine chemical properties. In conclusion, GLRaV-3 infection slowed grape ripening, but at equivalent ripeness to result in minimal effects on the juice and wine chemistry. Time of infection produced differences in specific plant physiological variables.

keywords: virus quantification, *Vitis vinifera* L., Sauvignon blanc cv., grape composition, virus spread, YAN, FAN, Free amino acids.

INTRODUCTION

Grapevine leafroll-associated virus 3 (GLRaV-3) is considered one of the most important viruses affecting grapevine because it is widespread in many vineyards around the world and results in significant economic losses (Martelli, 2012). This virus belongs to the genus *Ampelovirus*, family *Closteroviridae,* and is phloem-limited. Within the ampeloviruses, GLRaV-3 has the highest incidence in vineyards due to the higher amplification efficiency (Velasco et al., 2014 (Chapter 3)). The leaf symptoms of the infection are clearly visible in red cultivars, expressed as early red spotting, coalescing to a red purple colour leaving a green vein banding symptom. Leaves often curl downwards and become brittle. In white cultivars symptoms are less visually obvious. If symptoms express, they are likely to include inter-veinal yellowing of leaves and leaf rolling (Maree et al., 2013). Sauvignon blanc grown in Marlborough is usually asymptomatic thus it is more difficult to identify leafroll infected vines in the field.

These masked symptoms hinder disease diagnosis, timely insect vector control and effective removal of infected vines (Charles et al., 2009).

Sauvignon blanc is the most important grape cultivar in the Marlborough region of New Zealand. The regional growing conditions allow for a unique expression of flavour and aroma characteristics not seen in other Sauvignon blanc regions around the world. Low night temperatures and few hot days in Marlborough enables fruit and wine to retain acidity. Despite white cultivars being very important in many winegrowing regions around the world, there are few studies focused on the impact of GLRaV-3 on white grapes and wines (Charles et al., 2009; Gambino et al., 2012; Sampol et al,. 2003; Maree et al., 2013).

GLRaV-3 can lead to reductions in net leaf photosynthesis, content of soluble solids and vine productivity (Basso et al., 2010; Endeshaw et al., 2014; Lee et al., 2009; Mannini et al., 2012). These effects on plant physiology in turn generate an interest in exploring how GLRaV-3 infections alter berry sugars and organic acids that are responsible for final alcohol concentration and wine flavour and aroma (Bertamini et al., 2004; Cabaleiro et al., 1999; Lee & Martin, 2009; Ueno et al., 1985). Non-protein nitrogen-containing compounds found in grapes are the most important nutrients needed to carry out a successful fermentation. The concentrations of primary and secondary metabolites in juice at harvest depends on factors such as cultivar, vine nutrition, grape maturity and growing season (Bell & Henske, 2005; Ueno et al., 1985) and may be modified by vine virus status. Certain compounds determine the fermentation rate and completion of fermentation, especially ammonia and some free amino acids. These are known as yeast assimilable nitrogen (YAN). Low YAN can result in 'stuck' or 'sluggish' fermentation and which finishes before the intended point of dryness. Such problems in the fermentations may lead to the production of undesirable off-odours, caused by thiol-containing compounds and sulphides in the resulting wine. Fermentation conditions and juice components modify the yeast fermentation kinetics for diverse forms of available nitrogen (Taillandier et al., 2007). Di-ammonium phosphate (DAP) may be added in those cases where YAN compounds derived from grape are insufficient for a complete fermentation.

There is little information about the effects of virus titre (amount) on the physiological status of the infected plants. To our knowledge, no previous studies of

GLRaV-3 have measured the effect grapevine performance in relation to virus titre. Some studies have compared symptomatic with asymptomatic virus infected red grape leaves (Moutinho-Pereira et al., 2012; Endeshaw et al., 2014), but no work appears to have been done on white grape cultivars.

Nucleic-acid based methods have the advantage enabling the relationship between the virus titre to be related to the effects of the virus on the plant (Gambino et al., 2012; Montero et al., 2015 (Chapter 4)). The application of real-time reverse transcription PCR (RT–PCR) in particular has recently been used to study grapevine viruses (Douglas et al., 2009; Pacifico et al., 2011). While the effect of virus on plants has been studied over a number of seasons (Manini et al., 2012), the influence of virus on juice composition over time within a season is not well documented. In the present study, physiological variables of the grapes and the chemical profile of juice and wine were measured in non-infected and infected plants in order to determine the effects of GLRaV-3. Plants of Sauvignon blanc naturally infected and plants not infected by GLRaV-3 were selected for the experiment and the interaction between time of infection, virus titre and physiological components of wine production were measured.

MATERIAL AND METHODS

Vineyard site, environmental conditions and plant material

The experiment was carried out in a commercial vineyard at Rapaura area along the northern edge of the Wairau Valley, Marlborough region, New Zealand (41°29'33.72"S, 173°52'25.94"E). Sauvignon blanc vines (clone Mass Selected) grafted on rootstock SO_4 were planted in 1992 with a spacing of 1.8 m within the row and 2.4 m between rows, with rows oriented N–S and established to an annual pruning regime of four canes per vine (40–55 nodes per vine). Cane pruning was done in the winter 2013 using four canes vertical shoot position from the previous season and retaining 12 nodes per cane and lightly wrapped on fruiting wires 0.9 and 1.1 m from the soil surface (Smart & Robinson, 1991). Foliage wires were used to maintain a narrow canopy approximately 0.4 m face to face and 1.6 m high and vines were trimmed to maintain these dimensions three times during the growing season. Vines were drip irrigated, while industry standard practice was used to control insect pests and fungal diseases.

Temperature and rainfall were monitored during the experiment using a meteorological station (Plant & Food Research weather station), 41°29'28.9"S, 173°53'21.1"E and elevation 19 m above sea level nearby the field where the experiment was carried out.

Mid-day leaf water potential was determined using a Scholander chamber (Soil Moisture Equipment Corp., Santa Barbara, CA, USA) (Scholander et al., 1965).

Treatments and experimental design

Seven replicate vines of three treatments reflecting the spread of the virus: non-infected plants, plants infected by GLRaV-3 after 2008 and plants infected before 2008 were identified. Vines were assessed regularly from mid-February and harvested when fruit reached soluble solids content of 20.4 °Brix. Choosing a common °Brix value between treatments enabled the effects of the virus on the wine chemical profile to be investigated, without the confounding effect of variable °Brix at harvest.

Virus diagnosis and GLRaV-3 quantification

Virus status was tested in plants selected for the experiment in order to define the different treatments. Four rows, each with twenty-five plants, were analysed in 2001, 2006, 2008 and 2014 by enzyme-linked immunosorbent assay (ELISA) (Clark & Adams, 1977) using commercial coating and conjugate antibody preparations (Bioreba AG, Reinach, Switzerland). Tests were undertaken for *Grapevine Leafroll associated virus 1* (GLRaV-1), *Grapevine Leafroll associated virus 2* (GLRaV-2), and *Grapevine virus A* (GVA) were tested by ELISA to avoid any interactions with GLRaV-3 according to manufacturer's instructions.

For the experiment performed in 2014, the virus status of all plants was further confirmed and GLRaV-3 amount was quantified using multiplex reverse transcription PCR (Chooi et al., 2013) in one leaf per plant. Specimens were prepared using the SuperScript® III/Platinum® SYBR® Green One-Step qPCR Kit with ROX (Invitrogen, Carlsbad, CA, USA) according to manufacturer's instructions and performed in an ABI 7900HT real-time PCR thermocycler (Applied Biosystems, Foster City, CA, USA).

Gas exchange, chlorophyll content and growth measurement

Relative chlorophyll concentrations were measured twice a week, on four tagged leaves per plant, during fruit ripening from 6 March (around 16 ºBrix) to after harvest on 8 April using a SPAD-502 chlorophyll meter (Minolta, Tokyo, Japan). The measurements (expressed as SPAD units) were taken repeatedly at the three apices of a triangle drawn on each leaf lamina; the same leaves were used for gas exchange measurements. Net CO_2 assimilation (A_N) and stomatal conductance (g_s) were measured at the end of March (19–20 ºBrix) under saturating light (1500 µmol m^{-2} s^{-1}) and 400 µmol mol^{-1} CO_2. Leaf temperature was maintained at 27ºC and leaf-to-air vapour pressure deficit was kept between 1 kPa and 2 kPa during all measurements. A_N, g_s, transpiration (E) and intercellular CO_2 concentration (C_i) were determined simultaneously on leaves using a CIRAS2 portable photosynthesis system (PP Systems, Amesbury, MA, USA).

Trunk circumference in each plant was measured at the end of the experiment as described by Trought et al. (2011).

Yield components and basic fruit chemistry

A 30-berry sample was collected from all vines each week from shortly after veraison until harvest. Fruit was stored in chilled containers and transported to the laboratory where berry weight was measured before the fruit was processed into juice for analysis. Grape juice ºBrix were analysed using an Atago refractometer (Atago USA, Inc., Kirkland, Washington, USA), and the pH was measured using a 744 Metrohm AG (Herisau, Switzerland) pH meter. An automatic titrator, coupled to an auto sampler and control unit (Mettler Toledo DL50, Port Melbourne, Australia) was used to determine titratable acidity. All fruit was processed as mentioned before, within 24 h of sampling. Bunch numbers were recorded at harvest along with total yield on an individual vine basis.

Primary amino acids and wine chemical profiles

Quantification of tartaric, malic and citric acid was carried out by HPLC on a Shimadzu LC-20AT with a Restek Allure Organic Acids column (250 x 4.6 mm) using an isocratic mobile phase of 150 mM phosphate buffer (pH 2.5) at a flow rate of 0.5 ml

min^{-1}. Samples were centrifuged and filtered prior to analysis with a dilution factor of ten. All measurements were carried out in duplicate using a 4-point standard curve ($R^2 > 0.99$) with thiourea as an internal standard.

Quantification of individual amino acids was carried out according to previously published methods on an Agilent 1200 series HPLC equipped with a fluorescence detector (Henderson & Brooks, 2010). Samples were centrifuged and filtered prior to analysis with a dilution factor of two. All measurements were carried out in duplicate using a four-point standard curve ($R^2 > 0.99$).

Total phenolics were quantified in gallic acid equivalents using the Folin-Ciocalteu method. Free and total sulphur were quantified by a chemical assay purchased from Megazyme (Megazyme International Ireland, Co. Wicklow, Ireland). Reducing sugars were quantified by an enzymatic assay purchased from Megazyme. Ammonium was quantified by an enzymatic assay purchased from Vintessentials (Dromana, Australia). Primary amino acids were quantified in isoleucine (Nitrogen (N)) equivalents by the NOPA method (Dukes & Butzke, 1998). Optical densities at 420, 520 and 620 nm were quantified directly by spectrophotometric assay to determine juice and wine color. All samples were centrifuged or filtered prior to analysis and all analyses were carried out in duplicate. All spectrophotometric assays were run on a Molecular Devices Spectramax 384 Plus with a 1cm path length cuvette reference correction.

Wine making

For each treatment a representative 4 kg sample per plant (mean=20.4 °Brix) was taken for winemaking. Grapes were crushed and destemmed in a hand operated crusher and rachi removed by hand. The de-stemmed must was put in 4-l pails and sulphur dioxide (SO_2) at the rate of 40 mg l^{-1} was added. Must was given 1 hour of skin contact time at 10˚C under CO_2 cover. Fruit was pressed in a 4 kg sample press (Stainless Steel Systems, Blenheim, New Zealand) under a blanket of CO_2. The pressing regime was to fill the press basket with fruit, collect the free run juice, press for 45 seconds, release plunger and stir grape marc, press again for 45 seconds, release plunger and stir grape marc, then press for a final 45 seconds. To settle the juice, Rapidase enzyme (rate 0.03 ml l^{-1}) was added to the total juice. After 24 hours (h) at 10°C the juice was racked of

solids then 700 ml of juice was put into 750 ml bottles for fermentation processing, while 50 ml juice samples were frozen for further analysis. For fermentation, juice was warmed to 15˚C and inoculated with EC1118 rehydrating yeast (rate 250 mg l^{-1}) using a standard procedure. When fermentation was active and dropped 2–3 ºBrix, 30% DAP was added where YAN was below 250 mg l^{-1}. Fermentation was carried out at 15°C during 30 days. ºBrix and temperature were monitored daily during fermentation using an Anton-Paar DMA 35ɴ portable density meter. Temperature was increased the last 5 days of fermentation to 16°C to finish wines to dryness. Once ferments contained less than 2.0 g l^{-1} residual sugar, ferments were stopped with the addition of 50 mg l^{-1} SO$_2$ and particulates were allowed to settle for 24 h. Wine was centrifuged at 4600 g for 5 minutes using a Thermo Fisher Scientific Heraeus Multifuge 3SRPlus Centrifuge prior to wine samples being taken 75 ml for chemical analysis. All analyses were carried out on fresh (unfrozen) samples within 4 h of sampling time.

Statistical analysis

The physiological, vine, juice and wine data were analysed using R (http://.rproject.org/). One-way ANOVA and LSD multiple range tests were used for determining differences between the treatments for the parameters measured.

RESULTS

Environmental conditions and plant water status

During the summer of 2014, the weekly mean maximum temperature on the trial site never exceeded 25ºC. From September to December the weekly mean maximum temperature increased 10ºC, while in the months prior to the harvest, the weekly mean maximum temperature were very stable, with values between 23ºC and 24ºC (Figure 1).
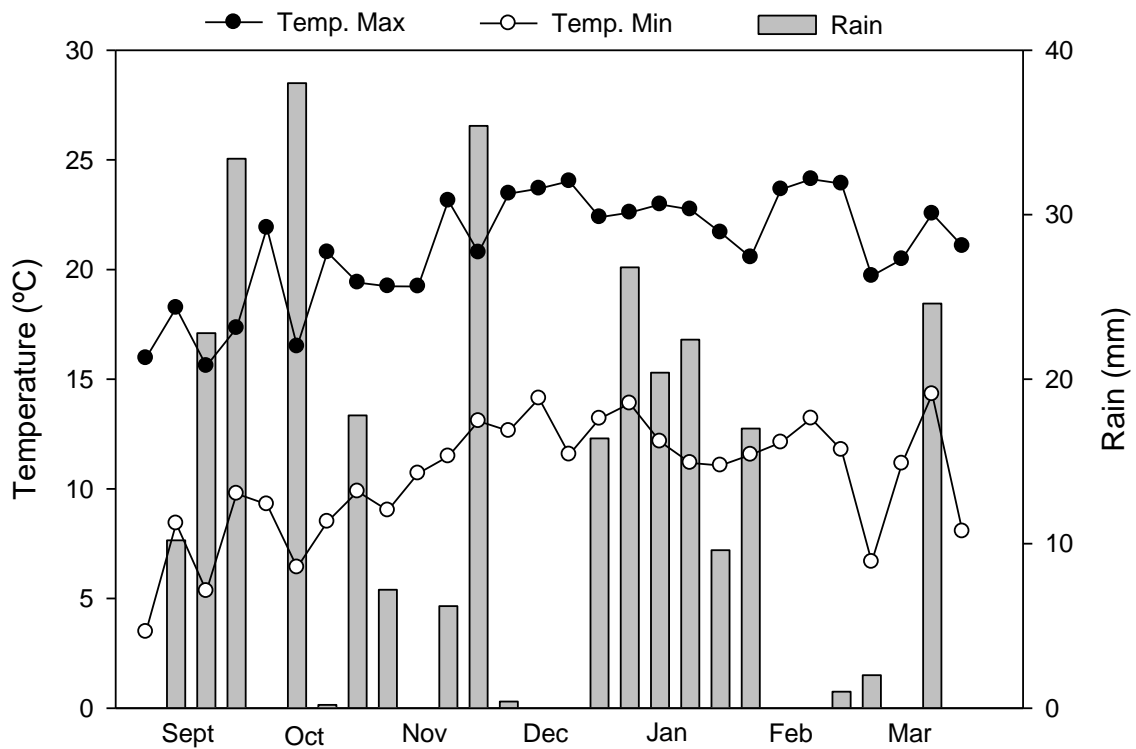
Figure 1. Weekly mean maximum and minimum temperature and rainfall data at the Marlborough Research Center (MRC), in Blenheim (Marlborough, New Zealand) using Plant & Food Research weather station, from September to March 2014.

However, during the first week of February and March, mean maximum temperature decreased by around 2ºC and 4ºC respectively. Weekly mean minimum temperature followed the same trend. Values were close to 3ºC in September and increased up to 14ºC in December. From December to harvest time mean minimum temperature decreased the last week of January and the first week of March by around 2ºC and 4ºC respectively. Rainfall during the season ranged from 20 to 90 mm per month (Figure 1). Maximum weekly rainfall was registered the second week of October with 38 mm. No rain fell in the first weeks of December and the last weeks of February; otherwise, close to harvest time there was 25 mm of rainfall. Midday leaf water potential measured was above –0.2 MPa (data not shown).

Virus diagnosis and GLRaV-3 quantification

In all three treatments, the absence of GLRaV-1, GLRaV-2 and GVA and the presence of GLRaV-3 was confirmed by ELISA. In the two treatments infected by GLRaV-3, virus amount did not differ between treatments (GLRaV-3 (+) Post 2008= 1.1±0.7 Log 10; GLRaV-3 (+) Pre=0.8±0.3 Log 10).

**Gas exchange, chlorophyll content and growth measurements.**

Net photosynthesis (A_N) in non-infected plants was significantly higher than in infected ones. The GLRaV-3 infection imposed a reduction of 21% in the assimilation rates in all infected plants. According to CO_2 diffusion parameters, stomatal conductance (g_s) was 24% lower in infected plants. As with the results obtained in A_N, no differences were found in g_s between the two treatments of infected plants. However, transpiration (E) was significantly lower in the plants infected before 2008 than in the other two treatments (Table 1).

Table 1. Net CO_2 assimilation (A_N), stomatal conductance (g_s), transpiration (E) and intercellular CO_2 for non-infected (GLRaV-3 (-)), virus infected after 2008 (GLRaV-3 (+) Post 2008) and virus infected before 2008 (GLRaV-3 (+) Pre 2008) plants. There are seven replicates for each treatment (letters; P = 0.05, LSD test).

Treatment	A_N (μmol CO_2 m^{-2} s^{-1})	gs (mmol CO_2 m^{-2} s^{-1})	E (mmol H_2O m^{-2} s^{-1})	Ci (mg L^{-1})
GLRaV-3 (-)	19.2±1.0a	423.35±29.83a	6.0±0.3ab	274.5±2.4a
GLRaV-3 (+) Post 2008	15.0±0.6b	322.85±22.03b	6.2±0.3a	272.2±2.5a
GLRaV-3 (+) Pre 2008	15.4±0.8b	315.92±18.94b	5.4±0.2b	274.1±2.4a

Relative chlorophyll content decreased through the summer in all treatments (Figure 2). However, the three treatments had significantly different relative chlorophyll contents, with highest values observed in non-infected plants and lowest in plants infected before 2008. Relative chlorophyll content slope was very stable even after harvesting for the non-infected plants treatment. In the case of the two treatments infected by GLRaV-3, the relative chlorophyll content suddenly decreased after harvesting (Figure 2).

Despite the effect on carbon assimilation, there were no differences in vine growth as measured by trunk circumference (data not shown), suggesting that overall vegetative growth was little affected by the virus.
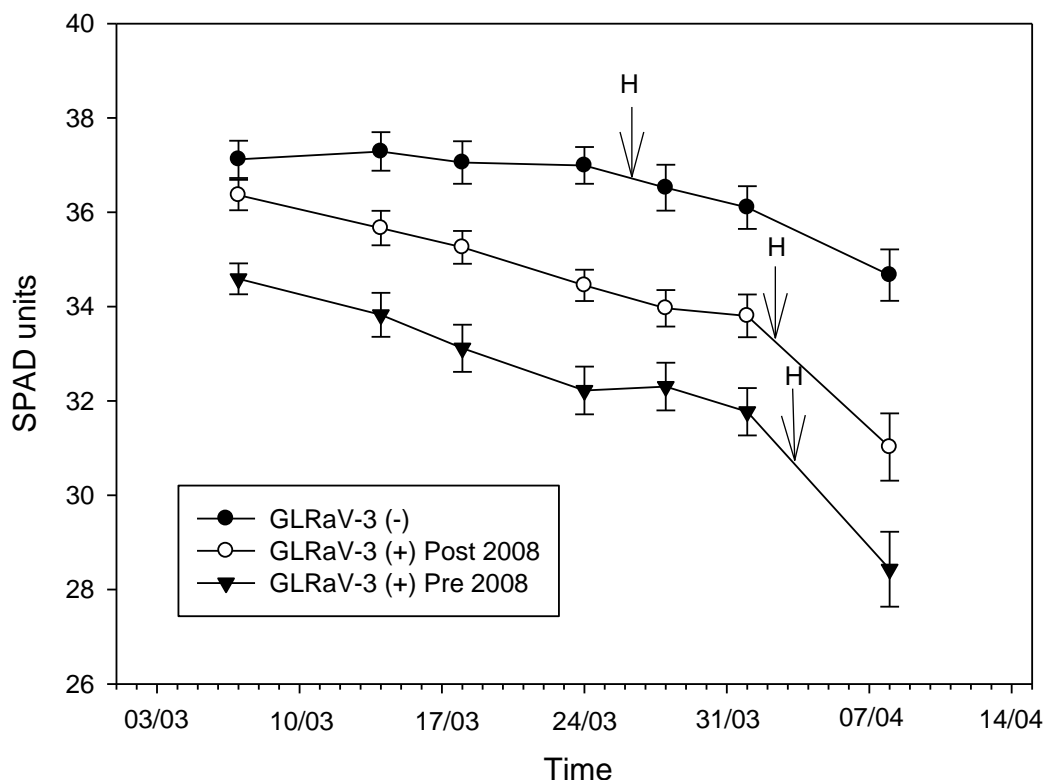
Figure 2. Chlorophyll relative content for non-infected (GLRaV-3 (-)), virus infected after 2008 (GLRaV-3 (+) Post 2008) and virus infected before 2008 (GLRaV-3 (+) Pre 2008) plants. Letter H represents harvest for each treatment. There are seven replicates for each treatment (letters; P = 0.05, LSD test).

Fruit maturity and yield components

Throughout the experimental period mean berry weight was higher in GLRaV-3 infected plants than in uninfected plants (Figure 3). However, by harvest time there were no significant differences in mean berry weight between the treatments.

The non-infected plants reached the juice soluble solids target (20.4 °Brix) on 26th March while plants infected after and before 2008 reached the same °Brix value on 2nd and 4th April, respectively. The TA of grapes from plants infected before 2008 was 4% higher than from plants infected after 2008, and 6% higher than from uninfected plants.
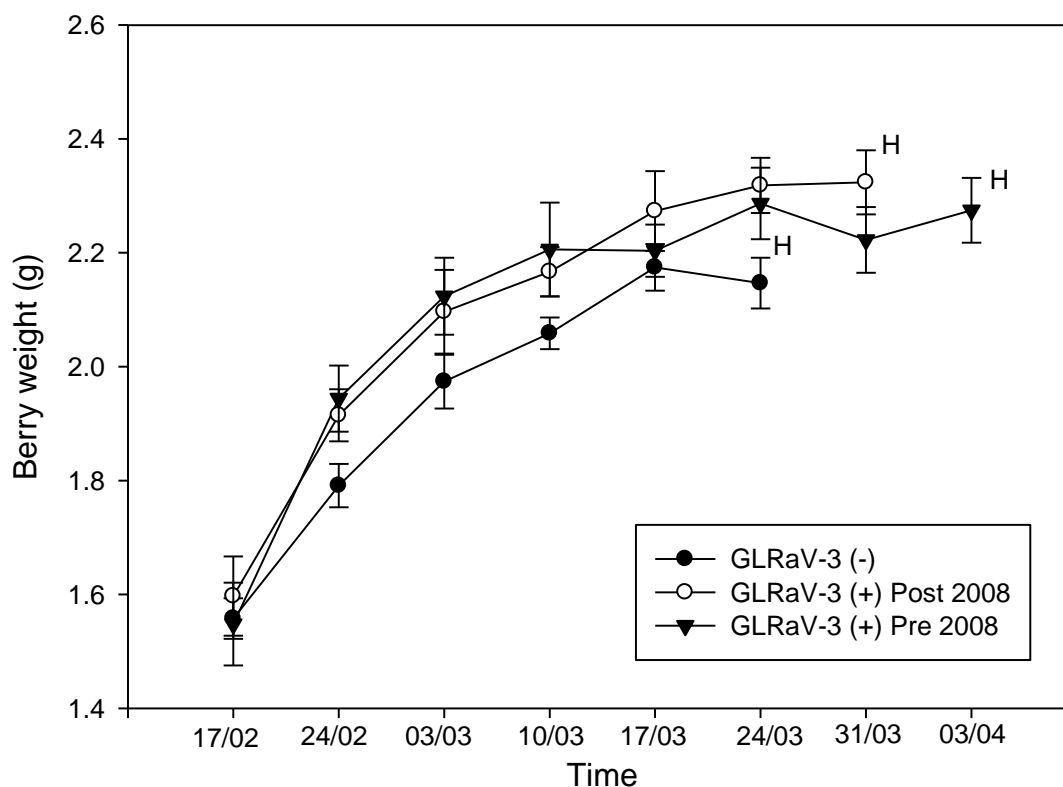
162

Figure 3. Berry weight for non-infected (GLRaV-3 (-)), virus infected after 2008 (GLRaV-3 (+) Post 2008) and virus infected before 2008 (GLRaV-3 (+) Pre 2008) plants. Letter H represents the soluble solid target at harvest. There are seven replicates for each treatment.

At the three harvest dates, TA was different for the three treatments, with highest value in plants infected after 2008 and lowest in plants infected before 2008 (Figure 4). GLRaV-3 infection appeared to delay the onset of ripening, but had relatively little effect on the rate of ºBrix accumulation. On 17th February there was a 1.3 ºBrix difference between infected and uninfected plants which increased to 1.6 ºBrix on 24th March.
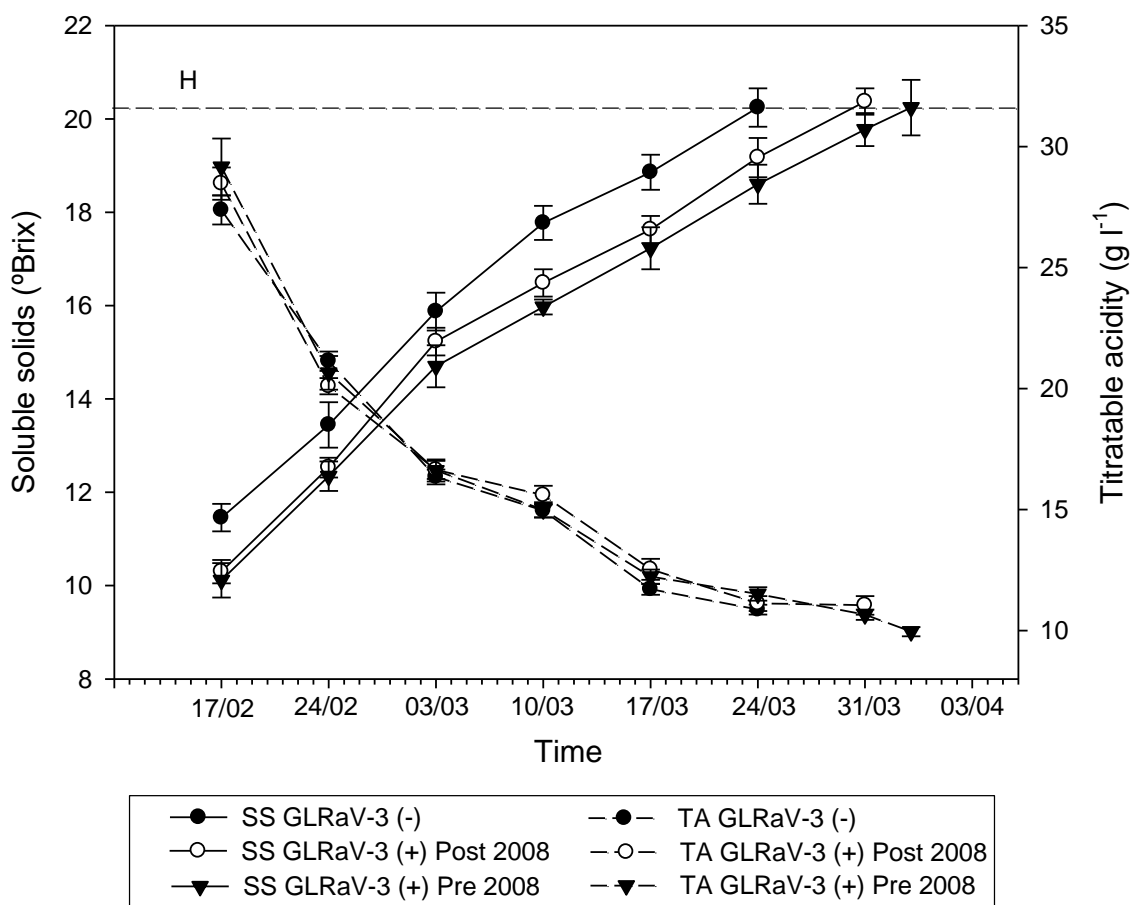
Figure 4. Soluble solids and titratable acidity in grapes, for non-infected (GLRaV-3 (-)), virus infected after 2008 (GLRaV-3 (+) Post 2008) and virus infected before 2008 (GLRaV-3 (+) Pre 2008) plants. Letter H represents the soluble solid target at harvest. There are seven replicates per treatment.

Yield, clusters per vine, cluster weight, berries per cluster, berry weight, seeds per berry and seed weight did not vary significantly between treatments (Table 2).

Table 2. Yield, clusters per vine, cluster weight, berries per cluster, berry weight, seeds per berry and seed weight for non-infected (GLRaV-3 (-)), virus infected after 2008 (GLRaV-3 (+) Post 2008) and virus infected before 2008 (GLRaV-3 (+) Pre 2008) plants, at harvest. There are seven replicates for each treatment (letters; P = 0.05, LSD test).

Parameter	GLRaV-3 (-)	GLRaV-3 (+) Post 2008	GLRaV-3 (+) Pre 2008
Yield (kg/vine)	9.65±0.50a	8.08±0.80a	10.21±1.08a
Clusters/vine (n)	64.83±4.65a	54.80±4.16a	68.57±6.43a
Cluster weight (g)	152.19±12.68a	146.70±3.79a	148.38±7.03a
Berries/Cluster (n)	70.75±5.62a	64.01± 2.72a	65.18± 2.44a
Berry weight (g)	2.15± 0.05a	2.30± 0.05a	2.27±0.05a
Seeds/berry (n)	1.43±0.05a	1.40±0.04a	1.45±0.08a
Seed weight (g)	1.06±0.03a	1.02±0.02a	1.04±0.06 a

Juice chemical profile

The amount of juice extracted from the 4 kg selected for the winemaking procedure was the same for the three treatments (around $0.6 \, l \, kg^{-1}$). Soluble solids from the 4 kg fruit lots were the same as the last maturity sample pre harvest for each treatment. Harvest juice analysis differed only in titratable acidity, being higher for uninfected plants. There were no differences between the two GLRaV-3 treatments (Table 3).

From the juice nitrogen concentration data GLRaV-3 did not affect the ammonia, total primary amino acids or YAN accumulation. However, there were differences in some of the individual amino acids (Table 3). Within the 15 amino acids analysed, those affected by the presence of GLRaV-3 were: aspartic acid (Asp), glycine (Gly), threonine (Thr), valine (Val), methionine (Met) and lysine (Lys). Individual free amino acids were grouped into the following five groups: Ala-Val-Leu family (Ala, Val, and Leu), aromatic amino acid family (Phe, Tyr and His), Asp family (Asp, Thr, Asn, Met, and Ile), Ser family (Ser and Gly), Glu family (Glu and Arg), and Lys based on chemical similarities and biosynthesis pathways (Lee et al., 2009). In summary the principal families affected by the virus were Ala-Val-Leu, Asp, Ser and Lys; the aromatic and Glu amino acid families were not affected by GLRaV-3 infection. The affected amino acid concentration decreased as a result of virus infection, with the exception of Val for both infection treatments and Lys for juice from vines infected after 2008 (Table 3).

Total phenolics in the three treatments were very similar, but juices from plants infected before 2008 had higher values than the plants infected after 2008. Colour intensity was lower in juice from uninfected plants, and it increased with the time of infection. However, tonality, a measure of the appearance of the colour (colour hue (A420/520)), was higher in the treatment of plants infected after 2008 and lower in juice from uninfected plants (Table 3).

Table 3. Harvest juice analysis (soluble solids, pH and titratable acidity), ammonia, individual free amino acids, total primary amino acids (FAN) and yeast assimilable nitrogen (YAN), phenolics and colour index in juice at harvest, for uninfected (GLRaV-3 (-)), virus infected after 2008 (GLRaV-3 (+) Post 2008) and virus infected before 2008 (GLRaV-3 (+) Pre 2008) plants, at harvest. There are seven replicates for each treatment (letters; P = 0.05, LSD test).

Variables	GLRaV-3 (-)	GLRaV-3 (+) Post 2008	GLRaV-3 (+) Pre 2008
Harvest juice analysis			
Soluble solids (ºBrix)	19.9±0.5a	20.4±0.2a	20.0±0.3a
pH	2.97±0.01a	2.98±0.01a	2.95±0.02a
Titratable acidity (g l^{-1})	12.11±0.26b	11.02±0.10a	10.79±0.16a
Harvest juice nitrogen concentration			
Ammonia (mg N l^{-1})	40.48±2.35a	46.19±5.09a	40.97±4.98a
Total Primary Amino Acids (mg N l^{-1})=FAN	146.05±6.60a	180.80±18.11a	174.74±15.74a
1- Aspartic Acid (Asp)	2.62±0.17b	1.99±0.16a	1.77±0.06a
2- Glutamic Acid (Glu)	7.75±0.22a	7.10±0.68a	7.30±0.39a
3- Serine (Ser)	4.11±0.20a	3.41±0.37a	3.16±0.31a
4- Histidine (His)	0.93±0.05a	0.90±0.13a	0.85±0.14a
5- Glycine (Gly)	0.19±0.01b	0.09±0.02a	0.10±0.01a
6- Threonine (Thre)	8.48±0.32b	7.45±0.86ab	6.40±0.57a
7- Arginine (Arg)	104.41±9.66a	92.29±13.96a	72.05±14.72a
8- Alanine (Ala)	14.83±0.62a	13.32±1.26a	12.62±1.36a
9- Tyrosine (Tyr)	0.40±0.03a	0.35±0.07a	0.30±0.06a
10- Valine (Val)	1.52±0.09a	2.51±0.31b	2.44±0.28b
11- Methionine (Meth)	1.20±0.32b	0.33±0.08a	0.35±0.09a
12- Phenylalanine (Phen)	1.43±0.24a	1.77±0.29a	1.60±0.33a
13- Isoleucine (Ile)	1.16±0.17a	1.24±0.32a	1.10±0.27a
14- Leucine (Leu)	1.43±0.21a	1.57±0.38a	1.33±0.34a
15- Lysine (Lys)	0.69±0.05a	0.99±0.27b	0.26±0.03a
YAN (mg l^{-1})	186.53±8.67a	227.00±23.10a	215.72±20.13a
Harvest juice phenolics and color index			
Phenolics (mg GAE l^{-1})	348.35±8.79ab	330.65±4.00b	350.76±5.01a
Colour intensity (A420)	0.225±0.002c	0.240±0.004b	0.255±0.003a
Colour hue (A420/520)	1.336±0.005c	1.416±0.011a	1.385±0.006b

In Juice, malic and tartaric acids were significantly lower in the two virus-infected plant treatments. Citric acid was higher in the juice obtained from plants infected after 2008 (Figure 5).
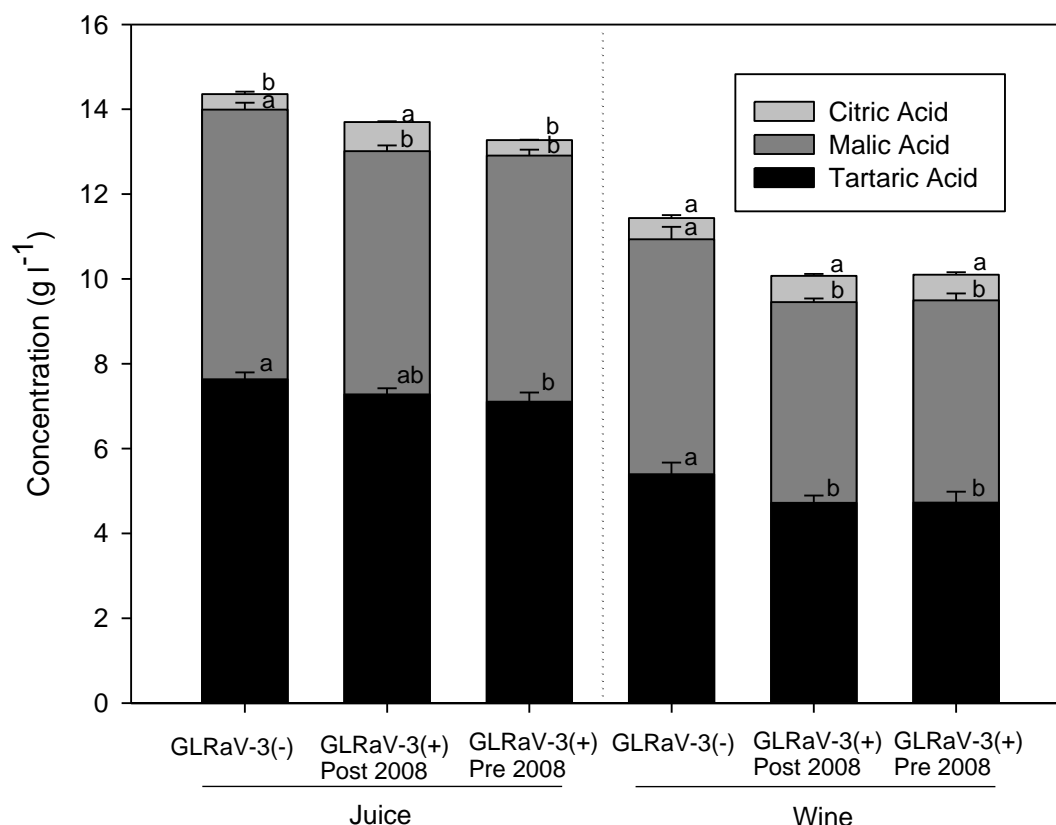
Figure 5. Organic acids presented in juice and wine. Citric, malic and tartaric acid in juice and wine for uninfected (GLRaV-3 (-)), virus infected after 2008 (GLRaV-3 (+) Post 2008) and virus infected before 2008 (GLRaV-3 (+) Pre 2008) plants, at harvest. There are seven replicates for each treatment (letters; P = 0.05, LSD test).

Wine chemical profile

Fermentation rates were very similar for the three treatments. However, the fermentation began one day and finished one week later for the treatment of plants infected after 2008 compared with the other two treatments. The fermentation curve trends were otherwise the same for the three treatments (data not shown).

Although free SO_2 was higher in wine from virus-infected plants, those values were always above the limit to inhibit oxidation in juice and wine (16.96±2.42 mg l^{-1} in wines from uninfected plants, 16.41±3.73 mg l^{-1} in wines from plants infected by GLRaV-3 after 2008 and 22.11±2.68 mg l^{-1} in wines from plants infected before 2008). Between treatments there were no differences in pH, alcohol content, phenolics, colour intensity and colour in wine; only TA was significantly lower in wines produced from plants infected before 2008 than the other two treatments (Table 4).

Table 4. Reducing sugars, pH, titratable acidity, alcohol content, phenolics, colour intensity and tonality (colour hue (A420/520) in wine, for uninfected (GLRaV-3 (-)), virus infected after 2008 (GLRaV-3 (+) Post 2008) and virus infected before 2008 (GLRaV-3 (+) Pre 2008). There are seven replicates for each treatment (letters; P = 0.05, LSD test).

Parameter	GLRaV-3 (-)	GLRaV-3 (+) Post 2008	GLRaV-3 (+) Pre 2008
Reducing sugar (g l^{-1})	2.40±0.75a	1.97±0.55a	2.45±0.47a
pH	2.96±0.01a	3.01±0.01a	2.99±0.03a
Titratable Acidity (g l^{-1})	11.60±0.10b	11.05±0.22ab	10.64±0.18a
Alcohol (% vol)	11.98±0.29a	12.19±0.16a	12.42±0.30a
Phenolics (mg GAE l^{-1})	213.79±8.01a	221.76±10.39a	220.46±10.15a
Color intensity (A420)	0.233±0.020a	0.253±0.019a	0.260±0.018a
Color hue (A420/520)	1.299±0.037a	1.337±0.029a	1.354±0.031a

The organic acids malic and tartaric acids were both higher in wines produced from non-infected plants than in infected ones. However, in GLRaV-3 infected wines, no differences in organic acids were found in wines produced from plants infected before and after 2008 (Figure 5).

DISCUSSION

Similar to many winegrowing regions around the world, some New Zealand vineyards are also highly infected with GLRaV-3 (Charles et al., 2009). The virus is established in North Island vineyards and is becoming increasingly prevalent in the Marlborough region of the upper South Island (Charles, 1993). Climatic conditions can influence virus titre; for example, when temperatures are extremely high (above 37ºC), virus multiplication can be interrupted (Gambino et al., 2012; Valero et al., 2003; Bota et al., 2014). Virus titre and time of infection besides vector activity are the principal variables affecting the virus infection process, along with factors such as cultivar, rootstock or vine age may contribute (Lee & Martin, 2009). The absence of differences in virus titre between treatments suggests the importance to the time of infection and the accumulative effect of the virus. However, the virus infection could be robust within the first six years of infection such that virus infection stage could not be distinguished by virus titre in that period.

Vine growth, yield, photosynthesis, and grape ripeness parameters have beendescribed as the principal factors affected by GLRaV-3 infection (Basso et al.,

2010; Endeshaw et al., 2014; Lee et al., 2009; Mannini et al., 2012). In the present study, no differences were found in trunk circumference; although the plants were infected by the virus a long time ago, there was no significant alteration in either the physiology of the vine and/or the resultant accumulation of trunk mass. Likewise, yield parameters were similar in the different treatments that were harvested at the same soluble solids value (Figure 4). According to Santini et al. (2011), presence of GLRaV-3 did not affect the yield from cv. Nebbiolo. Photosynthesis, stomatal conductance and transpiration were the main physiological parameters negatively affected by GLRaV-3 in the present study (Table 1). However, the limitations in those parameters by the virus infection was generally not as marked as in other studies performed with white and red cultivars (Mannini et al., 1996; Sampol et al., 2003, Cabaleiro et al., 1999; Bertamini et al., 2004). We also found a negative impact virus infection on relative chlorophyll content which increased over the time of infection. Thus, it appears nitrogen metabolism could be modified progressively by the time of infection. It is well known that GLRaV-3 affects grape maturity in red and white cultivars; however, the present study shows an influence by the duration of the virus infection (Figure 2). Normally during grape berry development, there is a rapid importation of carbohydrate that is employed for several processes including seed development, cell proliferation and expansion as carbohydrate accumulates in vacuoles within the berry pericarp cells which then expand in size, and finally the burst of organic acid synthesis at berry ripening (Coombe, 1992). The results from this study suggest that GLRaV-3 affects berry development, particularly at the later berry ripening phase, because we found that both malic and tartaric acids decreased in concentration in the presence of GLRaV-3 infection (Figure 5). A similar result has been reported by other studies (Lee et al., 2009; Kliewer et al., 1976).

The effect of the virus limiting carbohydrate importation at the last phase of berry development near harvest date could also explain the low rate of berry weight increase in infected plants compared to non-infected plants (Figure 3). However, there were no differences in berry weight at harvest time, a reflection of the later harvest date of the virus infected plants. Differences in grape ripeness probably began after seed development as there were no early differences between the three treatments in seed weight and number of seeds (Table 2).

A delay in sugar translocation could reduce the rate of soluble solids accumulation in grape berries (Table 2). After adjusting for grape ripeness by delaying the harvest date for infected plants, some significant parameters such as TA (Table 3) discriminated between non-infected and infected grapes. Therefore, acid to sugar ratio was changed possibly due to a delay in soluble solids accumulation in infected plants. GLRaV species infecting Burger grapes (Kliewer & Lider, 1976) were reported to have higher levels of TA compared to non infected grapes, and Giribaldi et al. (2011) reported significantly higher TA in grapes from plants with mixed infection of GLRaV-1, GVA and *Grapevine Rupestris Stem Pitting associated Virus* (GRSPaV) than from non infected plants. Mannini et al. (2012) reported lower TA and consequential higher pH in non-infected than GLRaV-3 infected plants.

There were no significant differences between treatments in phenolic compounds (Table 3). Phenolic compounds decrease throughout the ripening (Hellín et al., 2010); however, phenolic maturity does not always coincide with berry maturity as measured by sugar accumulation (Mannini et al., 2012), but higher phenolic content of infected berries has been linked to a response to biotic stress (Barlass et al., 1987). Plant defense response to the infection was undetectable by phenolic measurement in our study and even more dramatically, a lower total phenol content in GLRaV-3 infected vines was described by Mannini et al. (2012). Phenolic compounds can alter wine colour and body through oxidation with browning being the main effect of oxidation of phenolic compounds in white wines and the colour index value of the wines positively correlated that of the juice (Mannini et al., 2012; Martínez-Gil et al., 2012). This interesting oenological feature suggests the colour index in juice as a predictor of the quality of the wine (Martínez-Gil et al., 2012). However, this predictor was not effective in our study as the differences in colour intensity and tonality (hue) in juice did not result in differences in the wine (Table 4). In addition, differences obtained in colour intensity and hue of juice were unlikely to be due to oxidation, because TSO_2 and FSO_2 concentrations were always above the established threshold to prevent the negative effects of oxidation in juice and wine.

Five out of the fifteen individual primary amino acids measured in juice were affected by the virus infection (Table 3). Changes in some amino acids can modify volatile compounds in the wine and differences found in some of those amino acids can produce a delay in the wine reaching dryness (Mannini et al., 2012). However, in our

study no significant delay was found in the wine making and fermentation. According to Martínez-Gil et al. (2012), the concentration of all the amino acids increased significantly at the end of grape ripening, except for Asp, Tyr, and Met in Syrah, His in cv. Monastrell, and Ala in cv. Merlot. In our study regardless one week of difference of harvest date between treatments, Asp and Met were lower for infected plants, evidencing the effect of the virus on these amino acids. The amino acid most metabolised by yeast is Arg, followed by Lys, Ser, Thr, Leu, Asp, and Glu. The least metabolized amino acids are Gly, Tyr, Trp and Ala (Martínez-Gil et al., 2012). Although GLRaV-3 infection affected both groups of amino acids in Sauvignon blanc plants, YAN did not change between treatments significantly (Table 3). However, differences in some of primary amino acids analysed and YAN between treatments, regardless of whether they were not significant, suggested that there was probably an effect of virus, but it was not consistent from vine to vine. The absence of significant differences in YAN also could be due to the time-lapse between the harvest dates for the different treatments, as was reported by Mundy et al. (2007). YAN increases very quickly close to harvest and differences during the ripening could be explained by this factor. Lee et al. (2009) described no significant differences in individual free amino acids (FAN) or YAN between the grapes from non infected and GLRaV-2 and -3 infected vines. In the same study Val and Met content of non infected vines were significantly higher, compared to their infected counterparts.

In conclusion, the results showed that detection of virus presence is crucial to mitigate the negative effect on basic food chemistry. Principal changes observed related to berry ripening, which in turn affects harvest date, resulting in reduced organic acid concentrations. These changes appear to have had a greater effect on plants that had been infected before 2008. The duration of infection may have a stronger effect on plant physiology than absolute virus amount measured at any given time, perhaps due to compounding physiological impacts that are not directly correlated to plant growth, as measured by trunk circumference and yield, even when photosynthesis was reduced within individual leaves.

ACKNOWLEDGEMENTS

REFERENCES

Barlass M., Miller R.M., & Douglas T.J. (1987). Development of methods for screening grapevines for resistance to infection by downy mildew. II. Resveratrol production. *American Journal of Enology and Viticulture*, **38**, 65-68.

Basso M.F., Fajardo T.V.M., Eiras M., Ayub R.A., & Nickel O. (2010). Detecção e identificação molecular de vírus associados a videiras sintomáticas e assintomáticas. *Ciência Rural*, **40**, 2249-2255.

Bell S., & Henschke P.A. (2005). Implication of nitrogen nutrition for grapes, fermentation and wine. *Australian Journal of Grape and Wine Research*, **11**, 242-295.

Bertamini M., Muthuchelian K., & Nedunchezhian N. (2004). Effect of grapevine leafroll on the photosynthesis of field grown grapevine plants (*Vitis vinifera* L. cv. Lagrein). *Journal of Phytopathology*, **152**, 145-152.

Bota J., Cretazzo E., Montero R., Rossello J., & Cifre J. (2014). *Grapevine fleck virus* (GFkV) elimination in a selected clone of Manto negro Cv. and its effects on the photosynthesis. *Journal International des Science de la Vigne et du Vine*, **48**, 11-19.

Cabaleiro C., Segura A., & García-Berrios J.J. (1999). Effects of *Grapevine leafroll associated virus 3* on the physiology and must of *Vitis vinifera* L. cv. Albariño

following contamination in the field. *American Journal of Enology and Viticulture*, **50**, 40-44.

Charles J.G. (1993). A survey of mealybugs and their natural enemies in horticultural crops in North Island, New Zealand, with implications for biological control. *Biocontrol Science and Technology,* **3**, 405–418.

Charles J.G., Froud K.J., van der Brink R., & Allan D.J. (2009). Mealybugs and the spread of *Grapevine leafroll-associated virus 3* (GLRaV-3) in a New Zealand vineyard. *Australasian Plant Pathology*, **38**, 576-583.

Chooi K.M., Cohen D., & Pearson M.N. (2013). Generic and sequence-variant specific molecular assays for the detection of the highly variable *Grapevine leafroll-associated virus 3*. *Journal of Virological Methods*, **189**, 20-29.

Clark M.F., & Adams A.N. (1977). Characteristics of the microplate method of enzyme-linked immunosorbent assay for the detection of plant viruses. *Journal of General Virology*, **34**, 475-483.

Coombe B. (1992). Research on the development and ripening of the grape berry. *American Journal of Enology and Viticulture*, **43**, 101-110.

Douglas N., Pietersen G., & Krüger K. (2009). A Real-time RT-PCR assay for the detection and quantification of *Grapevine leafroll-associated virus 3* (GLRaV-3) in *Vitis vinifera* L. (Vitaceae) and *Planococcus ficus* (Signoret) (Hemiptera: Pseudococcidae). In: le Progrès Agricole et Viticole (Ed.), *Proceedings of the 16th Meeting of the International Council for the Study of Virus and Virus-like Diseases of the Grapevine*. ICVG, Dijon, France, pp. 292-293.

Dukes B.C., & Butzke C.E. (1998). Rapid determination of primary amino acids in must using an OPA/NAC spectrophotometric assay. *American Journal of Enology and Viticulture*, **49(2)**, 125-133.

Endeshaw S.T., Sabbatini P., Romanazzi G., Annemiek C., Schilder A.C., & Neri D. (2014). Effects of grapevine leafroll associated virus 3 infection on growth,leaf gas exchange, yield and basic fruit chemistry of *Vitis vinifera* L. cv. Cabernet Franc. *Scientia Horticulturae*, **170**, 228-236.

Gambino G., Cuozzo D., Fasoli M., Pagliarani C., Vitali M., Boccacci P., Pezzotti M., & Mannini F. (2012). Co-evolution between *Grapevine rupestris stem pitting-associated virus* and *Vitis vinifera* L. leads to decreased defense responses and increased transcription of genes related to photosynthesis. *Journal of Experimental Botany*, **63(16)**, 5919-5933.

Giribaldi M., Purrotti M., Pacifico D., Santini D., Mannini F., Caciagli P., Rolle L., Cavallarin L., Giuffrida M.G., & Marzachì C. (2011). A multidisciplinary study on the effects of phloem-limited viruses on the agronomical performance and berry quality of *Vitis vinifera* cv. Nebbiolo. *Journal of Protemomics*, **75(1)**, 306–315.

Hellín P., Manso A., Flores P., & Fenoll J. (2010). Evolution of aroma and phenolic compounds during ripening of 'Superior Seedless' grapes. *Journal of Agricultural and Food Chemistry*, **58(10)**, 6334-6340.

Henderson J.W., & Brooks A. (2010). Agilent application note: Improved amino acid methods using Agilent Zorbax Eclipse plus C18 columns for a cultivar of Agilent LC instrumentation and separation goals.
http://www.chem.agilent.com/Library/applications/5990-4547EN.pdf.

Kliewer W.M., & Lider L.A. (1976). Influence of leafroll virus on composition of Burger fruits. *American Journal of Enology and Viticulture*, **27**, 118-124.

Lee J., Keller K.E., Rennaker C., & Martin R.R. (2009). Influence of *Grapevine leafroll associated viruses* (GLRaV-2 and -3) on the fruit composition of Oregon *Vitis vinifera* L. cv. Pinot noir: free amino acids, sugars, and organic acids. *Food Chemistry*, **117**, 99-105.

Lee J., & Martin R.R. (2009). Influence of *Grapevine leafroll associated viruses* (GLRaV-2 and -3) on the fruit composition of Oregon *Vitis vinifera* L. cv. Pinot noir: Phenolics. *Food Chemistry*, **112**, 889-896.

Mannini F., Argamante N., & Credi R. (1996). Improvements in the quality of grapevine Nebbiolo clones obtained by sanitation. *Acta Horticulturae*, **427**, 319-324.

Mannini F., Mollo A., & Credi R. (2012). Field performance and wine quality modification in a clone of *Vitis vinifera* cv. Dolcetto after GLRaV-3 elimination. *American Journal of Enology and Viticulture*, **63**, 1.

Maree H.J., Almeida R.P.P., Bester R., Chooi K.M., Cohen D., Dolja V.V., Fuchs M.F., Golino D.A., Jooste A.E.C., Martelli G.P., Naidu R.A., Rowhani A., Saldarelli P.A., & Burger J.T. (2013). *Grapevine leafroll-associated virus 3*. *Frontiers in Microbiology*, **4**, 82.

Martelli G.P. (2012). Grapevine virology highlights 2010–2012. *Proceedings of the 17th Meeting of the International Council for the Study of Virus and Virus-like Diseases of the Grapevine.* ICVG, Davids, California, USA, October 7-14, 2012, pp. 13-32.

Martínez-Gil A.M., Garde-Cerdán T., Lorenzo C., Lara J.F., Pardo F., & Salinas M.R. (2012). Volatile compounds formation in alcoholic fermentation from grapes collected at 2 maturation stages: influence of nitrogen compounds and grape cultivar. *Journal of Food Science*, **77(1)**, 71-79.

Montero R., El aou ouad H., Pacifico D., Marzachì C., Castillo N., García E., Del Sáz N.F., Florez-Sarasa I., Flexas J., & Bota J. (2015). Absolute quantification of *Grapevine Leafroll associated Virus 3* (GLRaV-3) and its effects on the physiology in asymptomatic plants of *Vitis vinifera* L. (Submitted)

Moutinho-Pereira J., Correia C.M., Gonçalves B., Bacelar E.A., Coutinho J.F., Ferreira H.F., Lousada J.L., & Cortez M.I. (2012). Impacts of leafroll-associated viruses (GLRaV-1 and -3) on the physiology of the Portuquese grapevine cultivar "Touriga Nacional" growing under field conditions. *Annals of Applied Biology*, **160(3)**, 237-249.

Mundy D., Connolly P., & Neal S. (2007). Virus effects on Sauvignon Blanc wine quality: Progress report 2007. *New Zealand Winegrowers* (06-201 Year 1 report).

Pacifico D., Caciagli P., Palmano S., Mannini F., & Marzachì C. (2011). Quantitation of *Grapevine leafroll associated virus-1 and -3, Grapevine virus A, Grapevine fanleaf virus and Grapevine fleck virus* in field-collected *Vitis vinifera* L. 'Nebbiolo' by real-time reverse transcription-PCR. *Journal of Virological Methods*, **172**, 1-7.

Sampol B., Bota J., Riera D., Medrano H., & Flexas J. (2003). Analysis of the virus-induced inhibition of photosynthesis in malmsey grapevines. *New Phytologist*, **160**, 403-412.

Santini D., Roll L., Cascio P., & Mannini F. (2011). Modifications in chemical, physical and mechanical properties of Nebbiolo (*Vitis vinifera* L.) grape berries induced by mixed virus infection. *South African Journal of Enology and Viticulture*, **32(2)**, 183.

Scholander P.F., Bradstreet E.D., Hemmingsen E.A., & Hammel H.T. (1965). Sap pressure in vascular plants: Negative hydrostatic pressure can be measured in plants. *Science*, **148**, 339-346.

Smart R., & Robinson M. (1991). Sunlight into Wine: A Handbook for Winegrape Canopy Management. Winetitles, Adelaide. 88 pp.

Taillandier P., Portugal F.R., Fuster A., & Strehaiano P. (2007). Effect of ammonium concentration on alcoholic fermentation kinetics by wine yeasts for high sugar content. *Food Microbiology*, **24**, 95-100.

Trought M.C.T, & Bramley R.G.V. (2011). Vineyard variability in Marlborough, New Zealand: Characterising spatial and temporal changes in fruit composition and juice quality in the vineyard. *Australian Journal of Grape and Wine Research*, **17(1)**, 79-89.

Ueno K., Kinoshita K., Togawa H., & Iri M. (1985). Improvement of the wine quality by elimination of grapevine leafroll virus. *Journal of the Brewing Society of Japan*, **80**, 490-495.

Valero M., Ibañez A., & Morte A. (2003). Effects of high vineyard temperatures on the grapevine leafroll associated virus elimination from *Vitis vinifera* L. cv. Napoleon tissue cultures. *Scientia Horticulturae*, **97**, 289-296.

Velasco L., Bota J., Montero R., & Cretazzo E. (2014). Differences of three ampeloviruses multiplication in plant contribute to explain their incidences in vineyards. *Plant Disease*, **98**, 395-400.
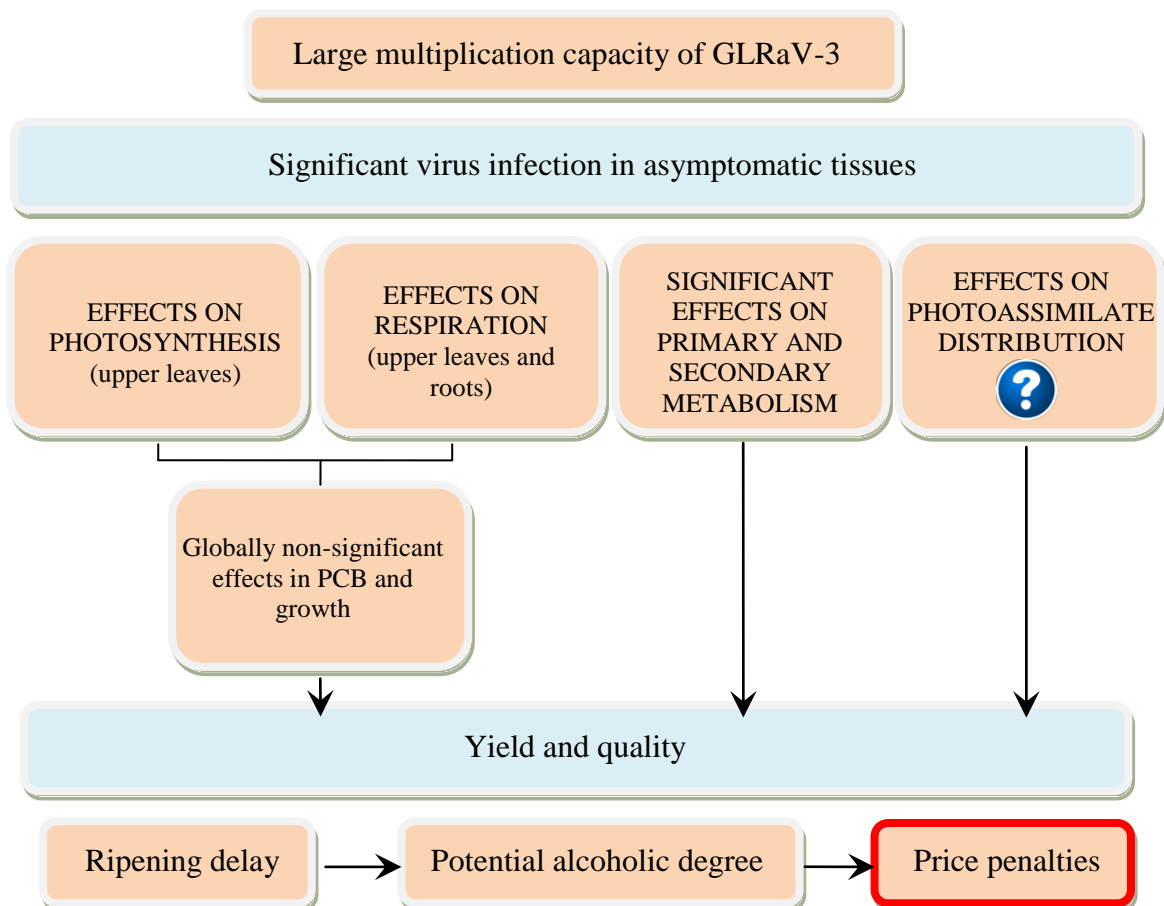
Chapter 8

GENERAL DISCUSSION

The results of this Thesis have been structured in five Chapters (3, 4, 5, 6 and 7) corresponding to each of the publications derived. The relevance of the findings is extensively discussed in each of Chapter, each of which deals with different specific objectives. Therefore, the present General Discussion Chapter focuses only on a broader and integrative view of all the observed effects of GLRaV-3 infection in asymptomatic plants of white grapevine cultivars, in an attempt to comprehensively linking each other, and highlighting potential future prospects to fight against the infection.

The first broad objective of this Thesis was to determine the reason of the high incidence of GLRaV-3 in vineyards. The results obtained showed a higher virus multiplication efficiency of GLRaV-3 than in the other two ampeloviruses studied in different cultivars (Figure 1).

Figure 1. Schematic diagram of GLRaV-3 effects on infected plants.

This could possibly explain the higher incidence in the field of GLRaV-3 (Chapter 3). In addition, different cultivar-sensitivity to virus infection could influence their incidence in vineyards, for instance Cabernet Sauvignon, Cabernet Franc, Pinot

Noir or Barbera have been described as high sensitive cultivars (Weber et al., 2002). Although cultivar sensitivity is an important factor that could determine virus incidence, other factors can affect virus spread such as vector specificity (Almeida et al., 2013; Martelli et al., 2012).

The GLRaV-3 virus can damage plant physiological processes even in asymptomatic situations (Figure 1). A_N was mainly affected by the virus, being the end of the growing season the period when the virus produced the most significant damages. Similar results were reported in other studies (Moutinho-Pereira et al., 2012; Endeshaw et al., 2014). However, virus amount conditioned the quantitative effects on photosynthesis. Different studies have described the effects of virus infection on photosynthesis, but the information about the relationship between virus amount and its effects on plant physiology remains scarce. The infected plants of Malvasía de Banyalbufar used in the experiments described in Chapter 4 had higher virus amount than the plants used in the rest of experiments described in the other Chapters. This highest virus concentration produced a bigger impact on A_N than in the other cases. At the leaf level, specific limitations to photosynthesis were studied, identifying CO_2 diffusion limitations, in the stomata and the mesophyll, as the responsible of A_N decreased in the first stage of GLRaV-3 infection while biochemical limitations were minor and appearing only at later stages of infection. Sampol et al. (2003) measured substantial declines in net assimilation rate identifying decreases in mesophyll conductance to CO_2 (g_m) and impaired Rubisco activity the principal limitations to photosynthesis. When virus concentration was low, for instance in infected plants of Girò Ros (Chapter 6), A_N was slightly affected. In this case, only leaves well exposed to light were affected by the virus only at the end of the growing season and only after midday. Respiration was little affected in any organ, thus globally non-significant effects in Plant Carbon Balance (PCB) and growth were observed, but PCB was decreased by 14% precisely at the end of the growing season (Figure 1). In this period ripening takes place, being crucial for the correct fruit development (Mannini et al., 2012).

Besides the parameters discussed above, in Chapter 5 more sensitive parameters affected by the virus were identified, but in this occasion related specially to the primary and secondary metabolism (Figure 1).

The auto-fluorescence of a sample is a highly sensitive and selective optical property that permits to establish non-destructive techniques for the assessment of plant status, like detecting the chlorophyll fluorescence (ChlF) related to stress phenomena. The results presented in this Thesis demonstrated that ChlF imaging (ChlFI) and multicolour fluorescence imaging (MCFI) could be used for early virus presence indicators. However, different results were obtained in non-photochemical quenching (NPQ) values between experiments described in Chapter 4 and 5. No differences were observed in this parameter in Chapter 4 between non infected and GLRaV-3 infected plants, while in Chapter 5 NPQ was higher in infected plants than non-infected ones. This could be due to the different experimental conditions performed in both experiments. Under control conditions, the effect of the virus on this variable can be studied more precisely. There are several studies where ChlFI and MCFI have been successfully tested for bacterial, virus and fungal infection detection (Pérez-Bueno et al., 2014; Granum et al., 2015; Morales et al., 2005). In all these cases the study was carried out under control conditions, as in the present Thesis. Currently, there are technical limitations that limit its use in field conditions, especially the MCFI techniques. However, recently an advanced MCFI and data analysis systems are being developed, opening new possibilities for the future (Konanz et al., 2014).

Some secondary metabolites as flavonols myricetin-3-*O*-rutinoside, quercetin-3-*O*-galactoside and quercetin-3-*O*-glucoside and hydroxycinnamic acids such as caffeic acid could be used as potential biomarkers for the identification of asymptomatic plants potentially infected by GLRaV-3 (Chapter 5). However, they accumulate in response to multiple infections (Morales et al., 2005; Parker et al., 2009) and, therefore, the presence of these compounds is not specific of the virus studied. Even so, these results provide new knowledge on the effects of GLRaV-3 that could be used for further investigations.

The results of this Thesis show that primary and secondary metabolisms are affected by the virus at leaf level (Chapters 4 and 5). However, it should be noted that these experiments were performed in potted plants without fruit. It will be important to confirm these results in vineyard plants. The presence of fruit strongly affects plant metabolism, reflecting the size of the carbon sink in the plant, even more than roots. There are evidences that grape berries are the most active sink of photosynthates in grapevines post veraison, importing up to 70-80% of the total assimilates obtained by

photosynthesis despite constituting only 20-30% of total plant dry matter (Bota et al., 2004). Therefore, virus-induced changes in photoassimilate distribution could influence fruit ripening in addition to phostosynthesis, respiration, and primary and secondary metabolism (Figure 1). Although this potential effect was not studied in depth in this Thesis (Chapter 6), other studies have shown that some plant viruses affect carbon partitioning and photoassimilate distribution (Shalitin & Wolf, 2000). It would be interesting to address this point in future studies using fruiting GLRaV-3 infected plants.

Scaling up to field grow plants enabled the effects of GLRaV-3 and the duration of the infection on fruit composition and chemical profile of juice and wine to be determined (Chapter 7). The results obtained suggest that GLRaV-3 affects berry development, particularly post verasion in the later berry ripening phase. This coincided with observed stronger effects on photosynthesis and plant carbon balance and decreases in both malic and tartaric acids in infected plants. The delay observed in berry ripening produced differences in soluble solids content between treatments. This delay could be particularly important in cold climates where infected vineyards would require a later harvest date to achieve the same or higher potential alcoholic degree in the juice as uninfected vineyards (Figure 1). However, this might be a means of counteracting earlier ripening and harvest associated with the potential consequences of climate change (Duchêne & Schneider, 2005; Jones et al., 2005). Low potential alcoholic degree in the juice means penalties to the final price paid for the fruit (Figure 1) (Cabaleiro et al., 2013). In vineyards with mealybug vectors spreading GLRaV-3 up to 100% in 15 years time-lapse, the virus can produced economic losses of 74,000 €/ha and year as demonstrated for Albariño cv. in the North of Spain (Cabaleiro et al., 2013). However, our results demonstrate that potential alcoholic degree did not change between treatments when vines of different treatments were harvested with common soluble solids target; therefore the penalties were avoided in this case. Attention must be taken to the parameters, such as acidity, which could be modified by delaying the harvest date and the influence on the final wine quality. Another way to minimise the virus effects on juice and wine quality is by removing leaves. Pereira-Crespo et al. (2012) reported an improvement in juice quality using this method; by decreasing titratable acidity by between 0.5 and 1.9 g l^{-1} of tartaric acid and increasing grape sugar content around 1 ºBrix. Partial defoliation of a number of leaves in the fruit zone of

each vine, between fruit set and ripening, modifies surrounding microclimate and promotes the ripening process (Pereira-Crespo et al., 2012). According to the results obtained in the present Thesis, perhaps the selective removal of upper leaves previous to ripening could also decrease virus impact on fruit quality, because these are the leaves showing stronger reductions in photosynthesis – i.e. reflecting stronger impacts of virus infection – specifically during the ripening period.

Early identification of virus presence by using ChlFI and MCFI techniques as proposed in this Thesis could be another method to fight against the infection, because the early determination of virus presence allows the rapid application of preventive controls of virus spread in large areas in the field. However, other biotic or abiotic stresses, such as water stress, produce similar effects on plant physiology and can produce similar changes in the ChlFI and MCFI signals in the field. Despite the recent interest on plant interaction with simultaneous water stress and pathogen, all previous studies were focused in crops other than grapevines (Carter et al., 2009; Sharma et al., 2007). In future studies, efforts should be focused on this particular stress combination due to the expected increase in global water scarcity due to climate change, and the possible increase of pathogen interactions.

Recently, unmanned aerial vehicles (drones) have been used to detect areas affected in the field by abiotic and biotic stresses. Parameters such as NDVI and canopy temperature have been proposed as indicators of water stress or fungi infections in different plant species (Baluja et al., 2012; Calderon et al., 2014). We are currently studying the potential of those parameters using unmanned aerial vehicles for virus presence determination in asymptomatic situations combined with drought stress in large areas in the field. In addition we are validating those physiological parameters found in this Thesis as more sensitive to the infection, in simultaneous drought stress and GLRaV-3 infection.

Chapter 9

CONCLUSIONS

From the experimental research presented in this Thesis, a series of conclusions have been reached regarding each of the specific objectives.

1. *To invetigate differences in the multiplication capacity of three ampeloviruses in order to understand the differences in their relative incidences in vineyards.*

1. GLRaV-3 is able to establish more efficient multiplication rates in the host than GLRaV-4 and 5-type ampeloviruses. This could be one of the main reasons of its high incidence in vineyards.

2. *To explore GLRaV-3 effects on several plant physiological and morphological parameters, identifying those most affected by the infection and possible correlations with virus amount.*

2. Asymptomatic grapevine plants showed the existence of virus effects on anatomical and physiological parameters, especially A_N and J_{flu}. These parameters decreased as the virus amounts increased.

3. *To determine whether changes in thermal and fluorescence patterns correlate with virus effects on primary and secondary metabolism.*

3. NPQ and BGF and derived ratios, measured in the abaxial side, were revealed as useful disease signatures for GLRaV-3.

4. Flavonols such as myricetin-3-*O*-rutinoside, quercetin-3-*O*-galactoside and quercetin-3-*O*-glucoside and hydroxycinnamic acids such as caffeic acid were identified as potential responsible metabolites for the observed changes in MCF parameters in response to the infection.

4. *To determine GLRaV-3 effects on the different components of carbon balance and biomass distribution identifying the most sensitive organs affected by the infection.*

5. Total carbon balance was lower in infected plants during the later stages of vine development.

6. Upper leaves and roots, were identified as the most sensitive parts of the plant to GLRaV-3 infection altering leaf CO_2 assimilation and leaf and root respiration.

5. *To study the effects of GLRaV-3 amount and the duration of the infection on fruit composition, juice and wine chemical profile.*

7. The most important virus-induced changes were observed in berry ripening, which in turn affects harvest date, resulting in reduced organic acid concentrations in the final product.

8. The duration of infection may have a stronger effect on plant physiology than absolute virus amount measured at any given time.

GENERAL REFERENCES

Adams I.P., Glover R.H., Monger W.A., Mumford R., Jackeviciene E., Navalinskiene M., Samuitiene M., & Boonham N. (2009). Next-generation sequencing and metagenomic analysis: a universal diagnostic tool in plant virology. *Molecular Plant Pathololology*, **10**, 537–545.

Agranovsky A.A., Koonin E.V., Boyko V.P., Maiss E., Frötschl R., Lunina N.A., & Atabekov J.G. (1994). *Beet yellows closterovirus*: complete genom estructure and identification of a leader papain-like thiol protease. *Virology*, **198**, 311–324.

Almeida R.P.P., Daane K.M., Bell V.A., Blaisdell G.K., Cooper M.L., Herrbach E. & Pietersen, G. (2013) Ecology and management of grapevine leafroll disease. *Frontiers in Microbiology*, **4**, 94.

Alzhanova D.V., Hagiwara Y., Peremyslov V.V., & Dolja V.V. (2000). Genetic analysis of the cell-to-cell movement of beet yellows closterovirus. *Virology*, **268**, 192–200.

Araya T., Noguchi K., & Terashima I. (2006). Effects of Carbohydrate Accumulation on Photosynthesis Differ between Sink and Source Leaves of *Phaseolus vulgaris* L. *Plant Cell Physiology*, **47(5)**, 644–652.

Atallah S.S., Gómez M.I., Fuchs M.F., & Martinson T.E. (2012). Economic Impact of Grapevine Leafroll Disease on *Vitis vinifera* cv. Cabernet franc in Finger Lakes Vineyards of New York. *American Journal of Enology and Viticulture*, **63**, 1.

Baluja J, Diago M.P., Balda P., Zorer R., Meggio F., Morales F., & Tardaguila J. (2012). Assessment of vineyard water status variability by thermal and multispectral imagery using an unmanned aerial vehicle (UAV). *Irrigation Science*, **30**, 511–522.

Basso M.F., Fajardo T.V.M., Eiras M., Ayub R.A., & Nickel O. (2010). Detecção e identificação molecular de vírus associados a videiras sintomáticas e assintomáticas. *Ciência Rural*, **40**, 2249-2255.

Bhat T.K., Singh B., & Sharma O.P. (1998). Microbial degradation of tannins--a current perspective. *Biodegradation*, **9(5)**, 343–357.

Bell S., & Henschke P.A. (2005). Implication of nitrogen nutrition for grapes, fermentation and wine. *Australian Journal of Grape and Wine Research*, **11**, 242-295.

Bell V.A., Bonfiglioli R.G.E., Walker J.T.S., Lo P.L., Mackay J. F., & McGregor S.E. (2009). *Grapevine leafroll-associated virus 3* persistence in *Vitis vinifera* remnant roots. *Journal of Plant Pathology*, **91**, 527–533.

Bertolini E., García J., Yuste A., & Olmos A. (2010). High prevalence of viruses in table grape from Spain detected by real-time RT-PCR. *European Journal of Plant Pathology*, **128**, 283–287.

Bester R., Jooste A.E.C., Maree H.J., & Burger J.T. (2012). Real-time RT-PCR high resolution melting curve analysis and multiplex RT-PCR to detect and differentiate grapevine leafroll-associated virus 3 variant groups I, II, III and VI. *Virology Journal*, **9**, 219.

Boller T. (1995). Chemoperception of microbial signals in plant cells. *Annual Review of Plant Biology*, **46**, 189–214.

Bota J., Stasyk O., Flexas J., & Medrano H. (2004). Effects of water stress on partitioning of 14C labelled photosynthates in *Vitis vinifera*. *Functional Plant Biology*, **31**, 697–708.

Botha C.E.J., & Cross R.H.M. (2000). Towards reconciliation of structure with function in plasmodesmata – who is the gatekeeper?. *Micron*, **21**, 713–721.

Botha C.E.J., & Cross R.H.M. (2001). Regulation within the supracellular highway-plasmodesma are the key. *South African Journal of Botany*, **67**, 1–9.

Boyer J.S. (1982). Plant productivity and environment. *Science*, **218**, 443–448.

Cabaleiro C., Pesqueira A.M., Barrasa M., & García-Berrios J.J. (2013). Analysis of the losses due to grapevine leafroll disease in Albariño vineyards in Rías Baixas (Spain). *Ciência e Técnica Vitivinícola*, **28(2)**, 43–50.

Cabaleiro C., Segura A., & García-Berrios J.J. (1999). Effects of *Grapevine leafroll associated virus 3* on the physiology and must of *Vitis vinifera* L. cv. Albariño

following contamination in the field. *American Journal of Enology and Viticulture*, **50**, 40–44.

Calderón R., Montes-Borrego M., Landa B.B., Navas-Cortés J.A., & Zarco-Tejada P.J. (2014). Detection of downy mildew of opium poppy using high-resolution multi-spectral and thermal imagery acquired with an unmanned aerial vehicle. *Precision Agriculture*, **15**, 639–661.

Carrington J.C., Kasschau K.D., Mahajan S.K., & Schaad M.C. (1996). Cell-to-cell and long-distance transport of viruses in plants. *Plant Cell*, **8**, 1669–1681.

Carter A.H., Chen X.M., Garland-Campbell K., & Kidwell K.K. (2009). Identifying QTL for high-temperature adult-plant resistance to stripe rust (Puccinia striiformis f. sp.tritici) in the spring wheat (*Triticum aestivum* L.) cultivar 'Louise'. *Theoretical and Applied Genetics*, **119**,1119–28.

Charles J.G., Cohen D., Walker J.T.S., Forgie S.A., Bell V.A., & Breen K.C.(2006). A review of the ecology of *Grapevine leafroll associated virus type 3* (GLRaV-3). *New Zealand Plant Protection*, **59**, 330–337.

Charles J.G., Froud K.J., van der Brink R., & Allan D.J. (2009). Mealybugs and the spread of *Grapevine leafroll-associated virus 3* (GLRaV-3) in a New Zealand vineyard. *Australasian Plant Pathology*, **38**, 576-583.

Cheng N.H., Su C.L., Carter S.A., & Nelson R.S. (2000).Vascular invasion routes and systemic accumulation patterns of tobacco mosaic virus in Nicotiana benthamiana. *Plant Journal*, **23**, 349–362.

Chooi K.M., Pearson M.N., Cohen D., & MacDiarmid, R.M. (2012). "Development of generic and variant specific molecular assays for the detection of the highly variable *Grapevine leafroll-associated virus-3*," in Proceedings of the. 17th Congress of ICVG 7–14 October (Davis: Foundation Plant Services), 142–143.

Coetzee B., Freeborough M., Maree H.J., Celton J., Rees D.J., & Burger J.T. (2010). Deep sequencing analysis of viruses infecting grapevines: virome of a vineyard. *Virology*, **400**, 157–163.

Cohen D., Chooi K.M., Bell V.A., Blouin A.G., Pearson M.N., & MacDiarmid R.M. (2012). "Detection of new strains of GLRaV-3 in New Zealand using ELISA and RT-PCR," in Proceedings of the 17th Congress of ICVG 7–14 October (Davis: Foundation Plant Services), 118–119.

Collins N.C., Webb C.A., Seah S., Ellis J.G., Hulbert S.H., & Pryor A. (1998). The isolation and mapping of disease resistance gene analogs in maize. *Molecular Plant-Microbe Interactions*, **11(10)**, 968–978.

Den Boon J.A., & Ahlquist P. (2010). Organelle-like membrane compartmentalization of positive-strand RNA virus replication factories. *Annual Review of Microbiology*, **64**, 241–256.

Ding S.W., & Voinnet O. (2007). Antiviral immunity directed by small RNAs. *Cell*, **130(3)**, 413-426.

Dixon R.A., Achnine L., Kota P., Liu C.J., Reddy M.S., & Wang L. (2002). The phenylpropanoid pathway and plant defense – a genomics perspective. *Molecular Plant Pathology*, **3**, 371–390.

Dolja V.V., Kreuze J.F., & Valkonen J.P.T. (2006). Comparative and functional genomics of closteroviruses. *Virus Research*, **117**, 38–51.

Duchêne E., & Schneider C. (2005). Grapevine and climatic changes: A glance at the situation in Alsace. *Agronomy for Sustainable Development*, **25**, 93-99.

Durango D., Quiñones W., Torres F., Rosero Y., Gil J., & Echeverri F. (2002). Phytoalexin accumulation in Colombian bean cultivars and aminosugars as elicitors. *Molecules*, **7**, 817–832.

Endeshaw S.T., Sabbatini P., Romanazzi G., Annemiek C., Schilder A.C., & Neri, D. (2014). Effects of *Grapevine leafroll associated virus 3* infection on growth,leaf gas exchange, yield and basic fruit chemistry of *Vitis vinifera* L. cv. Cabernet Franc. *Scientia Horticulturae*, **170**, 228-236.

Engel E.A., Escobar P.F., Rojas L.A., Rivera P.A., Fiore N., & Valenzuela P.D.T. (2010). A diagnostic oligonucleotide microarray for simultaneous detection of grapevine viruses. *Journal of Virological Methods*, **163**, 445–451.

Engel E.A., Girardi C., Escobar P.F., Arredondo V., Domininguez C., Pérez-Acle T., & Valenzuela P.D. (2008). Genome analysis and detection of a Chilean isolate of *Grapevine leafroll associated virus-3*. *Virus Genes*, **37**, 110–118.

Evert R.F. (1990). Dicotyledons. In sieve elements. Comparative structure, induction and development (eds H.-D. Behnke & R.D. Sjolund), pp. 103–137. Springer, Berlin, Germany.

Faoro F., Tornaghi R., Cinquanta S., & Belli, G. (1992). Cytopathology of leafroll-associated virus III (GLRaV-III). *Journal of Plant Pathology*, **2**, 67–83.

Faoro F., & Carzaniga, R. (1995). Cyotchemistry and immunocytochemistry of the inclusion bodies induced by *Grapevine leafroll-associated closteroviruses* GLRaV-1 and GLRaV-3. *Journal of Plant Pathology*, **5**, 85–94.

Feng J., Zeng R., & Chen J. (2008). Accurate and efficient data processing for quantitative real-time PCR using a tripartite plant virus as a model. *Biotechniques*, **44**, 901–912.

Flexas J., Bota J., Galmes J., Medrano H., & Ribas-Carbo M. (2006). Keeping a positive carbon balance under adverse conditions: responses of photosynthesis and respiration to water stress. *Physiologia Plantarum*, **127**, 343-352.

Florez-Sarasa I.D., Bouma T.J., Medrano H., Azcon-Bieto J., & Ribas-Carbo M. (2007). Contribution of the cytochrome and alternative pathways to growth respiration and maintenance respiration in Arabidopsis thaliana. *Physiologia Plantarum*, **129**, 143–151.

Freeborough M.J. (2003). A pathogen-derived resistance strategy for the broad-spectrum control of Grapevine leafroll-associated virus infection. University of Stellenbosch, PhD Thesis.

Gale G.(2002)."Saving the vine from phylloxera: an ever ending battle," in Wine: A scientific Exploration, eds J.Sandler and R.Pidler (London: Taylor and Francis),70–91.

Gambino G., Bondaz J., & Gribaudo I. (2006). Detection and elimination of viruses in callus, somatic embryos and regenerated plantlets of grapevine. *European Journal of Plant Pathology*, **114**, 397–404.

Gambino G., Perrone I., Carra A., Chitarra W., Boccacci P., Marinoni D.T., Barberis M., Maghuly F., Laimer M., & Gribaudo I. (2010). Transgene silencing in grapevine transformed with GFLV resistant genes: analysis of variable expression of transgene, siRNAs production and cytosine methylation. *Transgenic Research*, **19**, 17-27.

García-Ruiz F., Sankaran S., Maja J.M., Lee W.S., Rasmussen J., & Eshani R. (2013). Comparison of two aerial imaging platforms for identificaction of Huanglongbing-infected citrus trees. *Computers and Electronics in Agriculture*, **91**, 106-115.

Gaspar T., Franck T., Bisbis B., Kevers C., Jouve L., Hausman J.F., & Dommes J. (2002). Concepts in plant stress physiology. Application to plant tissue cultures. *Plant Growth Regulation*, **37**, 263–285.

Germundsson A., & Valkonen J.P.T. (2006). P1- and VPg-transgenic plants show similar resistance to *Potato virus A* and may compromise long distance movement of the virus in plant sections expressing RNA silencing-based resistance. *Virus Research*, **116**, 208–213.

Gershenzon J., & Croteau R. (1991). Terpenoids. In Herbivores their interaction with secondary plant metabolites, Vol I: The chemical participants, 2nd ed., G.A. Rosenthal and M.R. Berenbaum, eds, Academic press, San Diego, pp: 165–219.

Golino D.A., Sim S.T., Gill R., & Rowhani A. (2002). California mealybugs can spread grapevine leafroll disease. *California Agriculture*, **56**, 196–201.

Golino D. A.,Weber E., Sim S.T., & Rowhani A. (2008). Leafroll disease is spreading rapidly in a Napa Valley vineyard. *California Agriculture*, **62**, 156–160.

Gosalvez-Bernal B., Genoves A., Navarro J.A., Pallas V., & Sanchez-Pina M. (2008). Distribution and pathway for phloem-dependent movement of *Melon necrotic spot virus* in melon plants. *Molecular Plant Pathology*, **9**, 447–461.

Goszczynski D.E., Kasdorf G.G.F., & Pietersen G. (1995). Production and use of antisera specific to *Grapevine leafroll-associated viruses* following electrophoretic separation of their proteins and transfer to nitrocellulose. *African Plant Protection*, **1**, 1–8.

Gould J.M. (1983). Probing the structure and dynamics of lignin *in situ*. *What's New in Plant Physiology*, **14**, 25-91.

Gouveia P., Santos M.T., Eiras-Dias J.E., & Nolasco G. (2011). Five phylogenetic groups identified in the coat protein gene of *Grapevine leafroll-associated virus 3* obtained from Portuguese grapevine cultivars. *Archives of Virology*, **156**, 413–420.

Gowda S., Satyanarayana T., Ayllón M.A., Moreno P.R.F., & Dawson W.O. (2003). The conserved structures of the 5' non translated region of *Citrus tristeza virus* are involved in replication and virion assembly. *Virology*, **317**, 50–64.

Grannet J., Walker M.A., Kocsis L., & Omer A.D. (2001). Biology and management of grape phylloxera. *Annual Review of Entomology*, **26**, 387–412.

Granum E., Pérez-Bueno M.L., Calderón C.E., Ramos C., De Vicente A., Cazorla F.M., & M. Barón. (2015). Metabolic responses of avocado plants to stress induced by Rosellinia necatrix analysed by fluorescence and thermal imaging. *European Journal of Plant Pathology*, **142**, 625–632.

Gugerli P., Brugger J.J., & Bovey R. (1984). L'enroulement de la vigne: mise en évidence de particules virales et développement d'une méthode immunoenzymatique pour le diagnostic rapide. *Revue suisse de viticulture arboriculture horticulture*, **16**, 299–304.

Gutha R.L., Casassa L.F., Harbertson J.F., Rayapati A., & Naidu R.A. (2010). Modulation of flavonoid biosynthetic pathway genes and anthocyanins due to virus infection in grapevine (*Vitis vinifera* L.) leaves. *BMC Plant Biology*, **10**, 187.

Hanqing F., Kun S., Mingquan L., Hongyu L., Xin L., Yan L., & Yifeng W. (2010). The expression, function and regulation of mitochondrial alternative oxidase under biotic stresses. *Molecular Plant Pathology*, **11**, 429–40.

Hipper C., Brault V., Ziegeler-Graf V., & Revers F. (2013). Viral and cellular factors involved in phloem transport of plant viruses. *Frontiers in Plant Science*, **4**, 154.

Hoefert L.L., & Gifford E.M. (1967). *Grapevine leafroll virus*. History and anatomical effects. *Hilgardia*, **38**, 403–426.

Hristov I., & Abrasheva P. (2001). Effect of *Grapevine fanleaf virus* and *Grapevine leafroll associated virus 3* on vine plants under conditions of *in vitro* cultivation. *Rastenievudni Nauki*, **38**, 269–274.

Jarugula S., Gowda S., Dawson W.O., & Naidu R.A. (2010). 3'-coterminal subgenomic RNAs and putative cis-acting elements of *Grapevine leafroll-associated virus 3* reveals 'unique' features of gene expression. *Virology Journal*, **7**, 180.

Jones G.V., Duchene E., Tomasi D., Yuste J., Braslavska O., Shultz H., Martinez M.C., Boso S., Langellier F., Perruchot C., & Guimberteau G. (2005). Changes in European winegrape phenology and relationships with climate. *Comptes Rendus Proceedings GESCO*, Geisenheim, Germany, **1**, 55-61.

Jooste A.E.C., Maree H.J., Bellstedt D.U., Goszczynski D.E., Pietersen G., & Burger J.T. (2010). Three *Grapevine leafroll-associated virus 3* (GLRaV-3) variants identified from South African vineyards show high variability in their 5'UTR. *Archives of Virology*, **155**, 1997–2006.

Kangasjärvi S., Neukermans J., Li S., Aro E.M., & Noctor G. (2012). Photosynthesis, photorespiration, and light signalling in defense responses. *Journal of Experimental Botany*, **63**, 1619–1636.

Kim K. S., Gonsalves D., Teliz D., & Lee K.W. (1989). Ultrastructure and mitochondrial vesiculation associated with closteroviruslike particles in leafroll-diseased grapevines. *Phytopathology*, **79**, 357–360.

Kim H.R., Choi Y.M., Chung B.N., Choi G.S., & Kim J.S. (2002). Biological Assay and Cytopathological Characteristics of *Grapevine leafroll associated virus* 3 (GLRaV-3) and *Grapevine fanleaf virus* (GFLV). *Plant Pathology Journal*, **18(5)**, 244–250.

Krastanova S., Perrin M., Barbier P., Demangeat G., Cornuet P., Bardonnet N., Otten L., Pinck L., & Walter B. (1995). Transformation of grapevine rootstocks with the coat protein gene of *Grapevine fanleaf nepovirus*. *Plant Cell Reports*, **14**, 550–554.

Koh E.J., Zhou L., Williams D.S., Park J., Ding N., Duan Y.P., & Kang B.H. (2012). Callose deposition in the phloem plasmodesmata and inhibition of phloem transport in citrus leaves infected with "Candidatus liberibacter asiaticus". *Protoplasma*, **249**, 687–697.

Konanz S., Kocsányi L., & Buschmann C. (2014). Advanced Multi-Color Fluorescence Imaging system for detection of biotic and abiotic stresses in leaves. *Agriculture*, **4**, 79–95.

Koonin E.V., & Dolja V.V. (1993). Evolution and taxonomy of positive strand RNA viruses: implications of comparative analysis of amino acid sequences. *Critical Reviews in Biochemistry and Molecular Biology*, **28**, 375–430.

Kumar S., Baranwal V.K., Singh P., Jain R.K., Sawant S., & Singh S.K. (2012). Characterization of a *Grapevine leafroll-associated virus 3* from India showing in congruence in its phylogeny. *Virus Genes*, **45**, 195–200.

Lamb C., & Dixon R. A. (1997). The oxidative burst in plant disease resistance. *Annual Review of Plant Physiology and Plant Molecular Biology*, **48**, 251–275.

Lee J., Keller K.E., Rennaker C., & Martin R.R. (2009). Influence of *Grapevine leafroll associated viruses* (GLRaV-2 and -3) on the fruit composition of Oregon *Vitis vinifera* L. cv. Pinot noir: free amino acids, sugars, and organic acids. *Food Chemistry*, **117**, 99–105.

Lee J., & Martin R.R. (2009). Influence of *Grapevine leafroll associated viruses* (GLRaV-2 and -3) on the fruit composition of Oregon *Vitis vinifera* L. cv. Pinot noir: Phenolics. *Food Chemistry*, **112**, 889–896.

Lennon A.M., Neuenschwander U.H., Ribas-Carbo M., Giles L., Ryals J.A., & Siedow J.N. (1997). The effects of salicylic acid and *Tobacco mosaic virus* infection on the alternative oxidase of tobacco. *Plant Physiology*, **115**, 783-791.

Lewis N.G., & Yamamoto E. (1990). Lignin: Occurrence, biogenesis and biodegradation. *Annual Review of Plant Physiolgy and Plant Molecular Biology*, **41**, 455–496.

Li W., Zhao Y., Liu C., Yao G., Wu S., Hou C., Zhang M., & Wang D. (2012). Callose deposition at plasmodesmata is a critical factor in restricting the cell-to-cell movement of *Soibean mosaic virus. Plant Cell Reports*, **31**, 905–916.

Lichtenthaler H.K. (1996). Vegetation stress: an introduction to the stress concept in plants. *Plant Physiology*, **148**, 4–14.

Lichtenthaler H.K., & Schweiger J. (1998). Cell wall bound ferulic acid, the major substance of the blue-green fluorescence emission of plants. *Journal of Plant Physiology*, **152**, 272–282.

Ling K., Zhu H., Jiang Z., & Gonsalves D. (2000). Effective application of DAS-ELISA for detection of *Grapevine leafroll associated closterovirus 3* using a polyclonal antiserum developed from recombinant coat protein. *European Journal of Plant Pathology*, **106**, 301–309.

Ling K., Zhu H., Petrovic N., & Gonsalves D. (2001). Comparative effectiveness of ELISA and RT-PCR for detecting *Grapevine leafroll associated closterovirus 3* in field samples. *American Journal of Enology and Viticulture*, **52**, 21–27.

Ling K.S., Zhu H.Y., Drong R.F., Slightom J.L., McFerson J.R., & Gonsalves D. (1998). Nucleotide sequence of the 3'-terminal two-thirds of the *Grapevine leafroll associated virus 3* genome reveals a typical monopartite closterovirus. *Journal of General Virology*, **79**, 1299–1307.

Ling K.S.,Zhu H.Y., & Gonsalves D. (2004). Complete nucleotide sequence and genome organization of *Grapevine leafroll-associated virus 3*, type member of the genus Ampelovirus. *Journal of General Virology*, **85**, 2099–2102.

Liu Y.-P., Peremyslov V.V., Medina V., & Dolja, V.V. (2009). Tandem leader proteases of *Grapevine leafroll-associated virus-2*: host-specific functions in the infection cycle. *Virology*, **383**, 291–299.

Maghuly F., Leopold S., Machado A.D., Fernandez E.B., Khan M.A., Gambino G., Gribaudo I., Schartl A., & Laimer M. (2006). Molecular characterization of grapevine plants transformed with GFLV resistance genes: II. *Plant Cell Reports*, **25**, 546–553.

Mannini F., Mollo A., & Credi R. (2012). Field performance and wine quality modification in a clone of *Vitis vinifera* L. cv. Dolcetto after GLRaV-3 elimination. *American Journal of Enology and Viticulture*, **63**, 1.

Maree H.J., Freeborough M.J., & Burger J.T. (2008). Complete nucleotide sequence of a South African isolate of *Grapevine leafroll-associated virus 3* reveals a 50 UTR of 737 nucleotides. *Archives of Virology*, **153**, 755–757.

Maree H.J., Almeida R.P.P., Bester R., Chooi K.M., Cohen D., Dolja V.V, Fuchs M.F., Golino D.A, Jooste A.E.C., Martelli G.P., Naidu R.A., Rowhani A., Saldarelli P., & Burger, J. T. (2013). *Grapevine leafroll-associated virus 3*. *Frontiers in Microbiology*, **4**, 94.

Martelli G.P., & Boudon-Padieu E. (2006). Directory of infectious diseases of grapevines and viroses and viruslike diseases of grapevine: Bibliographic report 1998-2004. Opinions Mediterraneennes Serie B: Studies and Research.

Martelli G.P., Agranovsky A.A., Al Rwahnih M., Dolja V.V., Dovas C.I., Fuchs M., Gugerli P., Hu J.S., Jelkmann W., Katis N.I., Maliogka V.I., Melzer M.J., Menzel W., Minafra A., Rott M.E., Rowhani A., Sabanadzovic S., & Saldarelli P. (2012). Taxonomic revision of the family Closteroviridae with special reference to the grapevine leafroll-associated member soft hegenus Ampelovirus and the putative species unassigned to the family. *Journal of Plant Pathology*, **94**, 7–19.

Mazid M., Khan T.A., & Mohammad F. (2011). Role of secondary metabolites in defense mechanisms of plants. *Biology and Medicine*, **3(2)**, 232–249.

Maule A. (2008). Plasmodesmata: structure, function and biogenesis. *Current Opinion in Plant Biology*, **11**, 680–686.

Morales F., Cartelat A., Alvarez-Fernández A., Moya I., & Cerovic Z.G. (2005) Time-resolved spectral studies of blue-green fluorescence of artichoke (*Cynara cardunculus* L. var. Scolymus) leaves: identification of chlorogenic acid as one of the major fluorophores and age-mediated changes. Journal of Agricultural Food Chemistry 53(25): 9668–9678.

Moutinho-Pereira J., Correia C.M., Gonçalves B., Bacelar E.A., Coutinho J.F., Ferreira H.F., Lousada J.L., & Cortez M.I. (2012). Impacts of leafroll-associated viruses (GLRaV-1 and -3) on the physiology of the Portuquese grapevine cultivar "Touriga Nacional" growing under field conditions. *Annals of Applied Biology*, **3**,47–46.

Oparka K.J., & Cruz S.S. (2000). The great escape: phloem transport and unloading of macromolecules. *Annual Review of Plant Physiology and Plant Molecular Biology*, **51**, 323–347.

Oparka K.J., & Turgeon R. (1999). Sieve elements and companion cells – traffic control centers of the phloem. *Plant Cell*, **11**, 739–750

Orecchia M., Nolke G., Saldarelli P., Dell'Orco M., Uhde-Holzem K., Sack M., Martelli G., Fischer R., & Schillberg S. (2008). Generation and characterization of a recombinant antibody fragment that binds to the coat protein of Grapevine *leafroll associated virus 3*. *Archives of Virology*, **153**, 1075–1084.

Osman F., Leutenegger C., Golino D., & Rowhani A. (2007). Real-time RT-PCR (TaqMan®) assays for the detection of *Grapevine leafroll-associated viruses* 1–5 and 9. *Journal of Virological Methods,* **141**, 22–29.

Osman F., Leutenegger C., Golino D., & Rowhani A.(2008). Comparison o flow density arrays, RT-PCR and real-time TaqMan® RT-PCR in detection of grapevine viruses. *Journal of Virological Methods*, **149**, 292–299.

Osman F., & Rowhani A. (2006). Application of a spotting sample preparation technique for the detection of pathogens in woody plants by RT-PCR and real-time PCR (TaqMan®). *Journal of Virological Methods*, **133**, 130–136.

Pacottet B. (1906). Coloration anormale des feuilles de vigne. *Revue Viticulture*, **26**, 466–488.

Panattoni A., D'Anna F., & Triolo E. (2007). Antiviral activity of tiazofurin and mycophenolic acid against *Grapevine Leafroll-associated Virus 3* in *Vitis vinifera* explants. *Antiviral Research*, **73**, 206–211.

Pathirana R., & McKenzie M. J. (2005). A modified green-grafting technique for large-scale virus indexing of grapevine (*Vitis vinifera* L.). *Scientia Horticulturae*, **107**, 97–102.

Papadopoulou K., Melton R.E., Legget M., Daniels M.J., & Osbourn A.E. (1999). Compromised disease resistance in saponin-deficient plants. *PNAS*, **96**, 12923–12928.

Parker D., Beckmann M., Zubair H., Enot D.P., Caracuel-Rios Z., Overy D.P., Snowdon S., Talbot N.J., & Draper J. (2009). Metabolomic analysis reveals a common pattern of metabolic re-programming during invasion of three host plant species by Magnaporthe grisea. *Plant Journal*, **59**, 723–737.

Pérez-Bueno M.L., Pineda M., Díaz-Casado E., & Barón M. (2014). Spatial and temporal dynamics of primary and secondary metabolism in *Phaseolus vulgaris* challenged by *Pseudomonas syringae*. *Physiologia Plantarum*, **153**, 161–174.

Pereira-Crespo S., Segura A., García-Berrios J. & Cabaleiro C. (2012). Partial defoliation improves must quality of cv. Albariño infected by *Grapevine leafroll associated virus 3*. *Phytopathologia Mediterranea*, **51**, 383−389.

Pietersen G., Spreeth N., Oosthuizen T., VanRensburg A., Lottering D., & Tooth D. (2009)."A case study of control of grapevine leafroll disease spread on Vergelegen Wine Estate, South Africa, 2002–2008," in Proceedings of the 16th Congress of ICVG 31August–4 September (Dijon: Le Progres Agricole et Viticole), 230–231.

Pietersen G., & Walsh H. (2012). "Development of a LAMP technique for control of *Grapevine leafroll-associated virus type 3* (GLRaV-3) in infected white cultivar vines by rouging," in Proceedings of the 17th Congress of ICVG 7–14 October (Davis: Foundation Plant Services), 50–51.

Ravaz L, & Roos L. (1905). Le rougeau de la vigne. *Progrès Agricole et Viticole*, **22**, 39–40.

Ribas-Carbo M., Robinson S.A., & Giles L. (2005). The application of the oxygen-isotope technique to assess respiratory pathway partitioning. In Plant Respiration: From Cell to Ecosystem, *Advances in Photosynthesis and Respiration Series* (eds H. Lambers & M. Ribas-Carbo), **18**, 31–42. Springer, Dordrecht, The Netherlands.

Rice E.L., (1984). Allelopathy, second edition. Academic Press, New York.

Rinne P., & Schoot C. (2003). Plasmodesmata at the crossroads between development, dormancy, and defense. *Canadian Journal of Botany-Revue Canadienne de Botanique*, **81**, 1182–1197.

Roberts A.G., & Oparka K.J. (2003). Plasmodesmata and the control of symplastic transport. *Plant Cell Environment*, **26**, 103–124.

Roberts K., Love A.J. ,Laval V., Laird J., Tomos A.D., Hooks M.A., & Milner J.J. (2007). Long-distance movement of *Cauliflower mosaic virus* and host defense responses in Arabidopsis follow a predictable pattern that is determined by the leaf orthostichy. *New Phytologist*, **175**, 707–717.

Rodríguez-Moreno L., Pineda M., Soukupová J., Macho A.P., Beuzón C.R., M. Barón M. & Ramos C. (2008). Early detection of bean infection by *Pseudomonas syringae* in asymptomatic leaf areas using chlorophyll fluorescence imaging. *Photosynthesis Research*, **96(1)**, 27–35.

Rosenthal G.A. (1991). The biochemical basis for the deleterious effects of L-canavanine. *Phytochemistry*, **30**, 1055–1058.

Rowhani A., & Golino D.A. (1995). ELISA test reveals new information about leafroll disease. *California Agriculture*, **49**, 26–29.

Rowhani A., Uyemoto J.K., & Golino D.A. (1997). Acomparison between serological and biological assays in detecting *Grapevine leafroll-associated viruses*. *Plant Disease*, **81**, 799–801.

Ryals J.A., Neuenschwander U.H., Willits M.G., Molina A., Steiner H.Y., & Hunt M.D. (1996). Systemic acquired resistance. *Plant Cell*, **8**, 1809-1819.

Sampol B., Bota J., Riera D., Medrano H., & Flexas J. (2003). Analysis of the virus-induced inhibition of photosynthesis in malmsey grapevines. *New Phytologist*, **160**, 403–412.

Satyanarayana T., Gowda S., Ayllon M.A., Albiach-Marti M.R., & Dawson W.O. (2002). Mutational analysis of the replication signals in the 3'-non translated region of citrus tristeza virus. *Virology*, **300**, 140–152.

Savino V., Boscia D., D'Onghia A.M., & Martelli G.P. (1991)."Effect of heat therapy and meristem tip culture on the elimination of *Grapevine leafroll-associated closterovirus type III*," in Proceedings of the 10th Meeting of ICVG 3—7 September (Volos: ORES Publishing), 433–436.

Schaad N.W., Frederick R.D., Shaw J., Schneider W.L., Hickson R., Petrillo M.D., & Luster D.G. (2003). Advances in molecular-based diagnostics in meeting crop biosecurity and phytosanitary issues. *Annual Review of Phytopathology*, **41**, 305-324.

Schafer H., & Wink M. (2009). Medicinally important secondary metabolites in recombinant microorganisms or plants: progress in alkaloid biosynthesis. *Biotechnology Journal*, **4(12)**, 1684-1703.

Schaller A., & Ryan C.A. (1996). Systemin- a polypeptide signal in plants. *Bioessays*, **18**, 27–33.

Scheu G. (1935). Die Rollkrankheit des Rebenstockes. *Der Deutsche Wein-bau*, **14**, 222–223.

Schoelz J.E., Harries P.A., & Nelson R.S. (2011). Intracellular transport of plant viruses: finding the door out of the cell. *Molecular Plant*, **4**, 813–831.

Shalitin D., & Wolf S. (2000). Cucumber Mosaic Virus Infection Affects Sugar Transport in Melon Plants. *Plant Physiology*, **123**, 597–604.

Sharma R.C., Duveiller E., & Ortiz-Ferrara G. (2007). Progress and challenge towards reducing wheat spot blotch threat in the Eastern Gangetic Plains of South Asia: is climate change already taking its toll?. *Field Crops Research*, **103**, 109–18.

Shulaev V., Silverman P., & Raskin I. (1997). Airborne signalling by methyl salicylate in plant pathogen resistance. *Nature*, **385**, 718-721.

Silva M.S., Wellink J., Goldbach R.W., & Van Lent J.W.M. (2002). Phloem loading and unloading of *Cowpea mosaic virus* in *Vigna unguiculata*. *Journal of General Virology*, **83**, 1493–1504.

Smart R. 2013. Trunk diseases ... a larger threat than phylloxera?. *Wine & Viticulture Journal*, **28 (4)**, 16–18.

Stadler R., Wright K.M., Lauter-bach C., Amon G., Gahrtz M., Feuerstein A., Oparka K.J., & Sauer N. (2005). Expression of GFP-fusions in Arabidopsis companion cells reveals non-specific protein trafficking into sieve elements and identifies a novel post-phloem domain in roots. *Plant Journal*, **41**, 319–331.

Stapleton A.E., & V Walbot V. (1994). Flavonoids can protect maize DNA from the induction of ultraviolet radiation damage. *Plant Physiology*, **105(3)**, 881–889.

Taillandier P., Portugal F.R., Fuster A., & Strehaiano P. (2007). Effect of ammonium concentration on alcoholic fermentation kinetics by wine yeasts for high sugar content. *Food Microbiology*, **24**, 95-100.

Taiz L., & Zeiger E. (2006). *Plant Physiology*, 4th edition.

Tanaka Y., Sasaki N., & Ohmiya A. (2008). Biosynthesis of plant pigments: anthocyanins, betalains and carotenoids. *Plant Journal*, **54(4)**, 733-749.

Tsai C.W., Daugherty M.P., & Almeida R.P.P. (2012). Seasonal dynamics and virus translocation of *Grapevine leafroll-associated virus 3* in grapevine cultivars. *Plant Pathology*, **61**, 977–985.

Thompson J.R., Fuchs M., Fischer K.F., & Perry K.L. (2012). Macroarray detection of grapevine leafroll-associated viruses. *Journal of Virological Methods*, **183**, 161–169.

Tucker T., Marra M., & Friedman J.M. (2009). Massively parallel sequencing: The next big thing in genetic medicine. *American Journal of Human Genetics*, **85**, 142–154.

Turturo C., Salderelli P., Yafeng D., Digiaro M., Minafra A., Savino V., & Martelli G.P. (2005). Genetic variability and population structure of *Grapevine leafroll-associated virus 3* isolates. *Journal of General Virology*, **86**, 217–224.

Ueki S., & Citovsky V. (2007). "Spread throughout the plant: systemic transport of viruses," in Viral Transport in Plants, eds E. Waigmann and M. Heinlein (Berlin: Springer), 85–118.

Van Bel A.J.E. (2003). The phloem, a miracle of ingenuity. *Plant Cell Environment*, **26**, 125–149.

Van den Born E., Omelchenko M.V., Bekkelund A.,Leihne V., Koonin E.V., Dolja V.V., & Falnes P.Ø. (2008). Viral AlkB proteins repair RNA damage by oxidative demethylation. *Nucleic Acids Research*, **36**, 5451–5461.

van Dongen J.T., Gupta K.J., Ramírez-Aguilar S.J., Araújo W.L., Nunes-Nesi A., & Fernie A.R. (2011). Regulation of respiration in plants: A role for alternative metabolic pathways. *Journal of Plant Physiology*, **168**, 1434– 1443.

Von der Brelie D., & Nienhaus F. (1982). Histological and cytological studies on the infectious leafroll disease of the grapevine. *Zeitschrift für Pflanzenkrankheiten und Pflanzenschutz,* **89**, 508–517.

Walker J.T.S., Charles J.G., Froud K.J., & Connolly P. (2004). Leafroll virus in vineyards: Modeling the spread and economic impact. 19 pp. Report *to New Zealand Winegrowers Limited*, Auckland.

Walter B., Bass P., Legin R., Martin C., Vernoy R., Collas A., & Vesselle G. (2008). The use of a green-grafting technique for the detection of virus-like diseases of the grapevine. *Journal of Phytopathology,* **128**, 137–145.

Wang J., Sharma A.M., Duffy S., & Almeida, R.P.P. (2011). Genetic diversity in the 3' terminal 4.6-kb region of *Grapevine leafroll associated virus 3*. *Phytopathology*, **101**, 445–450.

Ward E., Foster S.J., Fraaije B.A., & McCartney H.A. (2004). Plant pathogen diagnostics: immunological and nucleic acid-based approaches. *Annals of Applied Biology*, **145**, 1–16.

Weber E., Golino D.A., & Rowhani A. (2002). Laboratory testing for grapevine virus diseases. *Practical Winery and Vineyard Journal*, **22**, 13–26.

Weber E., Golino D.A., & Rowhani A. (1993). Leafroll disease of grapevines. *Practical Winery and Vineyard Journal*, **14**, 21–24.

Xue B., Ling K., Reid C.L., Krastanova S., Sekiya M., Momol E.A., Süle S., Mozsar J., Gonsalves D., & Burr T.J. (1999). Transformation of five grapevine rootstocks with plant virus genes and a virE2 gene from Agrobacterium tumefaciens. *In Vitro Cellular and Developmental Biology-Plant*, **35**, 226–231.

Xu X., Jingwen Y. & Yuanguo C. (2011). Pharmacokinetic Study of Viral Vectors for Gene Therapy: Progress and Challenges, Viral Gene Therapy, Dr. Ke Xu (Ed.), ISBN: 978-953-307-539-6, InTech, DOI: 10.5772/21259.

Young N.D. (2000). The genetic architecture of resistance. *Current Opinion in Plant Biology*, **3**, 285-290.